Luíse Lopes Chaves

New technologies for the improvement of leprosy multidrug therapy: a Quality by Design approach

Tese do 3º Ciclo de Estudos Conducente ao Grau de Doutor em Ciências Farmacêuticas com Especialidade em Tecnologia Farmacêutica

Trabalho realizado sob a orientação do Professor Domingos de Carvalho Ferreira, e Co-orientação da Professora Maria de la Salette Hipólito Reis e do Professor Bruno Filipe Carmelino Cardoso Sarmento

U.PORTO
FACULDADE DE FARMÁCIA
UNIVERSIDADE DO PORTO

Abril de 2017

“Pedras no meu caminho? Guardo-as todas! Um dia hei de construir um castelo”.

Fernando Pessoa

Àquele que me fortalece, ao meu filho, quem me ensinou o amor incondicional, ao meu marido, meu eterno companheiro; aos meus pais, que me deram suporte sempre, e ao meu irmão, que foi amigo sempre que precisei.

Agradecimentos

Com o término desde doutoramento começo por refletir que nestas páginas não estão apenas o resumo de alguns anos de trabalho. Na verdade, nas entrelinhas desta tese estão, talvez, os anos de maior aprendizagem e crescimento pessoal que vivi, não só por estar a milhares de quilômetros das pessoas que considero de maior importância para mim, mas pelas experiências que tive oportunidade de vivenciar tanto pessoal como profissionalmente. Durante essa trajetória, muitas pessoas merecem minha eterna gratidão e serão sempre lembradas com carinho:

À Professora Doutora Salette Reis, por ter aceito minha co-orientação, e sempre ter-se mostrado tão disponível; pela paciência que sempre conduziu esta caminhada, com tanta sabedoria, estando sempre preocupada com meu bem-estar não só no ambiente de trabalho, como no âmbito pessoal, ajudando a superar todos os obstáculos que surgiram.

De maneira especial ao Professor Doutor José Luís Costa Lima, primeiramente por ter permitido que eu fizesse parte do grupo de pesquisa por ele coordenado, disponibilizando tudo que fosse necessário para realização do trabalho; e depois, por estar sempre atento e preocupado comigo em todos os aspectos. Agradeço imenso sua receptividade e sua simpatia, todas as oportunidades que me foram dadas, inclusivamente de realizar alguns passeios em sua companhia, que sempre foi agradabilíssima.

Ao professor Doutor Bruno Sarmento, por ter sido a primeira pessoa a ter aceito a minha orientação na Universidade do Porto e pela oportunidade de engrandecer meu conhecimento científico durante este percurso; e ao Professor Doutor Domingos Ferreira, por ter me aceitado como aluna de doutoramento na Faculdade de Farmácia.

À Doutora Sofia Costa Lima, que teve um papel fundamental para a conclusão deste trabalho, não só pela disponibilidade, como também pelo contributo cientifico. Agradeço também a convivência a as conversas, que sempre foram muito agradáveis.

Gostaria de demonstrar meu agradecimento a todo o grupo do departamento de Química Aplicada, com o qual tive o prazer de conviver durante alguns anos, e foram praticamente minha família durante esse período em que estive longe do meu país.

Particularmente, agradeço aos meus companheiros de laboratório Alexandre, Daniela, Catarina e Joana que tornaram os dias difíceis mais agradáveis, e compartilharam também os dias mais descontraídos; agradeço com carinho especial àqueles que tive oportunidade de conviver por mais tempo: Sofia CL, Nini, Mara, Catarina A, Virgínia, Cláudia Nunes, Marina Pinheiro, José Plácido, João Albuquerque, Miguel H, Alessandro S, Inês, Marieta, Marisa, Daniela R, Claudia S, obrigada por terem me ajudado a construir essa história!

Agradeço às amigas que fiz durante esse percurso Larini, Alessandra e Roberta por terem me confortado nos dias mais difíceis, rirem comigo e terem sido responsáveis pelos dias mais felizes que tive no Porto. Obrigada, vocês não sabem o quanto foram importantes!

Aos meu pais Mônica e Abiatar, que mesmo estando longes fizeram de tudo para que a realização deste sonho se tornasse realidade, me apoiando em tudo o que fosse necessário, por terem sido responsáveis pela pessoa que sou hoje através de seus ensinamentos e valores, terem me amado da maneira que sou, incondicionalmente. Amo vocês
Ao meu irmão Abiatar Neto por ter sido amigo quando mais precisei, pela força, pela companhia e cumplicidade. Amo vocês.

Aos meus sogros Vicente e Lúcia, e a Natália por terem me dado apoio durante esta caminhada.

Em especial, agradeço ao meu marido Alexandre por ter sido meu alicerce, meu amigo, meu companheiro, ter estado sempre presente quando mais precisei, sempre com paciência, buscando construir um ambiente de harmonia, apesar de todas as dificuldades que encontramos, que não foram poucas! Obrigada pela tolerância, por ter cuidado de mim quando fraquejei, por existir na minha vida de forma tão especial. Sem você, nada disso teria sido possível! Obrigada do fundo do meu coração. Principalmente, por ter me dado meu bem mais precioso, meu filho Alexandre Chaves a quem eu dedico esta tese e todo o meu amor.

Agradeço à CAPES pelo suporte financeiro relativo à bolsa de doutoramento 0831-12-3, e à todos que direta ou indiretamente fizeram parte deste trabalho.

FCT Fundação para a Ciência e a Tecnologia
MINISTÉRIO DA CIÊNCIA, TECNOLOGIA E ENSINO SUPERIOR
CAPES
COMPETE 2020
PORTUGAL 2020
UNIÃO EUROPEIA
Fundos Europeus Estruturais e de Investimento

Abstract

Leprosy is an infectious disease which is considered one of the most common causes of non-traumatic peripheral neuropathy worldwide. The actual treatment is based in a multidrug therapy (MDT), which is selected according to the classification of the disease. For the most complicated cases (multibacillary leprosy, MB), patients should take a daily dose of dapsone (DAP) and clofazimine (CLZ). The standardization of the MDT regarding duration and therapeutic agents seems seem to be a trend as may help to improve patient compliance. Despite the effectiveness of DAP and CLZ, their action is greatly limited by their physicochemical features, specially their low solubility. The main goal of this thesis was to develop new drug delivery systems for oral administration of DAP and CLZ, in order to overcome limitations associated with their poor water solubility using Quality by Design tools. The rational development of amorphous solid dispersions (SD) with DAP and polyvinylpyrrolidone K30(PVP K30) by freeze-drying improved drug solubility and dissolution rate by shifting DAP physical state from crystalline to the amorphous form. Further, the design of pH-sensitive DAP-loaded nanoparticles of Eudragit L100 (NPs—EL100-DAP) was performed by the application of Placket-Burman screening design (PBD) with subsequent optimization by Box-Behnken design (BBD). Fourier-transformed infrared spectroscopy (FTIR) and differential scanning calorimetry (DSC) analyses confirmed the association of DAP; transmission electron microscopy (TEM) micrographs revealed the spherical morphology of the nanoparticles. The DAP *in vitro* release assay from NPs-EL100-DAP confirmed the nanoparticles' pH sensitivity and the ability to deliver DAP at the intestinal environment. NPs-EL100-DAP demonstrated enhanced intestinal permeation in comparison to free DAP, in the Caco-2 monolayers model. Solid lipid nanoparticles (SLNs) loaded with CLZ (SLNs-CLZ) were developed aiming to improve its bioavailability and decrease its intrinsic toxicity. The study was conducted after preliminary risk assessment of the process and product variable which allowed the implementation of control actions. A new UV-Vis spectrophotometric method to quantify CLZ was developed and validated to determine the drug association efficiency (AE) of the optimized SLNs-CLZ. Optimized SLNs-CLZ presented suitable particles size (230 nm), zeta potential (-34.28 mV), AE (72%) and drug loading (2.4 %). Physicochemical characterization by FTIR and DSC confirmed the drug association within SLNs in amorphous state. The storage stability studies ensured stability over 12 weeks at 4ºC, and no significant toxic effect of SLNs-CLZ on gastric cells (MKN-28) and intestinal Caco-2 and HT29-MTX cells (up to 25 and 50 respectively) was observed. The optimized SLNs-CLZ showed to be suitable to orally deliver CLZ, even though some improvement in the

drug payload was found to be important for the application in leprosy treatment, aiming to reach the suitable systemic levels. For this purpose, poly(lactic-co-glycolic acid) (PLGA) CLZ-loaded nanoparticles (NPs-CLZ) were obtained after assessing the critical factors during nanoparticles formulation through PBD. The obtained NPs-CLZ had a particle size of 210.8 nm, polydispersity (PDI) of 0.211, an AE of 70% and DL of 12 %. NPs-CLZ were characterized regarding morphology and physicochemical properties which showed the spherical shape and amorphous state of associated CLZ within NPs-PLGA. *In vitro* drug release revealed the sustained release of CLZ. Cytotoxicity studies showed that the NPs-CLZ were not toxic on the studied intestinal cells (Caco-2 and HT29-MTX) while free CLZ exhibited an IC50 of 16.3 and 20.3 μg mL-1 for Caco-2 and HT29-MTX cells, respectively. Similar apparent permeability values for free CLZ and when associated within nanoparticles were found after 8 h of permeation assays across Caco-2. The obtained NPs-CLZ was found to be an alternative to the SLNs as they presented higher DL, being a promising platform to deliver of CLZ. Lastly, the DAP/ CLZ combinatory therapy used for MB leprosy was studied using the developed polymeric nanosystems *per se* and in association. After 8 h no toxicity was observed for Caco-2 incubated with DAP alone and within NPs, up to 100 μg mL^{-1}, while CLZ *per se* was toxic, reducing cell viability to 30% at 50 μg mL^{-1}. Caco-2 exposed to NPs-DAP/ NPs-CLZ (100 and 50 μg mL^{-1}, respectively) had 80% viability. No significant differences were observed between the nanosystems *per se* or in combination for the apparent permeability values and the amount of permeated drug. Thus, the two polymeric nanosystems containing DAP and CLZ in combination seemed to be a promising platform to deliver both drugs in association, representing an important step toward the improvement and of MB leprosy therapy, as they may decrease the toxicity associated with the drugs and increase patient compliance (a single dose with both MDT drugs). Overall, different platforms to deliver DAP and CLZ were obtained to overcome the limitations associated with both these drugs, showing to be promising systems for future use in leprosy treatment as single systems or in association. Nevertheless, complementary assays should be performed to better elucidate the effect and security of DAP/ CLZ association into nanodelivery systems.

Key words: Leprosy; Dapsone/ Clofazimine association; Solid dispersions; Nanocarriers, Design of Experiment

Resumo

A lepra é uma doença infecciosa considerada uma das principais causas de neuropatias não-traumáticas no mundo. O seu tratamento actual é baseado na poliquimioterapia (PQT), que é selecionada de acordo com a classificação da doença. Para os casos mais complicados de lepra multibacilar (MB) os pacientes tomam uma dose diária de dapsona (DAP) e clofazimina (CLZ). A padronização da PQT relativamente ao tempo de tratamento e aos agentes antimicrobianos parece ser uma tendência visto que poderá auxiliar na adesão dos pacientes ao tratamento. Apesar da eficácia da DAP e da CLZ, a ação destes fármacos é comprometida pelas suas características físico-químicas, especialmente devido à baixa solubilidade. O principal objetivo desta tese foi desenvolver novos sistemas para entrega de fármacos para administração oral da DAP e da CLZ, de modo a ultrapassar as suas limitações utilizando uma abordagem Quality by Design. Assim, o desenvolvimento racional de dispersões sólidas amorfas (DS) com DAP e polivinilpirrolidona K30 por liofilização promoveu um aumento da solubilidade e velocidade de dissolução da DAP através da mudança do seu estado de cristalino para o estado amorfo. Posteriormente, o desenho de nanopartículas de Eudragit L100, sensíveis ao pH, contendo DAP (NPs-EL100-DAP) foi realizado através da aplicação do Plackett-Burman design (PBD) e subsequente otimização pelo Box-Behnken design (BBD). As análises de espectroscopia na região do infravermelho, com transformada de Fourier (FTIR) e calorimetria exploratória diferencial (DSC) confirmaram a associação da DAP, enquanto a microscopia eletrónica de transmissão revelou a morfologia esférica das nanopartículas. O ensaio de libertação *in vitro* da DAP a partir das NPs-EL100-DAP confirmou a capacidade de entrega do fármaco em ambiente intestinal. As NPs-EL100-DAP conduziram a um aumento da permeabilidade intestinal da DAP, em comparação com o fármaco livre utilizando o modelo de monocamada de Caco-2. Nanopartículas lipídicas sólidas (SLNs) carregadas com CLZ (SLNs-CLZ) foram desenvolvidas com o objetivo de aumentar a biodisponibilidade da CLZ e, diminuir a sua toxicidade intrínseca. Uma avaliação preliminar permitiu identificar o risco das variáveis envolvidas no processo e na formulação. Um novo método espectrofotométrico UV-Vis para quantificação expedita da CLZ foi desenvolvido e validado. As SLNs-CLZ apresentaram tamanho de partícula, potencial zeta, eficiência de associação e capacidade de carga adequadas para administração oral. A caracterização físico-química por FTIR e DSC confirmaram a associação da CLZ nas SLNs no estado amorfo. Os estudos de estabilidade de armazenamento confirmaram a estabilidade das formulações no período de 12 semanas, a 4ºC, e nenhum efeito citotóxico foi observado para as SLNs-CLZ em células gástricas

(MKN28) e intestinais (Caco-2 e HT29-MTX). As SLNs-CLZ mostraram-se adequadas para entrega oral de CLZ, no entanto seria necessário aumentar a capacidade de carga para atingir níveis sistémicos adequados ao tratamento da lepra. Com esse propósito, nanopartículas de poli(acido lático-co-glicolico) (PLGA) veiculadas com CLZ (NPs-CLZ) foram obtidas após avaliação de fatores críticos na formulação das nanopartículas através de um PBD. As NPs-CLZ obtidas apresentaram características fisíco-químicas adequadas para administração oral. NPs-CLZ foram caracterizadas quanto à morfologia (esférica) e as propriedades físico-quimicas que evidenciaram estado amorfo da CLZ associada às NPs-PLGA. O estudo de libertação *in vitro* revelou uma entrega lenta de CLZ em meio ácido. Os estudos de citotoxicidade mostraram que NPs-CLZ não foram consideradas tóxicas nas células intestinais estudadas enquanto a CLZ na forma livre exibiu um IC50 de 16.3 e 20.3 μg mL^{-1} para Caco-2 e HT29-MTX, respectivamente. Os valores de permeabilidade aparente para CLZ associada às NPs-PLGA foram registados após 8 h de ensaio. As NPs-CLZ desenvolvidas mostraram ser uma alternativa às SLNs já que descritas, pois apresentam uma capacidade de associação mais elevada, podendo ser uma plataforma promissora para a entrega de CLZ. Por último, a combinação terapêutica DAP/ CLZ usada no tratamento da lepra MB foi estudada utilizando-se os nanosistemas poliméricos desenvolvidos *per se* e em combinação. Após 8 h nenhuma toxicidade foi observada para Caco-2 incubadas com DAP livre ou associada às NPs até 100 μg mL^{-1}, enquanto que a CLZ livre apresentou toxicidade, reduzindo a viabilidade celular para 30% a 50 μg mL^{-1}. Células Caco-2 expostas à combinação NPs-DAP/ NPs-CLZ (100 e 50 μg mL^{-1}, respectivamente) apresentaram 80% de viabilidade. Não foram observadas diferenças significativas entre os nanosistemas *per se* ou em combinação para os valores de permeabilidade aparente e a quantidade de fármaco permeado. Assim, os dois nanosistemas poliméricos contendo DAP e CLZ em combinação demonstraram ser plataformas promissoras para administrar os fármacos em associação, representando um passo importante para a melhoria e da terapia da lepra MB, uma vez que podem diminuir a toxicidade associada aos fármacos e aumentar adesão do paciente através de uma toma única com ambos os medicamentos da PQT. De um modo geral, foram obtidas diferentes plataformas para administrar DAP e CLZ para superar as limitações associadas a ambos os fármacos, mostrando terem sido desenolvidos sistemas promissores para uso futuro no tratamento da lepra como sistemas únicos ou em associação. No entanto, ensaios complementares devem ser realizados para melhor elucidar o efeito e a segurança da associação DAP /CLZ em nanosistemas de libertação controlada.

Palavras-Chave: Lepra; Associação dapsona/ clofazimina; Dispersões sólidas; Nanocarregadores; Desenho experimental.

Contents

List of Figures

CHAPTER II – THEORETICAL BACKGROUND

A. Leprosy disease: state of the art

B. Solid Dispersions

C. Nano-delivery systems

CHAPTER IV – PROGRESS BEYOND THE STATE OF THE ART

A. Rational and precise development of amorphous polymeric systems with dapsone by response surface methodology

B. pH-sensitive nanoparticles for improved oral delivery of dapsone: risk assessment, design, optimization and characterization

C. Optimization of solid lipid nanoparticles for clofazimine delivery: risk management, statistical design and physicochemical characterization

List of Tables

B. pH-sensitive nanoparticles for improved oral delivery of dapsone: risk assessment, design, optimization and characterization

C. Optimization of solid lipid nanoparticles for clofazimine delivery: risk management, statistical design and physicochemical characterization

D. Development of PLGA nanoparticles loaded with clofazimine for oral delivery: assessment of formu-lation variables and intestinal permeability

E. Polymeric nanosystems combination allows dapsone and clofazimine intestinal permeation

List of Abbreviations and Symbols

2θ	Diffraction angle
ε	Extinction coefficient related to the given substance
ΔH	Enthalpy variation
ACAT	Advanced compartmental absorption and transit
ANOVA	One-way analysis of variance
ATR	Attenuated Total Reflectance
BA	Bioavailability
BBD	Box–Behnken design
BCS	Biopharmaceutical Classification System
BL	Borderline Lepromatous
BT	Borderline Tuberculoid
CLZ	Clofazimine
cm s^{-1}	Centimeters per seconds
CMC	Critic Micellar Concentration
Co	Initial concentration
CPP	Critical Process Parameters
CQAs	Critical quality attributes
DAP	Dapsone
DHPS	Dihydropteroate synthase
DLS	Dynamic light scattering
DMEM	Dulbecco's Modified Eagle Medium
DMSO	Dimethyl sulfoxide
DoE	Design of Experiment
DS	Design Space
DSC	Differential Scanning Calorimetry
e.g.	*exempli gratia*
EL100	Eudragit L100
ELS	Electrophoretic Light Scattering
ENL	Erythema nodosum leprosum
f2	similarity factor
FaSSIF	Fasted Simulated Small Intestinal Fluid
FD	Freeze-Dried
FDA	Food and Drug Administration
FeSSIF	Fed State Simulated Intestinal Fluids

FT-IR	Fourier Transform Infrared
GIT	Gastrointestinal Tract
h	hours
HME	Hot-Melt Extrusion
HPLC	High-Performance Liquid Chromatography
HPMC	Cydroxypropylmethyl cellulose
HPMCAS	Hydroxypropylmethyl cellulose acetate/succinate
HPMCP	Hydroxypropylmethyl cellulose phthalate
i.e.	*id est*
IAM	Immobilized Artificial Membrane
IC50	50% Inhibition Concentration
ICH	International Conference on Harmonization
IFN-γ	Interferon gamma
IL	Interleukin
KN	Kneaded
LL	Lepromatous
LoD	Limit of Detection
LoQ	Limit of Quantification
M. leprae	Mycobacterium leprae
MB	Multibacillary
MDT	Multidrug therapy
mg	miligrams
mL	Milliliter
MTT	Thiazolyl blue tetrazolium bromide
NIR	Near Infrared
NLC	Nanostructured Lipid Carriers
nm	Nanometer
NMR	Nuclear Magnetic Resonance
NPs-EL100-DAP	Eudragit L100 DAP loaded Nanoparticles
NPs – CLZ	Polymeric nanoaprticles loaded with clofazimine
NPs – PLGA	Empty polymeric nanoparticles
^{o}C	Centigrade degrees
PABA	p-aminobenzoic acid
PAMPA	Parallel Artificial Membrane Permeability Assay
Papp	Apparent permeability
PAT	Process Analytical Technology
PB	Paucibacillary

PBD	Plackett-Burman Design
PBS	Phosphate Buffer Solution
PCA	Polyacrylates
PCR	Polymerase Chain Reaction
PDI	Poly-Dispersity iIndex
PDs	Polymeric Dspersions
PEG 1500	Polyethyleneglycol 1500
PEG 20000	Polyethyleneglycol 20000
PEG 4000	Polyethyleneglycol 4000
PEG 8000	Polyethyleneglycol 8000
PEGs	Polyethylene glycols
PLA	Polylactide
PLC	Polycaprolactone
PLGA	Poly(lactic-co-glycolic acid)
PM	Physical Mixture
PVA	Poly(vinyl alcohol)
PVP	Poly(vinylpyrrolidone)
QbD	Quality by Design
R2	Squared correlation coefficient
rpm	Rotation per minute
RPMI	Roswell Park Memorial Institute
RR	Reversal Reaction
RSM	Response Surface Methodology
SC	Schwann cells
SD	Solid Dispersions
SD	Standard Deviation
SEM	Scanning Electron Microscopy
SLN	Solid Lipid Nanoparticle
SLNs	Empty solid lipid nanoparticle
SLNs- CLZ	Solid lipid nanoparticle loaded with clofazimine
TEM	Transmission Electron Microscopy
Tg	Transition temperature
Th1	T helper cells type 1
TNF-α	Tumor Necrosis Factor alpha
TPQP	Target Product Quality Profile
TT	Tuberculoid
U-MDT	Uniform-MDT

UV-Vis	Ultraviolet-Visible
vs	Versus
w/v	Weight/volume
w/w	Weight/weight
WHO	World Health Organization
XRD	X-Ray Diffraction
XRPD	X-Ray Powder Diffraction
ZP	Zeta potential
$\mu g\ mL^{-1}$	Micrograms per milliliter
$\mu g\ s^{-1}$	Micrograms per second

Chapter I

Introduction

1. Motivation

Leprosy continues to be a significant issue of public health as it affects a large proportion of the World population [1, 2]. Brazil, India and Indonesia present the highest levels of the reported cases, accounting for 81% of new cases globally [3]. It is characterized as a chronic and infectious disease caused by an intracellular microorganism, the *Mycobacterium leprae* (*M. leprae*) [4], that mainly affects the peripheral nervous system, skin, and certain other tissues such as the reticuloendothelial system, bones and joints, mucous membranes, eyes, testis, muscles, and adrenals [1, 5]. Leprosy disease is one of the most common causes of non-traumatic peripheral neuropathy worldwide [6]. Acute episodes of clinical manifestations occurs during the chronic course of disease, affecting 30 to 50% of patients and often appear at the beginning of the treatment [1, 6]. Such reactions may cause permanent damage to the nerves, which lead to an increase in the morbidity due to sensory loss, dysfunction and eventual deformities in the skin and other organs [1, 6, 7]. To address issues related to leprosy control, new strategies have been proposed involving the improvement of political commitment and the reduction of patients disabilities in the next few years [3]. For treatment purposes, the World Health Organization suggests a simple scheme to classify leprosy patients based on visible symptoms and (ideally) the presence or absence of bacilli in slit-skin smears [1, 8]. Patients are classified as having paucibacillary (PB) leprosy (1 -5 skin patches) or multibacillary (MB) (with > 5 skin patches) [1, 8]. The actual recommended treatment for leprosy disease is based in a multidrug therapy (MDT), consisting of clofazimine (CLZ), dapsone (DAP) and rifampicin, as first line drugs. For patients with PB leprosy, rifampicin (600 mg) is monthly (supervised) administered and dapsone (100 mg) is daily (non-supervised) administered during 6 months; while MB patients are treated with rifampicin (200 mg) and clofazimine (300 mg) monthly (supervised) administered, and dapsone (100 mg) and clofazimine (50 mg) daily (son-supervised) administered, during 12 months [8].

The majority of the countries that have reported new leprosy cases in 2014 presented higher incidence of MB leprosy cases [3]. Thus, the standardization of the MDT regarding time of treatment and therapeutic agents seems to be a trend in leprosy eradication program as the implementation of a unique therapeutic regimen may help to improve patient compliance. In this context, DAP and CLZ which are the daily drugs used in MDT for MB cases become the most important components of leprosy therapy [9].

On the other hand, the idea of shortening the duration of MB treatment associated with the non-supervision of daily-drugs administration (DAP and CLZ) highlights the risk of antimicrobial resistance in leprosy [9]. Thus, research in the therapy of leprosy is still

needed, and some efforts must be done specially to improve delivery of drugs and compliance of patients, [5, 10, 11], as the research for alternative bactericidal agents are currently limited [12, 13].

Despite their proven effectiveness, the therapeutic potential of the anti-leprotic drugs is greatly limited by their physicochemical features, specially their insolubility in water [14]. This fact is especially relevant for daily dosages, i.e., for DAP and CLZ as they play an important role in the success of MDT. In this context, it seems to be of great relevance to develop new drug delivery systems with these drugs aiming to both overcome physicochemical limitations and improve their bioavailability, as well as to contribute to the improvement of leprosy therapy through the drug association.

2. Aims

Based on previous considerations, the main goal of this thesis was to develop new drug delivery systems with the first-line drugs used in leprosy MB treatment regimen, for daily administration of CLZ and DAP. The application of delivery systems aim to overcome limitations associated with their physicochemical characteristics particularly regarding poor water solubility. In parallel, this work intended to systematic design new drug delivery systems with DAP and CLZ through the application combined analytical approaches such as design of experiments (DoE) and response surface methodology (RSM), as Quality by Design tools.

More specifically, this thesis intended to develop and characterize: (i) amorphous solid dispersions with DAP to improve its dissolution rate; and (ii) pH sensitive polymeric nanoparticles targeted to intestinal environment, trying to avoid undesired DAP release under acidic conditions. Moreover, nano-delivery systems with CLZ, namely solid lipid and polymeric nanoparticles were also systematically developed and characterized aiming to overcome drug low bioavailability and associated toxic effects upon oral administration. Finally, the assessment of cell viability and *in vitro* permeability of DAP and CLZ were compared to the developed nano-delivery systems alone, and in association.

3. Structure

This thesis is organized in 5 chapters:

Chapter I: Introduction. This chapter includes the motivation for this work, as well as the definition of the main and specific goals. A brief description of the thesis organization and structure is also provided.

Chapter II: Theoretical background. This chapter started with the state of the art of leprosy disease, in which theoretical considerations, epidemiologic records, transmission, diagnosis and treatment were approached. Then, two published review works entitled "Quality by Design: Discussing and Assessing the Solid Dispersions Risk" and "Nanocarriers as strategy for oral bioavailability improvement of poorly water-soluble drugs" supported the strategies that have been used to overcome the drawbacks associated with the mainly anti-leprosy drugs: clofazimine and dapsone.

Chapter III: Methods. In this chapter, is presented a general overview of the fundamental aspects related to the techniques and methodologies used in this thesis to develop, characterize and validate the drug delivery systems developed in this thesis.

Chapter IV: Progress beyond the state of art. This chapter presents published and non-published works originated in the context of this thesis:

A. Rational and precise development of amorphous polymeric systems with dapsone by response surface methodology;

B. pH-sensitive nanoparticles for improved oral delivery of dapsone: risk assessment, design, optimization and characterization;

C. Optimization of solid lipid nanoparticles for clofazimine delivery: risk management, statistical design and physicochemical characterization;

D. Characterization of PLGA nanoparticles loaded with clofazimine for oral delivery: assessment of formulation variables and intestinal permeability;

E. Polymeric nanosystems combination allows dapsone and clofazimine intestinal permeation

F. Integrated Discussion

Chapter V: Concluding Remarks and Future Perspectives. In this final chapter, the main conclusions and perspectives are presented, considering the contributions of the present studies for the improvement of leprosy therapy as well as for the development of new delivery systems to overcome poor solubility of clofazimine and dapsone, enhancing its applicability in future associated therapy.

4. References

1. White, C. and C. Franco-Paredes, Leprosy in the 21st century. Clinical microbiology reviews, 2015. 28(1): p. 80-94.
2. Virmond, M., A. Grzybowski, and L. Virmond, Leprosy: A glossary. Clinics in Dermatology, 2015. 33(1): p. 8-18.
3. Organization, W.H., Weekly Epidemiological Record, 23 September 2016, vol. 91, 39 (pp. 441–460). 2016.
4. Nath, I., C. Saini, and V.L. Valluri, Immunology of leprosy and diagnostic challenges. Clinics in Dermatology, 2015. 33(1): p. 90-98.
5. Prasad, P.V.S. and P.K. Kaviarasan, Leprosy therapy, past and present: can we hope to eliminate it? . Indian Journal of Dermatology, 2010. 55(4): p. 316-324.
6. Bhat, R.M. and C. Prakash, Leprosy: An Overview of Pathophysiology. Interdisciplinary Perspectives on Infectious Diseases, 2012. 2012: p. 181089.
7. Gillis, T.P., Chapter 93 - Mycobacterium leprae A2 - Tang, Yi-Wei, in Molecular Medical Microbiology (Second Edition), M. Sussman, *et al.*, Editors. 2015, Academic Press: Boston. p. 1655-1668.
8. World Health Organization. Global Leprosy Programme. 2017 March 7]; Available from: http://www.searo.who.int/entity/global_leprosy_programme/disease/en/.
9. Prasad, P.V.S. and P.K. Kaviarasan, Leprosy therapy: past and present: can we hope to eliminate it? Indian Journal of Dermatology, 2010. 55(4): p. 316-324.
10. Grosset, J.H., Newer drugs in leprosy. International Journal of Leprosy and Other Mycobacterial Diseases, 2001. 69(2): p. S14.
11. Rodrigues, L.C. and D.N.J. Lockwood, Leprosy now: epidemiology, progress, challenges, and research gaps. The Lancet Infectious Diseases. 11(6): p. 464-470.
12. Kar, H.K. and R. Gupta, Treatment of leprosy. Clinics in Dermatology, 2015. 33(1): p. 55-65.
13. Legendre, D.P., C.A. Muzny, and E. Swiatlo, Hansen's Disease (Leprosy): Current and Future Pharmacotherapy and Treatment of Disease-Related Immunologic Reactions. Pharmacotherapy: The Journal of Human Pharmacology and Drug Therapy, 2012. 32(1): p. 27-37.
14. Islan, G.A., et al., Nanopharmaceuticals as a solution to neglected diseases: Is it possible? Acta Tropica, 2017. 170: p. 16-42.

Chapter II

Theoretical background

Partially published in:

Chaves, L., *et al.* "Quality by design: discussing and assessing the solid dispersions risk." Current Drug Delivery 11.2 (**2014**): 253-269.

Chaves, L., *et al.*, Nanocarriers as strategy for oral bioavailability improvement of poorly water-soluble drugs, in Nanoparticles in the Life Sciences and Biomedicine. **2017**, Pan Stanford Publishing. ISBN 978-981-4745-98-7.

A. Leprosy disease: state of the art

1. Introduction

Leprosy, also known as Hansen's disease, is a non-fatal ancient bacterial disease that, continues to be a significant issue of public health as it affects a large proportion of the World population [1, 2]. Currently it is one of the most common causes of non-traumatic peripheral neuropathy worldwide [6].

Epidemiologic data demonstrate that, despite important advances in the political, social, and economic status of developing countries, leprosy is still endemic in several countries of Africa, South-East Asia, and America. In Europe, it is considered a rare disease, although it is still a disease of concern among immigrants coming from risk areas [2].

Leprosy is characterized as a chronic and infectious disease caused by an intracellular microorganism, the *Mycobacterium leprae* (*M. leprae*) [4]. It mainly affects the peripheral nervous system, skin, and certain other tissues such as the reticuloendothelial system, bones and joints, mucous membranes, eyes, testis, muscles, and adrenals [1, 5].

Several clinical manifestations have been reported and depend on the host immune response [4]. Since the inflammation takes place, it is important to have immediate medical attention due to severe pain and to prevent nerve damage and deformity [4].

1.1 Epidemiology

The prevalence of leprosy globally decreased from >5 million cases in the mid-1980's to less than 200,000 in 2015 with the introduction of multidrug therapy [3]. Lower prevalence rates do not necessarily mean the reduction in the number of new cases found nor a decrease in *M. leprae* transmission; rather, it may be related to the shorter period of treatment recommended by the World Health Organization (WHO) or to the exclusion from registries of patients who have been cured or who have died [15].

According to data obtained from WHO, in 2015, several countries or territories reported cases of leprosy, namely: 28 cases from the African Region, 23 from the Region of the America, 11 from the South-East Asia Region, 20 from the Eastern Mediterranean Region, 28 from the European Region and 26 from the Western Pacific Region [16]. Figure 1 depicts the incidence of leprosy worldwide, based on WHO records.

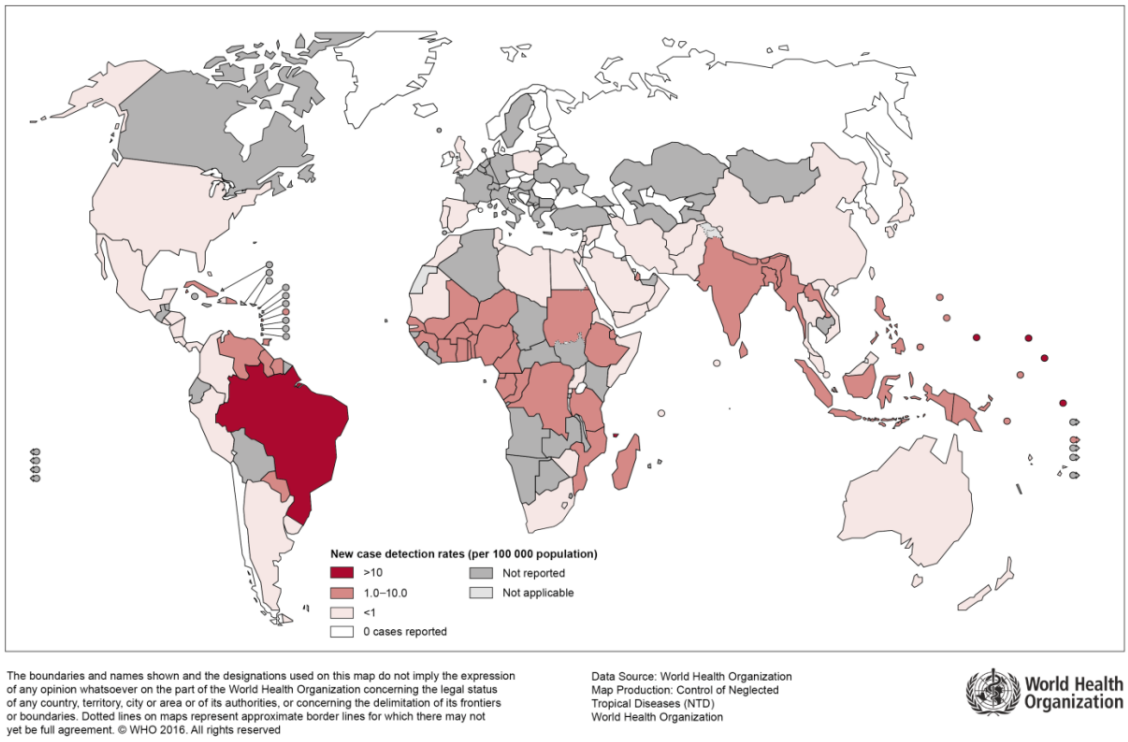

Figure 1. World distribution of new cases of leprosy in 2015, according to WHO [16].

At a global level, between 2005 and 2014 the number of new cases was maintained constant [3], which reveals that leprosy continuous to be highly prevalent in many countries. Among them, 13 countries reported >1,000 new cases (5 from Africa, 1 from America, 6 from South-East Asia and 1 Western Pacific), which together contributed to 94% of all new leprosy cases Worldwide [3]. Brazil, India and Indonesia, presented the higher levels of new cases with >10,000 new cases reported, accounting for 81% of new leprosy cases globally [3].

Regarding the diagnosis, 60.6% of new cases were classified as multibacillary, which indicate presence of advanced cases of leprosy and indirectly the magnitude of infection in the community [3]. Between 2007 and 2015, more than 110,000 people diagnosed with leprosy had physical deformities at diagnosis, an indicator of delayed detection [17]. The trend in the number of new cases indicates stagnation in leprosy control. Thus, early diagnosis and complete treatment with multidrug therapy continue to be key strategies for reducing disease burden due to leprosy [3].

To address issues related to stagnation in leprosy control, new strategies have been proposed and included (i) improved political commitment, (ii) reduction of patients disabilities, (iii) inclusion of persons affected by leprosy until 2020 [3].

1.2 Etiologic agent: *Mycobacterium leprae*

M. leprae (order *Actinomycetales* ; family *Mycobacteriaceae*) is an acid-fast obligate intracellular bacillus, differing from other mycobacteria that may grow beyond cells [15]. Morphologically the bacillus appears as pleomorphic rods with 1 to 8 μm long for 0.3 μm large [18], and replicate by binary diffusion [7, 15]. which takes from 12-13 days, in temperatures between 27-30°C [15].

M. leprae are naturally Gram-positive but can be differentially stained, appearing acid-fast using the Ziehl-Neelsen stain on smears or the Fite's acid fast stain in paraffin-embedded tissue sections [7]. The inability to culture *M. leprae in vitro* is one of the main specificities of that bacterium, and can be explained by its very long doubling time (14 days) [18]. Nowadays, it is still difficult to culture *M. leprae* in the laboratory, but it can be done by inoculating the bacterium into the footpad of female Swiss mice [18]. The *in vitro* replication allowed the research in the development of new antibiotic therapies and the study of drug resistance [18].

Despite the *M. leprae* be highly infective, the progression of the disease is slow due to the long incubation period of the bacteria [19, 20]. It shows tropism for cells of the reticuloendothelial and peripheral nervous system, more specifically for Schwann cells (SC), showing propensity to infect cold areas of the body as skin, nasal mucosa, and peripheral nerves [15]. Once inside cells, they get arranged in aggregates called globi [20, 21]. The specificity of *M. leprae* for SC is explained by the attachment to laminin-α2 and adhesins located in the basal lamina and to α-dystroglycan and ErbB2 receptors on the cell surface of peripheral nerves [1, 6]. When inside the SC, the pathogen triggers the differentiation into immature cells, creating a suitable environment for its proliferation [1]. The replication proceeds slowly until the recognition of the bacteria by T cells, starting up a chronic inflammatory reaction [15]. A schematic representation of the interaction between *M. leprae* and laminin-2 glycoprotein is represented in Figure 2. The infection of SC induces demyelination and loss of axonal conductance with consequent disability [6, 15, 20].

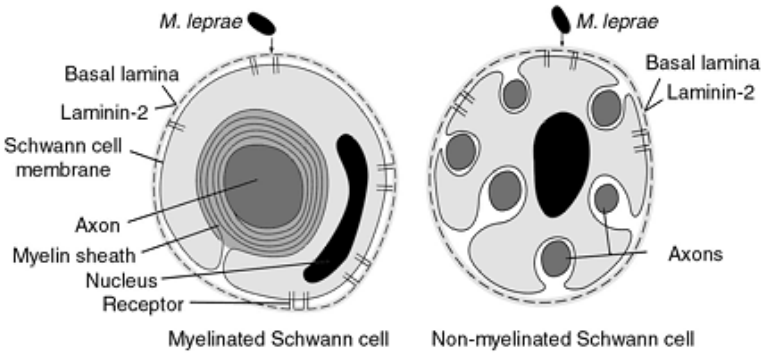

Figure 2. Schematic representation of the interaction between M. leprae and laminin-2 in the basal lamina of myelinated and non-myelinated Schwann-cell–axon units. Adapted from [20]

1.3 Transmission

The transmission and dissemination of *M. leprae* is low, and the mechanism by which the pathogen is transmitted is poorly understood [15]. *M. leprae* has been found in high numbers in the nasal mucosa. Thus, the respiratory tract may play a relevant role in its transmission as it may be a site of entry of the bacillus [15, 18].

No relationship between the *M. leprae* and a vector has been established, although the possibility cannot be ignored. Vertical transmission has been reported, so it is recommended to follow mother-child dyads [15].

The most contagious form of the disease is the lepromatous (see section 1.4) as patients usually have a very large number of bacilli, presenting up to 7 billion bacilli per one gram of tissue [18]. Although, the bacilli dissemination is not restricted to leprosy patients, healthy carriers and individuals with subclinical infections who carry *M. leprae* in their nasal and or oral mucosa may play an important role in the disease chain of transmission [22].

1.4 Classification

The classification of leprosy is determined by clinical prognosis and it serves to distinguish which cases may be potentially infectious [23]. In addition, the clinical determination of leprosy subtype may provide major pathophysiological information [23].

A more detailed and used system of classification, called Ridley and Jopling system, categorizes the disease into five types according to cell-mediated responses and these

include, from the least to the most severe tuberculoid (TT), borderline tuberculoid (BT), borderline borderline (BB), borderline lepromatous (BL), and lepromatous (LL) [1]. The borderline leprosy is considered an intermediate manifestation between lepromatous and tuberculoid leprosy, and the designation BT, BB and BL came to better characterize the borderline group that could comprise patients with different clinical, immunological, bacteriological, or histological findings [23].

Tuberculoid leprosy is characterized by the presence of few (or single) small lesions which may be hyposensitive or anesthetic, showing well-defined and elevated borders (papules and plaques), that can sometimes be infiltrated [2, 18]. Rare acid-fast bacilli are found in the damaged tissue [7]. If left untreated, they form copper colored papules or nodules known as leproma. Nerve damage is usually observed around skin lesions and is associated with sensory and/or motor impairment when the hands and feet are affected [18].

Borderline leprosy is classified according to the number of clinical signs, corresponding to a transition between TT and LL cases [2, 18]. The BT presentation of leprosy is defined by the presence of several asymmetrical and hypoesthetic lesions with peripheral macules or infiltration of the skin [18]. Lesions may vary in size, shape, and color, even in the same patient [2]. Histopathological analysis of skin smears may be negative or positive, even though bacteriologic index is usually low [2]. The BB presentation is defined by the presence of several non-anesthetic annular lesions characterized by infiltrated plaques with an apparent normal skin in the center and well-defined inner edge [2, 18]. The BL presentation is characterized by the disseminated presence and symmetric lesions, bilateral and non-anesthetic lepromas and annular lesions [2, 18]. The elevated number of lesion is due to the reduced immunologic resistance [2].

Lepromatous leprosy is caused by a strong inability for an immunologic reaction against *M leprae*. At skin levels, patients present a high number of bilateral and symmetrical not anesthetic leproma (20 to 100) that frequently occurs in the face, earlobes, fingers, and toes [15, 18]. Histopathology reveals very large numbers of bacilli in the dermis [7]. Non-skin manifestations may compromise the eyes, nose, bones, testis, spleen, liver, and adrenals, leading to systemic repercussions and more severe disability [2, 15].

For treatment purposes, WHO suggests a simple scheme to differentiate leprosy types. In this scheme, leprosy is classified based on visible symptoms and (ideally) the presence or absence of bacilli in slit-skin smears from cooler regions of the body (generally from earlobes, elbows, and/or knees) where bacilli proliferate [1, 8]. Patients with 1 -5 skin patches and no apparent bacilli in slit-skin smears are classified as having

"paucibacillary" (PB) disease, while those with > 5 skin patches and bacilli visible by microscopic analyses of skin smears are classified as having "multibacillary" (MB) disease. In areas without access to slit-skin smears, the criterion for diagnosis is the number of visible lesions [1, 8].

A schematic representation of leprosy classification according immune response, clinical manifestation and treatment is depicted in Figure 3.

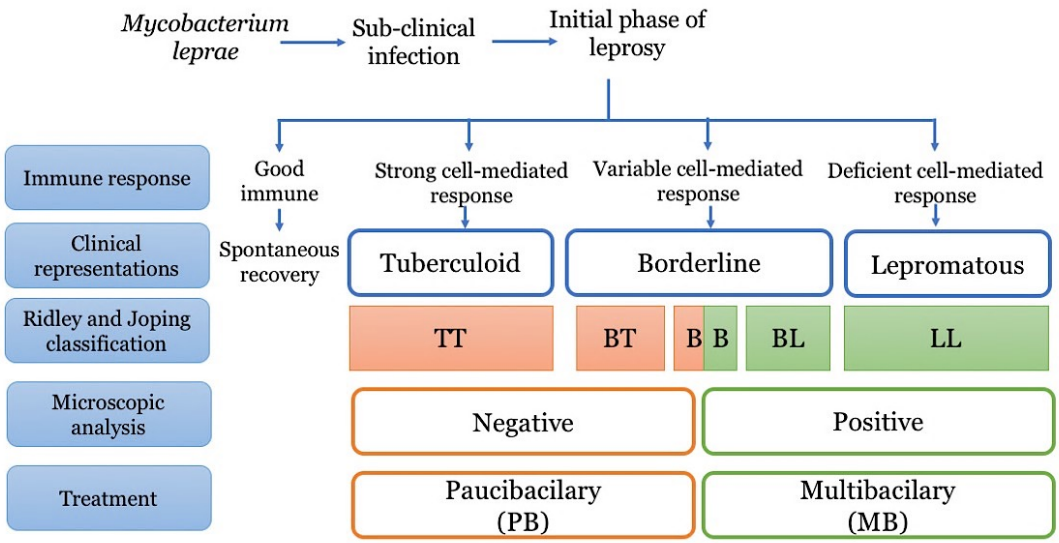

Figure 3. Schematic representation of leprosy classification according immune response, clinical manifestation and treatment. Adapted from [18].

Another important classification use by WHO to assess the efficacy of the public health program is to classify leprosy according disability grading system. This is a practical and simple classification that has been used as an epidemiological indicator [24, 25].Briefly, disability can be defined as any change that may compromises the proper functioning of the body, and may be at biological, activity, personal (psychological aspects), environmental or societal (context and participation) levels, which can be experienced by an individual affected by a disease or a special health condition [24, 25]. In this classification, Grade 0 means no impairment, Grade 1 means loss of sensation in the hand, eyes or foot, and Grade 2 means visible impairment [24, 25].

1.5 Leprosy reactions

Leprosy reactions are acute episodes of clinical inflammation which occurs during the chronic course of disease, affecting 30 to 50% of patients and often appear at the

beginning of the treatment [1, 6]. Reactions may cause permanent damage to the nerves, which lead to an increase in the morbidity such as sensory loss, dysfunction and eventual deformities. They can affect skin and other organs as well [1, 6, 7]. The appearance of the reactions are related to the immune system changes, that may be caused by the multidrug therapy, most often arising in the first two months after the beginning of the treatment, stress, or pregnancy [1, 6, 26]. They are classified as Type I also known as reversal reaction (RR); and Type II or erythema nodosum leprosum (ENL) reactions [26] .Both types of reactions have been found to cause neuritis, representing the primary cause of irreversible deformities [6].

Type I reaction occurs in 30% of patients, normally with borderline leprosy (BB or BL) [26] and, are associated with clinical and histopathological increased immunity toward *M. leprae* [7]. These reactions are characterized by edema and erythema of existing skin lesions, the formation of new skin lesions, neuritis, additional sensory and motor loss, and edema of the hands, feet, and face; however, systemic symptoms are uncommon [6, 7].

Type II reaction occurs mainly in patients with poor cellular immune responses but who have preserved humoral responses, for example in LL or LB patients with high levels of anti-*M. leprae* immunoglobulins [26]. The reactions are characterized by the appearance of tender, erythematous, subcutaneous nodules located on apparently normal skin, and is commonly accompanied by systemic symptoms, such as fever, malaise, enlarged lymph nodes, anorexia, weight loss, arthralgia, and edema. Other organs including the testis, joints, eyes, and nerves may also be affected [6, 7].

1.6 Immunological responses

The immune response to *M. leprae* is variable due to the large variability in host immune response to the bacillus [13, 15]. Different immune responses are observed among the 5 categories of the Ridley and Jopling classification system, especially when comparing the extremities of the manifestations [19]. Across the five-group Ridley and Jopling system, gradual reduction of cell-mediated immune responses is observed towards the lepromatous side of the spectrum (BL and LL), associated with increased bacillary load and high antibody titres [22].

The TT manifestation is characterized by vigorous T-cell responses (cell mediated immune response) (Th1), low antibody titers to *M. leprae* antigens, and the bacilli are organized in granulomas. Characteristic cytokine profile contains prevalence of interferon gamma [IFN-γ], interleukin (IL)-2, IL-15, and tumor necrosis factor alpha [TNF-α] [6, 26]. The primary skin lesions have epithelioid macrophages surrounded by

CD4+ T lymphocytes that activating macrophages to release inflammatory and proinflammatory cytokines that lead to cell-mediated immunity [27].
On the other hand, the immune response of LL patients is characterized by a Th2 immune response and the lesions are characterized by foamy macrophages heavily infected with bacilli, and predominantly CD8+ T cells, with production of IL-4 and IL-10 and activation of T regulatory cells [6, 19, 26, 28].
The different cytokines' patterns of the two poles of the disease form (TT or LL) play an important role in helping to identify the predominance of reactions through polymerase chain reaction (PCR)[19].

1.7 Diagnosis

Currently, the diagnosis of leprosy relies on a combination of the recognition of the clinical manifestations by physical examination, and skin biopsy and/or smear [13, 28]. The analysis of the clinical manifestations requires relatively high levels of expertise and experience to ascertain the differential diagnosis [28]. The proper classification of the disease plays an important role for the success of control programs and treatment standardizing [29].
According to the WHO, leprosy is diagnosed based on the presence of cardinal signs, and is made when an individual who has not completed a course of treatment presents one or more of the following signs: hypopigmented (or erythematous) anesthetic skin lesion; thickened peripheral nerve or positive skin smear or bacilli observed in a biopsy [8, 15]. Despite the consolidation of diagnostic and treatment guidelines, the immune responses observed during leprosy are occasionally used to complement clinical diagnosis [30]. A rapid molecular assay using real-time PCR to identify and quantify *M. leprae* DNA in tissue samples have been used to complement leprosy diagnosis [13]. More recently, the detection of antibodies of *M. leprae* antigens such as phenolic glycolipid-I and leprosy IDRI diagnostic-1 have been used for the classification of PB or MB forms of the disease [29, 30].

1.8 Conventional treatment

The leprosy treatment has gone under considerable evolution in the past century. The leprosy therapy firstly consisted of potassium iodide, arsenic, antimony, copper, sera, vaccines, aniline dyes, thymol, strychnine, baths, X-rays, radium, and electrical current [13]. In the late 19th and early 20th centuries, the chaulmoogra oil, extracted from

seeds of several species of the Hydnocarpus tree, was a hallmark of therapy with varying reports of documented success and indifferent results [13, 31].

In 1940's, the first sulfone drug was introduced to treat leprosy, the promin [32, 33]. Later on, dapsone monotherapy was introduced [1]. In patients on dapsone monotherapy, bacilli extinction was completed in 3 to 6 months, and complete clinical regression generally occurred within 2 to 3 years [12]. Patients had to maintain the treatment without interruption, otherwise resistance could develop [1].

In 1982 the WHO introduced multidrug therapy (MDT) consisting of clofazimine (CLZ), dapsone (DAP) and rifampicin, as first line drugs. For patients with PB leprosy, rifampicin (600 mg) is monthly (supervised) administered and DAP (100 mg) is daily (non-supervised) administered; while MB patients are treated with rifampicin (200 mg) and CLZ (300 mg) monthly (supervised) administered, in addition to DAP (100 mg) and CLZ (50 mg) daily (son-supervised) administered [8]. The introduction of MDT have altered the course of disease in leprosy patients and, nowadays, is the most common way to limit the dissemination of *M. leprae* [32].

The recommended treatment duration for MB leprosy is 12 months and this therapy includes patients presenting LL, BL, and BB leprosy according to the Ridley and Jopling system. For PB patients, the treatment duration is 6 months and includes patients with TT, and BT leprosy forms [15]. Since its introduction, MDT has not been revised except for the duration of therapy. Initially, the duration of treatment with MDT took 24 months or until smear negativity, which was responsible for decrease in patient compliance, resistance, and relapse, compared to dapsone monotherapy [12]. In 1997, it was implemented worldwide a fixed-duration treatment of 6 or 12 months for PB and MB respectively, which reduces significantly the number of relapses cases compared to the first adopted duration (24 months) [12].

Since 1995, the cocktail is provided in convenient monthly calendar blister packs by the WHO, free of charge to all endemic countries [8]. The MDT cocktail should be received by the patient under supervision [32]. The actual therapy for PB and MB in adults and child patients supplied by WHO are expressed in Figure 4.

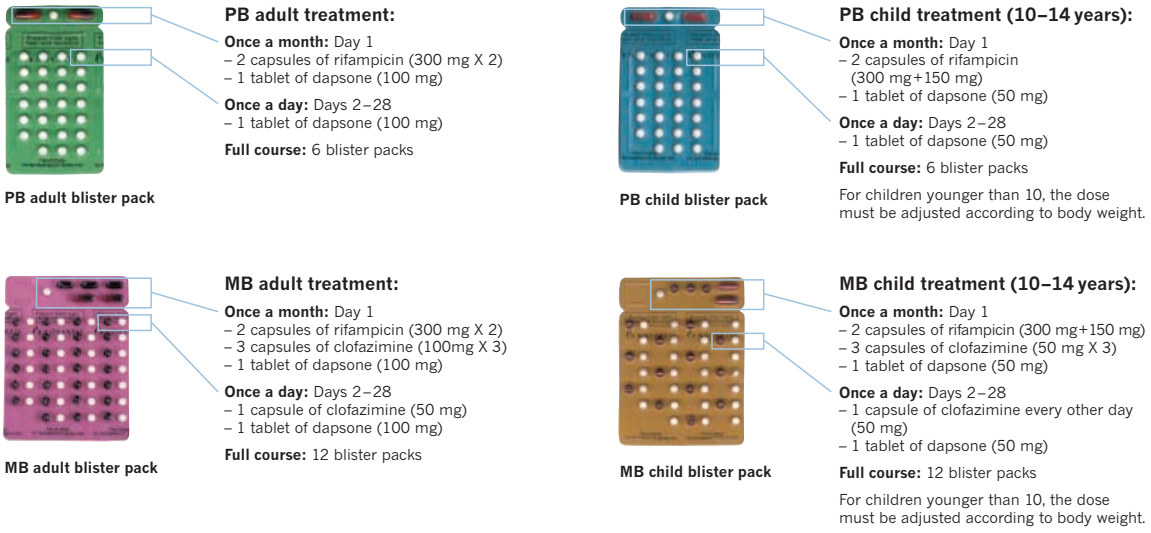

Figure 4. Leprosy treatment for adult and child: one month-pack blister distributed by WHO for paucibacillary (PB) and multibacillary (MB) leprosy [8].

Other alternative drugs as ofloxacin, minocycline, and clarithromycin have displayed significant activity against *M. leprae* and are among the drugs used as second-line treatments in humans [1, 34]. Even though they are not part of the WHO official regimen [34]. Attempts have been done to propose new combinations of these drugs in order to (i) overcome drug resistance, (ii) shorten the duration of the therapy, and (iii) improve the therapeutic efficacy [34].

Ofloxacin (4-fluooquinolone) is a fluorinated carboxy-quinolone that has moderate anti-*M. leprae* activity [7]. Fluoroquinolones mechanism of action against *M. leprae* is based on the inhibition of DNA gyrase and DNA replication and, transcription [13]. It is considered as an important option in leprosy treatment especially in patients with intolerance, resistance, or clinical failure to primary therapy [13]. Minocycline is the only member of the tetracycline group of antibiotics to demonstrate significant activity against *M. leprae*, presumably due to its lipophilic properties, which may enhance cell wall penetration. Its combination with dapsone and rifampicin presented additive activity against *M. leprae* [35]. Clarithromycin is a semisynthetic macrolide which displays significant bactericidal activity against *M. leprae* in humans [7, 35]. Despite the bactericidal effect of the this three-drug combination and the good therapeutic results observed in leprosy patients, the severe gastrointestinal side-effects related to the use of clarithromycin were sufficient to preclude the routine use of this drug in the field [7, 35].

1.8.1 Uniform multidrug therapy (MDT)

Despite the efficiency of the adopted classification system for treatment purposes, it is common to overestimate PB cases or underestimate MB diagnosis, which may jeopardize the adopted treatment [36, 37]. Moreover, another operational problem is patient compliance with long-term treatments for MB cases [36]. In this context, some efforts have been done to uniform MDT [38]. Recently, WHO have published this trend in leprosy treatment as a strategy to eradicate leprosy until 2020 [39, 40]. Some studies suggest the efficacy in shortening the duration of treatment of MB cases to 6 months. On the other hand, the addition of clofazimine in PB regimen seemed to improve the clinical outcome and produced disappearance of lesions and regression of granuloma [9]. As continued inflammatory response results in persistent activity in leprosy, clofazimine would contribute to PB patients therapy [38]. These trends open the door for introducing an uniform treatment regimen for both PB and MB cases with three drugs; hence, a single regimen for both forms of the disease, also known as Uniform-MDT (U-MDT) [40], which could simplify leprosy control, allowing its incorporation into primary health care units [36]. In this regard, new guidelines will be issued by WHO once the amount of supportive evidence is attained [40].

1.8.2 The daily multibacillary MDT agents

The proportion of MB cases globally is 60.6%, and among the countries that reported new cases in 2014, almost the totality presented higher incidence of MB leprosy cases [3]. In parallel, the treatment completion rate is one of the most important outcome indicators of case holding activity and reflects efficiency in patient management [3]. Thus, the standardization of the MDT regarding time of treatment and therapeutic agents aiming to enhance the global strategy for further reducing disease burden seems to be a tendency in leprosy eradication program.

In this context, CLZ and DAP which are the daily drugs used in MDT for MB cases become the most important components of leprosy therapy as their correct administration and compliance is essential for the efficacy of the treatment.

1.8.2.1 Dapsone

Dapsone (4,4'-diamino-diphenylsulfone) (Figure 5A) is a parent compound of sulfone drugs, which have long been the cornerstone of leprosy treatment [13, 41]. It was synthesized in 1908, even though its antibacterial characteristics were firstly not

noticed [41]. In 1945, it was adopted in the leprosy treatment as monotherapy, but resistance, estimated at 2–10%, has become a problem [13].

Chemically, DAP is an aromatic amine, aniline derivative [42, 43]. As a sulfone, it shows the structure of a sulphur atom linking two carbon atoms (Figure 5A). This group is essential for their pharmacological activity and toxicity [42]. It is considered as a very weak Lewis base with no readily dissociable hydrogen ion (H^+) [42]. DAP presents low solubility in water (0.16 mg mL^{-1}) being classified as a class II (poor solubility and high permeability) drug according the Biopharmaceutics Classification System [44].

Concerning the mechanisms of action, DAP combines both antimicrobial properties and anti-inflammatory effects resembling those of non-steroidal anti-inflammatory drugs [43]. As it is an analogue of *p*-aminobenzoic acid (PABA) its bacteriostatic activity is due to the competitive inhibition of the enzyme dihydrofolate synthetase, which is involved in the folate biosynthesis pathway in *M. leprae* [13, 44-46].

After oral administration, DAP is almost completely absorbed from the gastrointestinal tract (GIT) with a bioavailability of about 80%. The peak serum concentrations are generally attained within 2 to 8 h, and its half-life time is between 24 to 30 h [41, 47]. DAP is distributed through all organs and is able to cross the blood–brain and placenta barriers, being detectable in breast milk [47]. This antibacterial agent undergoes enterohepatic circulation after absorption, being metabolized both by the liver and activated polymorphonuclear leukocytes or mononuclear cells. The primary metabolites are products of acetylation by N-acetyltransferase and hydroxylation by cytochrome P-450 enzymes, originating monoacetyl-dapsone (Figure 5B) and dapsone hydroxylamine (Figure 5C), respectively [41, 47]. Approximately 20% of DAP is eliminated in urine as unchanged drug and 70% to 85% as water-soluble metabolites. Additionally, a small amount may be excreted in feces [47].

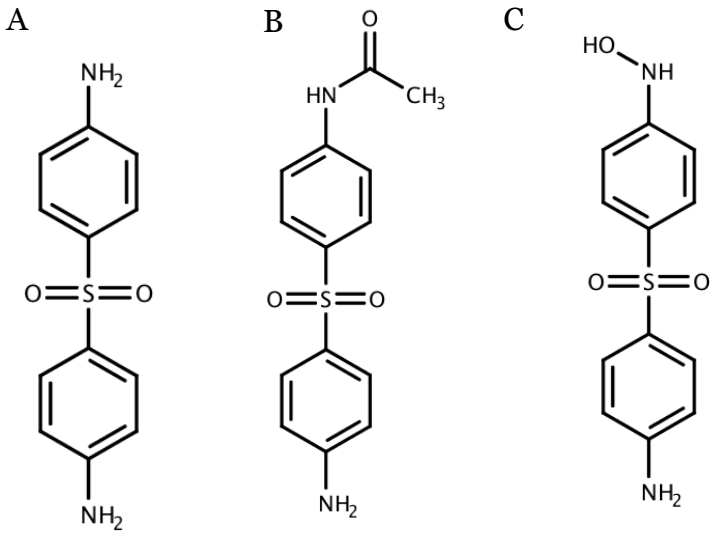

Figure 5. Chemical structures of (A) dapsone and its primary metabolites: (B) N-acetyltransferase (monoacetyl-dapsone) and (C) dapsone hydroxylamine (cytochrome P-450 enzymes).

Adverse reactions related to the use of DAP ranged from digestive problems such as nausea, vomiting to stomatitis. More severe occurrences as toxic hepatitis, cholestatic jaundice, cutaneous photosensitivity reactions and psychosis are unusual [48]. The metabolites of DAP, mainly hydroxylamine metabolite and other hydroxylated metabolites, are associated with a set of adverse effects called “sulfone syndrome” that includes fever, malaise, jaundice, exfoliative dermatitis or morbilliform rash, hepatic dysfunction, lymphadenopathy, methemoglobinemia, hemolysis, agranulocytosis, and hemolytic anemia [33, 41, 48].

The number of dapsone-resistant cases increased with the dapsone monotherapy, during the 1960s and 1970s [45], which forced the introduction of additional antimicrobial agents as clofazimine and rifampicin in the leprosy therapy [34]. One proposed mechanism of resistance is a mutation in the *M. leprae* gene that encodes dihydropteroate synthase (DHPS), called f*ol*p [13]. DHPS is a key enzyme during the folate systhesis, which participate in the condensation of PABA and 7,8-dihydro-6-hydroxymethylpterin-pyrophosphate to form 7,8-dihydropteroate [46].

1.8.2.2 Clofazimine

Clofazimine (Figure 6) is a rhimnophenazine which was first synthesized in 1954 as an anti-tuberculosis drug [49]. It has been used for the treatment of leprosy since 1969 [50]. This drug has both antimicrobial and anti-inflammatory activity, which is

associated to its efficacy in leprosy treatment as this feature may be potentially useful in controlling harmful ENL and RR in leprosy treatment [51].

The phenazine nucleus with an alkylimino and phenyl substituents are key features of the riminophenazines and essential for antimicrobial activity, varying according to the number and type of halogen atoms on the phenyl substituents [51]. The mechanism of action is undefined, but different studies have been suggesting that its antimicrobial activity is related to disruption of membrane structure and function [51], or it may act by increasing the activity of bacterial phospholipase A2 resulting in the release of lysophospholipids, enzymatic hydrolysis products toxic to *M. leprae* [52]. CFZ was also found to cluster with known respiratory modulators on transcriptional analysis, indicating that it may inhibit bacterial cell growth by interfering with electron transport [50].

CLZ is deep red to orange under normal conditions. It is a basic drug, presenting three amine groups, which may be protonated and charged at acidic pH and physiological conditions. Its color may change according to the pH shift, i.e., in more alkaline environment, CLZ remains uncharged and has an intense orange-yellow color; as the pH drops, the color became more red, tending to violet (very acidic environment) and it becomes more soluble [53, 54]. The changes in CLZ solubility according to pH shifts leads to drug precipitation *in vivo*, mainly along the GIT where different pH conditions are found [53, 55].

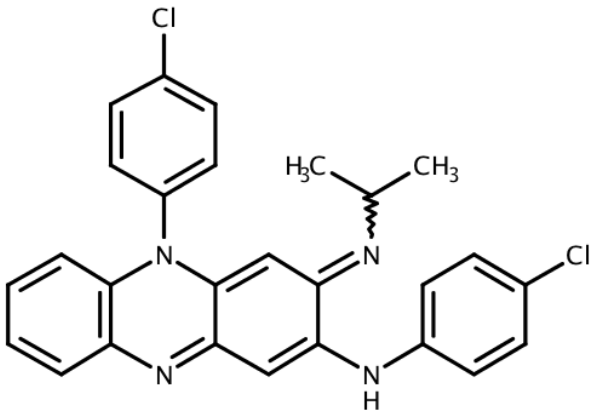

Figure 6. Chemical structure of clofazimine.

CLZ has very low solubility in water, being considered virtually insoluble, and highly lipophilic (logP > 7) which lead to its bioaccumulation as intracellular biocrystals [56]. In humans, the absorption of orally administered drug varies considerably (45%–62%) depending on whether the drug is taken with or without food. After oral

administration, the peak plasma concentration is after 8-12 h, depending on fed state [51]. Once absorbed, it concentrates in lipid-rich tissues, primarily at the reticuloendothelial system, but high concentrations are also found in the breasts, liver and intestines [57]. Its high lipophilicity ensures that the drug is slowly eliminated, mainly by renal and hepatic routes, with an elimination half-life of 70 days [55, 57, 58]. CLZ crosses the placenta and the blood–brain barrier in very small amounts [51].

The adverse effects of CLZ are generally dose-related, primarily affecting the skin, eyes and the GIT. Reddish-brown discoloration of the skin and conjunctiva are gradually reversible on cessation of therapy, even though patients often feel marked and stigmatized by this and withdraw CLZ from their treatments as a consequence [32, 51]. GIT adverse effects may be mild to moderate (abdominal/epigastric pain, nausea, diarrhea, vomiting, gastrointestinal intolerance), or, less frequently, severe (splenic infarction, bowel obstruction, bleeding) [51].

Recent works have been reporting that CLZ can form complexes with intracellular membranes, and precipitate as crystal aggregates, being phagocytized by the mononuclear phagocytic system [55, 56]. This phenomenon may be correlated with the undesired and toxicological effects, often resulting in patients' treatment noncompliance [59].

1.9 Issues and challenges

Despite significant improvements in leprosy treatment since the introduction of MDT, the global incidence remains high, and patients often have long-term complications associated with the disease [1]. Moreover, the availability of MDT in providing a microbiological cure is not enough to prevent nerve damage and sequelae associated with leprosy reactions [11], and the statistics commonly do not capture the disability and dysfunction that remain after treatment [1].

The treatment completion rates reported are sub-optimal in most of the leprosy programs. This highlights the risk of antimicrobial resistance in leprosy, which cannot be ignored [3]. The idea of shortening the duration of MB treatment through the U-MDT regimen associated with the non-supervision of daily-drugs administration (DAP and CLZ) may aggravate the resistance issue [9]. Thus, research in the therapy of leprosy is still needed, and some efforts must be done to improve delivery of drugs, compliance of patients, implement the prescribed drug regimens by medical staff associated with effective methods for monitoring drug resistance [5, 10, 11].

While there appears to be a need for alternative bactericidal agents and more combinations that can be used in leprosy therapy, these are currently limited [12] and

unfortunately, there is little novel drugs being explored for future treatment of leprosy [13].

2. Towards the improvement of leprosy MDT: the role of new drug delivery strategies

The therapeutic potential of leprosy drugs is greatly limited by their physicochemical features, specially their insolubility in water [14]. This fact is especially relevant for daily dosages, i.e., for DAP and CLZ as they play an important role in the success of MDT. Poorly water-soluble drugs often exhibit slow dissolution in the GIT, ultimately limiting their absorption [60, 61], resulting in low bioavailability after oral administration. The poor bioavailability commonly result into adjustment in the administered dosage aiming to reach the therapeutic range, which may aggravate toxicity [62]. Several approaches have been used to overcome drawbacks associated with poorly water-soluble drugs including micronization, salt formation, use of pro-drug, use of surfactant and lipids, co- solvents, nanocarriers, cyclodextrins, amorphous solid dispersions, and others [62]. Albeit, amorphous solid dispersions and nanocarriers present interesting advantages compared to other techniques, and seem to be promising strategies as drug delivery systems. The next sections will address in detail some of the most common techniques used for this purpose.

3. References

1. White, C. and C. Franco-Paredes, *Leprosy in the 21st century*. Clinical microbiology reviews, 2015. **28**(1): p. 80-94.
2. Virmond, M., A. Grzybowski, and L. Virmond, *Leprosy: A glossary*. Clinics in Dermatology, 2015. **33**(1): p. 8-18.
3. World Health Organization. *Weekly Epidemiological Record, 23 September 2016, vol. 91, 39 (pp. 441–460)*. 2016.
4. Nath, I., C. Saini, and V.L. Valluri, *Immunology of leprosy and diagnostic challenges*. Clinics in Dermatology, 2015. **33**(1): p. 90-98.
5. Prasad, P.V.S. and P.K. Kaviarasan, *Leprosy therapy, past and present: can we hope to eliminate it?* . Indian Journal of Dermatology, 2010. **55**(4): p. 316-324.
6. Bhat, R.M. and C. Prakash, *Leprosy: An Overview of Pathophysiology*. Interdisciplinary Perspectives on Infectious Diseases, 2012. **2012**: p. 181089.
7. Gillis, T.P., *Chapter 93 - Mycobacterium leprae A2 - Tang, Yi-Wei*, in *Molecular Medical Microbiology (Second Edition)*, M. Sussman, et al., Editors. 2015, Academic Press: Boston. p. 1655-1668.

8. World Health Organization. *Global Leprosy Programme*. 2017 March 7]; Available from: http://www.searo.who.int/entity/global_leprosy_programme/disease/en/.

9. Prasad, P.V.S. and P.K. Kaviarasan, *Leprosy therapy: past and present: can we hope to eliminate it?* Indian Journal of Dermatology, 2010. **55**(4): p. 316-324.

10. Grosset, J.H., *Newer drugs in leprosy*. International Journal of Leprosy and Other Mycobacterial Diseases, 2001. **69**(2): p. S14.

11. Rodrigues, L.C. and D.N.J. Lockwood, *Leprosy now: epidemiology, progress, challenges, and research gaps*. The Lancet Infectious Diseases. **11**(6): p. 464-470.

12. Kar, H.K. and R. Gupta, *Treatment of leprosy*. Clinics in Dermatology, 2015. **33**(1): p. 55-65.

13. Legendre, D.P., C.A. Muzny, and E. Swiatlo, *Hansen's Disease (Leprosy): Current and Future Pharmacotherapy and Treatment of Disease-Related Immunologic Reactions*. Pharmacotherapy: The Journal of Human Pharmacology and Drug Therapy, 2012. **32**(1): p. 27-37.

14. Islan, G.A., et al., *Nanopharmaceuticals as a solution to neglected diseases: Is it possible?* Acta Tropica, 2017. **170**: p. 16-42.

15. Eichelmann, K., et al., *Leprosy. An Update: Definition, Pathogenesis, Classification, Diagnosis, and Treatment*. Actas Dermo-Sifiliográficas (English Edition), 2013. **104**(7): p. 554-563.

16. World Health Organization. *Global Health Observatory (GHO) data*. 2016 [cited 2017 6 March]; Available from: http://www.who.int/gho/neglected_diseases/leprosy/en/.

17. Nobre, M.L., et al., *Multibacillary leprosy by population groups in Brazil: Lessons from an observational study*. PLoS Negl Trop Dis, 2017. **11**(2): p. e0005364.

18. Reibel, F., E. Cambau, and A. Aubry, *Update on the epidemiology, diagnosis, and treatment of leprosy*. Médecine et Maladies Infectieuses, 2015. **45**(9): p. 383-393.

19. Albuquerque, R.G., et al., *Sleep, Hansen's disease and the immune system--a not so harmonic triad*. Med Hypotheses, 2015. **84**(5): p. 456-9.

20. Rambukkana, A., *How does Mycobacterium leprae target the peripheral nervous system?* Trends in Microbiology, 2000. **8**(1): p. 23-28.

21. Grzybowski, A., et al., *Lepra: Various etiologies from miasma to bacteriology and genetics*. Clinics in dermatology, 2015. **33**(1): p. 3-7.

22. Reis, E.M., et al., *Mycobacterium leprae DNA in peripheral blood may indicate a bacilli migration route and high-risk for leprosy onset*. Clinical Microbiology and Infection, 2014. **20**(5): p. 447-452.

23. Gaschignard, J., et al., *Pauci- and Multibacillary Leprosy: Two Distinct, Genetically Neglected Diseases*. PLOS Neglected Tropical Diseases, 2016. **10**(5): p. e0004345.

24. World Health Organization, *International Classification of Functioning, Disability and Health: ICF*. 2001: World Health Organization.

25. de Souza, V., et al., *Is the WHO disability grading system for leprosy related to the level of functional activity and social participation?* Lepr Rev, 2016. **87**: p. 191-200.

26. Fonseca, A.B.d.L., et al., *The influence of innate and adaptative immune responses on the differential clinical outcomes of leprosy*. Infectious Diseases of Poverty, 2017. **6**(1): p. 5.

27. Mazini, P.S., et al., *Gene Association with Leprosy: A Review of Published Data*. Front Immunol, 2015. **6**: p. 658.

28. Freitas, A.A., et al., *Alterations to antigen-specific immune responses before and after multidrug therapy of leprosy*. Diagnostic Microbiology and Infectious Disease, 2015. **83**(2): p. 154-161.

29. Moura, R.S., et al., *Evaluation of a rapid serological test for leprosy classification using human serum albumin as the antigen carrier*. Journal of Immunological Methods, 2014. **412**: p. 35-41.

30. Hungria, E.M., et al., *Antigen-specific secretion of IFNγ and CXCL10 in whole blood assay detects Mycobacterium leprae infection but does not discriminate asymptomatic infection from symptomatic leprosy*. Diagnostic Microbiology and Infectious Disease, 2017. **87**(4): p. 328-334.

31. Sansarricq, H., *Multidrug therapy against leprosy : development and implementation over the past 25 years*. 2004, Geneva: World Health Organization. 28.

32. Duthie, M.S. and M.F. Balagon, *Combination chemoprophylaxis and immunoprophylaxis in reducing the incidence of leprosy*. Risk Management and Healthcare Policy, 2016. **9**: p. 43-53.

33. Zhu, Y.I. and M.J. Stiller, *Dapsone and sulfones in dermatology: Overview and update*. Journal of the American Academy of Dermatology, 2001. **45**(3): p. 420-434.

34. Anusuya, S. and J. Natarajan, *The eradication of leprosy: molecular modeling techniques for novel drug discovery*. Expert Opin Drug Discov, 2013. **8**(10): p. 1239-51.

35. World Health Organization, *WHO Expert Committee on Leprosy: Seventh Report*. 1998: World Health Organization.

36. Penna, M.L., et al., *Primary results of clinical trial for uniform multidrug therapy for leprosy patients in Brazil (U-MDT/CT-BR): reactions frequency in multibacillary patients*. Lepr Rev, 2012. **83**(3): p. 308-19.

37. Parkash, O., *Classification of leprosy into multibacillary and paucibacillary groups: an analysis*. FEMS Immunology & Medical Microbiology, 2009. **55**(1): p. 1-5.

38. Prasad, P., et al., *MDT-MB therapy in paucibacillary leprosy: A clinicopathological assessment*. Indian Journal of Dermatology, Venereology, and Leprology, 2005. **71**(4): p. 242.

39. Rao, P.N., S. Dogra, and S. Suneetha, *Global leprosy program: Does it need uniform-multi-drug therapy now?* Indian dermatology online journal, 2015. **6**(6): p. 425.

40. World Health Organization, *Global Leprosy Strategy 2016–2020: Accelerating towards a leprosy-free world*. Operational Manual. 2016: WHO Library Cataloguing-in-Publication data.

41. Sener, O., et al., *Severe dapsone hypersensitivity syndrome*. J Investig Allergol Clin Immunol, 2006. **16**(4): p. 268-70.

42. Oliveira, F.R., et al., *Clinical applications and methemoglobinemia induced by dapsone*. Journal of the Brazilian Chemical Society, 2014. **25**(10): p. 1770-1779.

43. Wozel, G. and C. Blasum, *Dapsone in dermatology and beyond*. Archives of Dermatological Research, 2014. **306**(2): p. 103-124.

44. Chaves, L.L., et al., *Rational and precise development of amorphous polymeric systems with dapsone by response surface methodology*. Int J Biol Macromol, 2015. **81**: p. 662-71.

45. Matsuoka, M., *Drug resistance in leprosy*. Jpn J Infect Dis, 2010. **63**(1): p. 1-7.

46. Williams, D.L., et al., *Dihydropteroate synthase of Mycobacterium leprae and dapsone resistance*. Antimicrobial agents and chemotherapy, 2000. **44**(6): p. 1530-1537.

47. Wozel, V.E.G., *Innovative Use of Dapsone*. Dermatologic Clinics, 2010. **28**(3): p. 599-610.

48. Coleman, M.D., *Dapsone-mediated agranulocytosis: risks, possible mechanisms and prevention*. Toxicology, 2001. **162**(1): p. 53-60.

49. Gopal, M., et al., *Systematic review of clofazimine for the treatment of drug-resistant tuberculosis [Review article]*. The International Journal of Tuberculosis and Lung Disease, 2013. **17**(8): p. 1001-1007.

50. Mafukidze, A., E. Harausz, and J. Furin, *An update on repurposed medications for the treatment of drug-resistant tuberculosis*. Expert Review of Clinical Pharmacology, 2016. **9**(10): p. 1331-1340.

51. Cholo, M.C., et al., *Clofazimine: current status and future prospects*. Journal of antimicrobial chemotherapy, 2011: p. dkr444.

52. Szeto, W., et al. *Clofazimine Enteropathy: A Rare and Underrecognized Complication of Mycobacterial Therapy*. in *Open Forum Infectious Diseases*. 2016. Oxford University Press.

53. Nunes, R., C. Silva, and L. Chaves, *Tissue-based in vitro and ex vivo models for intestinal permeability studies*, in *Concepts and Models for Drug Permeability Studies: Cell and Tissue based In Vitro Culture Models*. 2015. p. 203.

54. Reddy, V.M., J.F. O'Sullivan, and P.R. Gangadharam, *Antimycobacterial activities of riminophenazines*. Journal of Antimicrobial Chemotherapy, 1999. **43**(5): p. 615-623.

55. Baik, J. and G.R. Rosania, *Macrophages sequester clofazimine in an intracellular liquid crystal-like supramolecular organization*. PLoS One, 2012. **7**(10): p. e47494.

56. Yoon, G.S., et al., *Clofazimine Biocrystal Accumulation in Macrophages Upregulates Interleukin 1 Receptor Antagonist Production To Induce a Systemic Anti-Inflammatory State*. Antimicrobial agents and chemotherapy, 2016. **60**(6): p. 3470-3479.

57. Arbiser, J.L. and S.L. Moschella, *Clofazimine: a review of its medical uses and mechanisms of action*. Journal of the American Academy of Dermatology, 1995. **32**(2): p. 241-247.

58. Baik, J., et al., *Multiscale distribution and bioaccumulation analysis of clofazimine reveals a massive immune system-mediated xenobiotic sequestration response*. Antimicrobial agents and chemotherapy, 2013. **57**(3): p. 1218-1230.

59. Yoon, G.S., et al., *Phagocytosed Clofazimine Biocrystals Can Modulate Innate Immune Signaling by Inhibiting TNFalpha and Boosting IL-1RA Secretion*. Mol Pharm, 2015. **12**(7): p. 2517-27.

60. Khan, J., T. Rades, and B. Boyd, *The Precipitation Behavior of Poorly Water-Soluble Drugs with an Emphasis on the Digestion of Lipid Based Formulations*. Pharm Res, 2016. **33**(3): p. 548-62.

61. Nunes, R., C. Silva, and L. Chaves, *4.2 - Tissue-based in vitro and ex vivo models for intestinal permeability studies A2 - Sarmento, Bruno*, in *Concepts and Models for Drug Permeability Studies*. 2016, Woodhead Publishing. p. 203-236.

62. Chaves, L., et al., *Quality by design: discussing and assessing the solid dispersions risk*. Curr Drug Deliv, 2014. **11**(2): p. 253-69.

B. Solid Dispersions[1]

Send Orders for Reprints to reprints@benthamscience.net

Current Drug Delivery, 2014, *11*, 253-269 253

Quality by Design: Discussing and Assessing the Solid Dispersions Risk

Luíse L. Chaves[1*], Alexandre C.C. Vieira[1], Salette Reis[1], Bruno Sarmento[2,3] and Domingos C. Ferreira[4]

[1]*REQUIMTE, Laboratory of Applied Chemistry, Department of Chemical Sciences, Faculty of Pharmacy – University of Porto, Universidade do Portugal, Rua Jorge Viterbo Ferreira, 228, Edificio 3, piso 2, Laboratório de Química Aplicada, Postal Code: 4050-313 Porto;* [2]*IINFACTS - Instituto de Investigação e Formação Avançada em Ciências e Tecnologias da Saúde, Instituto Superior de Ciências da Saúde-Norte, Department of Pharmaceutical Sciences, CESPU, Gandra-PRD, Portugal;* [3]*INEB-Instituto de Engenharia Biomédica, New Therapies Group, Rua do Campo Alegre 823, 4150-180 Porto, Portugal;* [4]*Department of Pharmaceutical Technology, Faculty of Pharmacy – University of Porto, Universidade do Porto, Rua Jorge Viterbo Ferreira, 228 Edificio 3, piso 0, 4050-313, Porto, Portugal*

Abstract: The poor water solubility tops the list of undesirable physicochemical properties in the drug discovery and Solid Dispersions (SDs) has been frequently used to enhance dissolution of such compounds. Although, some challenges limit the studies of SD commercial application. During recent years, the Quality by Design (QbD) approach has begun to change drug development, and focus on pharmaceutical production, which shifted from an univariate empirical understanding for a systematic multivariate process. In this review, some possible variables during the development process, formulation and production of SDs were defined, introducing and applying the QbD concept. The proposed work presented important definitions as well as its application in the pharmaceutical product and process design, especially the challenges encountered during the development of formulations of poorly soluble drugs. In this aspect, the SD technique was deeply discussed, in which some important parameters during SD design and production were mentioned as method of production, polymers commonly used, methods for characterization and stability evaluation, in addition of biopharmaceutical considerations. Finally, a specific risk assessment for the design and production of SD and critical points were discussed, which was a positive evolution and may lead to better understanding of SD for a rational formulation.

Keywords: Low solubility, Process design, Product design, Quality by design, Risk assessment, Solid dispersions.

1. Introduction

In the pharmaceutical industry, a great effort has been made in the field of drug discovery, with the aim of improving existing therapies. During the compound screening, the five key physicochemical properties includes pKa, solubility, permeability, stability and lipophilicity [1]. Although, the poor solubility tops the list of undesirable compound properties [2]. Approximately 40% of potential new drugs identified by pharmaceutical companies are poorly soluble in water [3-5].

The aqueous solubility of a drug is a critical parameter of its dissolution rate during the biopharmaceutical phase of pharmaceutical products. The limited dissolution rate arising from low solubility frequently results in low bioavailability of orally administered drugs [6]. In such cases, an increase of the dose would be required until the blood drug concentration reaches the therapeutic range, which sometimes causes topical toxicity in the gastrointestinal tract upon oral administration [6].

[1] Published in: Chaves, L., *et al.* "Quality by design: discussing and assessing the solid dispersions risk." Current Drug Delivery 11.2 (**2014**): 253-269.

Improvement of oral bioavailability of poorly water-soluble drugs remains one of the most challenging aspects of drug development. Many technologies are available and have commonly been used to overcome drawbacks associated with poorly water-soluble drugs includes micronization, salt formation, use of pro-drug, use of surfactant and lipids, co-solvents, nanoparticles, cyclodextrins, amorphous solid dispersions, and others [7, 8].

Despite the variety of techniques that commonly have been used to increase dissolution rate of the drug, there are few practical limitations and the desired bioavailability enhancement may not always be achieved [7, 9].

One such formulation approach that has been shown to significantly enhance dissolution of such drugs is to formulate Solid Dispersions (SD). SD involves the dispersion of one or more active ingredients in an inert carrier or matrix at solid state [10]. These systems can increase dissolution rate and bioavailability of water insoluble drugs since, when they are exposed to aqueous media, the carrier dissolves, and the drug is released as very fine colloidal particles [7, 9]

In drug product development, the formulation design of a drug product with high drug load is most of the times difficult to achieve. Increasing drug load might result in poor powder properties, such as poor powder flowability and sticking tendency during granulation and tableting. In addition, the manufacturing cost would increase since a large amount of drug substance might be consumed to develop and manufacture the drug product [3, 6, 11, 12]. In this way, some problems limit the studies of solid dispersion commercial application including preparation method, the reproducibility of the physical and chemical properties, dosage formulation, manufacturing process and large-scale chemical stability of the drug and vehicle [12-14].

Most studies elucidated separately either the influence of formulation factors or process factors on solid dispersion stability [15-18]. During recent years, the Quality by Design (QbD) approach has begun to change drug development, and focus on the science of production, which shifted from an univariate empirical understanding for a systematic multivariate process in order to construction a systematically quality in the final pharmaceutical product [16].

QbD is a broad term that encompasses predefined target quality, with certain predictable quality through desired and predetermined specifications. Physicochemical, physiological, pharmacological and clinical considerations are relevant to obtain desired products that are safe and effective [19]. To attain this purpose, it is expected that variables associated with raw materials characteristics, product design, process and scale-up issues should be thoroughly investigated. Therefore, a very useful component of the QbD is the understanding of factors and

their interaction effects by a desired set of experiments. To understand the variables and their interactions, many statistical experimental designs have been recognized as useful techniques [20].

Although the QbD concept seems promising, currently, limited knowledge exists in the field of SD on the importance of process factors, as compared to formulation factors, for the physical stability of the drug [16].

The objectives of this review is to define some possible variables during the development process, formulation and production of SD as an alternative to increasing the solubility of poorly soluble drugs, introducing and applying the QbD concept.

1.1 Pharmaceutical *Quality by Design*

Pharmaceutical QbD is *"a systematic approach to pharmaceutical development that begins with predefined objectives and emphasizes product and process understanding based on sound science and quality risk management"* as defined by the International Conference on Harmonization (ICH) Q8 guideline [21-23].

In other words, it could be defined as the development of scientific understanding of critical process and product attributes, designing controls and testing based on the limits of scientific understanding at development stage, and utilizing this knowledge over the product's lifecycle to operate in continuous improvement [22].

The use of QbD principles increases process knowledge and product understanding, once during product development provides opportunities to facilitate innovation and continual improvement throughout the product lifecycle, compared to traditional approaches [22]. Besides promotes a higher level of assurance of product quality; increase efficiency of manufacturing process and reduce manufacturing cost and product rejects; minimize/eliminate potential compliance actions, costly penalties and re-calls; enhance opportunities for first cycle approval; maintains opportunities for continual improvement [24].

Some elements of the QbD framework have been used for many years. Besides the spotlight on these techniques has intensified in the pharmaceutical industry, in particular with the United States Food an Administration's (FDA) publication of their report "Pharmaceutical CGMPs for the 21st Century: A Risk-Based Approach to Product Quality Regulation Incorporating an Integrated Quality Systems Approach" [25].

The need for improving on-line monitoring and control methods to maintain high product quality during manufacturing operations [26] led to, shortly afterwards, the FDA guidance publication "PAT — A Framework for Innovative Pharmaceutical Development, Manufacturing and Quality Assurance" [27] in which was defined the

Process Analytical Technology (PAT) concept as a system for designing, analyzing, and controlling manufacturing through timely measurements (i.e., during processing) of critical quality and performance attributes of raw and in-process materials and processes, with the goal of ensuring final product quality [28]. In this way, the PAT concept was introduced by FDA as an initiative to bring an improved understanding of pharmaceutical manufacturing processes to increase the quality of their products [26, 29].

The move towards science-based development and manufacturing was embraced at an international level by ICH [30]. Four guidelines that support this vision, namely ICH Q8 on Pharmaceutical Development [23], ICH Q9 on Quality Risk-Management [31], ICH Q10 on Quality Systems [32] and the latest one, the Q11 on Development and manufacture of drug substances [33] were developed. ICH Q8 (R2), currently at Step 4, describes the principles of QbD and provides further explanations of key concepts [23].

QbD identifies characteristics that are critical to quality, translates them into the attributes that the drug product should possess, and establishes how the critical process parameters can be varied in order to achieve the desired characteristics. It means designing and developing formulations and manufacturing processes to ensure predefined product quality objectives [21, 34]. For these purpose, the relationships between formulation (drug and excipient attributes) and sources of variability of the manufacturing process should be established and identified. This knowledge is then used to implement a flexible and robust manufacturing process and products with the desired quality over time. [17, 21, 34].

1.1.1 Product Design

In the QbD context, for the product presents a consistent quality the sources of variability must be very well understood, which could come from the raw materials, the environment and/or the process itself. Afterwards, variability must be managed in such a way that ensures the final product quality [35-37].

A complete study QbD involves some important steps. At first, the Target Product Quality Profile (TPQP) must be set, defining the quality profile that the product should present, always based on prior scientific knowledge and its relevance *in vivo*. Subsequently, it is necessary to perform the product and process design, in order to ensure the quality profile predetermined. In this stage is important to identify, among the process parameters, which are the critical quality attributes (CQAs) as well as the sources of variability exist for risk assessment process. Once the CQAs are known, Design of Experiment (DoE) should be applied to perform a screening of the levels that

should be adopted during the experiments and defining the Design Space (DS) that means determining the real values which can be worked with in order to obtain the desired quality profile. Finally, control the manufacturing process to ensure product quality over time through an operation within the design space established [20, 38]. The figure 1 can summarize the QbD steps.

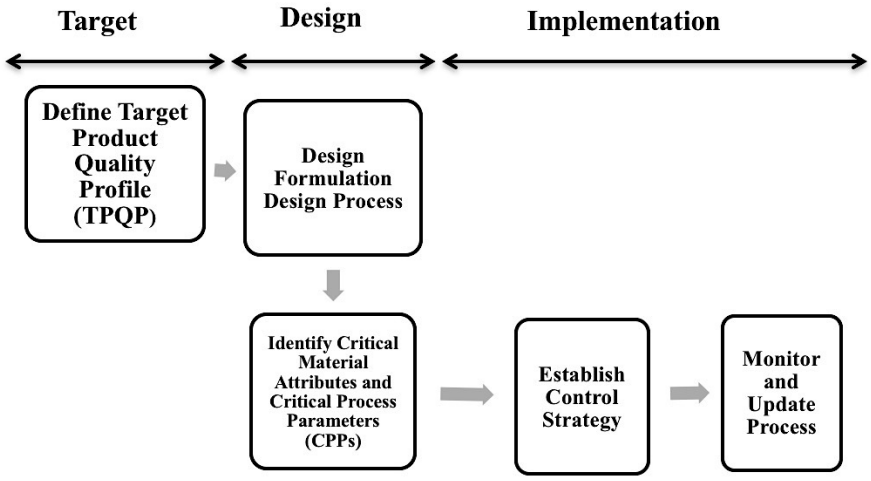

Figure 1. Overview of QbD [20].

The TPQP is the quality characteristics that the drug product should possess to reproducibly deliver the therapeutic benefit promised in the label [39]. Some physical, chemical, and biological properties must be evaluated in order to design and develop a robust product [23]. Physical properties may include physical description (particle size, shape, and distribution), polymorphism, aqueous solubility as function of pH, hygroscopicity, and melting points while chemical properties include pKa, chemical stability in solid state and in solution as well as photolytic, hydrolytic and oxidative stability [40]. Biological properties, on the other hand, include partition coefficient, membrane permeability, and/or oral bioavailability [1, 21].

CQAs could be defined as physical, chemical, biological or microbiological properties or characteristics that need to be controlled (directly or indirectly) to ensure product quality [20, 23]. The relationship between the process inputs (material attributes and process parameters) and the CQAs can be described in the Design Space. DS is defined as the space in which the quality of the product can be built. The wider the design space, the more robust and flexible the process is to accommodate variations. Risk assessment, multivariate experimental design, literature and prior

experience/knowledge contribute in defining the design space [37, 41, 42]. The ICH Q8 defines design space as *"the multidimensional combination and interaction of input variables (material attributes) and process parameters that have been demonstrated to provide assurance of quality. Working within the design space is not considered as a change; however, the movement out of the design space is considered a change and would normally initiate a regulatory post approval change process. Design space is proposed by the applicant and is subject to the regulatory assessment and approval"* [23].

To establish the design space, a design-of-experiments (DoE) approach was used effectively to determine the multi-dimensional relationships among causal factors and response variables [43]. In the DoE approach, process variables are first 'screened' to determine which are important to the outcome. This is followed up by 'optimization' where the best settings for the important variables are determined. In particular, factorial designs and response surface methodologies have been successfully applied in both discovery and development [37, 41, 42]. Thus, it is generally aimed to determine the levels of input variables from which a robust product with high quality may be produced. As each unit operation has many input and output variables as well as process parameters, it is impossible to experimentally investigate all of them. DoE results can help identify optimal conditions, the critical factors that most influence CQAs and those that do not, as well as details such as the existence of interactions and synergies between factors [21, 44].

1.1.2 Process Design

As mentioned before, not only the product must be designed, but also the control of the manufacturing process should be relevant. It is important to note that the goal of designing the process is not to eradicate variability but develop a process that can accommodate the range of acceptable variability for maintaining product quality [45].

The process design is the initial stage of process development where an outline of the manufacturing processes is identified and all the sources of variability as facility, equipment, material transfer, and manufacturing variables, should be taken into account [40]. Depending upon the product being developed, some knowledge about the type of process may be necessary, in order to conduct preliminary feasibility studies. For this purpose, the selection of the suitable process depends upon the formulation and the properties of the materials to be used [21, 24]. In this context, raw materials, process parameters and quality attributes must be investigated.

Physical, chemical or microbiological properties or characteristic of an input or output material is defined as an attribute, as well as the quality and quantity of drug substance, namely identity, purity, biological activity and stability [33]. On the other hand, process parameters include the type of equipment and equipment settings, batch size, operating conditions (e.g., time, temperature, pressure, pH, and speed), and environmental conditions such as moisture [21].

A pharmaceutical manufacturing process is usually composed of a series of unit operations, which is a discrete activity that involves physical changes, such as mixing, milling, granulation, drying, compaction, and coating. Therefore, the possibility of alterations in drug form during process development, i.e., change in the polymorphic form, must be considered [46]. According to ICH Q11 [33], all the potential drug alterations related to the process, from the beginning to the end, have to be controlled.

A useful approach to process design and optimization is to identify all the Critical Process Parameters (CPP) that could potentially affect the quality or performance of the product in order to and prepare a process optimization protocol [40]. In other words, CPP could be defined as any measurable parameter whose variability has an impact on CQAs, and for this reason, should be monitored and controlled to ensure the TPQP [23, 39].

Designing a process where the operating limits for one or more critical parameters are too narrow is a challenge, and frequently cannot be consistently achieved [40]. The ability of a manufacturing process to tolerate the expected variability of raw materials, operating conditions, process equipment, environmental conditions and human factors is referred to as robustness [47]. In process robustness studies, effects of variations in process parameters aid to identify CPPs which can potentially affect product quality or performance, establishes limits within which the quality of drug product is assured, and, in addition, avoid any potential impact of scale-up [48]. Nonetheless, when considering scale-up additional experimental work may be required once some critical process parameters are scale dependent and therefore, the model generated at the small scale could not be predictive at the large scale [21].

The QbD concept has been applied by several authors, who intended to improve pharmaceutical product design and/or process. In the Table 1 it could be seen some studies realized in this framework, in which were evaluated CQAs, in the case of formulation design, or CPPs in the case of process optimization.

Table 1. Studies realizes in the framework of pharmaceutical QbD.

PRODUCT DESIGN			**PROCESS DESIGN**		
Pharmaceutical Formulation	**CQAs**	**Ref.**	**Pharmaceutical Process**	**CPPs**	**Ref.**
Solid Lipid Nanoparticle (SLN) Formulation	Surface morphology Particle size Zeta potential Drug encapsulation efficiency Release behavior	[49]	Fluid bed granulation	Inlet air temperature Binder spray rate Air flow rate (Spraying and drying phases)	[36]
Liposome formulation	Particle size Zeta-potential, Drug encapsulation efficiency	[38]	Microfluidization	Milling time Microfluidization pressure Stabilizer type Processing temperature Stabilizer concentration	[50]
Matrix tablets	Dissolution efficiency Time necessary to dissolve 10%	[51]	Lyophilization	Primary drying temperature Secondary drying temperature and time Chamber pressure Freeze ramp rate	[52]
Dispersible tablet	Particle size Superdisintegrants Tablet hardness Lubricant level Packaging material	[53]	Spray Drying	Inlet temperature Spray flow rate Feed rate	[54]
Blends	Particle size and weight ratio Drug/excipients Particle shape Material density Cohesity	[55]	Blending	Order of addition Blend RPM Blending time Fill volume Equipment	[55]

1.1.3 QbD: An Approach based on Biopharmaceutical Classification System (BCS)

Establishing boundaries based on the clinical impact of the product design and manufacturing process is a challenge for pharmaceutical scientists, once manufacturing and composition variables need to be linked in order to establish the product clinical performance [56]. Pharmacokinetic parameters are considered to have a crucial role in the selection process and product development. Fundamental Biopharmaceutics Classification System (BCS) parameters, such as permeability, solubility and fraction dose absorbed should be useful in both the discovery and early development process [3, 57].

Class I compounds have a high solubility and permeability; therefore, their bioavailability will depend solely on the gastric emptying rate. For class II compounds with a low aqueous solubility and sufficient permeability the dissolution will be the rate limiting step [10]. Class III compounds have sufficient solubility but poor permeability and hence the absorption rate will be determined by passage through the gut wall. In the case of class IV compounds with both low solubility and permeability, the rate limiting step will differ case by case [6, 58].

The BCS has proven to be an extremely useful guiding tool for the prediction of *in vivo* performance of drug substances and development of new drug delivery system, from early to clinical stages, in order to ensure the performance of pharmaceutical product [57]. Thus, a greater understanding of dissolution and absorption behavior of drugs with low aqueous solubility is required to successfully formulate them into bioavailable drug products [3, 6, 9].

Dissolution is the only test that measures *in vitro* drug release as a function of time, which may reflect the reproducibility of the manufacturing process and, in some cases, the drug's *in vivo* performance [59]. Under the QbD framework, the dissolution tests should be developed to reflect *in vivo* performance as much as possible and must be representative to the conditions in the gastrointestinal tract [60].

Several physicochemical factors control the dissolution rate of the drugs. The factors affecting the drug dissolution rate are defined as the effective surface area, the diffusion coefficient, the diffusion layer thickness, the saturation solubility, the amount of dissolved drug, and the volume of dissolution media. Increases in the saturation solubility and the effective surface area have a positive impact on the dissolution rate of the drugs, and these factors could be increased by efforts of pre-formulation study and formulation design [6]. Crystal modification, particle size reduction, self-emulsification, pH modification, and amorphization are considered to be effective for improving the dissolution behavior of drugs poor water soluble [2].

1.2 Solid dispersions

The improvement of the drug water-solubility by SD is already described. The mixture of a poorly water soluble drug and highly soluble carriers creates a surface area in the dissolution medium, resulting in an increased dissolution rate and consequently improved bioavailability [61]. The amorphous state is reported to have more solubility as compared to crystalline state by the fact that in the amorphous state the molecules are arranged randomly and no energy is required to break, what happens with the ordered arrangement of crystalline state [62]. In figure 2, it could be seen the types of SD that may be achieved depending on polymer and drug characteristics. The drug can be dispersed in amorphous or in crystalline particles. When the drug is dispersed in the matrix in a single phase, it is called solid solution [63].

The use of SD has been extensively studied. Despite all the advantages, the commercial use of SD has been very limited, primarily due to the manufacturing difficulties and stability problems. A significant problem with the systems is the present difficulties in the formulation development and subsequent scaling-up. Thermo sensitive drugs and carriers may be destabilized during the melting or solvent-facilitated melting process since high melting temperatures are usually applied.

On the other hand, it is difficult to scale up the formulation of SD. The soft and tacky properties of solid dispersion powders result in poor flow ability, mixing property and compressibility, which may complicate the operations and render poor reproducibility of physicochemical properties of final products.

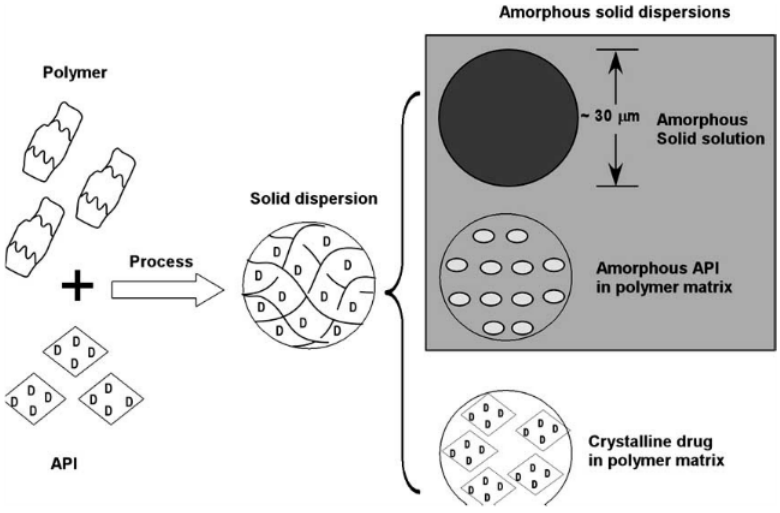

Figure 2. The solid dispersion formed from amorphous drug in a single phase (solid solution); amorphous drug in a separate-phase dispersion; and crystalline drug in a polymer matrix [63].

Despite extensive expertise with SD, they are not broadly used in commercial products, mainly because there is the possibility that during processing (mechanical stress) or storage (temperature and humidity stress) the amorphous state may undergo crystallization and dissolution rate decrease with ageing. The effect of moisture on the storage stability of amorphous pharmaceuticals is also a significant concern, because it may increase drug mobility and promote drug crystallization. Moreover, most of the polymers used in SD can absorb moisture, which may result in phase separation, crystal growth or conversion from the amorphous to the crystalline state or from a metastable crystalline form to a more stable structure during storage [64]. Table 2 can summarize the main methods of manufacturing, with theirs advantages and disadvantages; and the carriers commonly used for SD.

Table 2. Main methods of manufacturing, and carriers commonly used for SD

<table>
<tr><th colspan="2">METHODS OF OBTAINMENT</th><th>CARRIERS USED</th></tr>
<tr><td>Advantage</td><td>Disadvantage</td><td rowspan="2">Polymeric material:
poly(vinylpyrrolidone) (PVP), poly(vinylpyrrolidone/vinyl acetate copolymer), hydroxypropylmethyl cellulose (HPMC), hydroxypropylmethyl cellulose acetate/succinate (HPMCAS), hydroxypropylmethyl cellulose phthalate (HPMCP), acrylic acid-based enteric Eudragit systems.</td></tr>
<tr><td colspan="2">Solvent evaporation</td></tr>
<tr><td>Easy preparation
Feasible scale up</td><td>Toxicity
Residual amount</td><td rowspan="2">Sugars:
sucrose, dextrose, sorbitol, maltose, galactose, xylitol, chitosan, inulin, dextrin, cyclodextrin)</td></tr>
<tr><td colspan="2">Melting</td></tr>
<tr><td>Easy preparation
Feasible scale up</td><td>Drug degradation
Low solubility in molten carrier</td><td>Acids:
citric acid, tartaric acid, succinic acid</td></tr>
<tr><td colspan="2">Antisolvent</td><td rowspan="2">Surfactants:
polyoxyethylene stearate, poloxamer, deoxycholic acid, tweens, spans, compritol 888 ATO, gelucire 44/14 and 50/13, sodium lauryl sulfate, phospholipid)</td></tr>
<tr><td>Solvent-free</td><td>Low solubility in CO_2
Limited scale up</td></tr>
<tr><td colspan="2"></td><td>Miscellenous:
urea, urethane, hydroxyalkyl xanthene, pentaerythritol)</td></tr>
</table>

In this section, will be discussed the sources of variability that may affect the quality of SD, with the aim to make a risk assessment for the design and production of these system.

1.2.1 Methods of obtainment

Several studies have demonstrated that physical-chemical properties of solid dispersion obtained by different methods of preparation are directly related [16, 65]. This fact is

established as a prerequisite in solid dispersion developing, being necessary to evaluate interference of the method applied, in order to choose which is most efficient regarding to the dissolution and stability of the products obtained under the conditions of storage [13]. For many preparation techniques, demixing (partially or complete), and formation of different phases is observed. Phase separations like crystallization or formation of amorphous drug clusters are difficult to control and therefore unwanted [9], which may condition the method of preparation of SD.

There are mainly two processes for manufacture SD: the melt method, and those which involves solvent evaporation techniques [66]. Other techniques have gained increasing, as supercritical antisolvent methods, [65, 67] which will be discussed further.

Although the manufacturing methods to obtain SD be quite simple once the processing involves just few steps, they are individualized depending on the interaction between drug and carrier [62].

1.2.1.1 Solvent evaporation method

The solvent evaporation method aims to dissolve the drug and carrier simultaneously in a common solvent, followed by the removal of solvent by evaporation [2]. The solvent can be removed by various processes including vacuum drying, heating of the mixture, slow evaporation of the solvent at low temperature, the rotary evaporators, spray drying and freeze drying [68].

Identification of a common solvent for both drug and carrier can be problematic and complete solvent removal from the product can be a lengthy process [68]. Furthermore, the disadvantage of the solvent method is the use of organic solvents with toxicity problems, safety hazards and solvent residuals and also the possible precipitation of the drug into various polymorphic forms with different solubilities, which could vary bioavailability of the drug. [69].

Various strategies have been applied to dissolve the lipophilic drug and hydrophilic matrix material together in one solution. Low drug concentrations are used to dissolve both drug and matrix material in water, but this requires evaporation of high amounts of solvent, making the process expensive and impractical [61].

Some solubilizers or surfactants, as cyclodextrins, inulin, polysorbates, poloxamers, among others, have the capacity to increase the aqueous solubility of the drug substantially [66]. However, their use must be cautious once they may change the physical properties of the matrix, increase the water uptake of the formulation and, in addition, they can be toxic and not well tolerated *in vivo* [61, 70]

The nature of the solvent and its rate of evaporation and temperature are particularly critical in this method [16]. Chloroform [71], dichloromethane, ethanol [72] methanol [18], or mixtures of some of these solvents [73, 74], have been used to dissolve both drug and matrix simultaneously.

However, according to the ICH-Guidelines, these solvents belong to Class I, comprising the most toxic solvents [75]. Therefore, the use of these solvents is unacceptable and impractical because the amount of residual solvent present in the solid dispersion after drying has to be below the detection limits. One strategy for the dissolution of both drug and matrix is the use of solvent mixtures, in order to decrease the amount of each residual solvent and reduce toxicity. Water and ethanol or dichloromethane and have been used for this purpose. However, dissolution of drug and matrix in these mixtures is not always possible in the required concentration or ratio [13, 61].

Another challenge in the solvent method is to prevent phase separation, e.g. crystallization of either drug or matrix, during removal of the solvent(s). Drying at high temperatures speeds up the process and reduces the time available for phase separation. On the other hand, at high temperatures the molecular mobility of drug and matrix remains high, favoring phase separation [61].

Spray-drying is one of the most commonly used solvent evaporation procedures in the production of SD [66]. The spray drying process consists of four basic stages: atomization of the liquid, mixing of the liquid with the drying gas, evaporation of the liquid and separation of the dried particles from the gas. Due to the large specific surface area offered by the droplets, the solvent rapidly evaporates and the solid dispersion is formed within seconds, which may be fast enough to prevent phase separation [76]. Moreover, the SD prepared by spray drying consist of particles of which the size may be customized by changing the droplet size to meet the requirements for further processing or application (e.g., free flowing particles or articles for inhalation). Spray drying usually yields drug in the amorphous state, however sometimes the drug may have (partially) crystallized during processing [61].

The achievement of the solid dispersion by spray drying involves many variables such as the solvent used and the concentration of the drug and excipients in solution. Since many excipients are polymers, they can influence the non-covalent interactions between different solutes in solution [77].

SD can also be dried by the ultra-rapid freezing, frequently termed lyophilization [65]. The first step is a freezing stage, where water is converted into ice and the solutes are crystallized or transformed into solid. Later, it is followed by a drying step, which could be divided in two stages: Primary drying, where the ice crystals are removed by sublimation under vacuum (ice sublimation); and secondary drying (moisture desorption), where most

of the unfrozen water is removed by desorption [28, 78, 79]. After freeze-drying, the resulting product is a dry porous mass, very stable, with approximately the same size and shape as the original frozen mass [78, 79]. During lyophilization, it is crucial to ensure that the endpoint of all intermediate process steps is reached before the next process step is initiated and to monitor the solid state of the freeze-dried product [28]. The critical formulation properties include the collapse temperature of the formulation, the stability of the drug, and the properties of the excipients used [80, 81].

1.2.1.2 Melting method

The melting method involves melting of a physical mixture of drug and carrier to the liquid state followed by cooling until solidification [68]. The polymer could also be melted first, and then the drug incorporated into the melted matrix, followed by a Cooling. The cooling processes can be by room temperature or flash. Flash cooling could result in phase separation in some cases [62].
Although frequently applied, the melt method has serious limitations. This method is not suitable for thermolabile drugs and incomplete miscibility is observed between the solid drug [61]. When drug and matrix are incompatible two liquid phases or a suspension can be observed in the heated mixture, which results in an inhomogeneous solid dispersion [13]. This can be prevented by using surfactants. In addition, a problem can arise during cooling when the drug-matrix miscibility changes. In this case phase separation can occur. Indeed, it was observed that when the mixture was slowly cooled, crystalline drug occurred, whereas fast cooling yielded amorphous SD, degradation of the drug and or matrix can occur during heating to temperatures necessary to fuse matrix and drug [61].
Because of the toxicity and environmental problems associated with the use of organic solvents, the application of this method is advantageous in the preparation of SD when the drug has thermal stability. However, its use is inadequate when polymorphism occurs due to the transition that may occur during the merger between the polymorphic forms [13].
SD can be also prepared through a manufacturing method that involves both solvent evaporation and melting method in association. This method is called melt evaporation method. It involves preparation of SD by dissolving the drug in an appropriate solvent and then incorporating the solution directly into the melted polymer, which is then evaporated until the solvent layer disappears and forms a free-solvent film. The film is further dried to constant weight. This process is advantageous because the drug could be incorporated into a little amount of an organic solvent, which can be, in turn, incorporated into polymer without significant loss of its solid property. It is possible that the selected solvent or dissolved drug may not be miscible with the melt of the polymer and also the solvent used

may affect the polymorphic form of the drug, which precipitates as the solid dispersion. Besides, the efficacy and safety of SD with low therapeutic dose drugs could be compromised [82].

A number of convenient modifications of melt method have been developed to overcome problem of thermo-stability of drugs during melting process, which include hot melt extrusion, hot spin melting, meltrex-use of twin-screw extruder [62]. These techniques provide the opportunity to intensively mix a drug with a carrier at elevated temperatures in a continuous mode, without the need of a solvent [4, 12, 83]. Compared to the traditional fusion method, these techniques offer the possibility of continuous production, which makes it suitable for large-scale production. Furthermore, the product is easier to handle because at the outlet of the extruder the shape can be adapted to the next processing step without grinding [61]. The major disadvantage is the use of heat and the application of shear forces on the drug, which limits its use to heat stable compounds only [83].

One of the major problems associated with the melting method is that this process involves higher drug loadings and thus, there is a need for plasticizers to facilitate thermal processing, which can compromise the compositional glass transition temperature of the system, leading to the increase of the rate of drug crystallization [84]. In order to enhance the long term stability of amorphous systems, a novel high energy mixing process, KinetiSol® dispersing, was developed focused on providing improved compositional glass transition temperatures. In this processing, paddles within a cylindrical chamber containing raw materials rapidly rotate, generating all heat energy by a combination of shear and friction. The temperature in the chamber rapidly increase from room temperature to the desired ejection temperature, allowing for minimal thermal exposure [85]. The KinetiSol® dispersing has been already applied to prepare single phase SD of itraconazole in hypromellose, [86] and hydrocortisone [87].

With this technique, currently used in commercial polymer production, it is possible to prepare SD without the aid of solvents or plasticizers, which may translate into improved physicochemical properties and increased homogeneity of SD [84].

1.2.1.3 Supercritical antisolvent method

Supercritical fluid methods are mostly applied with CO_2, which is used as either a solvent for drug and matrix or as an antisolvent. When supercritical CO_2 is used as solvent, matrix and drug are dissolved and sprayed through a nozzle, into an expansion vessel with lower pressure and particles are immediately formed. The adiabatic expansion of the mixture results in rapid cooling. This technique does not require the use of organic solvents and

since CO_2 is considered environmentally friendly, this technique is referred to as “solvent free”. The application of this technique is very limited, because the solubility in CO_2 of most pharmaceutical compounds is very low (<0.01wt-%) and decreases with increasing polarity. Therefore, scaling up this process to kilogram-scale will be impractical [12, 61].

1.2.2 Carriers used in SD

It is crucial to select the right carrier based on the chemical structure of the drugs [76]. The selection of the carrier has the influence on the dissolution characteristics of the dispersed drug, since the dissolution rate of one component from the surface is affected by the other component in a multiple component mixture [4, 9]. The presence of functional groups that are either hydrogen donors or acceptors is an additional benefit, since specific interactions increase the solid solubility of the drug into its carrier and also seem to play an important role in inhibiting crystallization of a drug from a glass solution. The carrier should be pharmacologically inert and safe [4, 88].

Also, regarding to manufacturing SD, thermal stability and melt viscosity need to be considered for systems prepared by Hot-Melt extrusion; solubility in organic solvents is a prerequisite for carriers that are used for producing SD via solvent methods. In terms of drug release, it is obvious that the carrier should be soluble in water. The dissolved carrier will also influence the supersaturated drug solution that is formed following dissolution. Some carriers solubilize the released drug, whereas others will stabilize the supersaturated drug solution. A thorough insight in all of these aspects is imperative for a rational formulation strategy [4, 88].

The mainly carriers commonly used for SD are acids (citric acid, tartaric acid, succinic acid); sugars (sucrose, dextrose, sorbitol, maltose, galactose, xylitol); polymeric material (Polyvinyl pyrollidone, polyethylene glycol 4000 & 6000, carboxymythyl cellulose, hydroxypropylvcellulose, guar gum, xanthan gum, sodium alginate, dextrin, cyclodextrin); surfactants (polyoxyethylene stearate, poloxamer, deoxycholic acid, tweens and spans); and miscellenous (urea, urethane, hydroxyalkyl xanthene, pentaerythritol) [89].

Although, SD are usually prepared with water soluble low melting point synthetic polymers such as polyvinyl pyrrolidone (PVP), mannitol or polyethylene glycols (PEGs). These polymers show superior results in drug dissolution enhancement, but the amount of these polymers required is relatively large, around 1:2 to 1:8 (drug/ polymer) ratio. An obstacle of solid dispersion technology in pharmaceutical product development is that a large amount of carrier, i.e., more than 50% to 80% w/w, is required to achieve the desired dissolution [89].

PEGs are widely used as vehicles for SD with the melting method because of their low melting point, rapid solidification rate, capability of forming solid drug solutions, low toxicity and low costs. This often results in SD in which many drugs are incorporated as separate molecules in the helical structure present in a crystalline PEG. The helices are aligned in orderly fashion, illustrating that PEG easily crystallizes. However, at higher drug concentrations, the drug is often present in the crystalline form and the PEG dispersion may recrystallize over time, resulting in unstable formulations with lower dissolution rates [61, 69].

On the other hand, the ability to stabilize the amorphous state of drugs due to inhibition of drug recrystallization as well as a rapid solidification rate and low toxicity favors the PVP and some derivatives as PVP co-vinylacetate for the preparation of SD. PVPs are amorphous polymers with glass transition temperatures between 110 and 180◦C. [61, 69]. However, the relatively high glass and melting transitions limit the applicability of these polymers for the preparation of SD by the melting method [13]. The mode of incorporation of the drug depends on the PVP-drug miscibility and the preparation procedure, and therefore, grinding is required to obtain SD as powder that is easy to handle [61, 69].

Attempts have been made to increase the degree of drug dispersion by adding surfactants to the carrier, which was shown to be effective in originating high polymorphic purity and enhanced *in vivo* bioavailability [66, 70, 90, 91]. Adsorption of surfactant on solid surface can modify their hydrophobicity, surface charge, and other key properties that govern interfacial processes such as flocculation/dispersion, floatation, wetting, solubilization, detergency, and enhanced oil recovery and corrosion inhibition and thereby enhancing solubilization. Furthermore, they may help to prevent precipitation and/or protect a fine crystalline precipitate from agglomeration into much larger hydrophobic particles [82].

Some surfactants commonly used are inulin [92], inutec SP [93], compritol 888 ATO [94], gelucire 44/14 [95] and 50/13 [96], poloxamers 407/188 [91, 97], polysorbate 80 [98, 99], docusate sodium [70, 91], sodium lauryl sulfate [91, 100], phospholipids [101]. Poloxamers, includes a group of nonionic surfactants, have attracted considerable attention for application in formulation of SD [102-106]. These polymers are widely used as emulsifiers, solubilizing agents, and suspension stabilizers in pharmaceutical formulations and also act as wetting agents and plasticizers. Besides, have been reported for enhancing the solubility and bioavailability of sparingly soluble drugs in solid dosage forms [105, 106]. Phospholipids have the advantage of increasing the dissolution rate of drugs with low aqueous solubility, but at a much lower carrier concentration. In aqueous media, phospholipids disperse spontaneously to form spherical bilayer structures that can entrap or sequester the drug, which can be transported to the stationary or diffusion layer and subsequently yield more rapid and higher absorption [101]. Gelucires are glyceride-

based amphiphilic excipients composed of mixtures of mono, di, and tri glycerides with PEGs esters of fatty acids [62] Because they present an amphiphilic character, they are able to increase significantly the drug bioavailability.

Despite synthetic carriers have been commonly used to improve the solubility of lipophilic drugs, they present some problems, as high hygroscopicity, which may cause instability of SD. Therefore, continuous search for new carriers and new techniques have been done, which are useful for large-scale manufacturing [107].

Recently, the use of semi-synthetic hydrophilic polymers, as gum karaya [107] and chitosan [108-110] have been used as carriers to enhance the dissolution rate and bioavailability of poorly water-soluble drugs has been demonstrated by some of investigators.

Chitosan presents a vast number of applications in recent years and it is considered one of the most significant materials from the point of view of potential applications [108]. The positives attributes of chitosan are, mainly due to its complete biocompatibility, beside it is totally biodegradable, non-toxic, and also has a high adsorption capability [111]. From the technological point of view, it is miscible with other polymers, which could be very advantageous during the design of S formulations.

1.2.3 Techniques for characterization SD

Complete characterization of SD is important to assess quality of innovative and pre-approved products. Extensive characterization of their stability and physical-chemical properties are prerequisites to ensure their efficacy throughout their shelf-life [112]. Among the important characteristics, the most relevant are amorphous content, drug carrier miscibility, dissolution rate, surface properties, drug carrier interactions and physical stability.

Much effort has been put to differentiate amorphous and crystalline material once even small amounts of crystalline material can profoundly affect the *in vivo* performance of the amorphous material [63]. For this purpose, many techniques are available which detect the amount of crystalline material in SD. The amount of amorphous material can never be measured directly but can be derived from the amount of crystalline material in the sample [9].

Therefore, characterization of the structural state of the drug substance and their unambiguous identification in SD is a priority that still has remained a challenge [113]. Several methods for characterize SD, which has potential to evaluate their critical parameters are listed in table 3.

Amorphous SD is commonly characterized in terms of physical properties such as glass transition temperature (*Tg*), heat capacity, and miscibility [114]. Although, the analysis of *Tg* has been used frequently study once it is the fingerprint of a glassy material [4].

The *Tg* represents the temperature at which the non-equilibrium glass transforms to the super cooled liquid [63]. It is well known that compatible blends of amorphous materials exhibit one single *Tg* that is situated between the *Tg* of the individual components. There is a large number of relationships between the *Tg* of an amorphous system (mainly binary systems) and its composition, which seems to be a tool to measure physical stability of these systems. [88].

Besides, characterization of *in vitro* dissolution performance and, in particular, characterization of the supersaturated state with polymer-modulated interactions is desired to understand supersaturatable systems [115]. Some considerations regarding physical stability of SD and biopharmaceutical considerations will be given in the next sections.

Table 3. Methods for evaluate critical parameters of SD

PARAMETER	TECHNIQUE
Drug–carrier miscibility	Hot stage microscopy DSC Powder X-ray Diffraction (XRD) NMR 1H Spin lattice relaxation time
Drug carrier interactions	FT-IR spectroscopy Raman spectroscopy Solid state NMR DSC
Physical Structure	Scanning electron microscopy Surface area analysis
Surface properties	Dynamic vapor sorption Inverse gas chromatography Atomic force microscopy Raman microscopy
Amorphous content	Polarized light optical microscopy Hot stage microscopy Humidity stage microscopy DSC Powder XRD

NMR: Nuclear Magnetic Resonance; FT-IR: Fourier transform infrared; DSC: Differential Scanning Calorimetry; XRD: X-ray Diffraction.

There is an increasing demand for new approaches to understand the chemical and physical phenomena that occur during pharmaceutical unit operations [116]. With the introduction of the concept of PAT, the development of in-process analytics for process

monitoring are new efficient tools that have been used during pharmaceutical development, manufacturing, and quality control, maintaining or improving the current level of product quality assurance [116, 117].

Recently, some optical spectroscopy techniques, as Raman and Near Infrared (NIR) has been used a PAT tool (process analyzer) for the in-line and real time once they are non-destructive and solid samples can be analyzed in their native state without any sample preparation [80, 81, 118]. The IR spectra are generated by a change in the dipole moment of a molecule, while Raman scattering occurs as a result of changes in its polarisability [117, 118].

NIR and Raman spectroscopy present a number of applications in the pharmaceutical industry. In the case of NIR, it is commonly used for identity substances, measurement of water content, monitoring blends, drug substance content, etc. The usefulness of Raman spectroscopy, on the other hand, has been applied for monitoring synthesis and determination of polymorphic forms of the active component and also blend monitoring [118]

These spectroscopy techniques have been Also Implemented in the solid dispersion design / production framework [119-122].

Raman could be a very useful tool to predict the crystallinity of the solid dispersion and also monitor the presence of polymorphic forms during and after process manufacturing, in both real time and off-line [119, 122]. Besides, it can monitor the homogeneity in a mixture of polymers, compare powder samples that were prepared with different techniques, evaluate the chemical structure of drug and possible interactions, and others [119, 122].

NIR spectroscopy provides information about the spatial distribution of the components that compose the sample, in addition can provide important information of formulation chemical and physical parameters in order to measuring process performance [18, 120, 121].

1.2.3.1 Physical stability of SD

For a solid dispersion to be suitable as a pharmaceutical product it needs to show improved dissolution of an incorporated drug and, still, be stable on storage. Commonly the dissolution profile of the drug in a solid dispersion changes on storage due to physical instability which imposes phase separations and re-crystallizations of the dispersed components [90].

Phase instability as a function of time and/or triggered by storage conditions (temperature and/or elevated humidity) is often reported and contributes to the large discrepancy between scientific and developmental efforts [88].

Basically, changes occur in several systems in crystallinity and a decrease in dissolution rate with ageing and system may be destabilized through physical treatment such as pulverization. There is more deteriorating effect of moisture and temperature on SD than on physical mixtures [9].

A key formulation goal for an SD formulation is to prevent or predict nucleation and growth in drug-excipients matrix and dissolution medium. In the solid state, the inhibitory effects of polymers against crystallization have been attributed to some mechanisms including antiplasticization by the polymers, a reduction in local molecular mobility due to coupling between the polymer and drug substance, and an increase in the activation energy for nucleation [123].

In general, relatively small amounts of polymer in dispersions have been shown to significantly inhibit crystallization both in the solid state before administration and after introduction of the dispersion into dissolution media and gastrointestinal (GI) tract fluids [124].

Therefore, preparing a formulation with a high *Tg* by using high *Tg* excipients such as PVP or hydroxypropylmethycellulose, and storing it well below the *Tg* should slow down the solid-state transformation and prolong product shelf-life. On the contrary, the presence of a powerful plasticizer such as water may destabilize a solid dispersion [125].

The initial product *Tg* alone may not accurately reflect the physical stability of drug in a solid dispersion [125]. Several factors may influence the extent and rate of crystal nucleation and growth of amorphous drug substance which are quite complex, making it difficult to predict long-term stability as a function of temperature and relative humidity, as in studies conducted under accelerated conditions [124].

Therefore, it is important to understand the factors that could affect nucleation and growth of crystals in a solid solution such as temperature dependence of drug solubility supersaturation. In addition, the temperature dependence of both the molecular mobility and activation energy of nuclei formation needs to be known in order to predict the crystallization rate of amorphous drugs [125].

Unfortunately, the effect of interacting excipients on the physical stability of drugs is frequently observed but not predicted. Although, the use of mechanistic models can reduce cost to feasibility evaluations and facilitate solid dispersion formulation development [125].

1.3 Biopharmaceutical considerations

While determining the fundamental physicochemical properties of the drug, such as solubility and lipophilicity, are central to any oral formulation strategy, it is important not to focus solely on these parameters. The interaction between a drug and the gastrointestinal environment, or the biopharmaceutical properties of the drug, requires close consideration. The complex physiological factors that influence the rate of drug presentation at the intestinal surface, transmembranal transport process and finally release into the systemic circulation, are also essential and cannot be taken in isolation [126]. For example, low molecular weight drugs with moderate lipophilicity can be easily transported through passive transcellular pathway, while high lipophilicity drugs show poor permeation characteristics towards basolateral side due to being trapped inside the epithelial tight junctional cells. High molecular weight drugs with poor solubility show bioavailability problems as they cannot permeate through the barriers [127, 128].

Thus, if the physicochemical and biopharmaceutical limitations of the drug are known then appropriate excipient selection and logical formulation design is feasible [126].

The rate of absorption of many slightly soluble drugs from the GIT and other sites is limited by the rate of dissolution of the drug. A more physiologically relevant *in vitro* dissolution measurement is especially important for poorly water-soluble drugs formulated into supersaturatable systems where precipitation/crystallization of drug in GI tract is of a concern. Supersaturation and solution mediated phase transformation of the drug may result from pH-induced precipitation (e.g., free-base from salt/ionized form), precipitation from solution formulations (e.g., cosolvents, lipids), or amorphous/metastable to stable polymorph/ hydrate phase, transformations (e.g., crystallization of an amorphous solid dispersion) [115, 129].

Therefore, evaluating supersaturatable formulations with the use of biorelevant *in vitro* dissolution tests which can better represent *in vivo* conditions is more meaningful and highly desirable [115].

Several *in vitro-in vivo* screening methods are used as quality control tool to evaluate the intestinal permeability and real time bioavailability of drug formulations for oral administration, especially for drug belonging to BCS-II, once these assays provide reproducible results for bioavailability [130].

With respect to dissolution assays, the use of biorelevant fluids, especially Fasted Simulated Small Intestinal Fluid (FaSSIF), has been well established within the pharmaceutical industry. However, this medium represents only the proximal jejunum, and hence cannot take into account the rapid and dynamic changes in the conditions along the intestine [131]. For this reason, several modifications have been made for automation

of dissolution test with apparatus strongly resembling with simulated condition of stomach and intestines, while all conditions like temperature, peristaltic motion, pH, gastrointestinal transit time, secretion of gastric acid and enzymes, bile salts, pancreatic juice are maintained. Drugs belonging to BCS-II category with poor solubility are specially evaluated by such system [127].

Regarding to the intestinal permeability of drug formulations, several *in vitro* permeability assay methods are used. Mostly Caco-2 cell line, Parallel artificial membrane permeability assay (PAMPA) cells, MDCK cell line, immobilized artificial membrane (IAM), chromatography, advanced compartmental absorption and transit (ACAT) models are being used in screening the permeability of test formulations [127].

Typically, traditional *in vitro* dissolution methods and *in vivo* testing in animals serve as the primary tools to guide development of pharmaceuticals. Only at later stages, human *in vivo* bioequivalence trials are performed to verify therapeutic equivalence. However, introducing more clinically relevant methods during early stages of development, especially in the context of QbD, could make manufacturing more cost-effective while maintaining or even improving quality for the patients [131]

In this context, very recently, a new European project (OrBiTo) in the area of oral biopharmaceutics tools, including public and private institutions has addressed key gaps in the knowledge of GIT drug absorption and delivers in a framework for rational application of predictive biopharmaceutics tools for oral drug delivery [131].

This work tried to discuss mainly the directives of intestinal absorption; address biopharmaceutical aspects in oral pharmaceutical formulation development; give an approach about the current status of predictive biopharmaceutics tools; and finally introduce main objectives of the OrBiTo project.

The approach gives an unparalleled opportunity to initiate a transformational change in industrial research and development to achieve model-based pharmaceutical product development in accordance with the QbD concept, particularly for challenging projects such as low solubility molecules (BCS II and IV) [131].

1.4 Risk assessment of solid dispersions

During the solid dispersion formulation development phase, many factors originating from both formulations as well as processing can have decisive influence of the physical stability of the drug, and the importance of evaluating the combined influence of these factors has been highlighted. From a formulation perspective, numerous studies have investigated and found factors such as polymer-to-drug ratio, polymer type, and its molecular weight to have decisive influence for the drug physical stability. When solid

dispersion is prepared using the solvent evaporation method, several studies have highlighted the influence of various process parameters including solvent evaporation rate on solid dispersion physical stability [15].

According to QbD, pharmaceutical development includes identifying potential CQAs of the drug product, determining material attributes of excipients, selecting an appropriate manufacturing process (CPPs) and defining a control strategy.

Although CQAs define the objectives for formulation and process design, they are also very dependent upon other parameters of the final product as dosage form, formulation and manufacturing method chosen among many possible and clinically equivalent alternatives. Consequently, formulation and process development typically rely on empirical prior knowledge, small-scale feasibility studies and empirical statistical studies [132].

The identification of key factors (sources of variability) in early stages of development was done through risk assessment. In general, risk assessment is a systematic application of policies, procedures, and practices to identifying, assessing, analyzing, treating, monitoring, and communicating risks to life, property, or other valuables [133].

There are a number of different risk assessment tools available in a range of detail and complexity, and it is important to use a methodology suited to the purpose of the assessment.

The first step in the risk assessment is to systematically gather up all the possible factors that could influence product quality. To identify these factors, some reviewed the literature, past experiences, and data collected during the initial formulation development studies are useful. This information then could be hierarchically in a diagram using, for example, an Ishikawa or “fishbone”, which may help to identify the failure related to system, process step, or piece of equipment. From this information, the variables (CQAs) that need to be further studied and controlled can be identified [132].

Based on this and in all the topics discussed in this work, figure 4 shows an Ishikawa diagram proposed to risk management of design and production of SD, taking into account the desired characteristic of the product, i.e. the increased solubility of drugs. As mentioned before, all the parameters involved during pre-formulation and formulation step, as drug and polymer critical peculiarities as well as external factors related to the manufacturing process may affect the targeted profile of the final product.

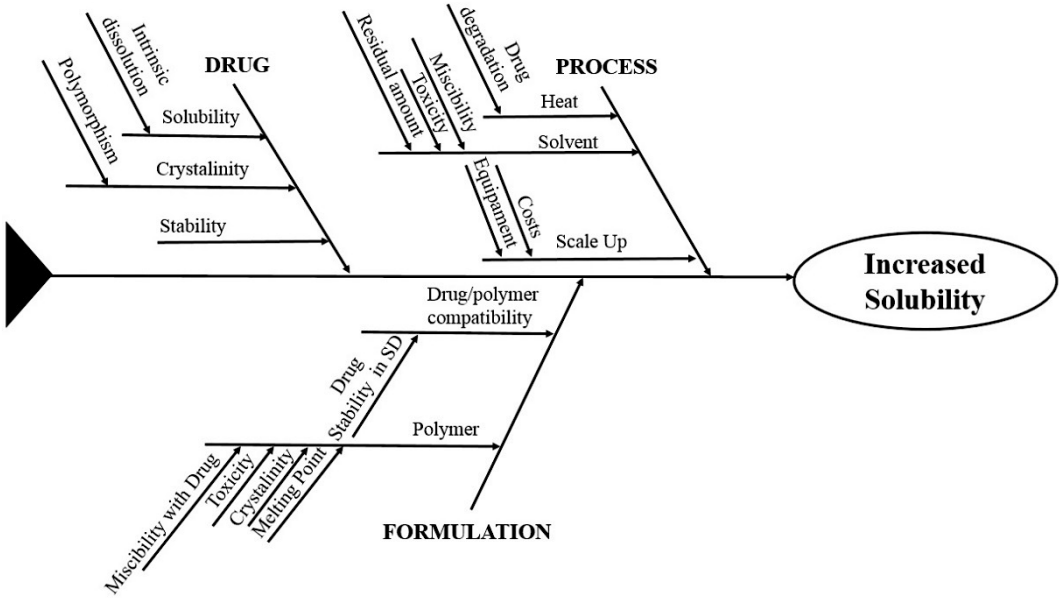

Figure 3. Ishikawa diagram for design and production of SD.

With the many factors influencing on the solid dispersion physical stability, an emerging recognized challenge is related to the systematic Design of Experiments (DoE) planning, and minimizing the complexity of the following multivariate modeling step, so that understanding of the underlying phenomena and latent factors influencing on the drug's physical stability can be maximized [15, 44].

Recent studies demonstrate the application of the QbD using the DoE for the development of SD. In 2011, Basalious *et al.* conducted a study that aimed to identify CQAs and the material attributes of the felodipine SD, which includes amount and type of hydrophilic carriers and/or surfactants, and determinate the process parameters for their preparation. For this study, Box –Behnken experimental design was applied to develop space design and determine the control space of the optimized felodipine SD that have maximum solubility, maximum dissolution, and ability to inhibit felodipine crystallization from supersaturated solution [44].

In 2009, Shrivastava and co-workers tried to improve the solubility of valsartan by formulating SD with gelucire 50/13, and evaluate the flow properties by surface adsorbent techniques, applying a full factorial experimental design. The independent variables were the ratio drug/gelucire and the amount of lubricant added in order to improve the flow properties. The dissolution rate, as amount dissolved in 10 and 30 minutes, and compressibility index were selected as dependent variables. Three-dimensional response surface plots and two-dimensional contour plots were drawn in order to estimate the effects of the independent variables on each response [134].

A similar study was done in 2013 by Katharia and co-workers, in which the authors tried to improve the dissolution rate of olanzapine by formulating SD using combination of hydrophilic polymers (PEG & PVP). A central composite design of two-factor and three level was used to determine the effect of content of PEG 20000 and PVP K 30 on the dissolution of drug and to statistically optimize the levels of these factors using multivariate analysis and response surface plots [135].

The adoption of statistical techniques based on the desirability approaches, and the evaluation of the optimization capability of response surface, in order to achieve optimized SD has been widely used and has shown to be an important tool during the design of SD. It is important to note that in all the studies cited, involving DoE and response surface analysis, the dissolution rate was adopted as dependent variable, which confirms and emphasizes the importance of this essay, which must always be a critical parameter in the development of DS.

As described in the Ishikawa diagram, the stability of the drug in SD, and even the stability of SD regarding the crystallinity have to be controlled once these parameters may affect the quality of the final formulation. In this way, the DoE has been applied in another framework. In 2012, Wu *et al.*, tried to assess and monitor the physical stability of SD during the development, using both formulation and process factors, in addition to long-term physical stability storage as a time factor [15].

The evidence and availability of recently marketed pharmaceuticals prepared by thermal processes reflect the benefits to the manufacture of solid dispersions at a large scale in a cost-effective manner, in particular hot melt extrusion and spray drying [136].

The spray drying process is a complex technological process that requires all processing conditions to be well controlled to avoid poor product performance [137]. Some of the conditions includes process parameters (inlet temperature, drying gas, flow rate, feed rate, nozzle size, compressed air flow rate) and formulation parameters (feed composition, solid content in feed and solvent type) [138]. Inadequate process conditions can lead to lower yields, sticking, or high moisture content in spray-dried SD [137]. On the other hand, hot-melt extrusion has stood out with advantages due to its single-step, simple and organic solvent-free preparation process, and gained increasing popularity. However, the elevated processing temperature has certainly limited the application of this technique for heat-sensitive drugs. In many cases, thermal degradation of drug is mainly related to the cumulative exposure to heat, which is a function of temperature and exposing duration [139].

Besides, in the phase of development, the process selection is also an important factor in. For example, for early stage or discovery-support activities, the availability of the drug in study is often limited, which tends to make spray drying the preferable process because its

feasibility can be determined with as little as 50 to 100 mg of drug, whereas several grams of the same are typically required to develop an initial hot-melt extrusion (HME) process [140].

Some recent studies have focused on the comparison between the two techniques in the design of DS. In 2013, Grawal, *et al.*, investigated systematically the effect of SD manufacturing methods such as hot-melt extrusion and spray drying on physicochemical properties and understand how these properties can affect manufacturability, physical stability and product performance of SD. The authors observed that the solid state properties and dissolution performance were similar for SD prepared by both processing techniques, although the different techniques impact the physical characteristics of SD, as morphological characteristics, surface area, bulk and tap density, and flow property. Also, under the accelerated stability conditions, SD dispersion prepared by spray drying process was physically less stable compared to the dispersion prepared by the hot-melt extrusion process [141].

In another study, Tian *et al.*, in 2013, in addition to use pre-formulation tools to rank polymers in terms of suitability to formulate molecular drug dispersions, the authors tried to understand the effects hot-melt extrusion and spray drying during the production of SD. The authors concluded that SD were affected by the nature of preparation technique; spray drying provided the greatest potential to generate SD across a wider concentration in which the sample should be thermodynamically unstable, and thus a high tendency to recrystallize, although it presented itself as a very fast technique. On the other hand, hot-melt extrusion has shown a limited window for extrusion in terms of temperature and drug composition; therefore, within this window, the viscosity of the system may prevent intimate mixing, and hence the inability to generate fully amorphous systems [142].

2. Conclusions

In spite of enormous research efforts both in academia and pharmaceutical industry very few products relying on solid dispersion technology reached the market. Moreover, the link between manufacturing process parameters and formulation parameters with the obtained physical structure and pharmaceutical performance of the solid dispersion is still not completely understood [88].

Understanding the functional relationship between quality attributes and process parameters as they progress through the manufacturing process is the most universally challenging aspect of QbD for drug development. Analytical specifications and control strategy aspects of the QbD plan remain the foundation for change throughout the evolution of the manufacturing process. Designed experiments generate the data required

to establish a design space for commercial manufacturing processes, while providing the process understanding that facilitates sound business decisions [53, 143].

Thus, it was clear that the influence of solid state and material properties on various aspects of SD such as product performance, physical stability and manufacturability should be considered by formulators. In addition, a systematic evaluation of SD prepared by different processing techniques can provide an early insight during initial stage of development to enable selection of an appropriate lead rational dispersion formulation and process in the pharmaceutical industry.

Acknowledgements

The authors thanks CAPES Foundation, Ministry of Education of Brazil for the Doctoral fellowship 0831-12-3.

References

1. Gopinath, R.; Naidu, R. A. S., Pharmaceutical Preformulation Studies – Current Review. *Int. J. Pharm&Bio. Arch.* **2011,** *2* (5), 1391-1400.
2. Jatwani, S.; Rana, A. C.; Singh, G.; Aggarwal, G., An overview on solubility enhancement techniques for poorly soluble drugs and solid dispersion as an eminent strategic approach. *Int. J. Pharm. Sci. Res.* **2012,** *3* (4), 942-956.
3. Buckley, S. T.; Fischer, S. M.; Fricker, G.; Brandl, M., *In vitro* models to evaluate the permeability of poorly soluble drug entities: Challenges and perspectives. *Eur. J. Pharm. Sci.* **2012,** *45* (3), 235-250.
4. Janssens, S.; Van den Mooter, G., Review: physical chemistry of solid dispersions. *J. Pharm. Pharmacol.* **2009,** *61* (12), 1571-1586.
5. Khutoryanskiy, V., Hydrogen-bonded interpolymer complexes as materials for pharmaceutical applications. *Int. J. Pharm.* **2007,** *334* (1-2), 15-26.
6. Kawabata, Y.; Wada, K.; Nakatani, M.; Yamada, S.; Onoue, S., Formulation design for poorly water-soluble drugs based on biopharmaceutics classification system: Basic approaches and practical applications. *Int. J. Pharm.* **2011,** *420* (1), 1-10.
7. Chaturvedi, A. K.; Verma, A., Solubility enhancement of poorly water soluble drugs by solid dispersion. *Int. J. Pharm. Sci.* **2012,** *3* (1), 26-34.
8. Dahan, A.; Beig, A.; Ioffe-Dahan, V.; Agbaria, R.; Miller, J., The Twofold Advantage of the Amorphous Form as an Oral Drug Delivery Practice for Lipophilic Compounds: Increased Apparent Solubility and Drug Flux Through the Intestinal Membrane. *The AAPS journal* **2012,** *15* (2), 347-353.
9. Kalia, A.; Poddar, M., Solid dispersions: An approach towards enhancing dissolution rate. *Int. J. Pharm. Sci.* **2011,** *3* (4), 9-19.
10. Bajaj, H.; Bisht, S.; Yadav, M.; Singh, V., Bioavailability Enhancement: A review. *Int. J. Pham&Bio. Sci.* **2011,** *2* (2), P.202-P.216.
11. Chen, H.; Khemtong, C.; Yang, X.; Chang, X.; Gao, J., Nanonization strategies for poorly water-soluble drugs. *Drug Discov. Today* **2011,** *16* (7–8), 354-360.

12. Karanth, H.; Shenoy, V.; Murthy, R., Industrially feasible alternative approaches in the manufacture of solid dispersions: A technical report. *AAPS PharmSciTech* **2006,** *7* (4), 31-38.

13. Alves, L.; Lyra, M.; Rolim, L.; Presmich, G.; Rolim-Neto, P., Avanços, propriedades e aplicações de dispersões sólidas no desenvolvimento de formas farmacêuticas sólidas. *Rev. Sci. Farm. Bas. Aplic.* **2012,** *33* (1), 17-25.

14. Tran, P. H. L.; Tran, T. T. D.; Park, J. B.; Lee, B. J., Controlled release systems containing solid dispersions: Strategies and mechanisms. *Pharm. Res.* **2011,** *28* (10), 2353-2378.

15. Wu, J. X.; Den Berg, F. V.; Søgaard, S. V.; Rantanen, J., Fast track to a solid dispersion formulation using multiway analysis of complex interactions. *J. Pharm. Sci.* **2012,** *102* (3), 904-914.

16. Wu, J. X.; Yang, M.; Berg, F. v. d.; Pajander, J.; Rades, T.; Rantanen, J., Influence of solvent evaporation rate and formulation factors on solid dispersion physical stability. *Eur. J. Pharm. Sci.* **2011,** *44* (5), 610-620.

17. Sammour, O. A.; Hammad, M. A.; Zidan, A. S.; Ayman, G. M., QbD approach of rapid disintegrating tablets incorporating indomethacin solid dispersion. *Pharm. Dev. Technol.* **2011,** *16* (3), 219-227.

18. Rahman, Z.; Zidan, A. S.; Khan, M. A., Risperidone solid dispersion for orally disintegrating tablet: Its formulation design and non-destructive methods of evaluation. *Int. J. Pharm.* **2010,** *400* (1–2), 49-58.

19. Zidan, A. S.; Sammour, O. A.; Hammad, M. A.; Megrab, N. A.; Habib, M. J.; Khan, M. A., Quality by design: Understanding the formulation variables of a cyclosporine A self-nanoemulsified drug delivery systems by Box–Behnken design and desirability function. *Int. J. Pharm.* **2007,** *332* (1–2), 55-63.

20. Lionberger, R.; Lee, S.; Lee, L.; Raw, A.; Yu, L., Quality by design: concepts for ANDAs. *The AAPS Journal* **2008,** *10* (2), 268-276.

21. Yu, L. X., Pharmaceutical Quality by Design: Product and Process Development, Understanding, and Control. *Pharm. Res.* **2007,** *25* (4), 781-791.

22. Garcia, T.; Cook, G.; Nosal, R., PQLI Key Topics - Criticality, Design Space, and Control Strategy. *J. Pharm. Inno.* **2008,** *3*, 60-68.

23. ICH, Q8(R2): Pharmaceutical Development. U.S, 2009.

24. Kharad, S. L.; Rane, S.; Sharma, N.; Velhankar, R., Quality By Design: Facilitate A Robust Pharmaceutical Process. *J. Pharm. Res.* **2011,** *4* (8), 2741-2743.

25. FDA, Pharmaceutical CGMPs for the 21 st Century: A Risk-Based Approach to Product Quality Regulation Incorporating an Integrated Quality Systems Approach. Services, U. S. D. o. H. a. H., Ed. U.S., 2002.

26. Glassey, J.; Gernaey, K.; Clemens, C.; Schulz, T.; Oliveira, R.; Striedner, G.; Mandenius, C.-F., Process analytical technology (PAT) for biopharmaceuticals. *Biotechnol. J.* **2011,** *6* (4), 369-377.

27. FDA, Guidance for Industry PAT — A Framework for Innovative Pharmaceutical Development, Manufacturing, and Quality Assurance. Services, U. S. D. o. H. a. H., Ed. Rockville, MD: U.S., 2004.

28. Read, E.; Shah, R.; Riley, B.; Park, J.; Brorson, K.; Rathore, A., Process analytical technology (PAT) for biopharmaceutical products: Part II. Concepts and applications. *Biotechnol. Bioeng*. **2010,** *105* (2), 285-295.

29. Strickley, R., Solubilizing excipients in oral and injectable formulations. *Pharm. Res*. **2004,** *21* (2), 201-230.

30. Korakianiti, E.; Rekkas, D., Statistical thinking and knowledge management for quality-driven design and manufacturing in pharmaceuticals. *Pharm. Res*. **2011,** *28* (7), 1465-1479.

31. ICH, Q9: Quality Risk Management. U.S., 2005.

32. ICH, Q10: Pharmaceutical Quality System. U.S., 2007.

33. ICH, Q11: Development and manufacture of drug substances. U.S., 2011.

34. Cui, Y.; Song, X.; Reynolds, M.; Chuang, K.; Xie, M., Interdependence of Drug Substance Physical Properties and Corresponding Quality Control Strategy. *Pharm. Tech* **2011,** *101* (1), 312-321.

35. Huiquan, W.; White, M.; Khan, M. A., Quality-by-Design (QbD): An integrated process analytical technology (PAT) approach for a dynamic pharmaceutical co-precipitation process characterization and process design space development *Int. J. Pharm*. **2011,** *405*, 63-78.

36. Lourenço, V.; Lochmann, D.; Reich, G.; Menezes, J. C.; Herdling, T.; Schewitz, J., A quality by design study applied to an industrial pharmaceutical fluid bed granulation. *Eur J Pharm Biopharm* **2012,** *81* (2), 438-447.

37. Rathore, A.; Winkle, H., Quality by design for biopharmaceuticals. *Nat. Biotechnol.* **2009,** *27* (1), 26-34.

38. Xu, X.; Costa, A. P.; Khan, M. A.; Burgess, D. J., Application of quality by design to formulation and processing of protein liposomes. *Int. J. Pharm.* **2012,** *434* (1–2), 349-359.

39. Roy, S., Quality by design: A holistic concept of building quality in pharmaceuticals. *Int. J. Pharm*. **2012,** *3* (2), 100-108.

40. Gibson, M., *Pharmaceutical preformulation and formulation*. Informa Healthcare USA: 2009.

41. Dayal, P.; Pillay, V.; Babu, R. J.; Singh, M., Box-Behnken experimental design in the development of a nasal drug delivery system of model drug hydroxyurea: Characterization of viscosity, in vitro drug release, droplet size, and dynamic surface tension. *AAPS PharmSciTech* **2005,** *6* (4), 573-585.

42. Gooding, O. W., Process optimization using combinatorial design principles: parallel synthesis and design of experiment methods. *Curr. Opin. Chem. Biol.* **2004,** *8* (3), 297-304.

43. Norioka, T.; Hayashi, Y.; Onuki, Y.; Andou, H.; Tsunashima, D.; Yamashita, K.; Takayama, K., A novel approach to establishing the design space for the oral formulation manufacturing process. *Chem. Pharm. Bull.* **2013,** *61* (1), 39-49.

44. Basalious, E. B.; El-Sebaie, W.; El-Gazayerly, O., Application of Pharmaceutical QbD for Enhancement of the Solubility and Dissolution of a Class II BCS Drug using Polymeric Surfactants and Crystallization Inhibitors: Development of Controlled-Release Tablets. *AAPS Pharmscitech* **2011,** *12* (3), 799-810.

45. Schmidt, B., Implementing Quality by Design: Are you ready, or not? *Pharmaqbd.com* **2010**.

46. Zhang, G. G.; Law, D.; Schmitt, E. A.; Qiu, Y., Phase transformation considerations during process development and manufacture of solid oral dosage forms. *Adv. Drug Delivery Rev.* **2004,** *56* (3), 371-390.

47. Glodek, M.; Liebowitz, S.; McCarthy, R.; McNally, G.; Oksanen, C.; Schultz, T., Process robustness—A PQRI white paper. *Pharm. Eng* **2006,** *26* (6), 1-11.

48. Martin-Moe, S.; Lim, F. J.; Wong, R. L.; Sreedhara, A.; Sundaram, J.; Sane, S. U., A new roadmap for biopharmaceutical drug product development: Integrating development, validation, and quality by design. *J. Pharm. Sci.* **2011,** *100* (8), 3031-3043.

49. Hao, J.; Fang, X.; Zhou, Y.; Wang, J.; Guo, F.; Li, F.; Peng, X., Development and optimization of solid lipid nanoparticle formulation for ophthalmic delivery of chloramphenicol using a Box-Behnken design. *Int. J. Nano* **2011,** *6*, 683-692.

50. Verma, S.; Lan, Y.; Gokhale, R.; Burgess, D., Quality by design approach to understand the process of nanosuspension preparation. *Int. J. Pharm.* **2009,** *377* (1-2), 185-198.

51. Furlanetto, S.; Cirri, M.; Maestrelli, F.; Corti, G.; Mura, P., Study of formulation variables influencing the drug release rate from matrix tablets by experimental design. *Eur. J. Pharm. Biopharm.* **2006,** *62* (1), 77-84.

52. Sundaram, J.; Hsu, C. C.; Shay, Y.-H. M.; Sane, S. U., Design Space Development for Lyophilization Using DOE and Process Modeling. *BioPharm. International* **2010,** *23* (9).

53. Charoo, N. A.; Shamsher, A. A. A.; Zidan, A. S.; Rahmand, Z., Quality by design approach for formulation development: A case study of dispersible tablets. *Int. J. Pharm. (Kidlington)* **2012,** *423*, 167-178.

54. Lebrun, P.; Krier, F.; Mantanus, J.; Grohganz, H.; Yang, M.; Rozet, E.; Boulanger, B.; Evrard, B.; Rantanen, J.; Hubert, P., Design space approach in the optimization of the spray-drying process. *Eur. J. Pharm. Biopharm.* **2012,** *80* (1), 226-234.

55. Adam, S.; Suzzi, D.; Radeke, C.; Khinast, J. G., An integrated Quality by Design (QbD) approach towards design space definition of a blending unit operation by Discrete Element Method (DEM) simulation. *Eur. J. Pharm. Sci.* **2011,** *42* (1–2), 106-115.

56. Dickinson, P.; Lee, W.; Stott, P.; Townsend, A.; Smart, J.; Ghahramani, P.; Hammett, T.; Billett, L.; Behn, S.; Gibb, R.; Abrahamsson, B., Clinical Relevance of Dissolution Testing in Quality by Design. *The AAPS Journal* **2008,** *10* (2), 380-390.

57. Lennernäs, H.; Abrahamsson, B., The use of biopharmaceutic classification of drugs in drug discovery and development: current status and future extension. *J. Pharm. Pharmacol.* **2010,** *57* (3), 273-285.

58. Frizon, F.; Eloy, J. d. O.; Donaduzzi, C. M.; Mitsui, M. L.; Marchetti, J. M., Dissolution rate enhancement of loratadine in polyvinylpyrrolidone K-30 solid dispersions by solvent methods. *Powder Technol.* **2013,** *235* (0), 532-539.

59. Tong, C.; Lozano, R.; Mao, Y.; Mirza, T.; Löbenberg, R.; Nickerson, B.; Gray, V.; Wang, Q., The Value of *In Vitro* Dissolution in Drug Development. *Pharmaceutical Technology* **2009,** *33* (4), 52-64.

60. D'Souza, S. S.; Lozano, R.; Mayock, S.; Gray, V., AAPS Workshop on the Role of Dissolution in QbD and Drug Product Life Cycle: A Commentary. *Diss. Tech.* **2010,** *17* (4), 41-5.

61. Dhirendra, K.; Lewis, S.; Udupa, N.; Atin, K., Solid Dispresion: A review. *Pak. J. Pharm. Sci* **2009,** *22* (2), 234-246.

62. Sinha, S.; Baboota, S.; Ali, M.; Kumar, A.; Ali, J., Solid Dispersion: An Alternative Technique for Bioavailability Enhancement of Poorly Soluble Drugs. *J. Dispersion Sci. Technol.* **2009,** *30*.

63. Nagapudi, K.; Jona, J., Amorphous active pharmaceutical ingredients in preclinical studies: Preparation, characterization, and formulation. *Curr. Bioact. Compd.* **2008,** *4* (4), 213-224.

64. Tiwari, R.; Tiwari, G.; Srivastava, B.; Rai, A. K., Solid Dispersions: An Overview To Modify Bioavailability Of Poorly Water Soluble Drugs. *Int. J. PharmTech Res.* **2009,** *1* (4), 1338-1349.

65. Badens, E.; Majerik, V.; Horváth, G.; Szokonya, L.; Bosc, N.; Teillaud, E.; Charbit, G., Comparison of solid dispersions produced by supercritical antisolvent and spray-freezing technologies. *Int. J. Pharm.* **2009,** *377* (1–2), 25-34.

66. Vasconcelos, T.; Sarmento, B.; Costa, P., Solid dispersions as strategy to improve oral bioavailability of poor water soluble drugs. *Drug Discov. Today* **2007,** *12* (23–24), 1068-1075.

67. Brion, M.; Jaspart, S.; Perrone, L.; Piela, G.; Evrard, B., The supercritical micronization of solid dispersions by Particles from Gas Saturated Solutions using experimental design. *J. Supercrit. Fluids* **2009,** *51*, 50-56.

68. Giri, T. K.; Kumar, K.; Alexander, A.; Ajazuddin; Badwaik, H.; Tripathi, D. K., A novel and alternative approach to controlled release drug delivery system based on solid dispersion technique. *Bulletin of Faculty of Pharmacy, Cairo University* **2012,** *50* (2), 147-159.

69. Bley, H.; Fussnegger, B.; Bodmeier, R., Characterization and stability of solid dispersions based on PEG/polymer blends. *Int. J. Pharm.* **2010,** *390* (2), 165-173.

70. Ghebremeskel, A.; Vemavarapu, C.; Lodaya, M., Use of surfactants as plasticizers in preparing solid dispersions of poorly soluble API: stability testing of selected solid dispersions. *Pharm. Res.* **2006,** *23* (8), 1928-1936.

71. Patel, T.; Patel, L.; Patel, T.; Makwana, S.; Patel, T., Enhancement of dissolution of Fenofibrate by Solid dispersion Technique. *Int. J. Res. Pharm. Sci.* **2010,** *1* (2), 127-132.

72. Sun, N.; Wei, X.; Wu, B.; Chen, J.; Lu, Y.; Wu, W., Enhanced dissolution of silymarin/polyvinylpyrrolidone solid dispersion pellets prepared by a one-step fluid-bed coating technique. *Powder Technol.* **2008,** *182* (1), 72-80.

73. Janssens, S.; Denivelle, S.; Rombaut, P.; Van den Mooter, G., Influence of polyethylene glycol chain length on compatibility and release characteristics of ternary solid dispersions of itraconazole in polyethylene glycol/hydroxypropylmethylcellulose 2910 E5 blends. *Eur. J. Pharm. Sci.* **2008,** *35* (3), 203-210.

74. Dahima, R.; Pachori, A.; Netam, S., Formulation and evaluation of mouth dissolving tablet containing amlodipine besylate solid dispersion. *Int. J. ChemTech. Res* **2010,** *2* (1), 706-15.

75. ICH, Q3C(R5). Impurities: Guideline for Residual Solvent. U.S.: 2011.

76. Paudel, A.; Worku, Z. A.; Meeus, J.; Guns, S.; Van den Mooter, G., Manufacturing of solid dispersions of poorly water soluble drugs by spray drying: Formulation and process considerations. *Int. J. Pharm.* **2013,** *453* (1), 253-84.

77. Al-Obaidi, H.; Brocchini, S.; Buckton, G., Anomalous properties of spray dried solid dispersions. *J. Pharm. Sci.* **2009,** *98* (12), 4724-4737.

78. Leuenberger, H., Spray freeze-drying–the process of choice for low water soluble drugs? *J. Nanopart. Res* **2002,** *4* (1), 111-119.

79. Chung, N.-O.; Lee, M.; Lee, J., Mechanism of freeze-drying drug nanosuspensions. *Int. J. Pharm.* **2012,** *437* (1-2), 42-50.

80. De Beer, T.; Allesø, M.; Goethals, F.; Coppens, A.; Heyden, Y.; De Diego, H.; Rantanen, J.; Verpoort, F.; Vervaet, C.; Remon, J.; Baeyens, W., Implementation of a process analytical technology system in a freeze-drying process using Raman spectroscopy for in-line process monitoring. *Anal. Chem.* **2007,** *79* (21), 7992-8003.

81. De Beer, T.; Vercruysse, P.; Burggraeve, A.; Quinten, T.; Ouyang, J.; Zhang, X.; Vervaet, C.; Remon, J.; Baeyens, W., In-line and real-time process monitoring of a freeze drying process using Raman and NIR spectroscopy as complementary process analytical technology (PAT) tools. *J. Pharm. Sci.* **2009,** *98* (9), 3430-3446.

82. Sharma, P.; Kapoor, A.; Bhargava, S., A review on: Solubility enhancement by implementing solid dispersion technique for poorly water soluble drug. *Res. J. Pharm. Bio. Chem. Sci* **2012,** *3* (1), 847-859.

83. Guns, S.; Mathot, V.; Martens, J. A.; Van den Mooter, G., Upscaling of the hot-melt extrusion process: Comparison between laboratory scale and pilot scale production of solid dispersions with miconazole and Kollicoat® IR. *Eur. J. Pharm. Biopharm.* **2012,** *81* (3), 674-682.

84. DiNunzio, J. C.; Brough, C.; Miller, D. A.; Williams III, R. O.; McGinity, J. W., Applications of KinetiSol®Dispersing for the production of plasticizer free amorphous solid dispersions. *Eur. J. Pharm. Sci.* 2010, *40* (3), 179-187.

85. Hughey, J. R.; Keen, J. M.; Brough, C.; Saeger, S.; McGinity, J. W., Thermal processing of a poorly water-soluble drug substance exhibiting a high melting point: The utility of KinetiSol®Dispersing. *Int. J. Pharm.* 2011, *419* (1), 222-230.

86. Dinunzio, J. C.; Hughey, J. R.; Brough, C.; Miller, D. A.; Williams Iii, R. O.; McGinity, J. W., Production of advanced solid dispersions for enhanced bioavailability of itraconazole using KinetiSol® Dispersing. *Drug Dev. Ind. Pharm.* 2010, *36* (9), 1064-1078.

87. DiNunzio, J. C.; Brough, C.; Hughey, J. R.; Miller, D. A.; Williams Iii, R. O.; McGinity, J. W., Fusion production of solid dispersions containing a heat-sensitive active ingredient by hot melt extrusion and Kinetisol® dispersing. *Eur. J. Pharm. Biopharm.* 2010, *74* (2), 340-351.

88. Van den Mooter, G., The use of amorphous solid dispersions: A formulation strategy to overcome poor solubility and dissolution rate. *Drug Discov. Today: Technologies* **2012,** *9* (2), 79-85.

89. Singh, M. C.; Sayyad, A. B.; Sawant, S. D., Review on various techniques of solubility enhancement of poorly soluble drugs with special emphasis on solid dispersion. *J. Pharm. Res.* **2010,** *3* (10), 2494-2501.

90. Unga, J.; Matsson, P.; Mahlin, D., Understanding polymer–lipid solid dispersions—The properties of incorporated lipids govern the crystallisation behaviour of PEG. *Int. J. Pharm.* **2010,** *386* (1–2), 61-70.

91. Alazar, N. G.; Chandra, V.; Mayur, L., Use of surfactants as plasticizers in preparing solid dispersions of poorly soluble API: Selection of polymer–surfactant combinations using solubility parameters and testing the processability. *Int. J. Pharm.* **2007,** *328*.

92. Visser, M. R.; Baert, L.; Klooster, G. v. t.; Schueller, L.; Geldof, M.; Vanwelkenhuysen, I.; de Kock, H.; De Meyer, S.; Frijlink, H. W.; Rosier, J.; Hinrichs, W. L. J., Inulin solid dispersion technology to improve the absorption of the BCS Class IV drug TMC240. *Eur. J. Phar.m Biopharm.* **2010,** *74* (2), 233-238.

93. Van den Mooter, G.; Weuts, I.; De Ridder, T.; Blaton, N., Evaluation of Inutec SP1 as a new carrier in the formulation of solid dispersions for poorly soluble drugs. *Int. J. Pharm.* **2006,** *316* (1–2), 1-6.

94. Jagdale, S.; Patil, S.; Kuchekar, B.; Chabukswar, A., Preparation and Characterization of Metformin Hydrochloride - Compritol 888 ATO Solid Dispersion. *Journal of young pharmacists: JYP* **2011,** *3* (3), 197-204.

95. Araújo, R.; Teixeira, C.; Freitas, L., The preparation of ternary solid dispersions of an herbal drug via spray drying of liquid feed. *Drying Tech.* **2010,** *28* (3), 412-421.

96. Jagdale, S.; Kuchekar, B.; Chabukswar, A.; Musale, V.; Jadhao, M., Preparation and in vitro evaluation of Allopurinol-Gelucire 50/13 solid dispersions. *Int. J. Adv. Pharm. Sci.* **2011,** *1* (1).

97. Ali, W.; Williams, A.; Rawlinson, C., Stochiometrically governed molecular interactions in drug: poloxamer solid dispersions. *Int. J. Pharm.* **2010,** *391* (1-2), 162-168.

98. Tejwani, R.; Joshi, H.; Varia, S.; Serajuddin, A., Study of phase behavior of poly (ethylene glycol)–polysorbate 80 and poly (ethylene glycol)–polysorbate 80–water mixtures. *J. Pharm. Sci.* **2000,** *87* (9), 946-950.

99. Okonogi, S.; Puttipipatkhachorn, S., Dissolution improvement of high drug-loaded solid dispersion. *AAPS PharmSciTech* **2006,** *7* (2).

100. de Waard, H.; Hinrichs, W.; Visser, M.; Bologna, C.; Frijlink, H., Unexpected differences in dissolution behavior of tablets prepared from solid dispersions with a surfactant physically mixed or incorporated. *Int. J. Pharm.* **2008,** *349* (1-2), 66-73.

101. Hussain, M. D.; Saxena, V.; Brausch, J. F.; Talukder, R. M., Ibuprofen–phospholipid solid dispersions: Improved dissolution and gastric tolerance. *Int. J. Pharm.* **2012,** *422* (1–2), 290-294.

102. Newa, M.; Bhandari, K.; Oh, D.; Kim, Y.; Sung, J.; Kim, J.; Woo, J.; Choi, H.; Yong, C., Enhanced dissolution of ibuprofen using solid dispersion with poloxamer 407. *Arch. Pharmacal. Res.* **2008,** *31* (11), 1497-1507.

103. Goddeeris, C.; Van den Mooter, G., Free flowing solid dispersions of the anti-HIV drug UC 781 with Poloxamer 407 and a maximum amount of TPGS 1000: investigating the relationship between physicochemical characteristics and dissolution behaviour. *Eur. J. Pharm. Sci.* **2008,** *35* (1-2), 104-113.

104. Passerini, N.; Albertini, B.; González-Rodríguez, M.; Cavallari, C.; Rodriguez, L., Preparation and characterisation of ibuprofen-poloxamer 188 granules obtained by melt granulation. *Eur. J. Pharm. Sci.* **2002,** *15* (1), 71-78.

105. Shah, T.; Amin, A.; Parikh, J.; Parikh, R., Process optimization and characterization of poloxamer solid dispersions of a poorly water-soluble drug. *AAPS PharmSciTech* **2007,** *8* (2).

106. Bandarkar, F. S.; Khattab, I. S., Lyophilized gliclazidepoloxamer solid dispersions for enhancement of invitro dissolution and invivo bioavailability. *Int. J. Pharm. Sci.* **2011,** *3* (2), 122-127.

107. Murali Mohan Babu, G.; Prasad, C. D. S.; Ramana Murthy, K., Evaluation of modified gum karaya as carrier for the dissolution enhancement of poorly water-soluble drug nimodipine. *Int. J. Pharm.* **2002,** *234* (1-2), 1-17.

108. Mura, P.; Zerrouk, N.; Mennini, N.; Maestrelli, F.; Chemtob, C., Development and characterization of naproxen–chitosan solid systems with improved drug dissolution properties. *Eur. J. Pharm. Sci.* **2003,** *19* (1), 67-75.

109. Papageorgiou, G.; Bikiaris, D.; Kanaze, F.; Karavas, E.; Stergiou, A.; Georgarakis, E., Tailoring the release rates of fluconazole using solid dispersions in polymer blends. *Drug Dev. Ind. Pharm.* **2008,** *34* (3), 336-346.

110. Zerrouk, N.; Mennini, N.; Maestrelli, F.; Chemtob, C.; Mura, P., Comparison of the effect of chitosan and polyvinylpyrrolidone on dissolution properties and analgesic effect of naproxen. *Eur. J. Pharm. Biopharm.* **2004,** *57* (1), 93-99.

111. Bhattarai, N.; Gunn, J.; Zhang, M., Chitosan-based hydrogels for controlled, localized drug delivery. *Adv. Drug Delivery Rev.* **2010,** *62* (1), 83-99.

112. Shah, R. B.; Zidan, A. S.; Funck, T.; Tawakkul, M. A.; Nguyenpho, A.; Khan, M. A., Quality by design: Characterization of self-nano-emulsified drug delivery systems (SNEDDs) using ultrasonic resonator technology. *Int. J. Pharm.* **2007,** *341* (1–2), 189-194.

113. Urbanova, M.; Brus, J.; Sedenkova, I.; Policianova, O.; Kobera, L., Characterization of solid polymer dispersions of active pharmaceutical ingredients by 19F MAS NMR and factor analysis. *Spectrochim. Acta, Part A* **2013,** *100* (0), 59-66.

114. Yang, J.; Grey, K.; Doney, J., An improved kinetics approach to describe the physical stability of amorphous solid dispersions. *Int. J. Pharm.* **2010,** *384* (1–2), 24-31.

115. Gao, P.; Shi, Y., Characterization of Supersaturatable Formulations for Improved Absorption of Poorly Soluble Drugs. *AAPS J.* **2012,** *14* (4), 703-713.

116. Rantanen, J.; Wikström, H.; Turner, R.; Taylor, L., Use of in-line near-infrared spectroscopy in combination with chemometrics for improved understanding of pharmaceutical processes. *Anal. Chem.* **2005,** *77* (2), 556-563.

117. Abu-Absi, N.; Kenty, B.; Cuellar, M.; Borys, M.; Sakhamuri, S.; Strachan, D.; Hausladen, M.; Li, Z., Real time monitoring of multiple parameters in mammalian cell culture bioreactors using an in-line Raman spectroscopy probe. *Biotechnol. Bioeng.* **2011,** *108* (5), 1215-1221.

118. Sparén, A.; Johansson, J.; Svensson, O.; Folestas, S.; Clayborn, M., Transmission Raman spectroscopy for quantitative analysis of pharmaceutical solids. *Am. Pharm. Rev* **2009,** *12* (1), 66-71.

119. Furuyama, N.; Hasegawa, S.; Hamaura, T.; Yada, S.; Nakagami, H.; Yonemochi, E.; Terada, K., Evaluation of solid dispersions on a molecular level by the Raman mapping technique. *Int. J. Pharm.* **2008,** *361* (1-2), 12-18.

120. Rahman, Z.; Zidan, A.; Khan, M., Formulation and evaluation of a protein-loaded solid dispersions by non-destructive methods. *The AAPS journal* **2010,** *12* (2), 158-170.

121. Zidan, A.; Habib, M.; Khan, M., Process analytical technology: nondestructive evaluation of cyclosporine A and phospholipid solid dispersions by near infrared spectroscopy and imaging. *J. Pharm. Sci.* **2008,** *97* (8), 3388-3399.

122. Saerens, L.; Dierickx, L.; Lenain, B.; Vervaet, C.; Remon, J. P.; Beer, T. D., Raman spectroscopy for the in-line polymer–drug quantification and solid state characterization during a pharmaceutical hot-melt extrusion process. *Eur. J. Pharm. Biopharm.* **2011,** *77*.

123. Konno, H.; Handa, T.; Alonzo, D. E.; Taylor, L. S., Effect of polymer type on the dissolution profile of amorphous solid dispersions containing felodipine. *Eur. J. Pharm. Biopharm.* **2008,** *70* (2), 493-499.

124. Newman, A.; Knipp, G.; Zografi, G., Assessing the performance of amorphous solid dispersions. *J. Pharm. Sci.* **2012,** *101* (4), 1355-1377.

125. Chow, K.; Tong, H. H. Y.; Lum, S.; Chow, A. H. L., Engineering of Pharmaceutical Materials: An Industrial Perspective. *J. Pharm. Sci.* **2007,** *97* (8), 2855-2877.

126. O'Driscoll, C. M.; Griffin, B. T., Biopharmaceutical challenges associated with drugs with low aqueous solubility—The potential impact of lipid-based formulations. *Adv. Drug Delivery Rev.* **2008,** *60* (6), 617-624.

127. Beg, S.; Swain, S.; Rizwan, M.; Irfanuddin, M.; Shobha Malini, D., Bioavailability enhancement strategies: basics, formulation approaches and regulatory considerations. *Curr. Drug Delivery* 2011, *8* (6), 691-702.

128. Cano-Cebrian, M. J.; Zornoza, T.; Granero, L.; Polache, A., Intestinal absorption enhancement via the paracellular route by fatty acids, chitosans and others: a target for drug delivery. *Curr. Drug Delivery* 2005, *2* (1), 9-22.

129. Florence, A. T.; Attwood, D., *Physicochemical Principles of Pharmacy*. Fourth edition ed.; Pharmceutical Press: London; Chicago, 2006; p 513.

130. FDA, Guidance to industry: Waiver of *in vivo* BA and BE studies for immediate release solid oral dosage forms based on a biopharmaceutical classification system. 2000.

131. Lennernäs, H.; Aarons, L.; Augustijns, P.; Beato, S.; Bolger, M.; Box, K.; Brewster, M.; Butler, J.; Dressman, J.; Holm, R.; Julia Frank, K.; Kendall, R.; Langguth, P.; Sydor, J.; Lindahl, A.; McAllister, M.; Muenster, U.; Müllertz, A.; Ojala, K.; Pepin, X.; Reppas, C.; Rostami-Hodjegan, A.; Verwei, M.; Weitschies, W.; Wilson, C.; Karlsson, C.; Abrahamsson, B., Oral biopharmaceutics tools – Time for a new initiative – An introduction to the IMI project OrBiTo. *Eur. J. Pharm. Sci.* In Press.

132. Fahmy, R.; Kona, R.; Dandu, R.; Xie, W.; Claycamp, G.; Hoag, S. W., Quality by Design I: Application of Failure Mode Effect Analysis (FMEA) and Plackett–Burman Design of Experiments in the Identification of "Main Factors" in the Formulation and Process Design Space for Roller-Compacted Ciprofloxacin Hydrochloride Immediate-Release Tablets. *AAPS PharmSciTech* 2012, *13* (4), 1243-1254.

133. Claycamp, H. G., Perspective on quality risk management of pharmaceutical quality. *Drug information journal* 2007, *41* (3), 353-367.

134. Shrivastava, A. R.; Ursekar, B.; Kapadia, C. J., Design, optimization, preparation and evaluation of dispersion granules of valsartan and formulation into tablets. *Curr. Drug Delivery* 2009, *6* (1), 28-37.

135. Katharia, A.; Kumar, R.; Sharma, R.; Singh, Y.; Teotia, U. V. S., Statistical Optimization of Olanzapine Ternary Solid Dispersions with Pvp K 30 and Peg 20,000 by Response Surface Methodology. *J. Appl. Pharm. Sci.* 2013, *3* (9).

136. Keen, J. M.; McGinity, J. W.; III Williams, R. O., Enhancing Bioavailability through Thermal Processing. *Int. J. Pharm.* 2013.

137. Patel, A.; Agrawal, A.; Dave, R., Development of polyvinylpyrrolidone-based spray-dried solid dispersions using response surface model and ensemble artificial neural network. *J. Pharm. Sci.* 2013, *102* (6), 1847-1858.

138. Patel, A.; Agrawal, A.; Dave, R., Investigation of the effects of process variables on derived properties of spray dried solid-dispersions using polymer based response surface model and ensemble artificial neural network models. *European journal of pharmaceutics and biopharmaceutics: official journal of Arbeitsgemeinschaft fur Pharmazeutische Verfahrenstechnik e.V* 2013.

139. Guo, Z.; Lu, M.; Li, Y.; Pang, H.; Lin, L.; Liu, X.; Wu, C., The utilization of drug–polymer interactions for improving the chemical stability of hot-melt extruded solid dispersions. *J. Pharm. Pharmacol.* 2013, n/a-n/a.

140. van Arnum, P., Bioavailability enhancement: When to use hot-melt extrusion versus spray drying: A Q&A with bend research. *Pharmaceutical Technology* 2012, *36* (8), 44-50.

141. Agrawal, A. M.; Dudhedia, M. S.; Patel, A. D.; Raikes, M. S., Characterization and performance assessment of solid dispersions prepared by hot melt extrusion and spray drying process. *Int. J. Pharm.* 2013, *457* (1), 71-81.

142. Tian, Y.; Caron, V.; Jones, D. S.; Healy, A. M.; Andrews, G. P., Using Flory–Huggins phase diagrams as a pre-formulation tool for the production of amorphous solid dispersions: a comparison between hot-melt extrusion and spray drying. *J. Pharm. Pharmacol.* 2013.

143. Ende, D. a.; Bronk, K. S.; Mustakis, J.; O'Connor, G.; Santa Maria, C. L.; Nosal, R.; Watson, T. J. N., API Quality by Design Example from the Torcetrapib Manufacturing Process. *J. Pharm. Inno.* 2007, *2*, 71-8.

C. Nano-delivery systems[2]

Chapter

Nanocarriers as strategy for oral bioavailability improvement of poorly water-soluble drugs

Luíse L. Chaves[1], Alexandre C. Vieira[1], Domingos Ferreira[2], Bruno Sarmento[3], Salette Reis[1], Sofia A. Costa Lima[1]

[1]UCIBIO/REQUIMTE, Department of Chemical Sciences, University of Porto, Rua Jorge Viterbo Ferreira, 228, Porto, Portugal
[2]Laboratório de Tecnologia Farmacêutica, Departamento de Ciências do Medicamento, Faculdade de Farmácia, Universidade do Porto, Portugal.
[3]I3S, Instituto de Investigação e Inovação em Saúde, Universidade do Porto, Portugal; INEB - Instituto de Engenharia Biomédica, Universidade do Porto, Portugal; CESPU, Instituto de Investigação e Formação Avançada em Ciências e Tecnologias da Saúde and Instituto Universitário de Ciências da Saúde, Gandra PRD, Portugal.

The oral route is still considered the most used way of administration due to its non-invasive nature and high patient compliance. However, the low solubility of drugs often results in poor bioavailability (BA) and, consequently, to inconstant plasma concentrations. The use of nanoformulations is one of the most promising strategies to overcome this issue due to their significant enhancement in the solubility and intestinal permeation. The major purpose of this chapter is to outline the main nanosystems commonly used to improve solubility of poorly-soluble drugs.

1. Introduction

The major portion of the drug delivery market is occupied by oral drug delivery systems [1]. The oral route is still considered the most convenient route for drug administration as it offers a high patient compliance allowing a flexible and controlled dosing schedule, especially important for chronic therapy [2]. It is associated with the low costs for both industry and patient, when compared to other administration routes [3]. Apart of the highlighted attributes, therapeutic efficacy of oral delivery systems is often concealed due

[2] Chaves, L., *et al*., Nanocarriers as strategy for oral bioavailability improvement of poorly water-soluble drugs, in Nanoparticles in the Life Sciences and Biomedicine. 2017, Pan Stanford Publishing. ISBN 978-981-4745-98-7.

to certain factors associated with physicochemical, anatomical, and biochemical, as well as physiological constraints [4]. Despite this complexity, the fundamental events controlling oral drug absorption are the solubility/dissolution of the drug in the gastrointestinal (GI) environment, and its permeability through the GI tract [4], which are the main causes of poor oral BA [5].

Nanocarriers have attracted increasing attention in recent years, for oral chemotherapy particularly for poorly soluble drugs [6]. Incorporation of drugs inside an appropriate nanocarrier seems to be a promising strategy, since the biodistribution of the drug will be dictated by the properties of the nanocarriers and not by the drug molecule itself [7].

This chapter will address the most commonly used nanocarriers to improve the BA of poorly soluble drugs, focusing on the main challenges during their formulation, the mechanisms of internalization, and the characterization techniques for nanocarriers with poorly soluble drugs.

2. Oral bioavailability

Oral BA is strictly related to pharmacokinetics of drugs and comprises two essential features: the rate of absorption which means how fast the drug enters the systemic circulation; and the extent of absorption which determines how much of the initial dosage reaches the circulation [6]. For both parameters, the solubility/dissolution rate is crucial since it determines how fast a drug reaches a maximum concentration in the luminal intestinal fluid, becoming available to be absorbed [8]. When a drug presents poor BA, the recommended dosage must be higher, as only a fraction of the drug enters the systemic circulation and reaches the site of action. On the other hand, a high drug dosage is often associated with the side effects and increased costs [6]. Poorly water-soluble drugs often exhibit slow dissolution in the GI tract, ultimately limiting their absorption [4].

Nowadays, poorly soluble compounds represent approximately 40% of the top oral marketed drugs. In addition, they stand for 90% of new chemical entities. This characteristic of poor water-solubility seems to be a tendency in the drug discovery field due to the sources used for this purpose such as combinatorial chemistry and high throughput screening, in which both aim to maximize drug-receptor interaction by stressing hydrophobic interactions [5].

A better understanding of the physicochemical and biopharmaceutical properties of drugs is not only helpful to develop new pharmaceutical products with already approved drugs, but also important during the screening of new drug candidates, allowing to identify potential absorption problems after oral administration [8]. In 1995, Amidon and co-workers stablished a Biopharmaceutical Classification System (BCS) based on their

solubility and intestinal permeability [9]. According to the Food and Drug Administration (FDA), a drug substance is considered "highly permeable" when the extent of absorption in humans is determined to be 90% or more of an administered dose, while is considered "highly soluble" when the highest dose strength is soluble in 250 mL or less of aqueous media over the pH range of 1–7.5 at 37 ºC [9, 10].

The BCS categorizes drug substances in four categories: high solubility/high permeability (class I), low solubility/high permeability (class II), high solubility/low permeability (class III), and low solubility/low permeability (class IV) [9]. Regarding formulation design, BCS can provide an indication of the experimental work difficulty. For instance, pharmaceutical formulations containing drugs belonging to class I or III can be prepared with a simple strategy, while for class II and IV drugs, formulation designs are often required [8].

Recently, the application of nanotechnology to improve BA of poorly water-soluble drug through incorporation in nanocarriers is gaining attention, as drug molecules size is reduced to the nanometer range. By downsizing drug molecules, thermodynamic and kinetic characteristics of the drug changes [6], and leads to a saturation solubility in the GI mucosa, thus consequent greater gradient concentration for drug absorption [11]. The nanocarriers affect drug molecules interfacial energy resulting in colloidal instability and spontaneous aggregation into a more thermodynamically stable state [12].

3. Nanocarriers for oral delivery

Nanocarriers are generally defined as a nanometer size scale system, consisting of at least two components in which one is the active compound [2].

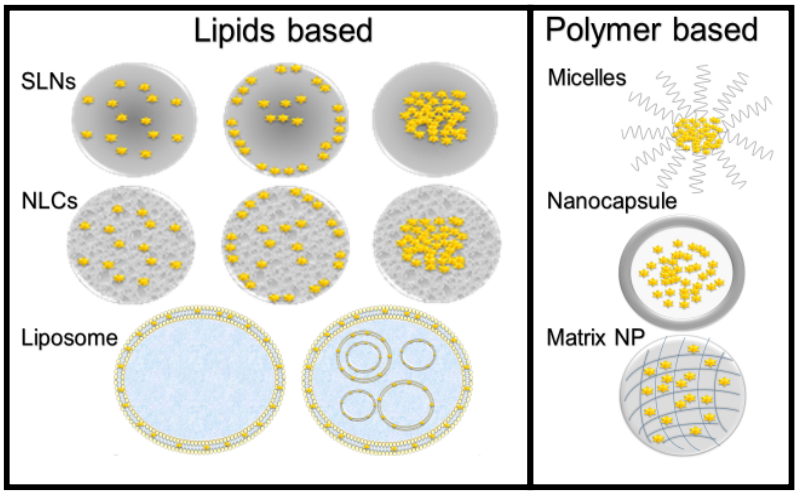

Figure 1. Different classes and types of nanocarriers.

The use of nanocarriers to encapsulate poorly soluble drugs offers additional advantages such as protection of the drug from GI degradation, improved circulation half-life, active and passive targeting to specific intestinal cells, reduced systemic side effects, co-delivery of multiple drug combinations using a single nanocarrier and the possibility to modulate drug release, which is often appropriate [7]. In addition, they may improve the oral BA by overcoming the first-pass effect and/or P-glycoprotein efflux, and enhancing cellular uptake [3].

There are several nanocarriers (Figure 1) already used for this purpose namely lipid-, phospholipid- or polymer-based, which may be designed case by case, in order to optimize their physicochemical features as well as *in vivo* efficacy [7]. In the case of lipophilic molecules only nanocarriers with enough high lipophilicity should be used.

The various types of nano-architectures mostly used to improve BA of poorly soluble drugs upon oral administration and their features will be addressed in the subsequent sections [11].

3.1 Polymeric-based nanocarriers

3.1.1 Polymeric nanoparticles

Polymeric nanoparticles are solid particles ranging from 10 to 1000 nm in size [13] and, compared to the lipid-based nanocarriers, have advantages such as higher stability in the GI tract, mainly in acidic environment, and possibility to achieve a more controlled drug release by modulating physicochemical characteristics [6].

Polymeric-based nanocarriers can be divided into two categories namely nanocapsules, which are vesicular systems with core like ”reservoir-type” where the drug is confined; or nanospheres, that are matrix systems where the drug may be uniformly dispersed. In the case of nanocapsules, the inner phase may store the drug in liquid (oily phase or water with surfactant) or solid state as a molecular dispersion, depending on the preparation method and raw materials used, which is an advantage compared to the nanospheres especially for poorly soluble drugs [13].

Nanoparticles may be composed of synthetic or natural polymers and their choice affects directly the drug association efficiency [14]. The synthetic polymers mostly used to formulate polymeric nanoparticles are polyesters derivatives such as polylactide (PLA), polylactide–polyglycolide copolymers such as poly(lactic-co-glycolic acid) (PLGA), polycaprolactones (PCL), and polyacrylates (PCA). PLGA is the most widely used polymer due to its biocompatibility and already described predictable biodegradability [6]. Natural polymers, also called biopolymers due to their biocompatibility, may also be used to

obtain nanoparticles. In general, biopolymers, such as alginate and albumin, exhibit lower immunogenicity than synthetic ones [14], and may also provide additional features as mucoadhesion and the possibility to chemical modification as chitosan [6].

Table 1. Examples of polymeric nanocarriers as oral delivery systems with poorly soluble drugs, and their main characteristics

Drug	Therapeutic class	Excipient(s)	Diameter (nm)	AE / LC (%)	Ref
Atazanavir*	Antiretroviral	Eudragit RL 100	466	60 / n.a.	[15]
Atorvastatin*	Antilipidemic	Zein	183	30 / 15	[16]
Celecoxib*	Anti-inflammatory	Ethyl cellulose	100-150	n.a / 10-50	[17]
Daidzein*	Hypertension, coronary heart disease, cerebral thrombosis, and menopause syndrome	PLGA	309-323	81-83 / 1.3-1.8	[18]
Lopinavir*	Antiretroviral	PCL	195	94 / n.a	[19]
Resveratrol*	Chemopreventive, cardiopreventive, antioxidant, anti-inflammatory	PLGA	170	78 / n.a	[20]
Paclitaxel**	Antineoplasic	Poly(anhydride)	178 - 188	75 -88 / n.a	[21]

*Belongs to Class II; **Belongs to Class IV

Regarding the method of fabrication, different methods can be reported such as nanoprecipitation, emulsion/solvent evaporation or emulsification, depending on the nature of the polymer as well as on the drug to be encapsulated [22]. One of the major disadvantages of the polymeric nanoparticles is the use of solvents, irrespective to the method of choice. The solvent choice is quite relevant for a successful encapsulation of poorly soluble drugs, as their proportion directly influence particle size and drug association efficiency [14].

When the objective is to encapsulate lipophilic drugs, the organic phase contains the polymer together with the drug. The emulsion-solvent evaporation is the most common method used to prepare polymeric nanoparticles, though the encapsulation of water-insoluble drugs is yet quite challenging [23]. It is crucial to define and control the critical parameters of the nanoparticles synthesis since they affect their physicochemical characteristics.

Polymeric nanoparticles increased the rate and extent of oral absorption of class II (eg. atazanavir, atorvastatin, celecoxib, daidzen, lopinavir and resveratrol) and class IV (eg. paclitaxel) drugs, resulting in augmentation in the values of drug plasma levels thus significant enhancement in the rate and extent of BA by the nanocarriers compared to

pure drug [17-23]. Table 1 illustrates some of the diversity of polymeric-based nanocarriers to improve BA of poorly soluble drugs.

3.1.2 Polymeric micelles

Polymeric micelles are nanosystems with an average hydrodynamic diameter less than 100 nm [24], composed by amphiphilic block co-polymers, with self-assemble properties. They are characterized by a core-shell structure, in which the core is a dense grid formed by the hydrophobic fragments, while the shell has hydrophilic characteristics [25]. One of the most commonly used hydrophilic fragment is poly(ethyleneglycol) (PEG), although other have been explored such as poly(N-vinylpyrrolidone) (PVP) and PCA.

For the hydrophobic core, cationic or anionic polymers may be used, although biodegradable polymers, such as PCL, PLA and poly(amino acids), are expected to be more promising for *in vivo* administration than the non-degradable ones [26]. They have the special feature of loading drugs with low solubility since their core serves as a reservoir due to the non-covalent hydrophobic drug/ polymer interactions, thus confer chemical stability to the drug inside the micelles [24]. Hydrophobic core characteristics are critical to determine the micelles loading capacity, and may be assessed by evaluating the degree of polarity between the drug and the polymer hydrophobic fragments [24].

By physical entrapping poorly-soluble drugs, polymeric micelles have the ability to increase their intrinsic water solubility and consequently drug BA in the targeted site of action. They generally have high thermodynamic stability and, compared to polymeric nanoparticles, they do not need organic solvent to be produced, which decrease the possibility of toxicity.

Besides polymer-drug miscibility, another important parameter that governs the association efficiency is the hydrophilic-lipophilic balance of the block co-polymers as well as polymer/ drug (P/D) ratio. As general rule, block co-polymers with longer hydrophobic fragments seem to promote a higher lipophilic drug loading. Furthermore, the drug loading tends to increase with the decreasing of the P/D ratio. Optimization of this parameter for lipophilic drugs allows high drug loading with minimum amount of polymer, as smaller amounts of polymer will be required for solubilizing a higher amount of drug [24].

Despite the advantages of the use of micelles to deliver poorly soluble drugs, their stability, mainly in physiological environment, is still an issue. Once administered, the micelles must resist to premature dissociation after dilution in the stomach and remain intact until reach intestinal environment. One of the parameters that dictate their stability is the critic micellar concentration (CMC) of the system. In general, lower CMC values

denote more resistance to effects of dilution and therefore confer greater stability [24]. Another disadvantage of micellar systems is their biocompatibility and cytotoxicity. Clinical studies have shown that these systems often may lead to unexpected adverse side effects. Minimal options of co-polymers that are safe are available and have been studied. On the other hand, there is still a lack of information about the effects that the amphiphilic co-polymers produce after oral administration. Thus, it is important to get know-how on the safety of micellar systems, by *in vitro* and *in vivo* studies [24].

Recently, Class II (efavirenz) and Class IV (oxcarbazepine, quercetin and paclitaxel) drugs were successfully incorporated into polymeric micelles (Table 2). Reports indicate for paclitaxel micelles higher *in vitro* cytotoxicity when compared with commercial formulation and the effective targeting to M-cells by micelles incorporating efavirenz with higher anti-HIV activity as compared to that of free drug. *In vivo* assays have been described with improvement quercetin BA by polymeric micelles as compared to free drug.

Table 2. Examples of micelles developed for oral delivery of poorly soluble drugs, and their main characteristics

Drug	Therapeutic class	Excipient(s)	Diameter (nm)	AE/ LC (%)	Ref
Efavirenz[*]	Antiretroviral	Carboxylated functional Pluronic F127	140	n.a / > 10	[27]
Oxcarbazepine[**]	Antiepileptic	Pluronic P84, F127 and F108	15-28	11-98 / n.a --	[28]
Paclitaxel[**]	Antineoplasic	H40-PCL-*b*-PCA-*b'*-methoxy PEG/PEG-folate	450	62 / 10	[29]
Quercetin[**]	Anti-inflammatory, antioxidant, anticancer	Soluplus®	79	96 / n.a	[30]

[*]Belongs to Class II; [**]Belongs to Class IV

3.2 Lipid-based nanocarriers

Lipid-based nanocarriers seem to have the most suitable features to load poorly soluble drugs since they may offer high drug loading, present suitable long-term storage stability and are feasible to scale-up compared to other colloidal carriers [31].

The variety of materials available, the biocompatibility of the lipids and other lipophilic substances as phospholipids and their ability to improve oral BA have made lipid

nanocarriers very attractive for oral delivery [1]. Lipid nanocarriers may enhance the solubility of lipophilic drugs through their interaction with the intestinal microenvironment and by modifying drug release, which prevent the supersaturation of the drug and consequent precipitation in the intestinal lumen, leading to BA improvement [32].

Furthermore, lipid systems may stimulate intestinal lymphatic drug transport, and the interaction with enterocyte-based transport processes, which can reduce undesired effects and may be of particular interest for dietary lipids and certain highly lipophilic compounds (for example, lipid-soluble vitamins and drugs) [32].

On the other hand, lipid nanocarriers are not universal platforms to delivery poorly soluble drugs due to the fact that lipophilic drugs do not necessarily display a high solubility in lipid phase. Therefore, besides the solubilization of the drug in the lipid phase, the partition of the drug between aqueous and oil phase should be taken into consideration.

A number of nanocarriers based on biocompatible lipids and oils have been efficiently used to improve the BA of poorly soluble drugs. The most commonly used will be discussed in this section.

3.2.1 Liposomes

Liposomes are vesicular structures made of natural or synthetic amphiphilic phospholipids that spontaneously self-assemble into bilayers when in contact with aqueous medium. Depending on the production conditions, they can form unilamellar or multilamellar vesicles, which make their size vary from 50 to >1000 nm. Inside the circular structures of the phospholipids, they form an aqueous compartment. Thus, due to its amphipathic nature, they are able to enclose hydrophilic drugs in the aqueous core and lipophilic drugs within the phospholipid membrane [14].

The most common production method of liposomes for drug delivery is based on the dehydration-rehydration technique, since it may provide a higher drug loading efficiency as compared to other methods [14]. Particularly for poorly soluble drugs, achieving a high drug loading is quite challenging, as the aqueous core space is much higher in comparison to the lipid bilayer that limits the accommodation of large amounts of drug. Thus, for drugs with very lipophilic characteristics, the utilization of multilamellar liposomes would be a better strategy, as their lipid bilayers structural organization should entrap more lipophilic drugs, compared to unilamellar vesicles. The composition of the bilayer can be easily changed in order to achieve a suitable partition between the drug and the phospholipid layer, without disrupting the integrity of the liposomal system [33].

There are still challenges regarding their stability under physiological conditions, mainly in the GI tract [39]. Once in the gastric environment, the phospholipids are found to be highly susceptible to gastric acid, bile salts and lipases, whose destructive effects commonly lead to losing of the liposomal integrity and leakage of the drug. In addition, even if the liposomes can reach the intestinal lumen, another challenge is the permeation of the vesicles across the GI epithelia due to its physicochemical characteristics and the presence of the mucus layer [40]. In order to overcome these limitations, many attempts have been made to ameliorate their stability by modifying constituents, and to improve liposomal BA. Surface modification is one of the most used strategy as this parameter may alter both stability and introduce new functionalities to improve their cellular internalization [40]. The surface modification may be achieved by the attachment of surfactants as bile salts or polysorbates (Tweens), or by coating with functional polymers such chitosan or PEG [40]. For instance, chitosan may increase the liposome residence time in the intestinal mucosa due to its mucoadhesive properties, leading to an enhanced BA [40].

Table 3 Examples of liposomes as oral delivery systems with poorly soluble drugs, and their main characteristics

Drug	Therapeutic class	Excipient(s)	Diameter (nm)	AE / LC (%)	Ref
Daidzein*	Hypertension, coronary heart disease, cerebral thrombosis, and menopause syndrome	Soybean phospholipid, sodium oleate and glycerol monostearate	45	92 / n.a	[34]
Resveratrol*	Chemopreventive, cardiopreventive, antioxidant, anti-inflammatory	Distearoyl phosphatidyl choline and cholesterol	493	92-100 / n.a	[35]
Cyclosporine A**	Immunosuppressant	Cholesterol and lecithin	63 - 72	~98 / ~9	[36]
Nimodipine**	Cardiovascular agent	Soybean phospholipid	317 - 379	73-85 / n.a	[37]
Sorafenib**	Antineoplasic	Lipoid e80 cholesterol	165	91 / 4	[38]

*Belongs to Class II; **Belongs to Class IV

Recently, polymersomes have been applied to improve oral BA of poorly soluble drugs, as they exhibit enhanced stability and tunable properties [41]. These polymeric nanocarriers are self-assembled vesicles similar in the structure and function to liposomes. To improve incorporation of low water soluble drugs an amphiphilic β-cyclodextrin-centered tri-arm star polymer (mPEG2k-PLA3k)3-CD is used resulting in a considerable drug loading capability.

In vivo assays revealed that Class IV drugs (e.g. nimodipine, sorafenib and cyclosporine A) incorporated into liposomes exhibited higher drug plasma level and improved biological activity as compared to free drug. Few reports indicate higher pharmacokinetic profile of Class II drugs (daidzein and resveratrol) loaded in liposomes than plain drug. Table 3 shows the potential of liposomes to enhance BA of poorly soluble drugs for oral administration.

3.2.2 Solid lipid nanoparticles

Solid lipid nanoparticles (SLN) are composed by lipids that are solid at room temperature, and in aqueous medium, the colloidal system must be stabilized by an emulsifier. The resultant nanosystem generally contains submicron particles with size between 50 and 1,000 nm [31].

SLN combine advantages of polymeric nanocarriers such as possibility to achieve a drug controlled release and efficient encapsulation, together with the biocompatibility of the material used as in the case of lipid-based nanocarriers [33]. Additional advantages of SLN include: improved stability both in storage and in the GI tract, feasibility to scale-up, low cost, and production without the use of organic solvents [1].

A broad range of solid lipids with huge degrees of polarity are available to produce SLN, ranging from non-polar, as triglycerides and waxes through glyceride mixtures, to fatty acids and emulsifying wax. Furthermore, many surfactants may also be used to stabilize the nanoformulation as phospholipids, bile salts, non-ionic surfactants as polysorbates and poloxamers [32]. In addition, particularly for poorly soluble drugs, the possibility to screen different biocompatible lipid compositions according to their compatibility with the drug is an added value, as this kind of study may improve physicochemical characteristic of the systems as well as drug association.

Regarding the methods of production, SLN are usually produced by the formation of an oil-in-water emulsion, followed by the solidification of the dispersed lipid phase. Other methods have been reported such as high-shear homogenization, high-pressure homogenization and ultrassonication. Still, the production of lipid nanocarriers with suitable diameter and narrow polydispersity index remains a challenge, and a critical step during SLN design [3].

Depending on the method of production and on the constituents, the drug may be incorporated into the particles in different ways. For example, high-pressure homogenization process usually produces particles with matrix-like behavior, in which the drug is dispersed molecularly in the lipid phase. On the other hand, in the case of drug enriched shell type, the drug is dispersed in the outer shell of the lipid phase, which

happens when phase separation occurs during cooling process. The drug may also stay in the inner core of the nanocarrier when the drug concentration is close to the saturation solubility in the lipid, and starts to precipitate, while a lipid shell with fewer drugs is formed around the core [42].

The crystallinity of the solid lipids is one of the most important issues during SLN design, which are commonly associated with polymorphism and dynamic transition, leading to low drug incorporation, drug expulsion and consequent drug release due to the lipid rearrangement, and tendency to particle aggregation [42].

In vitro studies described an improved cytotoxicity of classe II (eg. paclitaxel) drugs when loaded in SLNs as compared to free drug, and also enhanced drug cellular uptake, suggesting potential as an oral drug delivery system. Others report biocompatibility of SLN containing class II drugs (risperidone) and enhanced *in vitro* permeability for class IV drug curcumin loaded in SLN. *In vivo* assays revealed oral BA improvement for class II drugs (eg. Efavirenz, raloxifene, miconazole, glibenclamide, dapsone) when delivered by SLN in comparison to plain drug. Some Class II and Class IV compounds have been successfully incorporated into SLN for enhanced oral BA and are detailed on Table 4.

Table 4. Examples of SLN as oral delivery systems with poorly soluble drugs, and their main characteristics

Drug	Therapeutic class	Excipient(s)	Diameter (nm)	AE / LC (%)	Ref
Dapsone[*]	Antibiotic	Cetyl palmitate	308	68 / 17	[43]
Efavirenz[*]	Antiretroviral	Compritol 888 ATO	160	86 / 39	[44]
Glibenclamide[*]	Antidiabetic	Gelucire 44/14 Precirol® ATO5	105-112	20-70 / n.a	[45]
Miconazole[*]	Antifungal	Precirol ATO5	22	90 / n.a	[46]
Raloxifene[*]	Prevention and treatment of osteoporosis	Glyceryl tribehenate	167	92 / n.a	[47]
Curcumin[**]	Antioxidant, anti-inflammatory, antibacterial, antifungal and chemopreventive	Compritol 888 ATO	270	80 / 2	[48]
Paclitaxel[**]	Chemotherapeutic agent	Stearic acid	251	71 / n.a	[49]

[*]Belongs to Class II; [**]Belongs to Class IV

3.2.3 Nanostructured lipid carriers

In order to overcome some drawbacks associated with the SLN, mainly regarding stability and loading capacity, a second generation of lipid-based nanocarriers were developed. The nanostructured lipid carriers (NLC) are systems composed by a blend in appropriate proportion of solid and liquid lipids as a core matrix, in which the final physical state is still solid [50].

Table 5 Examples of NLC as oral delivery systems with poorly soluble drugs, and their main characteristics.

Drug	Therapeutic class	Excipient(s)	Diameter (nm)	AE / LC (%)	Ref
Budesonide[*]	Corticosteroid	Precirol ATO 5 and miglyol 812	204	96 / n.a	[51]
Resveratrol[*]	Chemopreventive, cardiopreventive, antioxidant, anti-inflammatory	Cetyl palmitate, miglyol 812	150-250	≈70 / n.a	[52]
Vinpocetine[*]	Vasodilators, treatment of chronic cerebral vascular ischemia, acute stroke, senile cerebral dysfunction and alzheimer's disease	Compritol 888 ATO or monostearin, miglyol 812	136	95 / 2	[53]
Curcumin[**]	Antioxidant, anti-inflammatory, antibacterial, antifungal and chemopreventive	Precirol ATO 5 and miglyol 812	280	95 / n.a	[54]
Saquinavir[**]	Antiretroviral	Precirol ato 5, miglyol 812	165- 1090	99 / 1	[55]

[*]Belongs to *Class II; [**]Belongs to Class IV

The presence of liquid and solid lipids allow the immobilization of higher amounts of drugs, compared to SLN, thus increasing the loading capacity, and prevent the premature expulsion of the drug, providing a greater long-term stability. This happens due to the chemical differences between the two types of lipids, which lead to imperfections inside the matrix. The larger this imperfection, the higher is the association efficiency, which can be modulated by varying the ratio solid/ liquid lipid, and their composition [50]. Another mechanism by which NLC may improve drug loading is probably by the partition of the solubilized drug between solid/liquid lipids. Many times, in SLN the drug is soluble in molten lipids before preparation and reaches saturation, but during the cooling phase it may precipitate resulting in immediate expulsion of the drug. In NLC, this saturation may not occur as the solubilized drug may be partitioned within solid and liquid lipid, as they

have different polarity, avoiding the precipitation [50]. This feature is even more important when the drug used has very high lipophilicity, since the lipids are able to solubilize easier these types of drugs.

Unlike SLN, NLC may exhibit a biphasic drug release, i.e., an initial burst release followed by a second release phase more controlled. This fact occurs due to the presence of a considerable amount of drug in the outer oily layer of the nanocarriers, which is rapidly expulsed; while in the second release phase the drug is released at a constant rate from the lipid core. Modulation of the release profiles as a function of the lipid matrix composition is very advantageous. These single features make nowadays, NLC the "smarter" lipid systems, having improved properties in contrast to other lipid-based formulations [50].

Table 5 presents some examples of these lipid nanocarriers for oral delivery of poorly soluble drugs from class II and IV. Few reports indicate *in vitro* potential of NLC to improve oral BA of class IV (eg. saquinivir) and class II drugs (eg. resveratrol). *In vivo* studies revealed the contribution of NLC significantly improve the biological activity of classe IV (eg. curcumin) and class II (eg. budenoside) drugs and in few cases enhanced oral BA (eg. vinpocetine).

3.3 Oral absorption: crossing the intestinal barrier

The understanding of how different nanocarriers interact with biological systems is important as it dictates the rate of absorption to reach systemic circulation and where the medicinal effects take place [56]. For oral route, the absorption step involves several stages and is determined by the drug's physicochemical and formulation properties.

The human GI tract is a dynamic structure that, besides the role of absorption, acts as an efficient barrier against undesired bacteria and toxins. To overcome this barrier is still a challenge during the development of drug nanosystems for oral delivery [4]. Upon ingestion, the first obstacle for nanosystems is to retain their integrity in the complex gastric medium, that contains numerous compounds such as bile salts, ions, lipids, cholesterol, and enzymes, and an extremely acidic pH environment [4]. Afterwards, upon reaching the small intestine portion, where approximately 90% of the absorption occurs, nanocarriers can be absorbed or internalized.

In the intestinal lumen nanocarriers find at the mucus layer, which cover the epithelium and is constantly renewed. The mucus consists of mucin glycoproteins, enzymes, electrolytes and water, and due to its cohesive and adhesive nature, the passage of nanocarriers with certain physicochemical properties may be a challenge [57]. To overcome this drawback, development of nanosystems with mucoadhesion properties may increase the residence time at the absorption site [14].

Below the mucus layer, particles will find the intestinal epithelium which is formed by a monolayer composed by a heterogeneous population of cells derived from undifferentiated cells called crypt. The cells from the crypt may differentiate into absorptive cells (enterocytes); mucus secreting cells (goblet); endocrine cells; Paneth cells, which secrete large amounts of protein-rich materials; and in M cells that compose a lymphoid region called Peyer's patches, which are specialized in antigen sampling [4].

Despite this heterogeneity, the enterocytes are the most predominant cells in the intestine. Although the mechanisms by which they absorb or internalize nanocarriers varies and will be addressed in the next section. In addition, M cells also represents a target in the drug delivery framework due to its specialization in phagocytosis, which may be useful to transfer nanocarriers from the lumen to the basolateral membrane, where there are several populations of lymphocytes and mononuclear phagocytes, as macrophages, which serves as host cells for innumerous diseases [4]. Despite this heterogeneity, the enterocytes are the most predominant cells in the intestine.

3.4 Nanocarrier absorption mechanisms

Oral absorption initiates in the mouth and follows to the stomach, small intestinal until reaching the colon. This process occurs throughout the GI tract membranes by mechanisms of passive transport and carrier-mediated transport. The primary route of membrane permeation for many drugs and small size nanocarriers, in several cells of the intestinal membrane, is the passive diffusion. Drugs with low passive permeation are often transported through a transport carrier, and ligand-targeted nanocarriers by an endocytosis-mediated mechanism.

Biological cell membranes are fluidic hydrophobic barriers composed of a lipid bilayer, cholesterol and membrane anchor proteins (eg. transporters).

3.4.1 Passive transport

Passive diffusion occurs when substances (free drug or drug nanocarriers) diffuse across a cell membrane from a region of high concentration to one of low concentration. It can take place by two pathways: the paracellular pathway, in which substances diffuses through the intercellular space between the intestinal enterocytes [58]; and the transcellular (or lipophilic) pathway, which requires substances travel through the cell, passing through both the apical membrane and basolateral membrane (Figure 2).

The tight junctions between the intestinal enterocytes are negatively charged, thus positively charged substances cross through more readily and negatively charged

substances are repelled [59]. Paracellular route (Figure 2, II) represents less than 0.01% of the total surface area of intestinal membrane, and closer to the colon the junctional complex become tighter. The transcellular route (Figure 2, I) is the major responsible for the intestinal absorption of substances. It involves the movement of substances based on a diffusion gradient and may include transcellular diffusion, active carrier mediated transportation (Figure 2, IV) and transcytosis (Figure 2, V). The physicochemical properties of the substances control the rate of transport through the transcellular pathway [60].

The lipid bilayer portion of the cell membrane is fluidic with no specific binding sites, thus passive transport is not saturable, not subject to inhibition, and non-sensitive to molecules stereospecific structure [61]. The lipid bilayer portion of cell membrane is similar to most cells, thus passive diffusion occurs regardless of cell type, but may be dependent on the membrane lipid composition.

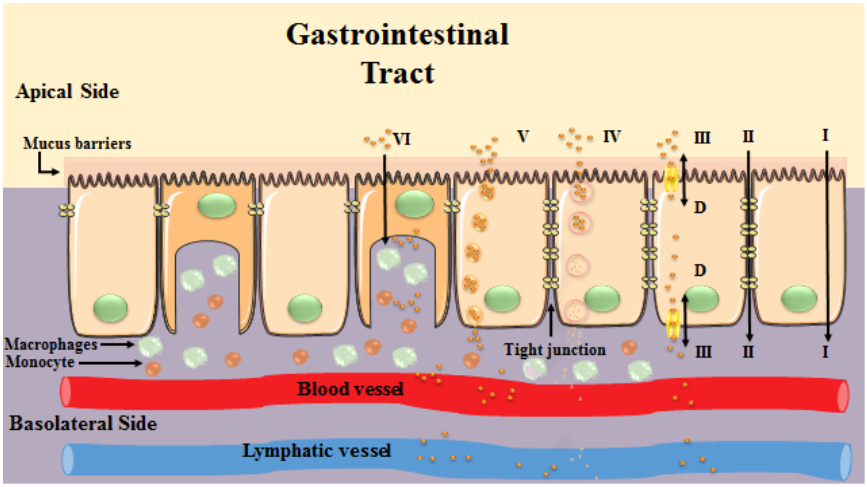

Figure 2. Schematic representation the transport pathways across the intestinal barrier: (I) transcellular passive diffusion, (II) paracellular passive diffusion, (III) influx/efflux facilitated transport by membrane proteins, (IV) endocytosis with lysosome degradation, (V) transcytosis and (VI) uptake by M cells.

Usually, the absorption of colloidal carriers (e.g. polymer based nanocarriers) follows mechanistic pathways involving intracellular uptake by M-cells of Peyer's patches (Figure 2, VI) or/and intercellular/paracellular uptake through the intestinal membrane [62]. By the intracellular pathway drug reaches the systemic circulation through the lymphatic system. This way enables nanocarriers to avoid the hepatic first-pass effect, thus increasing plasma drug concentration. For lipid-based nanocarriers containing self-emulsifying agents, absorption can be driven by lipase-mediated chylomicron formation towards the lymphatic system [63]. The chylomicron formation also aids the absorption of

water-insoluble molecules as it enhances the dissolution and assimilation of lipophilic molecules [64].
Lipid-based nanocarriers can be transported through intracellular Peyer's patches uptake and by the chylomicron formation, evading first-pass effect and targeting drugs to the lymphatic system with special relevance in lymphatic cancers and some infections therapy.

3.4.2 Carrier-mediated transport

Molecules transport across a membrane involving a protein is designated as carrier-mediated transport (Figure 2, III). If the transport process requires energy it is named active transport (e.g. endocytosis, influx/efflux), and may involve transport against a concentration gradient. When the process is not driven by energy is defined as facilitated transport (e.g. phagocytosis), and is based on the concentration gradient of a substrate.
Interaction of nanocarriers with the outer surface of the cells and cellular membranes leads to internalization into intracellular vesicles, and initiates the endocytosis process. This invagination of plasma membrane surrounding the nanocarriers can have different sizes, compositions and internal environment, accordingly to the internalization pathway (e.g. endosomes, phagosomes or macropinosomes). Endocytosis pathway is determined by the size, morphology and surface chemistry of the nanocarriers and, may also depend on the cell type. Phagocytosis, macropinocytosis, chlatrin-mediated, caveolin-mediated and clathrin/ caveolin-independent endocytosis are internalization mechanism described so far. Usually the internalization of nanocarriers in vesicles results in their degradation at the late endosomes (lysosomes containing enzymes and acidic pH) and, prevents them from reaching their target sites (cytoplasm, mitochondria, nucleus). Nanocarriers escape from endosome is challenging but can be achieved by using endosomolytic polymers (e.g. poly(amidoamine) or peptides to increase the intracellular delivery and avoid lysosomal degradation. Exocytosis of the vesicle contents is also a possible pathway for the excretion of nanocarriers from cells. Direct translocation of nanocarriers across the plasma membrane may occurs independent on the metabolic activity of the cells. This pathway named transduction is mediated by peptides known as cell penetrating peptides and is characterized by being energy- and receptor-independent [65].
Carrier-mediated transport is selective and may involve transporters through mechanism of active drug influx and efflux. More than 400 membrane transporters have been described. In carrier-mediated transport the physicochemical properties of the molecules and their potential affinity for various transport proteins play essential roles [66]. Nanocarriers coupled to affinity moieties that target GI surface markers (eg. ICAM-1,

cobalamin receptor), involved in transport, may improve BA. Enterocytes express various transporters on the apical and basolateral membranes conducting the influx (solute carrier, SLC family) or efflux (ATP-binding cassette, ABC family) of endogenous molecules and xenobiotics. Contrary to the passive transport process, the carrier-mediated transport is saturable, subject to inhibition, stereospecific and occurs in the specific cells expressing the transporter.

3.4.3 Factors affecting nanocarriers absorption

The rate and extent of oral drug absorption is influenced by physicochemical and biopharmaceutics factors. Physicochemical data is heterogeneous but indicates that ionization state, molecular weight and lipophilicity affect small molecules BA. Nanocarriers are design to enhance drug solubility and protect the encapsulated therapeutic agents from the extreme conditions found in the GI tract. Particle size, surface charge and chemical composition are essential parameters to consider in order to improve drug oral BA.

The molecule's ionization determines its dissolution rate and passive diffusion across the GI tract. Therefore, the pH value is a crucial parameter in oral drug absorption and dissolution [67]. Physiological aspects influence the pH, as the luminal secretions alter the local environment. At the luminal side the pH is acidic and can be as low as 2.3. While in the duodenum, the secretion of pancreatic bicarbonate and bile neutralizes the pH and, along the small intestine the pH progressively becomes alkaline. pH-sensitive nanocarriers can be design taking advantage of this specific feature of the GI tract. Accordingly, to their composition, drug release will occur under the intended pH and the body regions with physiological pH will not be affected [41].

The particle size matters in orally drug delivered nanocarriers. Small particles (ca. 100 nm) have been reported to exhibit higher absorption as compared to larger (ca. 500 nm) particles [64]. However, larger nanocarriers show longer retention periods in the Peyer's patches facilitating transport to the lymphatic system.

Surface charge and hydrophobicity also affect the oral BA and thus the nanocarriers interaction with the GIT. Nanocarriers with high hydrophobicity exhibited improved accumulation in the Peyer's patches [64]. Contrary to size, nanocarrier charge is a crucial parameter for the interaction with intestinal *in vitro* models [68]. M cells uptake is highly affected by surface charge. Specific targeting to M-cells, e.g. lectin ligand, also improves cellular uptake [69]. Positively charged nanocarriers present higher cellular toxicity compared to negatively charged and may even lead to reactive oxygen species production, and mitochondrial damage [70]. Most probably, these effects are related to the

electrostatic interaction between the surface particles and cell membranes. In the intestinal membrane *in vitro* model, the receptor-mediated endocytic pathway plays a role in the internalization and transport of positively charged nanocarriers, while the lipid raft pathway mediates the uptake and transport of negatively charged nanocarriers [68].

The surface charge of nanocarriers alters upon absorption due to plasma protein adsorption. This phenomenon determines the biological nanocarriers fate, as it can lead to phagocytosis, long-term blood circulation or specific targeting. Protein adsorption on nanocarriers may reduce mean resident time and increases first-pass metabolism [71].

Oral drug delivery poses a significant challenge due to the short residence time of the formulations within the GI tract. Therefore, to increase the effectiveness of therapy, delivery systems with ability to adhere to the oral mucosa or target specific parts of the GI tract would be advantageous. Although the mechanisms governing oral absorption remain unknown, various strategies proved to be effective, for example, improvement of mucoadhesiveness, polymer coating and ligand-mediated targeting to epithelia. Polysaccharides and chitosan reinforce the mucoadhesion by interfering with the tight junctions thus enhancing absorption of the drug. Coating lipid-based nanocarriers with chitosan leads to inversion of surface potential from negative to positive, preventing the pH triggered aggregation of lipid nanocarriers in the stomach [31]. In fact, positively charged chitosan has a high affinity to bind with negatively charged mucin and mucosal surfaces [72]. Also, modification with tocopheryl polyethylene glycol 1000 succinate and pluronics could enhance oral absorption by inhibition of intestine efflux pumps, as P-glycoproteins [73].

Nanocarriers taken from the GI tract can reach the systemic circulation or be cleared by the immune system. To improve oral BA nanocarriers recognition and elimination can be overcome by coating with hydrophilic polymers, such as PEG [74]. The impact of PEGylation in inhibiting lipid digestion, mediated by gastric and pancreatic lipases, is dependent on the molecular weight and the packing density of PEG molecules, as increasing the molecular weight and the packing density of PEG headgroups result on improved steric hindrance of digestive enzymes thus protecting the lipid core [75].

Ligand-mediated targeting to epithelia takes advantage of the specific receptors expression on the cell surface. Active targeting to M-cells, by receptor mediated phagocytosis, can be achieved using lectins [76]. The potential of transenterocytic phagocytic pathway has also been explored, targeting several receptors (eg. vitamins, carbohydrate and proteins) [69].

3.5 Nanocarriers Characterization: Issues and challenges

Properly characterization of nanocarriers is a critical step to control product quality, stability and safety. Although it is not an easy work due to the complexity and diversity of these formulations. Parameters must be studied according to the type of nanocarrier chosen as well as the nature of the materials used. Despite the diversity of the nanocarriers available, there are basic common characterization techniques for particle size and shape, and the homogeneity of the system (polydispersity index). Accurate and sensitive techniques have already been used for these purposes, which are able to provide excellent qualitative and quantitative information [1].

The dynamic light scattering (DLS) is one of the most popular techniques used to estimate the size distribution of small particles in solution or suspension. The data obtained provide information about a population of nanocarriers in each sample solution, and not from each particle. Main strengths of DLS include: short experiment duration, noninvasive technique, able to measure diluted samples in a different wide range of concentrations and even small amounts of higher molecular weight species can be detected. Even though, the high accuracy of the technique can, sometimes, lead to a wrong interpretation of the data as the presence of even a small percentage of aggregates may interfere in the scattering intensity, increasing the size of measured particle. In the case of nanocarrier with poorly soluble drugs, proper dilution sometimes is not enough to solubilize unentrapped drug in suspension, and these particles are also measured, giving the false result of bigger nanocarriers. Besides the mentioned basic characterization parameters, there are some other critical that must be studied more deeply and carefully.

Association efficiency together with drug loading and drug release kinetics are important not only for therapeutic purposes, as it dictates the rate of drug that may reach the site of action, but also should be well determined, without having super estimation or false results, which are common for insoluble drugs [77]. Furthermore, the physical state of the drug in the nanocarriers, i.e., in amorphous state or in crystal form, may be important as it directly influences drug loading in nanocarriers as well as the release characteristics of the encapsulated drug [77].

The next sections will address with more details these critical parameters and the possible issues that its determination may give rise to.

3.5.1 Polymorphism and crystallinity

Drug stability, solubility, dissolution, efficacy and, consequently, BA are parameters directly related to the physical state of the drug in nanocarriers. The drug may be

encapsulated in a crystalline or amorphous state, which will depend on several parameters of the nanocarrier design. In addition, the crystalline form of the drug may change, leading to a formation of a polymorph of the drug.

Polymorphs are chemically identical, although the different arrangement of the molecules lead to a different configuration of the crystal, which can vary from each other significantly in solubility and stability [78].

Several factors can alter the physical state of the drug for instance the use of the organic solvent as well as its type, the method of obtaining, and even some drying processes as lyophilization. Because most of the techniques applied to obtain nanocarriers with poorly soluble drugs use organic solvents, it is important to check if polymorphs of the drug have been already reported, and monitor this parameter during all the steps of the formulation. The assessment of the polymorphic form and the crystallinity of the drug may be performed using different techniques that may be correlated with each other, as differential scanning calorimetry (DSC), X-ray diffraction (XRD) and microscopy [78].

3.5.2 Drug association

In general, poorly soluble drug encapsulation is influenced by several factors such as nature of the nanocarrier, matrix polymorphism, method of preparation, surfactants, and use of organic solvents to dissolve the drug [33]. As already mentioned, regardless the nature of the nanocarrier matrix used, the miscibility between the drug and the carriers must be well determined, since the higher is the affinity between both components, the higher seems to be the association efficiency, and lower is the ratio carrier/drug necessary to achieve suitable formulation [33]. Furthermore, the association of the drug inside nanocarriers is also dependent on the distribution and partition of the drug between the external phase, which is usually aqueous, and the matrix [33]. It has already been reported that poorly soluble drugs tend to precipitate in the external phase, when the method of preparation involves an oil-in-water emulsion, leading to low association efficiency [77].

The association efficiency may be determined by destroying the nanocarriers, with previous separation from the unentrapped drug (direct method); or measuring only the drug present on the external phase (indirect method). In both cases, the separation of the obtained nanocarriers should be done, despite the small size of these particles makes it difficult to separate the colloids and the dispersion medium and, for lipophilic drugs, the drug theoretically soluble is present as a precipitate, leading to an overestimation of the drug loading capacity.

Basically two methods are used to measure association efficiency, namely centrifugation and ultra-filtration, depending on the nature of the material used. For instance, for

polymeric-based nanocarriers, it is common to use the centrifugation method as with high speeds of centrifugation they form a pellet, and the supernatant may be collected, despite the force used do perform the technique. On the other hand, ultra-filtration is often successfully used for lipid-based nanocarrier, as most of the lipids have low density and are not able to form pellet, at considerable high speed of centrifugation. This technique utilizes membranes with different molecular weight cutoffs that retain the nanocarriers, while the solubilized drug passes through the membrane [78]. None of the mentioned methods are completely suitable to estimate the association efficiency of poorly soluble drugs, as the presence of precipitated drug is common, turning this characterization one of the most difficult challenges during the design of the formulations.

3.5.3 Drug release profile

As already mentioned along this chapter, the solubility of the drug in aqueous medium may be indicative of its *in vivo* performance, as the precipitation of the drug reduces the total amount of drug absorbed, decreasing its BA. Thus, the best way to mimic *in vitro* the behavior of the drug solubilization upon oral administration is through a dissolution test, also called release profile in the case of nanocarriers. The *in vitro* release profile, if properly performed, can inform the rate by which the drug becomes available to be absorbed, in different conditions encountered *in vivo* such as different pH, the presence of digestion proteins and protein binding [79].

Some critical conditions must be established during the *in vitro* release assay in order to provide some predictive potential, such as the release media and sampling methods. The choice of the medium should simulate *in vivo* systems. Phosphate buffer solution (PBS) is the simplest and common medium used for this purpose, despite significant underestimation of the intestinal fluid environment [79]. Thus, serum-containing buffers may be a reasonable choice of release medium for mimicking a physiological fluid, especially for poorly water-soluble drugs, since they have a more complex composition that seems to affect solubilizing properties (e.g. fasted or fed state simulated intestinal fluids (FaSSIF and FeSSIF, respectively)) [79].

The first challenge to be solved during an *in vitro* drug release of nanocarriers containing poorly soluble drugs is to satisfy sink conditions, which is defined as the volume of medium at least three fold higher than the volume necessary to reach a supersaturated solution of drug. It means that, to obtain realistic results, suitable volume of release medium must be used, implying the use of very low concentration of formulation in the case of poorly soluble drugs, compromising sometimes the accuracy of the quantification analysis. With the use of simulated intestinal fluids is even more useful to achieving sink

conditions compared to PBS due to the solubilizing effects of the proteins. Likewise, this difficulty may be alleviated by concentrate the samples prior to analysis, or adding surfactants of co-solvents in the release medium to increase the drug solubility [80].
Besides the composition and the volume of the release media, it is important to select the more appropriate method, depending on the formulation to be studied. Centrifugation and dialysis are most widely used for this purpose, although both have critical limitations. The first method is based on the centrifugation of the samples at each time point, at high speeds to separate the nanoformulations from the free drug. The main disadvantages of this method are that the pressure generated during the centrifugation can force the release of the drug and, for lipophilic drugs, precipitation of drug in the pellet may occur. In addition, the compression of the pellet is often excessive, turning the resuspension difficult, or sometimes the separation is incomplete, leading to cumulative errors in measurement of the released drug [80].
In the dialysis, the nanocarrier suspension is placed inside a dialysis bag with a specified molecular weight cutoff, and the released drug molecules diffuse out of the bag, for further quantitative analysis. In this case, the major difficulty is to achieve real concentration of poorly soluble drugs in the receptor compartment due to premature precipitation of the drug inside the dialysis bag.

3.5.4 Permeability assays

One of the last steps during formulation design, but not less important, is the evaluation of its permeability characteristics in order to compare the *in vitro* absorption profile with pure drug. In face of all the challenges associated with the conception of drug delivery systems containing poorly soluble drugs, a significant increasing in the number of reports in this framework has been done, applying techniques from the most basic models including non-cellular-based (artificial membrane), cell or tissue based models (*in vitro*), to more complex and time consuming methods as *in situ*, *in vivo* intestinal perfusion, and *in silico* [4]. Nevertheless, the *in vitro* techniques are preferred as they are less laborious and less expensive as compared to *in vivo* animal studies, and can represent an alternative to animal use mainly during initial stages research.
Currently, there are a variety of human immortalized cell lines that are able to easily grow into confluent monolayer models, which can mimic with good correlation with *in vivo* results the intestinal epithelium for transport studies. The commonly used cells for this purpose are endothelial cells (e.g. Caco-2 cells). Caco-2 cells differentiate both structurally and functionally into cells resembling mature enterocytes and have also been shown to express several transport systems of different molecules [81]. The successful application of

in vitro models to predict drug absorption across the intestinal mucosa depends on how closely they mimic the characteristics of the *in vivo* intestinal epithelium [4]. Thus, other cell lines were started to be used in co-cultures together with Caco-2 due to the need to develop models with greater predictability, that involves other mechanism of absorption, and have the ability to provide a more realistic mucus barrier [82]. In this context, several studies have been done applying co-cultures of Caco-2 and mucus secreting goblet cells (HT29) [83], or Caco-2 co-culture with Raji B lymphocytes, that has been developed to mimic the M cells [84].

Despite good correlations have been encountered between *in vivo*/*in vitro* values of permeability with these models, there are still several difficulties associated in the prediction of absorption of poorly soluble drugs, especially for drug belonging to BCS class IV. As already discussed, the absorption of these drugs are extremely influenced by physiological environment, as the presence of endogenous surfactants, as well as the presence or absence of food, which are factors very difficult to mimic *in vitro*. In addition, gastric emptying rate, GI transit rate and GI pH cannot be incorporated in the results interpretation [81].

Likewise, the limit of detection of analytical methods, together with the tendency for drug precipitate before permeation is one more obstacle during *in vitro* permeability assays for poorly soluble drugs, leading to uncertain results. Besides, it is common to find high levels of toxicity in many cell lines, which turns the concentration of drug in the sample even lower. One recent strategy to overcome the solubilization problem during *in vitro* permeability tests is the use of solubilizing agents (eg. poloxamers, Tritons), which may partially eliminate the detection limit challenge, turning possible the estimation of the permeability [85].

4. Conclusions

Despite the vast and growing therapeutic application of poorly soluble drugs it was demonstrated that there are still severe issues regarding the development of oral dosage forms. Along the previous sections, it could be seen that the use of different systems either polymeric- or lipid-based has been studied as nanocarriers to improve oral BA of class II and class IV drugs. In this framework, the use of nanotechnology has been proven to be a promissory and efficient strategy to improve solubility, dissolution kinetics and oral BA of hydrophobic drugs. Few reports already describe *in vivo* assays with a significant enhancement of drug-loaded nanocarriers oral BA as compared to free drug. It was shown along this chapter that there are several different nanocarriers used for this purpose, with different features, which allows developing tailor-made nanotherapeutics for different

drugs. With rapid scientific and technological advances in nanosizing hydrophobic drugs, its potential can be vital for clinical applications. This whole field will thus require more attention in the future, in particular regarding to *in-vitro–in-vivo* correlations, in order to elucidate in detail all effects involved and to provide an adequate basis for appropriate carrier selection.

Acknowledgments

LL thanks the CAPES Foundation, Ministry of Education of Brazil (0831-12-3); and AV thanks to the CNPq (246514/2012-4). SACL thanks Operação NORTE-01-0145-FEDER-000011 (Qualidade e Segurança Alimentar — uma abordagem (nano) tecnológica) for her Investigator contract. The Authors also thank the financial support of National Funds from FCT (Fundação para a Ciência e a Tecnologia) and FEDER under Program PT2020 (project 007728 -UID/QUI/04378/2013).

5. References

1. Das, S. and A. Chaudhury, *Recent advances in lipid nanoparticle formulations with solid matrix for oral drug delivery*. AAPS PharmSciTech, 2011. **12**(1): p. 62-76.
2. Plapied, L., et al., *Fate of polymeric nanocarriers for oral drug delivery*. Current Opinion in Colloid & Interface Science, 2011. **16**(3): p. 228-237.
3. Harde, H., M. Das, and S. Jain, *Solid lipid nanoparticles: an oral bioavailability enhancer vehicle*. Expert Opin Drug Deliv, 2011. **8**(11): p. 1407-24.
4. Nunes, R., C. Silva, and L. Chaves, *4.2 - Tissue-based in vitro and ex vivo models for intestinal permeability studies A2 - Sarmento, Bruno*, in *Concepts and Models for Drug Permeability Studies*. 2016, Woodhead Publishing. p. 203-236.
5. L Chaves, L., et al., *Quality by design: discussing and assessing the solid dispersions risk*. Current drug delivery, 2014. **11**(2): p. 253-269.
6. Pathak, K. and S. Raghuvanshi, *Oral bioavailability: issues and solutions via nanoformulations*. Clin Pharmacokinet, 2015. **54**(4): p. 325-57.
7. Narvekar, M., et al., *Nanocarrier for poorly water-soluble anticancer drugs—barriers of translation and solutions*. AAPS PharmSciTech, 2014. **15**(4): p. 822-833.
8. Kawabata, Y., et al., *Formulation design for poorly water-soluble drugs based on biopharmaceutics classification system: basic approaches and practical applications*. International Journal of Pharmaceutics, 2011. **420**(1): p. 1-10.
9. Amidon, G.L., et al., *A Theoretical Basis for a Biopharmaceutic Drug Classification: The Correlation of in Vitro Drug Product Dissolution and in Vivo Bioavailability*. Pharmaceutical Research, 1995. **12**(3): p. 413-420.
10. FDA, *Waiver of in vivo bioavailability and bioequivalence studies for immediate-release solid oral dosage forms based on a biopharmaceutics classification system: guidance for industry*. Food and Drug Administation Rockville, MD.

http://www/. fda. gov/downloads/drugs/guidancecomplianceregulatoryinformation/guidances/ucm 070246. pdf. Accessed 12th June, 2015.

11. Desai, P., A. Date, and V. Patravale, *Overcoming poor oral bioavailability using nanoparticle formulations–opportunities and limitations*. Drug Discov Today Technol, 2012. **9**(2): p. e87-e95.

12. Merisko-Liversidge, E.M. and G.G. Liversidge, *Drug nanoparticles: formulating poorly water-soluble compounds*. Toxicologic pathology, 2008. **36**(1): p. 43-48.

13. Akash, M.S.H., K. Rehman, and S. Chen, *Polymeric-based particulate systems for delivery of therapeutic proteins*. Pharmaceutical development and technology, 2015: p. 1-12.

14. Zazo, H., C.I. Colino, and J.M. Lanao, *Current applications of nanoparticles in infectious diseases*. J Control Release, 2016. **224**: p. 86-102.

15. Singh, G. and R.S. Pai, *Atazanavir-loaded Eudragit RL 100 nanoparticles to improve oral bioavailability: optimization and in vitro/in vivo appraisal*. Drug Delivery, 2016. **23**(2): p. 532-539.

16. Hashem, F.M., et al., *Optimized zein nanospheres for improved oral bioavailability of atorvastatin*. Int J Nanomedicine, 2015. **10**: p. 4059-69.

17. Morgen, M., et al., *Polymeric Nanoparticles for Increased Oral Bioavailability and Rapid Absorption Using Celecoxib as a Model of a Low-Solubility, High-Permeability Drug*. Pharmaceutical Research, 2012. **29**(2): p. 427-440.

18. Ma, Y., et al., *The comparison of different daidzein-PLGA nanoparticles in increasing its oral bioavailability*. Int J Nanomedicine, 2012. **7**: p. 559-579.

19. Ravi, P.R., et al., *Design, optimization and evaluation of poly-ε-caprolactone (PCL) based polymeric nanoparticles for oral delivery of lopinavir*. Drug Development and Industrial Pharmacy, 2015. **41**(1): p. 131-140.

20. Singh, G. and R.S. Pai, *Optimized PLGA nanoparticle platform for orally dosed trans-resveratrol with enhanced bioavailability potential*. Expert Opinion on Drug Delivery, 2014. **11**(5): p. 647-659.

21. Zabaleta, V., et al., *Oral administration of paclitaxel with pegylated poly(anhydride) nanoparticles: Permeability and pharmacokinetic study*. European Journal of Pharmaceutics and Biopharmaceutics, 2012. **81**(3): p. 514-523.

22. Moritz, M. and M. Geszke-Moritz, *Recent Developments in the Application of Polymeric Nanoparticles as Drug Carriers*. Adv Clin Exp Med, 2015. **24**(5): p. 749-58.

23. Alshamsan, A., *Nanoprecipitation is more efficient than emulsion solvent evaporation method to encapsulate cucurbitacin I in PLGA nanoparticles*. Saudi Pharmaceutical Journal, 2014. **22**(3): p. 219-222.

24. Lu, Y. and K. Park, *Polymeric micelles and alternative nanonized delivery vehicles for poorly soluble drugs*. International journal of pharmaceutics, 2013. **453**(1): p. 198-214.

25. Gothwal, A., I. Khan, and U. Gupta, *Polymeric micelles: recent advancements in the delivery of anticancer drugs*. Pharmaceutical research, 2016. **33**(1): p. 18-39.

26. Elsabahy, M. and K.L. Wooley, *Design of polymeric nanoparticles for biomedical delivery applications*. Chem Soc Rev, 2012. **41**(7): p. 2545-61.

27. Roy, U., et al., *Preparation and characterization of anti-HIV nanodrug targeted to microfold cell of gut-associated lymphoid tissue*. International Journal of Nanomedicine, 2015. **10**: p. 5819-5835.

28. Singla, P., S. Chabba, and R.K. Mahajan, *A systematic physicochemical investigation on solubilization and in vitro release of poorly water soluble oxcarbazepine drug in pluronic micelles*. Colloids and Surfaces A: Physicochemical and Engineering Aspects.

29. Tabatabaei Rezaei, S.J., et al., *pH-responsive unimolecular micelles self-assembled from amphiphilic hyperbranched block copolymer for efficient intracellular release of poorly water-soluble anticancer drugs*. Journal of Colloid and Interface Science, 2014. **425**: p. 27-35.

30. Dian, L., et al., *Enhancing oral bioavailability of quercetin using novel soluplus polymeric micelles*. Nanoscale Research Letters, 2014. **9**(1): p. 1-11.

31. Luo, Y., et al., *Solid lipid nanoparticles for oral drug delivery: Chitosan coating improves stability, controlled delivery, mucoadhesion and cellular uptake*. Carbohydr Polymers, 2015. **122**: p. 221-229.

32. Porter, C.J., N.L. Trevaskis, and W.N. Charman, *Lipids and lipid-based formulations: optimizing the oral delivery of lipophilic drugs*. Nature Reviews Drug Discovery, 2007. **6**(3): p. 231-248.

33. Narvekar, M., et al., *Nanocarrier for poorly water-soluble anticancer drugs--barriers of translation and solutions*. AAPS PharmSciTech, 2014. **15**(4): p. 822-33.

34. Zhang, Z., et al., *Daidzein-phospholipid complex loaded lipid nanocarriers improved oral absorption: in vitro characteristics and in vivo behavior in rats*. Nanoscale, 2011. **3**(4): p. 1780-7.

35. Basavaraj, S. and G.V. Betageri, *Improved oral delivery of resveratrol using proliposomal formulation: investigation of various factors contributing to prolonged absorption of unmetabolized resveratrol*. Expert Opinion on Drug Delivery, 2014. **11**(4): p. 493-503.

36. Deng, J., et al., *The studies of N-Octyl-N-Arginine-Chitosan coated liposome as an oral delivery system of Cyclosporine A*. J Pharm Pharmacol, 2015. **67**(10): p. 1363-70.

37. Sun, C., et al., *Liquid Proliposomes of Nimodipine Drug Delivery System: Preparation, Characterization, and Pharmacokinetics*. AAPS PharmSciTech, 2013. **14**(1): p. 332-338.

38. Xiao, Y., et al., *Sorafenib and gadolinium co-loaded liposomes for drug delivery and MRI-guided HCC treatment*. Colloids and Surfaces B: Biointerfaces, 2016. **141**: p. 83-92.

39. Wu, W., Y. Lu, and J. Qi, *Oral delivery of liposomes*. Therapeutic Delivery, 2015. **6**(11): p. 1239-1241.

40. Nguyen, T.X., et al., *Recent advances in liposome surface modification for oral drug delivery*. Nanomedicine (Lond), 2016. **11**(9): p. 1169-85.

41. Hu, M., et al., *Polymersomes via Self-Assembly of Amphiphilic β-Cyclodextrin-Centered Triarm Star Polymers for Enhanced Oral Bioavailability of Water-Soluble Chemotherapeutics*. Biomacromolecules, 2016. **17**(3): p. 1026-1039.

42. H Muller, R., R. Shegokar, and C. M Keck, *20 years of lipid nanoparticles (SLN & NLC): present state of development & industrial applications*. Current drug discovery technologies, 2011. **8**(3): p. 207-227.

43. Vieira, A.C.C.C., L.L.; Pinheiro, M.; Ferreira, D.; Sarmento, B.; Reis, S., *Design and statistical modeling of mannose-decorated dapsone-containing nanoparticles as a strategy of targeting intestinal M-cells*. International Journal of Nanomedicine, 2016. **11**: p. 2601-2617.

44. Makwana, V., et al., *Solid lipid nanoparticles (SLN) of Efavirenz as lymph targeting drug delivery system: Elucidation of mechanism of uptake using chylomicron flow blocking approach*. International Journal of Pharmaceutics, 2015. **495**(1): p. 439-446.

45. Gonçalves, L.M.D., et al., *Development of solid lipid nanoparticles as carriers for improving oral bioavailability of glibenclamide*. European Journal of Pharmaceutics and Biopharmaceutics, 2016. **102**: p. 41-50.

46. Aljaeid, B.M. and K.M. Hosny, *Miconazole-loaded solid lipid nanoparticles: formulation and evaluation of a novel formula with high bioavailability and antifungal activity*. Int J Nanomedicine, 2016. **11**: p. 441-7.

47. Ravi, P.R., et al., *Lipid nanoparticles for oral delivery of raloxifene: Optimization, stability, in vivo evaluation and uptake mechanism*. European Journal of Pharmaceutics and Biopharmaceutics, 2014. **87**(1): p. 114-124.

48. Righeschi, C., et al., *Enhanced curcumin permeability by SLN formulation: The PAMPA approach*. LWT - Food Science and Technology, 2016. **66**: p. 475-483.

49. Baek, J.-S. and C.-W. Cho, *2-Hydroxypropyl-β-cyclodextrin-modified SLN of paclitaxel for overcoming p-glycoprotein function in multidrug-resistant breast cancer cells*. Journal of Pharmacy and Pharmacology, 2013. **65**(1): p. 72-78.

50. Khan, S., et al., *Nanostructured lipid carriers: An emerging platform for improving oral bioavailability of lipophilic drugs*. International journal of pharmaceutical investigation, 2015. **5**(4): p. 182.

51. Beloqui, A., et al., *Budesonide-loaded nanostructured lipid carriers reduce inflammation in murine DSS-induced colitis*. International Journal of Pharmaceutics, 2013. **454**(2): p. 775-783.

52. Neves, A.R., et al., *Novel resveratrol nanodelivery systems based on lipid nanoparticles to enhance its oral bioavailability*. International Journal of Nanomedicine, 2013. **8**: p. 177-187.

53. Zhuang, C.-Y., et al., *Preparation and characterization of vinpocetine loaded nanostructured lipid carriers (NLC) for improved oral bioavailability*. International Journal of Pharmaceutics, 2010. **394**(1–2): p. 179-185.

54. Beloqui, A., et al., *A comparative study of curcumin-loaded lipid-based nanocarriers in the treatment of inflammatory bowel disease*. Colloids and Surfaces B: Biointerfaces, 2016. **143**: p. 327-335.

55. Beloqui, A., et al., *Mechanism of transport of saquinavir-loaded nanostructured lipid carriers across the intestinal barrier*. Journal of Controlled Release, 2013. **166**(2): p. 115-123.

56. Bannunah, A.M., et al., *Mechanisms of nanoparticle internalization and transport across an intestinal epithelial cell model: effect of size and surface charge.* Molecular pharmaceutics, 2014. **11**(12): p. 4363-4373.

57. des Rieux, A., et al., *Targeted nanoparticles with novel non-peptidic ligands for oral delivery.* Adv Drug Deliv Rev, 2013. **65**(6): p. 833-44.

58. Lennernas, H., *Does fluid flow across the intestinal mucosa affect quantitative oral drug absorption? Is it time for a reevaluation?* Pharm Res, 1995. **12**(11): p. 1573-1582

59. Karlsson, J., et al., *Paracellular drug transport across intestinal epithelia: influence of charge and induced water flux.* Eur. J. Pharm. Sci., 1999. **9**(1): p. 47-56.

60. Avdeef, A., *Physicochemical profiling (solubility, permeability and charge state).* Curr. Top. Med. Chem., 2001. **1**(4): p. 277-351.

61. Sugano, K., et al., *Coexistence of passive and carrier-mediated processes in drug transport.* Nat Rev Drug Discov, 2010. **9**(8): p. 597-614.

62. Kreuter, J., *Peroral administration of nanoparticles.* Adv Drug Deliv Rev, 1991. **7**: p. 71-86.

63. Sanjula, B., *Effect of poloxamer 188 on lymphatic uptake of carvedilol-loaded solid lipid nanoparticles for bioavailability enhancement.* J Drug Target, 2009. **17**: p. 249-256.

64. Bargoni, A., et al., *Solid lipid nanoparticles in lymph and plasma after duodenal administration to rats.* Pharm Res, 1998. **15**(745-750).

65. Elsabahy, M. and K.L. Wooley, *Design of polymeric nanoparticles for biomedical delivery applications.* Chem Soc Rev, 2012. **41**(7): p. 254-2561.

66. Varma, V.M., et al., *Targeting intestinal transporters for optimizing oral drug absorption.* Curr Drug Metab, 2010. **11**(9): p. 730-742.

67. DeSesso, J.M. and C.F. Jacobson, *Anatomical and physiological parameters affecting gastrointestinal absorption in humans and rats.* Food Chem. Toxicol., 2001. **39**(3): p. 209-228.

68. Bannunah, A.M., et al., *Mechanisms of nanoparticle internalization and transport across an intestinal epithelial cell model: effect of size and surface charge.* Mol Pharm. 2014 Dec 1;11(12):4363-73. , 2014. **11**(12): p. 4363-4373.

69. des Rieux, A., et al., *Targeted nanoparticles with novel non-peptidic ligands for oral delivery.* Adv. Drug Deliv. Rev., 2013. **65**(6): p. 833-844.

70. Nangia, S. and R. Sureshkumar, *Effect of nanoparticle charge and shape anisotropy on translocation through cell membranes.* Langmuir, 2012. **28**(51): p. 17666-17671.

71. Göppert, T.M. and R.H. Müller, *Adsorption kinetics of plasma proteins on solid lipid nanoparticles for drug targeting.* . Int J Pharm., 2005. **302**: p. 172-186.

72. Hombach, J. and A. Bernkop-Schnürch, *Mucoadhesive drug delivery systems.* Handb Exp Pharmacol, 2010. **197**: p. 251-266.

73. Chen, D., D. Xia, and X. Li, *Comparative study of Pluronic F127-modified liposomes and chitosan-modified liposomes for mucus penetration and oral absorption of cyclosporine A in rats.* Int. J. Pharm., 2013. **449**: p. 1-9.

74. Knop, K., et al., *Poly(ethylene glycol) in drug delivery: Pros and cons as well as potential alternatives*. Angew Chem Int Ed Engl, 2010. **49**: p. 6288-6308.

75. Feeney, O.M., et al., *'Stealth' lipid-based formulations: Poly(ethylene glycol)-mediated digestion inhibition improves oral bioavailability of a model poorly water soluble drug*. J Control Release 2014. **192**: p. 219-227.

76. Zhang, X. and W. Wu, *Ligand-mediated active targeting for enhanced oral absorption*. Drug Discov. Today, 2014. **19**(7): p. 898-904.

77. Panyam, J., et al., *Solid-state solubility influences encapsulation and release of hydrophobic drugs from PLGA/PLA nanoparticles*. Journal of pharmaceutical sciences, 2004. **93**(7): p. 1804-1814.

78. Kathe, N., B. Henriksen, and H. Chauhan, *Physicochemical characterization techniques for solid lipid nanoparticles: principles and limitations*. Drug development and industrial pharmacy, 2014. **40**(12): p. 1565-1575.

79. Buckley, S.T., et al., *Biopharmaceutical classification of poorly soluble drugs with respect to "enabling formulations*. Eur J Pharm Sci , 2013. **50**: p. 8-16.

80. Abouelmagd, S.A., et al., *Release kinetics study of poorly water-soluble drugs from nanoparticles: are we doing it right?* Mol Pharm, 2015. **12**: p. 997-1003.

81. Antunes, F., et al., *Models to predict intestinal absorption of therapeutic peptides and proteins*. Current drug metabolism, 2013. **14**(1): p. 4-20.

82. Gamboa, J.M. and K.W. Leong, *In vitro and in vivo models for the study of oral delivery of nanoparticles*. Advanced drug delivery reviews, 2013. **65**(6): p. 800-810.

83. Béduneau, A., et al., *A tunable Caco-2/HT29-MTX co-culture model mimicking variable permeabilities of the human intestine obtained by an original seeding procedure*. European Journal of Pharmaceutics and Biopharmaceutics, 2014. **87**(2): p. 290-298.

84. Lasa-Saracíbar, B., et al., *In Vitro Intestinal Co-Culture Cell Model to Evaluate Intestinal Absorption of Edelfosine Lipid Nanoparticles*. Current Topics in Medicinal Chemistry, 2014. **14**(9): p. 1124-1132.

85. Fischer, S.M., et al., *In-vitro permeability of poorly water soluble drugs in the phospholipid vesicle-based permeation assay: the influence of nonionic surfactants*. Journal of Pharmacy and Pharmacology, 2011. **63**(8): p. 1022-1030.

Chapter III

Methods

1. Experimental design

Experimental design, also known as design of experiments (DoE), is the methodology used to systematically conduct and plan experiments aiming to extract the maximum amount of information with the lowest number of analyses [1].

Before the construction of an experimental design, is important to select the variables that will be investigated, the ones that can be changed independently of each other (independent variables) within the experimental domain. Experimental domain describes the experimental field that must be investigated and is defined by the minimum and maximum limits of the experimental variables studied, also called levels [2]. Lastly, the responses or dependent variables are the measured values of the results from experiments.

When the experimental variables and the responses have been defined the experiments can be planned and performed in such a way that a maximum of information is gained from a minimum of experiments [3]. The experimental designs are constructed with a specific set of experiments defined by a matrix composed by the different level combinations of the variables studied [2, 3]. The type of design is chosen depending on the proposed model and the objectives of the study, which may be screening, factor influence, optimization, among others [3, 4].

The experimental design tool was used along this entire thesis aiming to provide a rational and systematic development of the drug delivery systems.

1.1 Empirical models

The outcome of an experiment is usually dependent on the experimental conditions. It, therefore, can be described as a function $f(x)$ which represents a reasonable description of the relationship between the experimental variables and the responses within a limited experimental domain [3].

Two types of models are mainly used to investigate the experimental system, namely linear and polynomial models. The polynomial model contains additional terms that describe the interaction between different experimental variables and are divided into second order interaction model or quadratic model. The last one can determine optimum (maximum or minimum) levels by the introduction of a quadratic term. For the different models, different types of experimental designs are needed [3].

The linear model is mathematically expressed by the following equation:

$$y = b_0 \sum_{i=1}^{k} b_i x_i + \varepsilon$$

where k is the number of variables, b_o is the constant term, b_i represents the coefficients of the linear parameters, x_i represents the variables, and ε is the residual associated to the experiments [2].

The next level of the polynomial model should contain additional terms, which describe the interaction between the different experimental variables. The second-order model for an interaction presents the following terms [2]:

$$y = b_0 \sum_{i=1}^{k} b_i x_i + \sum_{1 \le i \le j}^{k} b_{ij} x_i x_j + \varepsilon$$

where b_{ij} represents the coefficients of the interaction parameters.

Critical point (maximum, minimum, or saddle), can be determined by the introduction of quadratic terms [2] according to the equation presented below:

$$y = b_0 \sum_{i=1}^{k} b_i x_i + \sum_{i=1}^{k} b_{ii} x_i^2 + \sum_{1 \le i \le j}^{k} b_{ij} x_i x_j \, \varepsilon$$

1.2 Full factorial designs

Full factorial is the design that has every possible combination of factors at the designated levels. There are L^k combinations of k factors at L levels [5]. The simplest design in the 2^k series with only two factors, at two levels ("low" and "high"). This design is called a 2^2 factorial design [6].

1.3 Screening: Plackett-Burman design

A screening experiment is performed in order to determine the experimental variables and interactions that have significant influence on the result, measured in one or several responses [3, 7]. This kind of experimental design can be applied when many factors must be examined to identify which are the ones that may potentially influence one or more responses of interest, aiming to reduce the number of factors to be investigated in further experimentation [1]. Thus, minimizing the number of experiments while maximizing information is the ultimate goal [1].

Plackett-Burman design (PBD), are one of the most popular screening designs and are used to investigate n−1 variables in n experiments, in a multiple of four sample size, i.e.,

$4k$ observations with $k = 1, 2, \ldots n$. Thereby PBD require fewer experiments than the highly fractionated factorial designs that include the same number of factors. The projective property of the PBD is that it allows an efficient separation of main effects and interaction for further studies [1, 7].

1.4 Box-Behnken design

A Box–Behnken design (BBD) has three or more levels and can be applied to problems having three or more factors. There are no factorial or extreme points and the design requires $2k(k-1) + n_{cp}$ (n_{cp} = number of central points) [5]. In BBD, the experimental points are located on a hypersphere equidistant from the central point, which allows the efficient estimation of the first- and second-order coefficients of the mathematical model. These designs are, in this way, more efficient and economic than their corresponding $3k$ designs, mainly for a large number of variables [2, 8]. The construction of this design requires that all factor levels have to be adjusted only at three levels (−1, 0,+1) with equally spaced intervals between these levels [2].

2. Response Surface Methodology

Response surface methodology (RSM) is a collection of mathematical and statistical techniques based on the fit of a polynomial equation to the experimental data obtained by experimental design. It must help to better understand the behavior of experimental collection aiming to make statistical previsions. It is useful when a response or a set of responses of interest are influenced by several variables, and allows to simultaneously optimize the levels of these variables to achieve the best system performance. For these purposes, linear or square polynomial functions are employed to describe the system studied and, consequently, to explore experimental conditions until its optimization [2].
The application of RSM implies in the following steps: (i) selection of independent variables that could potentially interfere on the system through screening studies, as well as the delimitation of the experimental domain; (ii) correct choice of the experimental design and performance of the experiments according to the selected experimental matrix; (iii) mathematic–statistical treatment of the obtained experimental data through the fit of a polynomial function; (iv) evaluation of the model's fitness; (v) obtaining the optimum values for each studied variable [2].

3. Solid Dispersions

Solid dispersions are defined as a dispersion of the drug in an inert carrier or matrix at solid state, aiming to enhance the oral bioavailability of poorly water-soluble drugs by modulating drug release profile. It has been demonstrated that solid dispersion, may improve drug solubility by the reduction of particle size, which are generally molecularly dispersed in the matrix [9-11]. When the solid dispersion is exposed to aqueous media and the carrier dissolves, the drug is released as very fine colloidal particles due to the increase in the surface area [9-11]. This mechanism has been reported to be responsible for the bioavailability enhancement of poorly soluble drugs [9-11]. Several methods have been reported to prepare solid dispersions [9-11]. The kneading and solvent evaporation the most widely used due to their advantages.

3.1 Kneading

Kneading is perhaps the simplest technique to prepare solid dispersions in which the drug is dispersed in the carrier as microcrystals or in amorphous state. According to this procedure, the drug and the selected carrier are triturated together using a small volume of ethanolic (1:1 – w/w) solution to give a thick paste. The drug or at least the carrier used should be soluble in water or in ethanol.
The obtained paste is kneaded for a pre-defined time, to disperse the drug into the carrier, and then the formulation is dried at medium temperature (40 – 60°C) in an oven. The dried mass is pulverized and the particles are calibrated by passing through appropriate mesh sieve size. The solid dispersion powder obtained by this technique are physico-chemically stable and can be easily formulated in a tablet dosage form by direct compression method [12].

3.2 Solvent evaporation

Solvent evaporation processes consist in solubilizing both drug and carrier(s) in common solvents or in a mixture of solvent followed by solvent removal. Non-covalent molecular interactions between drug and carrier(s) during solvent removal are responsible for the formation of an amorphous product [9]. Solvent evaporation processes can be divided in four major groups depending on solvent removal conditions: (i) high temperature and normal pressure, (ii) high temperature and negative pressure, (iii) freeze-drying, or (iv) supercritical fluids [9].

3.2.1 Freeze-drying

Freeze-drying comprises freezing a solution/suspension of drug and carrier(s) followed by reducing the surrounding pressure to allow water and solvents in the sample to undergo solid–gas transition. In a freeze-drying process, drug and carrier(s) maintain their molecular dispersion structure observed upon dissolution [9].

4. Nanoparticles

Nanoparticles are solid, colloidal particles consisting of macromolecular substances that vary in size from 10 nm to 1000 nm. Typically, the drug of interest is dissolved, entrapped, adsorbed, attached and/or encapsulated into or onto the matrix. Depending on the method of preparation nanoparticles, nanospheres, or nanocapsules can be achieved, and each of them present different properties and drug release characteristics [13].
The mechanism by which nanoparticles can improve drug solubility is based on the formation of a fine colloidal dispersion, at the same time that entraps the drug, providing a large surface area of absorption in the gastrointestinal tract [14]. Several nanostructures have been already used for this purpose namely lipid-, phospholipid- or polymer-based nanoparticles [15]. In this thesis, polymeric and solid lipid nanoparticles were developed.

4.1 Polymeric nanoparticle

4.1.1 Nanoprecipitation method

The nanoprecipitation method is also called solvent displacement or interfacial deposition. In this method, there is an aqueous phase, generally containing a surfactant acting as stabilizer, and an organic phase, consisting of a solvent solution with the polymer and the drug. The solvent used for this method should be miscible with the aqueous phase. The nanoparticles are obtained as a colloidal suspension formed when the organic phase is added slowly and with moderate stirring to the aqueous phase. Several polymers have been reported to produce polymeric nanoparticles by nanoprecipitation method. In this thesis, the polymeric nanoparticles were based on Eudragit L100 (methacrylic acid - methyl methacrylate copolymer (1:1)) [16-18].

4.2 Solid lipid nanoparticles

Solid lipid nanoparticles (SLNs) consist of a physiological compatible solid lipid core and of an amphiphilic surfactant shell. The main characteristic of the lipid phase is that they remain in solid state at room temperature [19, 20].
SLNs can be prepared using a wide variety of lipids including fatty acids, glyceride mixtures or waxes, stabilized with selected biocompatible surfactants (non-ionic or ionic). Besides, SLNs presents low cytotoxicity due to their biodegradable and biocompatible lipid composition, and are feasible to scale-up with an associated low cost [19, 21].

4.2.1 Hot homogenization and ultrasonication technique

Several methods to produce SLNs have been already described [22, 23]. In this thesis, we have used the hot homogenization and ultrasonication technique. In this method, the lipid and the drug are first melted above the melting point of the lipids (generally 5ºC) followed by the addition of aqueous phase heated to same temperature. Then, are emulsified by probe sonication. The ultrasonication is based on the mechanism of cavitation, which disperses the melted lipid to minute droplets [24]. The cooling of the nanoemulsions allows the crystallization of the lipids and subsequent formation of lipid nanoparticles.

5. Formulations characterization

5.1 Microscopy techniques

The morphology of the formulation may be assessed by images obtained through microscopic techniques, such as scanning electron microscopy (SEM) and transmission electron microscopy (TEM).
SEM allows to obtain three dimensional images of the surfaces of the formulations, in this case solid dispersions, and the respective physical mixtures. The samples are irradiated with an electron beam and the signals generated from the interaction of the electron beam with the sample comprise secondary electrons, backscattered electrons, characteristic x-rays, and other photons which can be used to investigate different features of the sample surface [25].
On the other hand, TEM utilizes energetic electrons which cross the samples to provide morphologic and crystallographic information, in this work was used for the nanoparticles. The images are generated by the interaction between the samples and the energetic electrons in the vacuum chamber, which generates high-resolution, two-

dimensional, black and white images [25].

5.2 X-Ray diffraction

The X-ray diffraction (XRD) can be described as the reflection of a collimated beam of X-rays incident on the crystalline planes of an examined compound. Typically, XRD, based on wide-angle elastic scattering of X-rays, is a tool for characterizing crystalline size, shape and lattice distortion by long-range order, but is limited to disordered materials [25].
The XRD technique represents the primary method for obtaining fundamental structural information on crystalline substances including the determination of crystal structures, evaluation of polymorphism and solvate structures, evaluation of degrees of crystallinity, and the study of phase transitions [26]. XRD techniques used to characterize solids include the analysis of single crystals or powders, this last case is also called X-ray powder diffraction (XRPD). In powder XRD, the typical output is a plot of intensity versus the diffraction angle (2θ). Such a plot can be considered a fingerprint of the crystal structure, and is useful for determination of crystallographic sameness of samples by pattern comparison. A crystalline material will exhibit peaks indicative of reflections from specific atomic planes. The same will be exhibited for all repeating planes with the same spacing. An amorphous sample, on the other hand, will exhibit a broad hump in the pattern called an amorphous halo [27].
In this thesis, the XRD technique was employed to assess the degree of crystallinity of solid dispersions, compared to the pure drug.

5.3 Dynamic light scattering

The measurement of nanoparticles was conducted by dynamic light scattering (DLS) technique, which consists in the incidence of a laser beam through the sample with particles in suspension and that promotes a light scattering whose intensity fluctuations is measured by a detector. The fluctuations are caused by the random Brownian motion of the nanoparticles that can be faster in the case of small particles, or slower in the case of larger particles, according to the Stokes-Einstein equation.
The polydispersity index can also be determined and describes the distribution width of the particle size (from 0 to 1) [25].

5.4 Electrophoretic light scattering

The electrophoretic light scattering (ELS), commonly called zeta potential, is a physical

property which indicates the surface charge of the nanoparticles. The presence of charge on the particles surface affects the ion distribution the aqueous medium, resulting in the creation of an electrical double layer constituted by the charged surface and the counter-ions distributed in a diffuse way in the aqueous medium. This solvating layer is held to the surface, and in the edge of the layer (Stern layer) zeta potential can be measured. When an electric field is applied, charged particles in suspension are attracted towards the electrode of opposite charge. When the equilibrium is reached, the particles move with constant velocity, also known as electrophoretic mobility which can be correlated with the zeta potential [25].

The magnitude of the zeta potential gives an indication of the long-term stability of the colloidal dispersions. Nanoparticles in suspension will tend to suffer repulsion between them if they have a large absolute value of zeta potential and will be considered stable when this value is higher than |30| mV [76].

5.5 Differential scanning calorimetry

Differential scanning calorimetry (DSC) is a technique able to study thermally induced transitions and particularly, the conformational transitions of biological macromolecules [28]. This thermal analysis has been frequently used to investigate the physical state, degree of crystallinity and polymorphism of compounds. Specifically, to lipid based nanosystems, it has been applied to evaluate crystal ordering of the lipid nanoparticles.

The DSC thermal analytical technique measures how physical properties of a sample change, along with temperature against time, allowing to measure the heat capacity of a substance and the enthalpy variation (ΔH). During a change in temperature, DSC measures a heat quantity, which is radiated or absorbed by the sample based on a temperature difference between the sample and the reference material. The sample material is enclosed in a pan (generally aluminum pan) and an empty reference pan is placed on a thermoelectric disk surrounded by a furnace which is heated at constant rate [28, 29]. The energy is introduced simultaneously into the samples and the reference pans, so that temperatures of both cells are raised identically over time. The difference in the input energy required to match the temperature of the sample to that of the reference would be the amount of excess heat absorbed or released by the sample (during an endothermic or exothermic process, respectively). This difference is measured in terms of ΔH, calculated from the area under the transition peak [28, 29].

In this thesis, DSC measurements were performed to assess physical state of drug after production of either polymer- and lipid-based nanoparticles, and to identify potential chemical interactions between the drugs and other constituents of the formulation.

5.6 Fourier Transform Infrared spectroscopy

Fourier transform infrared spectroscopy (FT-IR) is a technique which measures the vibrational frequency of specific chemical bonds, allowing the identification of functionalgroups present in the samples. By analyzing the absorption bands that is given in the infrared spectrum, it is possible to identify vibrational modes associated to the presence of specific molecules [25]. Moreover, infrared spectroscopy technique may allow to assess significant differences between crystalline and amorphous phases and hence are used to infer crystalline degree of the sample as the intensity of the vibrational bands is directly proportional to the concentration of the concerned phase [30].
FT-IR analysis was used to investigate the stability of the used drugs after preparation through the assessment of chemical interactions between drug and other excipients. Moreover, this tool could provide information about the influence of the process on the degree of crystallinity of the final formulations and the physical state of the drug in the systems.

6. Drug quantification

6.1 Spectrophotometry

When light passes through or is reflected from a sample, the amount of light absorbed is the difference between the incident radiation and the transmitted radiation.
The amount of light absorbed is proportional to the number of absorbing molecules through which the light passes, and may be expressed as either transmittance or absorbance. Although, for quantitative applications, absorbance values are most widely used as the relationship between absorbance and concentration, path length is normally linear, and is expressed following the Beer-Bouguer-Lambert law:

$$A = \varepsilon bc$$

where A is the absorbance; ε is the extinction coefficient related to the given substance; b is the path length (usually in centimeters) and c is the substance concentration.
As ε is characteristic of a given substance at defined set conditions, and c is always constant, in practice, these parameters are not used for quantitative analysis, instead a calibration curve for the substance to be analyzed is constructed using one or more standard solutions with known concentrations of the analyte.

The simple linear relationship between absorbance and concentration and the relative ease of measurement of ultraviolet-visible (UV-Vis) light have made UV-Vis spectroscopy is the basis for several quantitative analytical methods [31].
The UV-Vis spectrophotometry technique was applied to quantify the selected drugs in the developed drug delivery systems and to estimate the drug association in nanoparticles formulations.

6.2 High-performance liquid chromatography

The chromatographic technique is a separation technique based on the sample partitioning between a moving phase, in this case liquid, and a stationary phase, which is solid [27]. The high-performance liquid chromatography (HPLC) is currently the most suitable method for meeting most of the criteria for quantitative analysis in the pharmaceutical framework. It is a reliable quantitative precise and accuracy quantification method sufficient to allow for the determination of the drug and related substances simultaneously using a variety of detectors, with excellent reproducibility [26].
The proposed combined therapy using different systems with two different drugs for the treatment of leprosy imply the development of a quantitative and sensitive HPLC method that could separate both drugs and the excipients used in the preparation of the formulations. The method was developed to quantify dapsone and clofazimine isolated or in combination in the different obtained drug delivery systems. Also, the developed method allowed to quantify the drugs in culture medium, from permeation studies using Caco-2 cell monolayer.

6.3 Association efficiency and drug loading

The association efficiency may be determined by destroying the nanoparticles, with previous separation from the unentrapped drug (direct method); or measuring only the drug present on the external phase (indirect method). In both cases, the separation of the nanoparticles should be done [32].
The separation of the nanoparticles may be done by centrifugation of ultra-filtration, depending on the nature of the material used. For polymeric nanoparticles, it is common to use the centrifugation method as the material characteristics allow to obtain pellets with reasonable centrifugation speeds, enabling to collect supernatant and quantify the non-entrapped drug. On the other hand, ultra-filtration is often successfully used for lipid nanoparticles. This method requires the use of membranes with a defined molecular weight cutoff that retain the nanocarriers, while the solubilized drug passes through the

membrane [32].
The indirect method was the main method used for association efficiency estimation, even though the direct method was applied for confirmation purposes. Centrifugation and ultra-filtration separation techniques were used for polymeric and solid lipid nanoparticles, respectively. The drug was quantified by UV-Vis spectroscopy.

7. *In vitro* studies

7.1 *In vitro* dissolution

In vitro dissolution tests are relevant for the prediction of *in vivo* performance as drug absorption after oral administration depend on drug release from the formulation and the dissolution under physiological conditions. The selection of appropriate dissolution conditions is important to the successful *in vitro* evaluation of oral solid dosages and must be designed to closely simulate the GIT environment [33, 34].
General guidelines exist for the selection of dissolution media, volume, stirring rate, and temperature to be used with each type of apparatus. The selection of the dissolution testing conditions should be based on the ability to detect product variation, the stability changes, and the correlation with *in vivo* results in situations where these studies are performed [27]. For oral dosage forms, it is important that the dissolution medium ranges in pH from 1.2 to 6.8, even though, it is most important to simulated gastro-intestinal fluids. Sink conditions are desirable but not mandatory [33, 34], especially for the evaluation of solid dispersions where the theoretical solubility of an amorphous form is often predicted to be much higher than the experimentally observed value, and is important to assess the improvement on the drug dissolution profile [35].
In this thesis, the dissolution tests were performed to assess the drug dissolution profile and the solubility increment provided by the developed amorphous solid dispersions, by two different methods, which were compared to physical mixtures and pure drug. The assays were performed under pH 6.8 to simulate intestinal environment.

7.2 *In vitro* release

The *in vitro* release studies are commonly performed by two methods, depending on the nature of the carrier. Centrifugation and dialysis are the most widely used for this purpose. The first method is based on the centrifugation of the samples at each time point, at 20,000 x*g* to separate the nanoformulations from the free drug, for further quantification. This method is suitable for polymeric nanoparticles. In the dialysis, the nanoparticles suspension is placed inside a dialysis bag with a specific molecular weight

cutoff, and the released drug molecules diffuse out of the bag, for further quantitative analysis [36].
Both methods were applied is this thesis, depending on the testing formulation.

8. Cell studies

8.1 Cell viability

Cell viability studies were conducted to assess the toxicity of nanoparticles, using different cell lines representative of the GIT. The MTT assay is a colorimetric assay used to access cell metabolism, measuring the activity of cellular enzymes that reduce the thiazolyl blue tetrazolium bromide (MTT) substrate to formazan, resulting in a dark purple color which is spectrophotometrically quantified [37].

8.2 *In vitro* permeability assays

Permeability studies can be important to simulate the transport of nanoparticles through intestinal barrier. These assays are performed on 12-well transwell cells with Caco-2 monolayers by seeding cells on membrane inserts for 21-23 days. The cells grow on the apical chamber until the monolayer achieves a transepithelial electrical resistance (TEER) value around 400 Ω.cm² [38].
The permeability was carried out by adding diluted formulations in the apical side of the transwell system. At predetermined time intervals aliquots were sampled from the basolateral compartment and replaced with fresh culture medium. The amount of drug in the samples was analyzed by HPLC. The cumulative amounts of transported drug across the monolayers can be calculated from the concentrations measured in the basolateral compartment. The permeability profile may be expressed as apparent permeability (*Papp*), which is calculated following the equation:

$$Apparent\ permeability\ (Papp) = \frac{dQ}{dt} \times \frac{1}{A \times C_0}$$

where, *Papp* is the apparent permeability coefficient (cm/sec), *dQ/dt* is the linear appearance rate of the compound on the receiver end based on its cumulative transport for 8 h (μg/sec), *A* is the surface area of the cell monolayer (cm) and C_o is the initial concentration of compound in the donor chamber (μg/ml) [39].

9. References

2. Vanaja, K. and R. Shobha Rani, Design of experiments: concept and applications of Plackett Burman design. Clinical research and regulatory affairs, 2007. 24(1): p. 1-23.
3. Bezerra, M.A., et al., Response surface methodology (RSM) as a tool for optimization in analytical chemistry. Talanta, 2008. 76(5): p. 965-77.
4. Lundstedt, T., et al., Experimental design and optimization. Chemometrics and intelligent laboratory systems, 1998. 42(1): p. 3-40.
5. Lewis, G.A., D. Mathieu, and R. Phan-Tan-Luu, Pharmaceutical experimental design. 1998: CRC Press.
6. Hibbert, D.B., Experimental design in chromatography: A tutorial review. Journal of Chromatography B, 2012. 910: p. 2-13.
7. Myers, R. and D. Montgomery, Response Surface Methdology: Product and Process Optimization Using Designed Experiments. 1995, New York: Wiley.
8. Plackett, R.L. and J.P. Burman, The design of optimum multifactorial experiments. Biometrika, 1946. 33(4): p. 305-325.
9. Box, G.E. and D.W. Behnken, Some new three level designs for the study of quantitative variables. Technometrics, 1960. 2(4): p. 455-475.
10. Vasconcelos, T., et al., Amorphous solid dispersions: Rational selection of a manufacturing process. Advanced Drug Delivery Reviews, 2016. 100: p. 85-101.
11. Chaves, L., et al., Quality by design: discussing and assessing the solid dispersions risk. Curr Drug Deliv, 2014. 11(2): p. 253-69.
12. Fahr, A. and X. Liu, Drug delivery strategies for poorly water-soluble drugs. Expert Opinion on Drug Delivery, 2007. 4(4): p. 403-416.
13. Bikiaris, D.N., Solid dispersions, Part I: recent evolutions and future opportunities in manufacturing methods for dissolution rate enhancement of poorly water-soluble drugs. Expert Opinion on Drug Delivery, 2011. 8(11): p. 1501-1519.
14. Singh, R. and J.W. Lillard, Nanoparticle-based targeted drug delivery. Experimental and molecular pathology, 2009. 86(3): p. 215-223.
15. Attama, A. and C. Umeyor, The use of solid lipid nanoparticles for sustained drug release. Ther Deliv, 2015. 6(6): p. 669-684.
16. Narvekar, M., et al., Nanocarrier for poorly water-soluble anticancer drugs—barriers of translation and solutions. AAPS PharmSciTech, 2014. 15(4): p. 822-833.
17. Vauthier, C. and K. Bouchemal, Methods for the preparation and manufacture of polymeric nanoparticles. Pharmaceutical research, 2009. 26(5): p. 1025-1058.
18. Mora-Huertas, C., H. Fessi, and A. Elaissari, Polymer-based nanocapsules for drug delivery. International journal of pharmaceutics, 2010. 385(1): p. 113-142.
19. Reis, C.P., et al., Nanoencapsulation I. Methods for preparation of drug-loaded polymeric nanoparticles. Nanomedicine: Nanotechnology, Biology and Medicine, 2006. 2(1): p. 8-21.
20. Righeschi, C., et al., Enhanced curcumin permeability by SLN formulation: The PAMPA approach. Food sci technol, 2016. 66: p. 475-483.

21. Vieira, A.C., et al., Design and statistical modeling of mannose-decorated dapsone-containing nanoparticles as a strategy of targeting intestinal M-cells. Int J Nanomedicine, 2016. 11: p. 2601-17.

22. Narvekar, M., et al., Nanocarrier for poorly water-soluble anticancer drugs--barriers of translation and solutions. AAPS PharmSciTech, 2014. 15(4): p. 822-33.

23. Muchow, M., P. Maincent, and R.H. Müller, Lipid nanoparticles with a solid matrix (SLN®, NLC®, LDC®) for oral drug delivery. Drug development and industrial pharmacy, 2008. 34(12): p. 1394-1405.

24. Müller, R.H., K. Mäder, and S. Gohla, Solid lipid nanoparticles (SLN) for controlled drug delivery – a review of the state of the art. European Journal of Pharmaceutics and Biopharmaceutics, 2000. 50(1): p. 161-177.

25. Mehnert, W. and K. Mader, Solid lipid nanoparticles: production, characterization and applications. Adv Drug Deliv Rev, 2001. 47(2-3): p. 165-96.

26. Lin, P.-C., et al., Techniques for physicochemical characterization of nanomaterials. Biotechnology advances, 2014. 32(4): p. 711-726.

27. Ahuja, S. and S. Scypinski, Handbook of modern pharmaceutical analysis. Vol. 10. 2010: Academic press.

28. Ohannesian, L. and A. Streeter, Handbook of pharmaceutical analysis. 2001: CRC Press.

29. Bruylants, G., J. Wouters, and C. Michaux, Differential scanning calorimetry in life science: thermodynamics, stability, molecular recognition and application in drug design. Current medicinal chemistry, 2005. 12(17): p. 2011-2020.

30. Gill, P., T.T. Moghadam, and B. Ranjbar, Differential scanning calorimetry techniques: applications in biology and nanoscience. J Biomol Tech, 2010. 21(4): p. 167-193.

31. Shah, B., V.K. Kakumanu, and A.K. Bansal, Analytical techniques for quantification of amorphous/crystalline phases in pharmaceutical solids. Journal of pharmaceutical sciences, 2006. 95(8): p. 1641-1665.

32. Primer, A., Fundamentals of UV-visible spectroscopy. Copyright Hewlett-Packard Company, Hewlett-Packard publication, 1996(12-5965).

33. Kathe, N., B. Henriksen, and H. Chauhan, Physicochemical characterization techniques for solid lipid nanoparticles: principles and limitations. Drug development and industrial pharmacy, 2014. 40(12): p. 1565-1575.

34. Food, U. and D. Administration, Guidance for industry: Dissolution testing of immediate release solid oral dosage forms. Center for Drug Evaluation and Research, Rockville, 1997.

35. He, Y. and C. Ho, Amorphous solid dispersions: utilization and challenges in drug discovery and development. Journal of pharmaceutical sciences, 2015. 104(10): p. 3237-3258.

36. Konno, H., et al., Effect of polymer type on the dissolution profile of amorphous solid dispersions containing felodipine. European journal of pharmaceutics and biopharmaceutics, 2008. 70(2): p. 493-499.

37. Abouelmagd, S.A., et al., Release kinetics study of poorly water-soluble drugs from nanoparticles: are we doing it right? Molecular pharmaceutics, 2015. 12: p. 997-1003.

38. Mosmann, T., Rapid colorimetric assay for cellular growth and survival: Application to proliferation and cytotoxicity assays. Journal of Immunological Methods, 1983. 65(1): p. 55-63.

39. Freichels, H., et al., Targeting nanoparticles to M cells with non-peptidic ligands for oral vaccination. Eur J Pharm Biopharm, 2009. 73(1): p. 16-24.

40. Bhushani, J.A., N.K. Kurrey, and C. Anandharamakrishnan, Nanoencapsulation of green tea catechins by electrospraying technique and its effect on controlled release and in-vitro permeability. Journal of Food Engineering, 2017. 199: p. 82-92.

Chapter IV

Progress beyond the state of the art

Published:

Chaves, L.L., *et al.*, Rational and precise development of amorphous polymeric systems with dapsone by response surface methodology. Int J Biol Macromol, 2015. 81: p. 662-71.

Submitted:

1. pH-sensitive nanoparticles for improved oral delivery of dapsone: risk assessment, design, optimization and characterization.
2. Optimization of solid lipid nanoparticles for clofazimine delivery: risk management, statistical design and physicochemical characterization;
3. Development of PLGA nanoparticles loaded with clofazimine for oral delivery: assessment of formulation variables and intestinal permeability.

In preparation:

1. Polymeric nanosystems combination allows dapsone and clofazimine intestinal permeation

Integrated discussion

A. Rational and precise development of amorphous polymeric systems with dapsone by response surface methodology.[3]

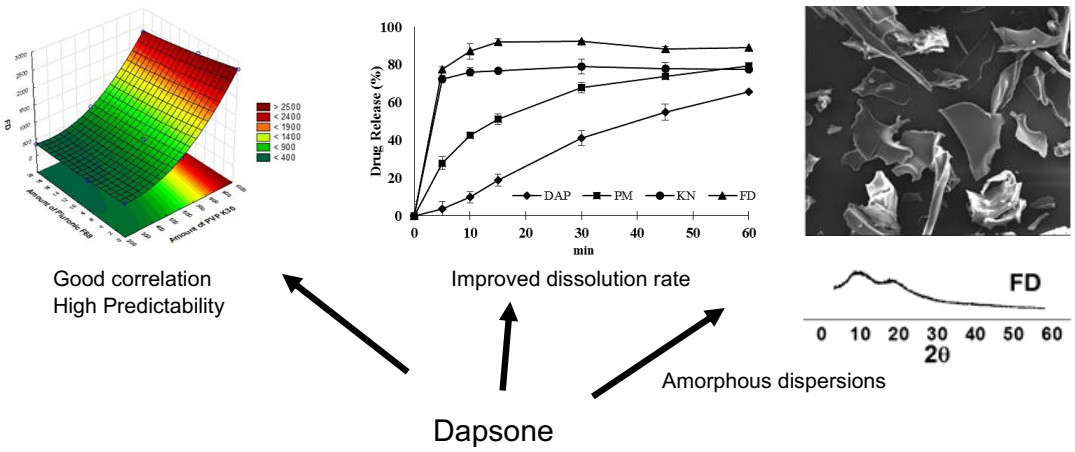

Published: Chaves, L.L., *et al.*, Rational and precise development of amorphous polymeric systems with dapsone by response surface methodology. Int J Biol Macromol, 2015. 81: p. 662-71.[3]

International Journal of Biological Macromolecules 81 (2015) 662–671

Contents lists available at ScienceDirect

International Journal of Biological Macromolecules

journal homepage: www.elsevier.com/locate/ijbiomac

Rational and precise development of amorphous polymeric systems with dapsone by response surface methodology

Luíse L. Chaves[a], Alexandre C.C. Vieira[a], Domingos Ferreira[b], Bruno Sarmento[c,d,e], Salette Reis[a,*]

[a] UCIBIO, REQUIMTE, Departamento de Ciências Químicas, Faculdade de Farmácia, Universidade do Porto, Porto, Portugal
[b] Laboratório de Tecnologia Farmacêutica, Departamento de Ciências do Medicamento, Faculdade de Farmácia, Universidade do Porto, Portugal
[c] I3S, Instituto de Investigação e Inovação em Saúde, Universidade do Porto, Portugal
[d] INEB – Instituto de Engenharia Biomédica, Universidade do Porto, Portugal
[e] CESPU, Instituto de Investigação e Formação Avançada em Ciências e Tecnologias da Saúde and Instituto Universitário de Ciências da Saúde, 4585-116 Gandra PRD, Portugal

ARTICLE INFO

Article history:
Received 17 June 2015
Received in revised form 24 July 2015
Accepted 4 August 2015
Available online 24 August 2015

Keywords:
PVP K30
Kneading
Freeze drying
Design of experiments
Quality by design

ABSTRACT

This work aimed to design dapsone (DAP) amorphous Polymeric Dispersions (PD) using design of experiments (DoE) and response surface methodology (RSM) as optimization tools in order to tailor the biopharmaceutical properties toward its oral delivery. A two-factor, three-level (3^2) statistical design was implemented to study the influence of input variables (amount of PVP K30 and Pluronic F68) on the equilibrium solubility of DAP of the physical mixture (PM), kneaded (KN) and freeze dried (FD) PDs. Through the analysis, it was found that equilibrium solubility of DAP was improved with increasing of PVP K30, mainly for FD PDs, but decreased with increasing Pluronic F68 concentration. XRD and FTIR spectrum revealed the amorphous characteristic of FD PDs and SEM confirmed the homogeneity of the system leading to enhanced surface area and consequent dissolution rate. The *in vitro* dissolution rate of PDs was significantly faster compared to DAP and PM, and all the similarity factors (*f2*) were below 50, demonstrating the differences on the dissolution profiles. The results established the effectiveness of PDs for improvement of dissolution and solubility of DAP and the success in the implementation of DoE and RSM as QbD tools in the design of PDs.

1. Introduction

Leprosy is a chronic infectious disease that continues to be a serious public health problem in several developing countries, caused by *Mycobacterium leprae* (*M. Leprae*) [1]. It is a slowly growing intracellular bacillus, transmitted from an infected person to others via their nasal secretions [2]. The disease affects peripheral nerves, especially Schwann cells, as well as skin and multiple internal organs such as the reticulo-endothelial system, bones and joints, mucous membranes, eyes, testes, muscles, and adrenals [3]. Its clinical manifestations are related to the level of cell-mediated immunity of individual patients [1, 4]. The multidrug therapy consists in combinations of dapsone (DAP), rifampicin, and clofazimine to treat multibacillary leprosy (MB), while DAP in combination with rifampicin is usually used to treat paucibacillary (PB) leprosy [1].

Dapsone (4,4'-diamino-diphenylsulfone, DAP) is a bacteriostatic drug that acts by competitive inhibition of the enzyme dihydrofolate synthetase and dihydrofolate

reductase, key enzymes in the folate biosynthesis pathway in *M. leprae* [1, 5]. Despite its therapeutic potential, DAP is classified as a class II compound according to the Biopharmaceutics Classification System (BCS) [6], and its low solubility was found to result in a low therapeutic index and high microbial resistance [7]. Several approaches have been attempted in order to improve DAP water solubility, such as encapsulation into nanoparticles [8], inclusion complexes with cyclodextrins [9], nanoemulsion [10, 11] and co-crystals [7]. However, these strategies are often confronted with few practical limitations and the desired bioavailability enhancement may not always be achieved [12]. In this framework, solid dispersion system is one of the promising methods to improve the aqueous solubility of poorly soluble drugs, especially for oral solid dosage forms.

In these formulations, the drug dissolution rate may be improved by reducing the drug particle size to almost a molecular level and by modifying the drug crystallinity to generate a completely or partially amorphous state, increasing their saturation solubility in gastrointestinal fluids [13, 14].

In the last few years, the International Conference on Harmonization Q8 guidelines, described the concept of Quality by Design (QbD) [15], which is getting great attention in pharmaceutical formulation development, focusing on the science of production, to construct a systematically quality in the final pharmaceutical product [12, 16]. It is widely known that formulation optimization can be implemented by the use of a combination of analytical approaches, such as design of experiments (DoE), response surface methodology (RSM), and optimization [17]. DoE is a structural and organized procedure for determination of critical factors that could affect the process or product in order to ensure their reliability and robustness [16, 18]. Likewise, RSM is applied to describe correlations between causal factors and response variables, enabling to improve understanding of the influence of different excipients and their interactions as well as predicting optimized formulations with the desired profile [18, 19].

Although the QbD concept seems promising, currently, few works have been developed in the field of solid dispersions on the importance of process and formulation factors [16, 18, 20, 21].

The present study aimed to develop DAP amorphous Polymeric Dispersions (PDs) by using DoE and RSM as optimization tools. For this purpose, a suitable carrier was chosen from an initial polymer screening, and the improvement on the equilibrium solubility was chosen as critical parameter. Additionally, it was determined the influence of PDs process in the selected polymer and also the influence of a third component on the drug equilibrium solubility. It was used two types of solvent evaporation methods (kneading and freeze-drying), due to their simplicity and

potential for scale-up, to manufacture PDs. The PDs were subsequently characterized regarding their crystallinity, morphology and molecular interactions. *In vitro* drug dissolution study was then performed with the formulations.

2. Material and methods

2.1 Material

DAP was purchased from CHEMOS GmbH (Regenstauf, Germany). Polyethyleneglycols (PEG 1500, PEG 4000, PEG 8000 and PEG 20000), low molecular weight chitosan and Pluronic® F-68 were purchased from Sigma-Aldrich (St. Louis, USA); hydroxypropyl methylcellulose (HPMC; METHOCEL™ E5LV) was obtained from Colorcon Limited, UK. Polyvinylpyrrolidone (PVP K30) was obtained from Fluka (Buchs, Switzerland). Compritol® ATO 888 and Gelucire® 44/14 were gifted from Gatefossé (Saint-Priest, France) and inulin was kindly provided by Sensus (Roosendaal, the Netherlands). Ethanol (VWR chemicals), acetonitrile (VWR chemicals) and ultra-pure water (MilliQ) were used in preparation of the solid dispersions.

2.2 Methods

2.2.1 Equilibrium solubility of DAP at different pH aqueous solutions

Solubility studies of DAP were performed according to the shake flask method [22]. An excess amount of drug (± 20 mg) was weighed in test tubes containing 10 mL of ultra-pure water, or selected buffer solutions, namely hydrochloric acid buffer pH 1.2, acetate buffer pH 4.5 and phosphate buffer pH 6.8 and 7.4 [23]. The samples were mechanically stirred in a thermostatic water bath at 37±1°C, for simulating physiological conditions [22], or 25 ±1°C for 48 h. Subsequently, the suspensions were filtered using paper filters (Whatman n°5), and quantified by spectrophotometry at 291nm. All the experiments were conducted in triplicates.

2.2.2 Screening of different polymeric carrier

The effect of different carriers on the solubility of DAP was studied by formulating physical mixtures (PM) of DAP and several hydrophilic and hydrophobic carriers (PEG 1500, PEG 4000, PEG 8000, PEG 20000, Pluronic F68, chitosan, inulin, Gelucire®44/14, Compritiol ATO 888; HPMC and PVP K30) at the ratio 1:1 and 1:5

(w/w). The equilibrium solubility was the parameter chosen (quality attribute) for the selection of the suitable carrier for the improvement of DAP solubility, which were performed similarly to the equilibrium solubility of DAP in ultra-pure water, at 37±1°C, for 48h.

2.2.3 Preparation of physical mixture

PM were prepared by weighing known amounts of DAP and the respective amounts of carriers, respecting the ratios studied which were merely mixed vigorously with a vortex during 5 minutes for complete homogenization.

2.2.4 Preparation of solid dispersions

2.2.4.1 Kneading Method

Kneaded (KN) PDs were prepared with DAP: polymer ratios of 1:1, 1:3 and 1:5 (w/w). Accurately weighed quantity of polymer and drug were mixed with a mortar and a pestle, with sufficiently amount of a hydro-alcoholic solution (50:50 water/ethanol), which was dripped while the mixture was kneaded until the obtaining of a smooth and homogeneous mass. Finally the mass was dried in an oven at 60 °C for 2h and then passed through a #100 sieve. The PD were then stored in desiccator.

2.2.4.2 Freeze-drying method

Firstly, known amounts of DAP and PVP K30 were dissolved in acetonitrile and water respectively, respecting the ratios studied (1:1, 1:3 and 1:5 (w/w)). The solutions were maintained in magnetic stirring during 48h, for the complete solvent evaporation and better interaction drug-polymer. The final solutions were then frozen at -84°C for 24h. The samples were freeze-dried (Lyoquest ECO, Telstar) using a condenser temperature of -65°C and pressure of 0.5 mbar, during 48h, in order to obtain a dry cake. The samples were stored in desiccator for a complete drying.

2.2.5 Design of experiments

The experiments were carried out following a full factorial design to optimize and evaluate the effect of material attributes on the equilibrium solubility of DAP PDs obtained by two different methods (kneading and freeze-drying) and the respective PM.

A two factor, three level (3^2) design were performed in order to explore response surfaces and constructing second-order polynomial models with STATISTICA 10 (Statsoft Inc, USA). The factors studied were the amount of polymer and the influence of a surfactant as a third component in the formulation. The levels and factors are given in Table 1. The response adopted was the equilibrium solubility after 48h, at 25ºC. The ANOVA analysis of the experimental data was performed by RSM. The polynomial model given by Eq. (1) was applied as the response function.

$$Y = A_0 + A_1X_1 + A_2X_2 + A_3X_1X_2 + A_4X_1^2 + A_5X_2^2$$

Where:

Y = dependent variable (equilibrium solubility)

X_1 = Amount of polymer (mg) PVP K30;

X_2 = Amount of surfactant (mg) Pluronic F68;

X_1X_2 = represent the interaction term;

Xi^2 = quadratic terms; and

Ai = polynomial coefficients.

The effects of the factors were considered significant when the ANOVA results indicated a significance level higher than 5% ($p < 0.05$).

Tables 1. Independent variables and their corresponding levels of PD preparation.

Variables	***Levels***		
	-1	**0**	**+1**
X_1	200 mg	600 mg	1000 mg
X_2	0	8 mg	20 mg

2.2.6 Solid dispersions characterization

2.2.6.1 X-Ray diffraction

The X-ray power diffraction (XRD) data were collected with a PANalytical Empyrean X-ray diffractometer equipped with a Cu-Kα monochromatic radiation source. The scanning angle ranged from 2 to 60° in 2θ steps of 0.26° and a counting time of 5 s/step.

2.2.6.2 Scanning electron microscopy

The surface morphology of PM, KN and FD PDs were observed by scanning electron microscopy (SEM) on a FEI Quanta 400 FEG SEM from FEI (Hillsboro, Oregon, USA). The powder samples were also observed were mounted onto a metal stubs and vacuum-coated with a layer of gold/palladium prior observation in microscope.

2.2.6.3 Fourier transformed-infrared spectroscopy (FT-IR)

FT-IR spectroscopy was used to investigate the physicochemical interactions occurring PM, KN and FD PDs. The IR spectra were obtained using the PerkinElmer® (Spectrum 400) equipped with an attenuated total reflectance (ATR) device and zinc selenite crystals. The samples were transferred directly to the ATR compartment, and the result was obtained by combining the 16 scans. The spectra were recorded between 4000 and 600cm^{-1} with a resolution of 4 cm^{-1}.

2.2.6.4 *In vitro* drug release

The *in vitro* dissolution profiles of DAP, PMs and PDs were conducted using the USP paddle apparatus for all the samples. The samples were dropped into 900 mL of phosphate buffer pH 6.8 maintained at a temperature of 37°C ± 0.5 °C and stirred at a speed of 100 rpm for 60 min. A 5 mL aliquot of the sample was withdrawn at 5, 10, 15, 30, 45, 60 min and further replaced with same volume of dissolution medium kept at the same temperature. Samples were filtered and analyzed by spectrophotometry at 291 nm.

The release profiles were assessed by calculating the similarity factor *f*2 for each sample pair, according to the Eq. 2 [24, 25].

$$f2=50 \times log\left\{\left[1+(1/n)\sum_{j=1}^{n}\left|R_j-T_j\right|^2\right]^5 \times 100\right\}$$

Where n is the number of dissolution points, Rj and Tj are the reference and test dissolution values at time t. Two dissolution profiles are considered similar when the *f*2 value is 50–100 [26].

3. Results and discussion

3.1 Equilibrium solubility of DAP in different pH

The values of DAP solubility determined at different pH, are present in Fig. 1. The observed behavior of solubility dependence on pH was due to the chemical characteristics of DAP, and the presence of amino groupings. At lower pH (1.2), the major micro-species of the drug is with both amino group protonated, which increase the solubility of the drug. On the other hand, as the pH increases, the solubility decreases, once at pH 4.5, 6.8 and 7.4 the drug maintain its molecular structure.

Moreover, it was observed that at physiological temperature (37°C) the solubility was almost two fold higher.

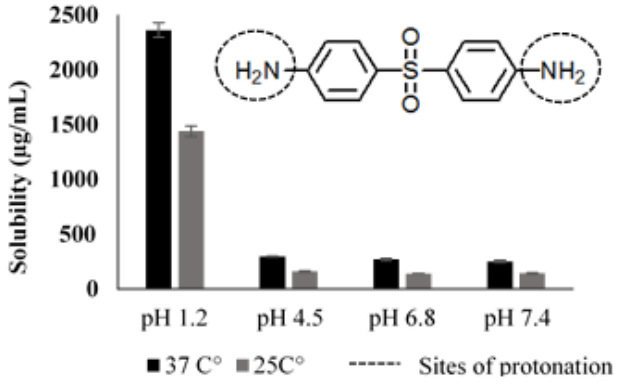

Figure 1. Effect of temperature and pH on the solubility of DAP (n=3).

Drug permeation occurs mainly in the small intestine, and depends on several physiological and physical-chemical parameters concerning pharmaceutical dosage [27].

Despite the high protonation of DAP at lower pH leading to its high solubility, the luminal pH of the small intestine, where the majority of the drug is absorbed, ranges between 5.5 and 7.0. At these range of pH DAP molecule is almost totally unionized (pKa 2.41) which may lead to recrystallization in the lumen, hindering permeation rate [28].

3.2 Screening of different carrier

Various carriers were used to evaluate the enhancement of DAP solubility, in two different ratios, in order to observe the tendency of DAP solubility with the amount of

the carriers. The equilibrium solubilities of the different DAP PMs in ultra-pure water are shown in Fig. 2.

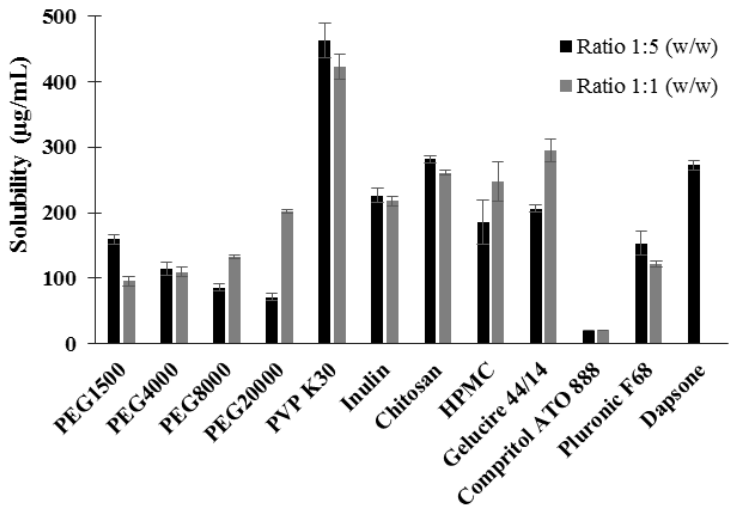

Figure 2. Effect of different carriers on the equilibrium solubility of DAP in water at 37ºC, (n=3).

Due to the hydrophobic characteristics of Gelucire 44/14 and Compritol ATO 888, it was expected that DAP solubility would not increase merely by preparing PM. These type of carriers are non-swellable lipophilic material, presenting a surface activity of self-emulsifying properties. Thus it is necessary to first melt the carriers and then disperse drug. Generally, hydrophobic carriers tend to promote sustain the release of the drug [29, 30], which is not the purpose of this work.

The PM with carbohydrates carriers (inulin and chitosan) did not show great potential in the increment of solubility of the DAP. Hydrophilic systems, i.e., polymeric matrices, are the most used to develop PDs [30]. Among the hydrophilic polymers tested (PEGs, HPMC and PVP K30), only the PVP K30 was found to significantly influence DAP solubility, and this increment seems to be proportional to the amount of polymer used. On the other hand, HPMC provided a slight decrease on DAP solubility inversely proportional to the amount of polymer, probably due its gelling properties, leading to drug association. Moreover, PEGs did not demonstrate any positive effect on DAP solubility, and a positive correlation between the concentration of PEG and the molecular weight was observed on DAP solubility. Despite the extensive use of PEGs in PDS, the decrease in DAP solubility in PM suggests that the interaction between the drug and the polymer should be studied deeper.

The use of PVP K30 to formulate PDs was previously proposed [16, 18, 31-33]. The mechanism by which it leads to increased equilibrium solubility is due to wetting and

decreased surface tension effects [32, 33]. In addition, due to the amorphous characteristic of PVP, the system became partially crystalline, which is more favorable to be completely amorphous when formulating PDs, where the drug has a better chance to be molecularly dispersed in the carrier [29], especially when there is a possibility of hydrogen interactions between the carrier and the drug [30].

Based on the results, the PVP K30 was the polymer that seems to be most suitable to increase DAP solubility, which solubility increases as the amount of PVP increases. It is expected that applying different processes to obtain PDs, better results may be achieved. Therefore, PVP K30 was chosen as polymer model for further studies.

Recent studies have shown that during the accelerated dissolution of binary PDs, an unavoidable supersaturation of drug and its consequent recrystallization may occur. In this context, the properties of the carrier can be tailored to the needs of the system, e.g., stabilization of a solid solution or improvement of the dissolution rate [34]. The inclusion of surfactants as a third component in the PDs may help to avoid drug recrystallization and to stabilize the systems [35, 36]. It was already reported that the use of Pluronic® may maintain solution concentrations that were higher than the equilibrium solubility of crystalline drug due to solubilizing effect and surface activity of these polymeric surfactants [20].

3.3 Optimization and evaluation of PDs by Design of Experiments and Response Surface Methodology

RSM is a collection of mathematical and statistical techniques based on the fit of a polynomial equation to the experimental data, which must describe the behavior of a data set with the objective of making statistical previsions. Before applying the RSM methodology, it is first necessary to choose an experimental design that will define which experiments should be carried out in the experimental region being studied [37]. DoE, on the other hand, is an optimization technique that aims to evaluate all the potential factors simultaneously, systematically and speedily, and can be applied for process or products [38]. Together they are useful tools during formulation design, and has been applied successfully during the optimization of PDs [16, 18, 20, 39, 40].

In order to promote further solubility of DAP, a novel ternary PDs system consisting of DAP, PVP and Pluronic F68 were investigated through DoE. PDs systems were obtained by kneading (KN) and freeze drying (FD) methods, in order to evaluate the influence of the process.

The experimental results with the respective observed responses of the dependent variables are shown in Table 2. The maximum equilibrium solubility after 48h varied

between 100.9 and 192.7 µg/mL for PM, from 198.2 and 459.7 µg/mL for KN and from 344.2 and 994.6 for FD solid dispersion. The highest value of equilibrium solubility was obtained from the sample 7 of the FD PD, being also the formulation that originated higher solubility values using KN. All the values obtained from FD solid dispersions were higher than those obtained from KD, proving that this method was more efficient in the improvement of DAP solubility. Likewise, in all the cases, the influence of the Pluronic F68 as a third component of solid dispersions was not positive, according to the results of equilibrium solubility.

Table 2. Equilibrium solubility obtained from physical mixtures (PM), and PDs o tained by kneading (KN) and freeze-drying (FD)

Sample	Independent Variable				Dependent Variables		
	X_1		X_2		Physical mixture (PM) µg/mL	Kneading (KN) µg/mL	Freeze Dried (FD) µg/mL
	Real (mg)	Coded	Real (mg)	Coded			
1	200	-1	0	-1	150.2 ± 7.9	252.3 ± 11.5	408.5 ± 22.6
2	200	-1	8	0	144.2 ± 10.8	198.2 ± 4.9	344.2 ± 22.0
3	200	-1	20	+1	134.7 ± 55.8	198.3 ± 7.8	353.1 ± 21.7
4	600	0	0	-1	166.2 ± 10.5	315.6 ± 5.8	502.4 ± 18.2
5	600	0	8	0	172.4 ± 16.5	249.7 ± 3.5	380.0 ± 30.1
6	600	0	20	+1	100.9 ± 10.3	253.0 ± 12.5	355.1 ± 21.0
7	**1000**	+1	**0**	**-1**	189.8 ± 8.1	459.7 ± 4.4	**994.6 ± 47.7**
8	1000	+1	8	0	192.7 ± 11.2	399.4 ± 9.8	835.0 ± 22.8
9	1000	+1	20	+1	190.4 ± 12.1	329.1 ± 9.0	515.4 ± 48.5

Based on these results, the process inputs and the response variables were related using a quadratic equation with statistical analysis through STATISTICA 10 software. X_1 represent amount of PVP K30 and X_2 represent the amount of Pluronic F68. The results of the regression coefficients of the obtained equations, the R squares calculated and the $F_{calculated}$ for each model are shown in Table 3. As observed, all the F calculated were much higher than the F_{critic} (9.02) with 95% of confidence, proving that the models are statistical significant, and could be used to achieve a suitable input values. The larger the coefficient is, the higher is the influence of the material attribute on the response. It can be inferred from Table 3 that the PVP K30 as material attribute have a significant effect on the equilibrium solubility of DAP in all the techniques used.

With the equations obtained, 3D responses surface plots were obtained, as shown in Fig. 3. The RSM models shows correlations coefficient (R^2) of 0.989 for PM, 0.989 for KN and 0.999 for FD method, which prove that the models obtained are very well correlated. The qualities of the models were evaluated by plotting correlation plots (predicted data *vs* experimental data) and residual plots (residual *vs* experimental

data) (Fig. 4). It could be seen that all the models show high predictability coefficients, with few outliers, mainly for FD process, thus the predicted values for the three models were reasonably similar to the experimental data. In addition, the residual plots provided a better visual comprehension of the capability of the models, since all the data were widely scattered in predicting DAP solubility, as all of the points are tightly distributed along the horizontal axis (Fig. 4b,d,f). Thus, they can be judged as suitable models, with no trend in the data. These data reflect greater robustness in the freeze-drying process, since all the process parameters may be controlled, which is of great value to the scale-up stage.

Table 3. Regression analysis for responses for physical mixtures (PM), and PDs obtained by kneading (KN) and freeze-drying (FD)

Reg. Coefficients	**PM**	***p*-value**	**KN**	***p*-value**	**FD**	***p*-value**
Intercept.	213.225	-	446.254	-	692.565	-
X_1 (L)	-0.378	0.0521	-0.878	0.0770	-1.844	**0.0028**
X_1 (Q)	0.0006	**0.0090**	0.0016	**0.0099**	0.004	**0.0002**
X_2 (L)	-2.299	0.5904	-18.230	0.1808	-10.551	0.1983
X_2 (Q)	-0.258	0.2095	0.786	0.1753	0.438	0.2050
$X_1.X_2$	0.002	0.4872	-0.006	0.4682	-0.0207	**0.0198**
R^2	**0.989**		**0.989**		**0.999**	
$F_{calculated}$	**56.63**		**408.67**		**3287.90**	

The influence of the amount of PVP K30 in the FD process was more relevant, comparing to KN and PM, confirmed by the values of the intercept of the equations obtained, which are the arithmetic means responses of all the runs [39], i.e., in all the FD PDs, the equilibrium solubility was higher than the others. In addition, for all the processes the quadratic coefficient had positive effect on the responses, indicating that the effect of the PVP on the equilibrium solubility is more important at higher amounts. On the other hand, the linear term of the amount of PVP had a negative impact for the freeze drying process. It can be explained by the fact that the freeze drying process itself is able to improve DAP solubility, and small amount of PVP would not influence on the response, and even lead to a decrease on the final result, only being advantageous if used in higher concentrations.

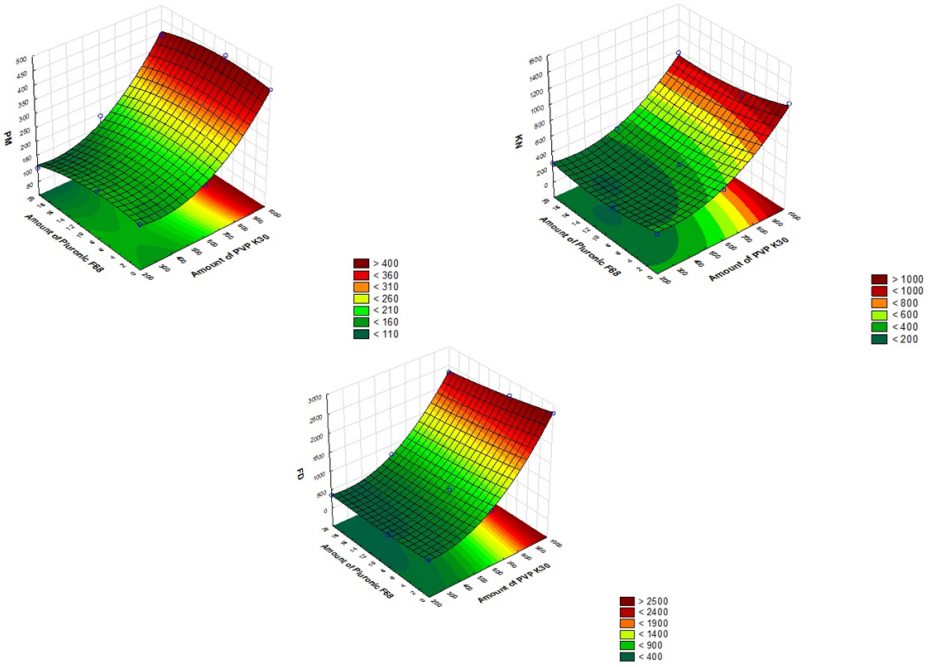

Figure 3. Response surface plot showing the effect of the amount of PVP K30 and Pluronic F68 on the equilibrium solubility of DAP from physical mixtures (PM), and PDs obtained by kneading (KN) and freeze-drying (FD).

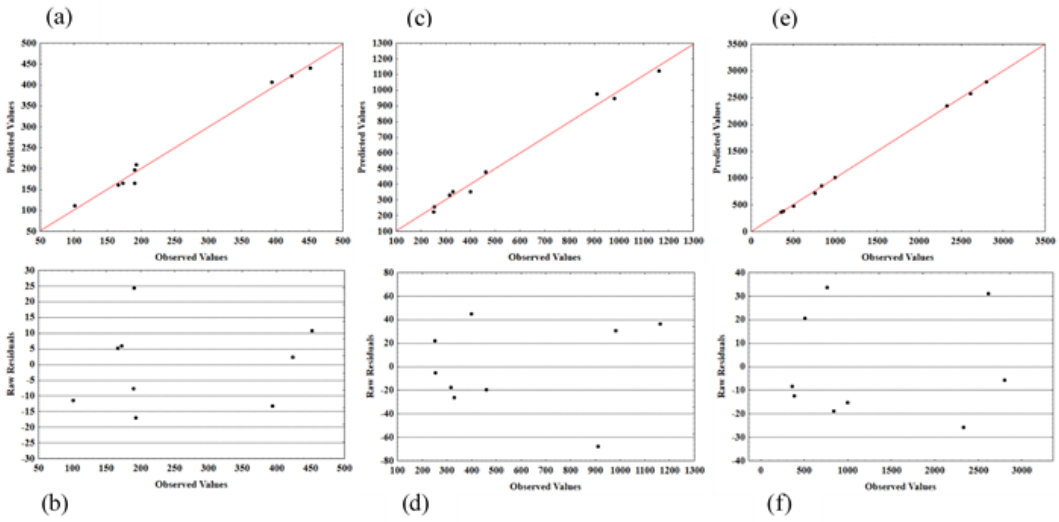

Figure 4. Predicted vs experimental data plots (top) and residual plots (bottom) for data obtained by RSM where: a and b are from PM, b and c are from KN, e and f are from FD.

Moreover, the amount of Pluronic F68 influenced negatively, i.e., decreased the positive effect of PVP K30, once the regression coefficient of X_1X_2 was also relevant, but with negative signal. It was expected that the addition of a surfactant may increase the equilibrium solubility of DAP, as already described in other studies. Although, due to

the amphiphilic structure of Pluronic F68, which has the properties to self-assemble into micelles in aqueous solution when the concentration was above the critical micellar concentration, DAP might be entrapped by micelles formed, which may become an obstacle to the further solubilization after the 48h [34]. Thus, for further characterization, sample 7 of the FD PD was chosen.

3.4 Solid dispersions characterization

For the characterization of the solid dispersions, sample 7 was selected, according to the results of the formulation optimization.

3.4.1 X-Ray diffraction

The XRD patterns of PDs indicate changes in its crystalline structure. The diffractograms of DAP, PVP K30, and PDs obtaining by kneading and freeze drying method are depicted in Fig. 5. The crystalline character of DAP is explicit in the XRD, reflected in the intense peaks between 10º and 30 º [9], while the PVP K30 is completely amorphous, with complete absence of peaks. Regarding the PDs, it could be seen that the kneading method did not generate a completely amorphous material, although the intensity and some peaks is decreased, and in some cases, disappeared. On the other hand, in the freeze dried PDs XRD patterns, it was not found any characteristic peak of DAP, which indicates that the material is completely amorphous, due to a strong intermolecular interaction between the drug and the polymer, better explained in the further characterization, and due to the influence of the lyophilization process itself, already described in the literature, responsible to produce amorphous material, with very low density [32].

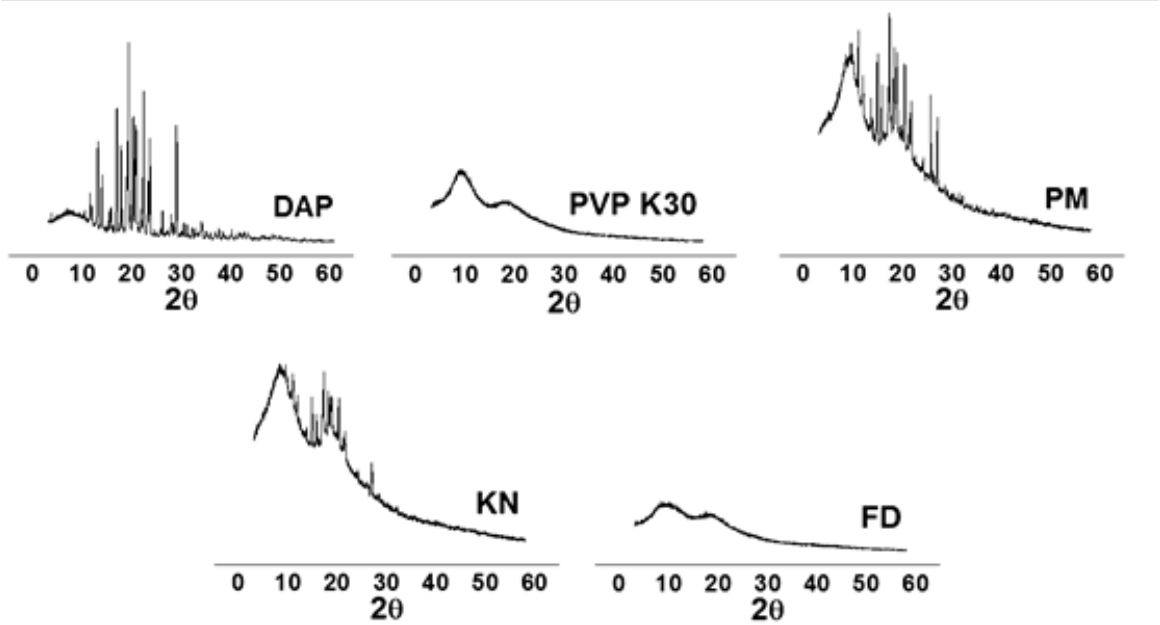

Figure 5. X-ray diffractograms of dapsone (DAP) and PVP K30 raw material; physical mixtures (PM), and PDs obtained by kneading (KN) and freeze-drying (FD).

3.4.2 Scanning electron microscopy

The Fig. 6 shows SEM images of DAP, PVP K30, PM, and PDs obtained by kneading and freeze dried process. The crystalline profile of DAP and the amorphous character of PVP K30, with rounded shapes, are well defined. In the SEM images of PM, the drug interacts only superficially, while in the images obtained from KN PD, the particles present new shapes, not spherical, where the drug appear to be inserted in the polymeric matrix, in its crystalline form. This phenomenon is able to improve the drug solubility due to a higher interaction between the drug and the PVP K30, leading to a decrease of the superficial tension.

In the case of the FD PD, the images show irregular particles with flake-like appearance, which is typical of freeze-dried materials [32, 41]. In these images it was not possible to identify the crystals of DAP neither the rounded shapes of PVP K30. Instead, a homogeneous distribution was observed, wherein the drug appears to be dispersed within the polymer. This homogeneous matrix reflects the best results obtained during the formulation optimization, once in this case the interaction between the drug and the polymer was at molecular level, which facilitate the dissolution process.

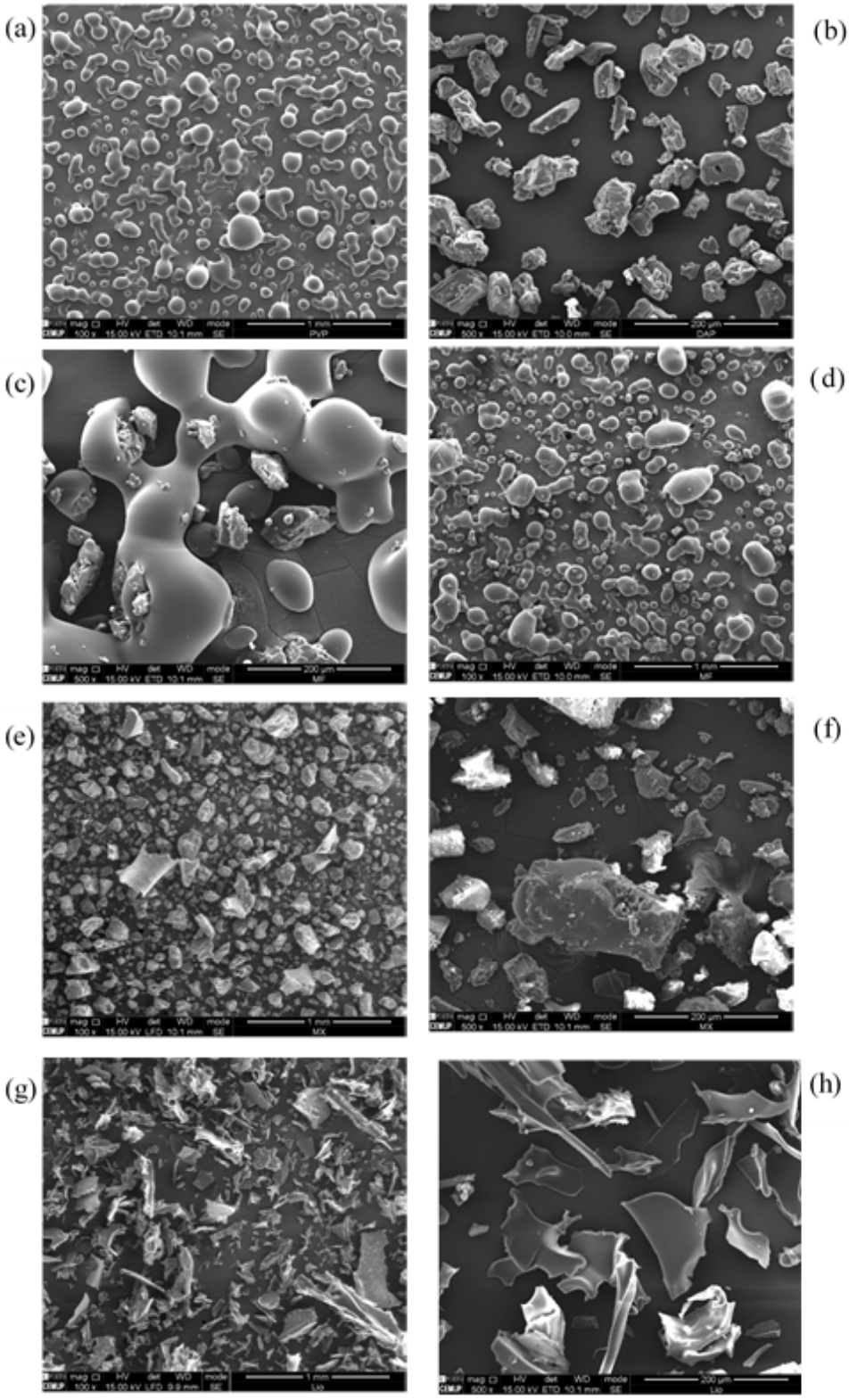

Figure 6. Representative scanning electron microscope (SEM) images of PVP K30 (a), and DAP raw material (b); physical mixtures (PM) (c,d), and PDs obtained by kneading (KN) (e,f), and freeze-drying (FD) (g,h).

3.4.3 Fourier transformed-infrared spectroscopy (FT-IR)

In the FT-IR spectra from DAP (Fig. 7), it can be observed a band at 3300–3400 cm^{-1} corresponding to the stretch of the amine group (N-H), and peaks corresponding to bend vibration of $–NH_2$ groups between 1590 and 1550 cm^{-1}. The bands at 1143 and 1180 cm^{-1} are ascribed to the symmetric and asymmetric vibrations of the sulfone group ($-SO_2$) [42]. PVP contains an amide carbonyl on the pyrrolidone monomer, which is a strong hydrogen bond acceptor [43]. The –C=O group of PVP is considered to be the most favorable site for interaction due to the steric constraints on the N atom [44]. The spectra of the PVP starting material showed, among others, important bands at 2955 cm−1 (C–H stretch) and 1665 cm−1 (C=O) [32].

Regarding the PDs, compared to the PM, it could be seen that the region corresponding to the N-H bonding showed a lower intensity and hypochromic shift, especially in the case of FD, which can be explained by hydrogen bond between the drug and PVP K30 at a molecular level. Moreover, the broadening of the stretching region could be attributed to changes in the crystal structure, particle shape and size [45]. Intermolecular interactions in the amorphous solids can directly affect their molecular mobility [46] causing changes in the oscillating dipole of the molecules, which may lead to changes in the frequency and bandwidth of interacting groups in the spectrum [47]. Thus, drug–polymer interactions in PDs can be explored using IR spectroscopy, whereby the presence of specific interactions is often used to infer miscibility. Specific interactions between the drug and polymer are usually hydrogen bonding [48]. Additionally, amorphous systems may involve a weakening or strengthening of hydrogen bonds thus leading to decrease in band intensities, due to the general diffusion and broadening [46].

DAP molecule contains considerable potential moieties for intermolecular interactions via $–NH_2$ and $–SO_2–$ functional groups [46, 49]. The $–SO_2$ group has a strong electron withdrawing nature, although this phenomenon may lose its electron-accepting capability due to the presence of aromatic ring directly bonded, which lead to a stabilization of its electrons at the neighborhood. On the other hand, the $–NH_2$ group becomes much more susceptible to donate protons, which is probably the most available site for hydrogen bonding.

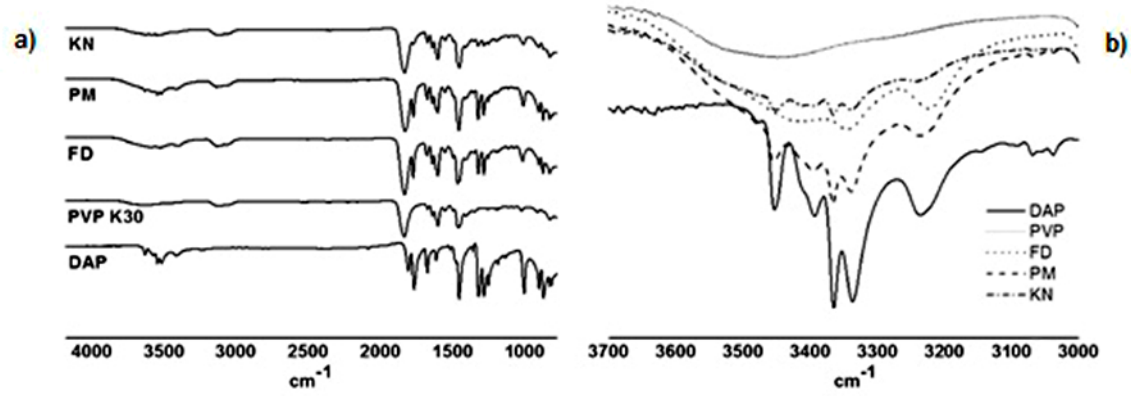

Figure 7. FT-IR spectra (a) and detailed N-H stretching region (3700–3000 cm–1) (b) of DAP, PVP K30, physical mixture (PM), kneaded (KN) PD, and freeze-dried (FD) PD.

3.4.4 *In vitro* drug release

The release profiles of DAP from PDs in comparison with DAP powders and PMs is depicted in Fig. 8. DAP powder exhibited a poor dissolution rate with 41% of drug dissolved after 30 min. PM presented a slight improvement in the dissolution properties in comparison with the pure drug. These results suggested that PVP itself might act as a weak solubilizer in PMs, contributing to the limited increase in drug dissolution, as well as in preventing drug aggregation [34]. Nevertheless, it was evident that PDs exhibited faster dissolution rates than DAP powders and corresponding PMs. The drug release from PD formulations were considerably increased, indicating a fast and burst release of DAP in dissolution media, since more than 75% of drug was released in first 10 minutes, when compared to the pure drug, which dissolution was very slow, less than 10% in the same period of time.

The dissolution rate improvement of the drug in the PDs may be attributed to the high hydrophilicity of the PVP, smaller particle size and consequently larger surface area (especially in freeze-dried PDs) and decreasing in drug crystallinity [33, 45].

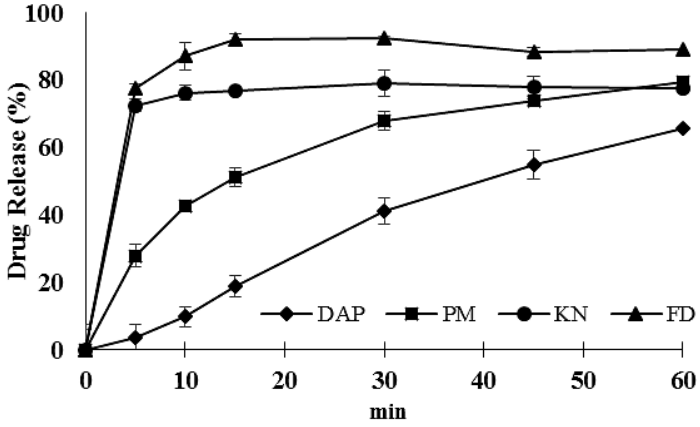

Similarity Factor (f2)					
DAP vs PM	*DAP vs KN*	*DAP vs FD*	*PM vs KN*	*PM vs FD*	*KN vs FD*
27,4	13,3	9,3	27,6	21,3	44,7

Figure 8. Dissolution profiles of dapsone (DAP) raw material, physical mixtures, and PDSs obtained by kneading (KN) and freeze-drying (FD) processes, and the similarity factors between all the formulations and pure drug.

The similarity factor, f2 has been used by the FDA for the comparison of dissolution profiles. *f*2 values between 50 and 100 to indicates similarity between two dissolution profiles and *f*2 values of 100 for two identical profiles [25]. From the results, none similarity was observed between the dissolution profiles of pure drug, PM and both PDs formulation, since all the correlations provided *f*2 values below 50 (Table 5). This corroborates with the morphological and crystallinity differences observed within FD and KN samples. Despite the burst effect in the drug release profile, the dissolution in the first 10 min was faster for FD dispersions compared with the KN samples. This phenomenon may be attributed to the very wettable and needle shaped particles, in addition to a completely amorphous powder obtained by freeze drying method, which not can be obtained from the kneading process, from which was obtained a partially crystalline powder, as observed from the XRD and SEM analysis. Accordingly, the particle size and particle shape of the PDs powders may be considered as the main cause of the drug release rate enhancement, since in all formulations the amount of PVP was the same, so its hydrophilic character did not interfere for differentiate the profiles [32, 45].

Despite the freeze-drying process has improved DAP solubility and immediately released the drug, and the fact that this process can be easily scale-up with low losses, the kneading process also provided satisfactory results considering the simplicity low-cost of the technique.

4. Conclusion

In this study, QbD was successfully applied for pharmaceutical development of DAP PDs, through the application of DoE and RSM as tools. A full-factorial design was developed to investigate the effect of the variables (amount of PVP K30 and amount of Pluronic® F68) on the equilibrium solubility of the PM, KN and FD PDs. Implementation of response surface plot and regression correlation analysis revealed the relationship between the variables and the responses. It was observed that the solubility of DAP increased directly with the increase in amount of PVP K30, which was not observed with the addition of Pluronic® F68. This phenomenon was more evident for the formulations obtained by the freeze-drying method. These findings could be explained by the improved wettability caused by the highly hydrophilic polymer PVP, mainly by particle size reduction, by the conversion of the crystalline form to the amorphous form and by the molecular interactions between drug and polymer in resultant dispersions, as supported by the FT-IR spectra.

Results show that the PDs preparation method had a significant effect on the dissolution performance of DAP. Of the two processes studied, freeze-drying was more effective in producing PDs with higher dissolution rates than kneading. Although, despite the substantial differences between them from a manufacturing perspective, both solvent evaporation techniques used were able to improve DAP solubility and immediately released the drug. Freeze-drying can be advantageous in terms of dissolution enhancement but the associated production costs should be considered before applying this technology.

The combination of preliminary studies and experimental design performed in the present study together with image and spectral analysis represent one step towards DAP PDs formulation development on the basis of Quality by Design, and showed increased prediction efficiency during the optimization procedure.

Acknowledgments

The authors thanks the European Union (FEDER funds through COMPETE) and National Funds (FCT) through project Pest-C/EQB/LA0006/2013. The work also received financial support from the European Union (FEDER funds) by the European Regional Development Fund (ERDF) through the Programa Operacional Factores de Competitividade – COMPETE, by Portuguese funds through FCT in the framework of the project PEst-C/SAU/LA0002/2013, and co-financed by North Portugal Regional Operational Programme (ON.2 – O Novo Norte) in the framework of project SAESCTN-PIIC&DT/2011, under the National Strategic Reference Framework (NSRF).

We are also grateful to Dr. Tito Trindade (CICECO) and Dr. Daniela Silva (CEMUP) for the expert help with the X-Ray Diffraction analysis and Scanning Electron Microscopy, respectively. and Luíse Chaves thanks the CAPES Foundation, Ministry of Education of Brazil for the Doctoral fellowship 0831-12-3; and Alexandre Vieira thanks to the CNPq to the fellowship 246514/2012-4.

5. References

[1] Yamasaki PR, do Nascimento DC, Chelucci RC, de Faria Fernandes Belone A, Rosa PS, Diorio SM, *et al.* Synthesis and evaluation of novel dapsone-thalidomide hybrids for the treatment of type 2 leprosy reactions. Bioorg Med Chem Lett. 2014;24(14):3084-3087.

[2] Anusuya S, Natarajan J. The eradication of leprosy: molecular modeling techniques for novel drug discovery. Expert Opin Drug Discov. 2013;8(10):1239-1251.

[3] Talhari C, Talhari S, Penna GO. Clinical aspects of leprosy. Clin Dermatol. 2015;33(1):26-37.

[4] Bhat RM, Prakash C. Leprosy: an overview of pathophysiology. Interdiscip Perspect Infect Dis. 2012;2012:181089.

[5] Kar HK, Gupta R. Treatment of leprosy. Clin Dermatol. 2015;33(1):55-65.

[6] Bergstrom CA, Andersson SB, Fagerberg JH, Ragnarsson G, Lindahl A. Is the full potential of the biopharmaceutics classification system reached? European journal of pharmaceutical sciences : official journal of the European Federation for Pharmaceutical Sciences. 2014;57(0):224-231.

[7] Jiang L, Huang Y, Zhang Q, He H, Xu Y, Mei X. Preparation and Solid-State Characterization of Dapsone Drug–Drug Co-Crystals. Cryst Growth Des. 2014;14(9):4562-4573.

[8] Santos GSd, Pereira GG, Bender EA, Colomé LM, Guterres SS, Carvalho DCMd, *et al.* Desenvolvimento e caracterização de nanopartículas lipídicas destinadas à aplicação tópica de dapsona. Quim Nova. 2012;35(7):1388-1394.

[9] Grebogi IH, Tibola APOV, Barison A, Grandizoli CWPS, Ferraz HG, Rodrigues LNC. Binary and ternary inclusion complexes of dapsone in cyclodextrins and polymers: preparation, characterization and evaluation. J Incl Phenom Macro. 2012;73(1-4):467-474.

[10] Monteiro LM, Lione VF, do Carmo FA, do Amaral LH, da Silva JH, Nasciutti LE, *et al.* Development and characterization of a new oral dapsone nanoemulsion system: permeability and in silico bioavailability studies. Int J Nanomedicine. 2012;7:5175-5182.

[11] Borges VR, Simon A, Sena AR, Cabral LM, de Sousa VP. Nanoemulsion containing dapsone for topical administration: a study of *in vitro* release and epidermal permeation. Int J Nanomedicine. 2013;8:535-544.

[12] Chaves LL, Vieira AC, Reis S, Sarmento B, Ferreira DC. Quality by design: discussing and assessing the solid dispersions risk. Curr Drug Deliv. 2014;11(2):253-269.

[13] Duret C, Wauthoz N, Sebti T, Vanderbist F, Amighi K. Solid dispersions of itraconazole for inhalation with enhanced dissolution, solubility and dispersion properties. Int J Pharm. 2012;428(1-2):103-113.

[14] Zhaojie M, Ming Z, Shengnan W, Xiaojia B, Hatch GM, Jingkai G, *et al*. Amorphous solid dispersion of berberine with absorption enhancer demonstrates a remarkable hypoglycemic effect via improving its bioavailability. Int J Pharm. 2014;467(1-2):50-59.

[15] ICH. Q8(R2): Pharmaceutical Development. U.S2009.

[16] Patel AD, Agrawal A, Dave RH. Investigation of the effects of process variables on derived properties of spray dried solid-dispersions using polymer based response surface model and ensemble artificial neural network models. Eur J Pharm Biopharm. 2014;86(3):404-417.

[17] Li Z, Cho BR, Melloy BJ. Quality by Design Studies on Multi-response Pharmaceutical Formulation Modeling and Optimization. J Pharm Innov. 2013;8(1):28-44.

[18] Patel AD, Agrawal A, Dave RH. Development of polyvinylpyrrolidone-based spray-dried solid dispersions using response surface model and ensemble artificial neural network. J Pharm Sci. 2013;102(6):1847-1858.

[19] Ren S, Mu HL, Alchaer F, Chtatou A, Mullertz A. Optimization of self nanoemulsifying drug delivery system for poorly water-soluble drug using response surface methodology. Drug Dev Ind Pharm. 2013;39(5):799-806.

[20] Basalious EB, El-Sebaie W, El-Gazayerly O. Application of pharmaceutical QbD for enhancement of the solubility and dissolution of a class II BCS drug using polymeric surfactants and crystallization inhibitors: development of controlled-release tablets. AAPS PharmSciTech. 2011;12(3):799-810.

[21] Barmpalexis P, Kachrimanis K, Georgarakis E. Solid dispersions in the development of a nimodipine floating tablet formulation and optimization by artificial neural networks and genetic programming. Eur J Pharm Biopharm. 2011;77(1):122-131.

[22] FDA. Food and Drug Administration. Guidance for industry: waiver of *in vivo* bioavailability and bioequivalence studies for immediate-release solid oral dosage forms based on a biopharmaceutics classification system. Food and Drug Administration, Rockville, MD2000.

[23] USP. United States Pharmacopeia and National Formulary (USP 31-NF 26). Vol 2. Rockville, MD: United States Pharmacopeia Convention. 2008.

[24] Vranić E, Grizić D, Planinšek O, Srčič S, Bilensoy E. Binary, ternary and microencapsulated celecoxib complexes with β-cyclodextrin formulated via hydrophilic polymers. J Incl Phenom Macrocycl Chem. 2014;80(1-2):139-146.

[25] Odeku OA, Okunlola A, Lamprecht A. Microbead design for sustained drug release using four natural gums. Int J Biol Macromol. 2013;58(0):113-120.

[26] Lucio D, Zornoza A, Martinez-Oharriz MC. Influence of chitosan and carboxymethylchitosan on the polymorphism and solubilisation of diflunisal. Int J Pharm. 2014;467(1-2):19-26.

[27] Dahan A, Miller JM, Amidon GL. Prediction of solubility and permeability class membership: provisional BCS classification of the world's top oral drugs. AAPS J. 2009;11(4):740-746.

[28] Zecevic DE, Meier R, Daniels R, Wagner KG. Site specific solubility improvement using solid dispersions of HPMC-AS/HPC SSL--mixtures. Eur J Pharm Biopharm. 2014;87(2):264-270.

[29] Tran PH, Tran TT, Park JB, Lee BJ. Controlled release systems containing solid dispersions: strategies and mechanisms. Pharm Res. 2011;28(10):2353-2378.

[30] Paudel A, Worku ZA, Meeus J, Guns S, Van den Mooter G. Manufacturing of solid dispersions of poorly water soluble drugs by spray drying: Formulation and process considerations. Int J Pharm. 2013;453(1):253-284.

[31] Al-Obaidi H, Ke P, Brocchini S, Buckton G. Characterization and stability of ternary solid dispersions with PVP and PHPMA. Int J Pharm. 2011;419(1-2):20-27.

[32] Dontireddy R, Crean AM. A comparative study of spray-dried and freeze-dried hydrocortisone/polyvinyl pyrrolidone solid dispersions. Drug Dev Ind Pharm. 2011;37(10):1141-1149.

[33] Frizon F, Eloy JD, Donaduzzi CM, Mitsui ML, Marchetti JM. Dissolution rate enhancement of loratadine in polyvinylpyrrolidone K-30 solid dispersions by solvent methods. Powder Technology. 2013;235:532-539.

[34] Li J, Liu P, Liu JP, Zhang WL, Yang JK, Fan YQ. Novel Tanshinone II A ternary solid dispersion pellets prepared by a single-step technique: *in vitro* and *in vivo* evaluation. Eur J Pharm Biopharm. 2012;80(2):426-432.

[35] Vasconcelos T, Sarmento B, Costa P. Solid dispersions as strategy to improve oral bioavailability of poor water soluble drugs. Drug Discov Today. 2007;12(23-24):1068-1075.

[36] Szuts A, Lang P, Ambrus R, Kiss L, Deli MA, Szabo-Revesz P. Applicability of sucrose laurate as surfactant in solid dispersions prepared by melt technology. Int J Pharm. 2011;410(1-2):107-110.

[37] Bezerra MA, Santelli RE, Oliveira EP, Villar LS, Escaleira LA. Response surface methodology (RSM) as a tool for optimization in analytical chemistry. Talanta. 2008;76(5):965-977.

[38] Singh B, Kapil R, Nandi M, Ahuja N. Developing oral drug delivery systems using formulation by design: vital precepts, retrospect and prospects. Expert Opin Drug Deliv. 2011;8(10):1341-1360.

[39] Shrivastava A, Ursekar B, Kapadia C. Design, Optimization, Preparation and Evaluation of Dispersion Granules of Valsartan and Formulation into Tablets. Curr Drug Delivery. 2009;6(1):28-37.

[40] Verma S, Rudraraju VS. Disintegration mediated controlled release supersaturating solid dispersion formulation of an insoluble drug: design, development, optimization, and *in vitro* evaluation. AAPS PharmSciTech. 2015;16(1):85-97.

[41] Kasper JC, Friess W. The freezing step in lyophilization: physico-chemical fundamentals, freezing methods and consequences on process performance and quality attributes of biopharmaceuticals. Eur J Pharm Biopharm. 2011;78(2):248-263.

[42] Vuković GD, Tomić SZ, Marinković AD, Radmilović V, Uskoković PS, Čolić M. The response of peritoneal macrophages to dapsone covalently attached on the surface of carbon nanotubes. Carbon. 2010;48(11):3066-3078.

[43] Wegiel LA, Mauer LJ, Edgar KJ, Taylor LS. Mid-infrared spectroscopy as a polymer selection tool for formulating amorphous solid dispersions. JPharmPharmacol. 2014;66(2):244-255.

[44] Gupta P, Thilagavathi R, Chakraborti AK, Bansal AK. Role of molecular interaction in stability of celecoxib-PVP amorphous systems. Mol Pharm. 2005;2(5):384-391.

[45] Mohammadi G, Hemati V, Nikbakht M-R, Mirzaee S, Fattahi A, Ghanbari K, *et al*. *In vitro* and *in vivo* evaluation of clarithromycin–urea solid dispersions prepared by solvent evaporation, electrospraying and freeze drying methods. Powder Technology. 2014;257:168-174.

[46] Kaushal AM, Chakraborti AK, Bansal AK. FTIR studies on differential intermolecular association in crystalline and amorphous states of structurally related non-steroidal anti-inflammatory drugs. Mol Pharm. 2008;5(6):937-945.

[47] Gupta P, Bansal AK. Molecular interactions in celecoxib-PVP-meglumine amorphous system. JPharmPharmacol. 2005;57(3):303-310.

[48] Wegiel LA, Zhao Y, Mauer LJ, Edgar KJ, Taylor LS. Curcumin amorphous solid dispersions: the influence of intra and intermolecular bonding on physical stability. Pharm Dev Technol. 2014;19(8):976-986.

[49] Jiang L, Huang Y, Zhang Q, He H, Xu Y, Mei X. Preparation and Solid-State Characterization of Dapsone Drug–Drug Co-Crystals. Crystal Growth & Design.

B. pH-sensitive nanoparticles for improved oral delivery of dapsone: risk assessment, design, optimization and characterization[4]

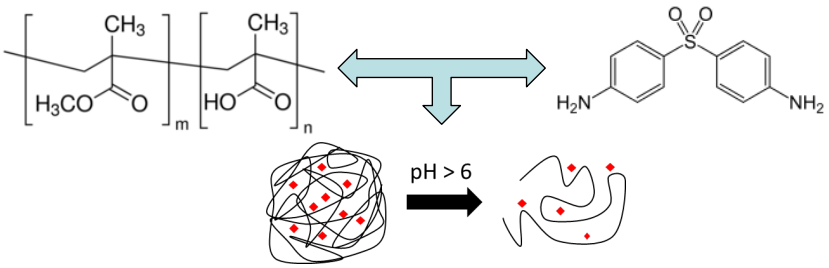

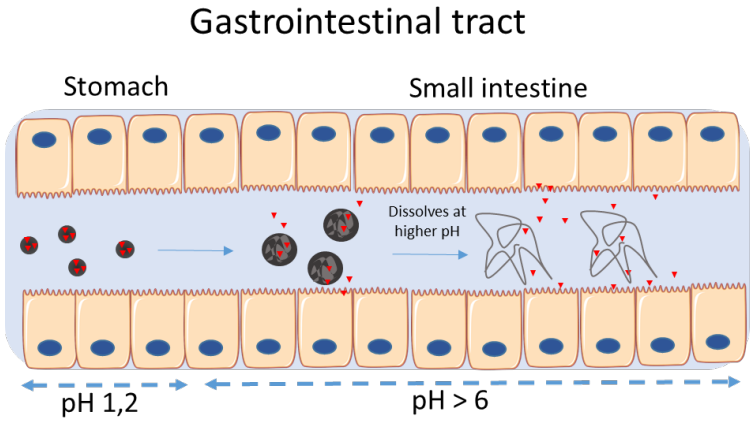

[4] Submitted

pH-sensitive nanoparticles for improved oral delivery of dapsone: risk assessment, design, optimization and characterization

Luíse L. Chaves[a], Sofia A. Costa Lima[a], Alexandre C.C.Vieira[a], Luísa Barreiros[a], Marcela A. Segundo[a], Domingos Ferreira[b], Bruno Sarmento[c,d,e], Salette Reis[*a]

[a]UCIBIO, REQUIMTE, Departamento de Ciências Químicas, Faculdade de Farmácia, Universidade do Porto, Porto, Portugal
[b]UCIBIO, REQUIMTE, Laboratório de Tecnologia Farmacêutica, Faculdade de Farmácia, Universidade do Porto, Portugal
[c]I3S, Instituto de Investigacão e Inovação em Saúde, Universidade do Porto, Portugal
[d]INEB – Instituto de Engenharia Biomédica, Universidade do Porto, Portugal
[e]CESPU, Instituto de Investigacão e Formação Avançada em Ciências e Tecnologias da Saúde and Instituto Universitário de Ciências da Saúde, Gandra, Portugal

ABSTRACT

Aim: To optimize the production of pH-sensitive dapsone (DAP) nanoparticles based on Eugradit L100 (NPs-EL100-DAP) for oral delivery. **Materials & methods:** NPs-EL100-DAP were optimized using a Plackett–Burman design and a Box-Behnken design. The physicochemical properties of the obtained nanoparticles were monitored by microscopy, dynamic light scattering, UV-visible and Fourier-Transform Infrared spectroscopies, differential scanning calorimetry, *in vitro* release assays, and examined for cytotoxicity and permeation across intestinal barrier. **Results:** The *in vitro* release assay of NPs-EL100-DAP confirmed the nanoparticles' pH sensitivity and the ability to deliver DAP at intestinal environment. NPs-EL100-DAP demonstrated enhanced intestinal interactions in comparison to free DAP, across Caco-2 monolayers. **Conclusion:** These studies demonstrate the potential of NPs-EL100-DAP as a therapeutic platform for oral treatment of leprosy.

Key words: Eudragit L100, Caco-2 cell, leprosy, Box-Behnken design, Plackett–Burman design, *in vitro* release assay

1. Introduction

The oral route is still considered the safest and most convenient route of drug administration, as it provides higher patient compliance compared to other routes [1]. On the other hand, factors like low aqueous solubility, rapid metabolism of drug in the gastrointestinal tract (GIT) and low mucosal permeability commonly limit its *in vivo* performance [2]. Many approaches have been reported to overcome the limitations associated with drugs administered orally, especially regarding poorly soluble drugs. The main strategies are based on the reduction of drug particle size and increasing the dissolution rate. Among the emerging strategies, the use of nanoparticles as drug delivery systems has been shown to be a promising tool due to their powerful advantages by providing an enhanced safety and efficacy of the drugs, promoting targeted and/or prolonged delivery, and offering improved stability of drug against GIT chemical/enzymatic degradation [3].

Besides, recent studies have demonstrated the advantages of the use of stimuli-responsive systems as pH-sensitive nanoparticles for targeted intestinal delivery of drugs, avoiding undesired gastric absorption, preventing potential degradation in the stomach environment which may lead to the formation of toxic compounds, and ensuring the drug release in the intestine [2, 4, 5].

Several polymers have the ability to protect the drug against the action of the stomach enzymes and acidic gastric fluids [6], remaining intact in low pH environments, and dissolving at higher pH conditions [5]. Eudragit L100 (EL100) which is an anionic copolymerization product of methacrylic acid and methyl methacrylate, is an enteric pH-dependent copolymer, which is soluble above pH 6, thus being commonly used for the preparation of enteric solid dosage forms [4-8].

Dapsone (4,4′-diaminodiphenylsulfone) (DAP) is a sulfone group drug with unique properties as its dual antimicrobial and anti-inflammatory therapeutic activity. It has been used as the drug of choice in the multidrug therapy of leprosy due to its bacteriostatic action against *Mycobacterium leprae,* inhibiting the synthesis of the folic acid via competition with p-aminobenzoate [9, 10]. However, severe side effects as hemolytic anemia and peripheral neurophathy have been reported after oral administration [10]. The systemic effects are related to the occurrence of toxic metabolic products, although relevant digestive problems such as nausea, vomiting, and stomatitis may occur. Besides, the clinical use of DAP is limited due to its physicochemical properties namely water low solubility, being classified as a Class II agent according to the biopharmaceutical classification system, which leads to an inadequate oral bioavailability [9].

The aim of this study was to screen and optimize the production of pH-sensitive Eudragit L100 DAP loaded nanoparticles (NPs-EL100-DAP) by evaluating the variables that affect the selected critical parameters. First, a Plackett–Burman screening design (PBD) was used to identify the main factors affecting NPs-EL100-DAP, followed by a Box-Behnken design (BBD) which was applied to optimize formulation parameters of the nanoparticles. Further, the optimized nanoparticles were characterized regarding particle size distribution, polydispersity index (PDI), association efficiency (AE), morphology and *in vitro* dissolution testing under different pH conditions (pH 1.2 and 6.8). Cell viability of the obtained formulations was also assessed with three different cell lines, in order to evaluate the toxicity of the particles when in contact with gastric (MKN-28) and intestinal (Caco-2 and HT29-MTX cells). Finally, the *in vitro* permeability of NPs-EL100-DAP through Caco-2 monolayers was performed in order to monitor the performance of the developed system.

2. Materials and methods

2.1 Materials

DAP was purchased from CHEMOS GmbH (Regenstauf, Germany); Pluronic® F-68, and polyvinyl alcohol (PVA) were purchased from Sigma–Aldrich (St. Louis, USA); poly(methacrylic acid-co-methyl methacrylate) 1:1 (Eudragit® L100, Evonik Roehm GmbH, Darmstadt, Germany), ethanol (VWR chemicals, Carnaxide, Portugal) and acetone (JGMS, Odivelas, Portugal) were used to produce the nanoparticles.
Caco-2 and MKN28 cell lines were purchased from the American Type Culture Collection (ATCC, Wesel, Germany) (passage number 35 - 55); HT29-MTX cell line was kindly provided by Dr. T. Lesuffleur (INSERM U178, Villejuif, France). Dulbecco's Modified Eagle Medium (DMEM), Roswell Park Memorial Institute (RPMI), fetal bovine serum (South America origin), Pen-Strep (penicillin, streptomycin) and Trypsin-EDTA were all obtained from Gibco (Paisley, UK). Thiazolyl blue tetrazolium bromide (MTT) was obtained from Sigma–Aldrich.

2.2 Eudragit L100 nanoparticles preparation

Dapsone-loaded Eudragit L100 nanoparticles (NPs-EL100-DAP) were prepared via the nanoprecipitation method, previously described [4, 11], with slight modifications. Briefly, known amounts of Eudragit L100 and DAP were co-dissolved in a mixture of ethanol-acetone (1:1), in defined volumes, according to the experimental design. The

organic solution was subsequently slowly dripped (0.5 mL min^{-1}) in the aqueous phase containing the surfactant (PVA 1% (w/v)), previous acidified to pH 3 to promote the polymer precipitation. The final solution was maintained under magnetic stirring at 350 rpm (RT 15 Power IKAMAG Multiposition Magnetic Stirrer, Staufen, Germany) and room temperature until complete solvent diffusion. The particles were centrifuged using an Allegra X-15R centrifuge (Beckman Coulter), at 11,200 x*g* for 30 min, and the supernatant was discarded. This procedure was performed three times with acidified water (pH 3) to eliminate non-encapsulated drug. The resultant particles were freeze-dried for 48 h, using a LyoQuest 85 plus v.407 Telstar freeze dryer (Telstar® Life Science Solutions, Terrassa, Spain).

2.3 Experimental design

2.3.1 Preformulation screening: Plackett-Burman

A Plackett-Burman design (PBD) was performed to screen and evaluate the process and formulation parameters that may influence the desired profile of the nanoparticles, allowing to evaluate a wide number of variables at the same time with good level of accuracy. Moreover, this experimental design aimed to select the main effects for the subsequent studies. The design was constructed with seven factors and eight experiments, using the STATISTICA 10 (StatSoft®, Dell Software, Round Rock, TX, USA) software. The parameters studied were chosen on the basis of preliminary investigation and on the literature. All the non-studied variables such as the type of polymer (EL100), organic solvent (ethanol:acetone, 1:1 v/v) and solvent evaporation method (magnetic stirring at 300 rpm, room temperature) were kept constant. The selected dependent variables were: particles size (Y_1), polydispersity index (Y_2) and association efficiency (Y_3). The independent variables were: (X_1) volume of aqueous phase; (X_2) type of surfactant; (X_3) surfactant concentration (w/v); (X_4) ratio polymer/drug; (X_5) polymer concentration (w/v); (X_6) volume of organic phase; and (X_7) method of preparation (coded and real levels in Table S1).

2.3.2 Optimization: Box-Behnken Design

After the assessment of the critical parameters by the PBD, a three factor-three level Box-Behnken Design (BBD) was applied to optimize the nanoparticle formulation, with 15 runs including 3 replicates of the central point. The selection of factors (independent variables) and their respective levels were based on the PBD results. All the other

variables not used in the BBD were maintained constant, namely volume of aqueous phase (10 mL); type of surfactant (PVA); surfactant concentration (1%, w/v) and method of nanoparticle production (nanoprecipitation).

The data was analyzed by the regression coefficient of each response, following the equation:

$$Y = b_0 + b_1X_1 + b_2X_2 + b_3X_3 + b_{12}X_1X_2 + b_{13}X_1X_3 + b_{23}X_2X_3 + b_{11}X_1^2 + b_{22}X_2^2 + b_{33}X_3^2$$

Where Y is the response, b_0 is the intercept representing the mean of the results while b_1 to b_{33} are the associated coefficient; X_1, X_2 and X_3 are the independent variables, reassigned as ratio polymer/drug (X_1); polymer concentration (X_2); and volume of organic phase (X_3). The combination of factors and quadratic terms are expressed as X_iX_j and X_i^2 respectively.

The polynomial equations were statistically examined through the analysis of variance (ANOVA) and the factors were considered significant when the values of p of the regression coefficients were < 0.05. The correlation coefficients (R^2) and lack of fit were also obtained in order to predict the accuracy of the models. Graphical correlations between two independent variables and a single response were depicted in 3D responses surface plots, and optimum values for each variable were assessed based on the desirability profile. In order to evaluate the robustness of the developed models, the desired particle was obtained in triplicated as a check-point, where the magnitude of the error between observed and predicted values was evaluated following the equation:

$$Bias\ (\%) = \frac{|\text{predicted value} - \text{observed value}|}{observed\ value} \times 100$$

2.4 Nanoparticles characterization

2.4.1 Particle size and polydispersity index

The mean particle size as well as the polydispersity index (PDI) were analyzed using a ZetaPALS, Zeta Potential Analyzer (Brookhaven Instrument Corps, Holtsville, NY, USA), at 25°C with a light incidence angle of 90°. The fresh particles were properly diluted with ultrapure water until reaching a suitable concentration (Kcps 300-500), and the obtained value is the representation of multiples runs (n=6).

2.4.2 Association efficiency

For the determination of drug association in the different formulations of the experimental design, nanoparticles were diluted 5 times with acidified ultrapure water (pH 3) and centrifuged at 11,200 g for 30 min. Absorbance of supernatant was measured at 391 nm, which corresponds to DAP maximum absorption wavelength, by UV-VIS spectroscopy (Jasco V-660, Easton, MD, USA). The percentages of association efficiency (AE) was calculated based on the following equation:

$$AE = \frac{initial\ amount\ of\ DAP - recovered\ DAP}{initial\ amount\ of\ DAP} \times 10$$

2.4.3 Fourier-Transform Infrared

The spectra of DAP, NPs-EL100 and NPs-EL100-DAP were obtained in order to evaluate possible chemical interactions between DAP and the excipients used to formulate the nanoparticles. The Fourier-Transform Infrared (FT-IR) spectra were obtained using the PerkinElmer® Spectrum 400 (Waltham, MA, USA) equipped with an attenuated total reflectance (ATR) device and zinc selenite crystals. The samples were transferred directly into the ATR compartment, and the result was obtained by combining the 16 scans. The spectra were recorded between 4000 and 600 cm^{-1} with a resolution of 4 cm^{-1}.

2.4.4 Morphology

The morphology of the optimized nanoparticles was examined employing transmission electron microscopy (TEM, JeolJEM-1400, JEOL Ltd., Tokyo, Japan). Images were obtained after dropping diluted colloidal dispersions over a grid followed by negative staining with uranyl acetate. The grid was exposed at the accelerating voltage of 60 kV.

2.4.5 Differential scanning calorimetry

Differential scanning calorimetry thermograms of DAP, EL100, NPs-EL100 and NPs-EL100-DAP were obtained aiming to evaluate the physical changes in DAP crystallinity before and after the production process. The thermal analysis was performed using a DSC 200 F3 Maia (Netzsch, Selb, Germany).

Accurately weighted samples (1-2 mg) were poured into aluminum pans and hermetically sealed. An empty pan was used as reference. The samples were scanned from 30 to 250 ºC, at 10 ºC/min. Nitrogen gas was used as purge gas, at 40 mL/min.

2.4.6 *In vitro* drug release

In vitro DAP release profile from the optimized nanoparticles was evaluated using the dialysis bag diffusion [12-14] method, in two different pH conditions, 1.2 and 6.8, to simulate gastric and intestinal physiological conditions, respectively. The assay was carried out in sink conditions.

Briefly, 1 mL of unwashed colloidal dispersions (containing the equivalent of 750 μg.ml^{-1} in DAP) was placed into dialysis bag with a molecular weight cutoff of 3,500 Da. The dialysis bags were immersed into 40 mL of dissolution media, and stirred magnetically (RT 15 Power IKAMAG Multiposition Magnetic Stirrer, Staufen, Germany) at 350 rpm and 37.0 ºC ± 0.5ºC. The dialysis bag was the donor compartment, and at regular interval times, 200 μL of the outside dissolution media were withdrawn and replaced by the same amount of fresh media. Subsequently, the samples were read spectrophotometrically in a microplate reader (SynergyTM HT, Biotek, Winooski, VT, USA), at specific wavelengths (288 nm for pH 1.2 and 291 for pH 6.8) for each different dissolution media. The release profile was evaluated during 2 h, for the pH 1.2, and during 6 h for the pH 6.8, in order to simulate the transit time of the particles in stomach and small intestine, respectively [15, 16]. The experiment was performed in triplicate (n = 3) for each pH condition.

2.5 Cell studies

Caco-2 and HT29-MTX cell lines were cultured in DMEM, and MKN-28 cells were cultured in RPMI, both medium supplemented with 10% (v/v) of fetal bovine serum (FBS), and 1% (v/v) penicillin-streptomycin. Cells were grown in a humidified incubator at 37 ºC, 5% CO_2 and 95% relative humidity, and the cells were detached using a trypsin solution when reaching 80% confluence.

2.5.1 Cell viability

Cell viability assays were performed using the MTT assay with Caco-2, HT29- MTX and MKN-28 cell lines in order to evaluate the effect of NPs-EL100 and NPs-EL100-DAP along the GI tract. The three types of cells were seeded in 96-well microplates at a

density of 5 x 10^4 cells per well for Caco-2 and HT29-MTX; and at 10^5 cells per well for MKN-28.

The nanoparticles suspensions and free DAP were tested in a concentration-dependent range (25 – 400 μg mL^{-1} in relation to DAP concentration) prepared in culture medium. Free DAP samples were prepared from a stock solution in DMSO, and properly dilutions were performed immediately before the assays, so that the maximum concentration of DMSO did not exceed 4% (v/v). 100 μL of each sample were incubated for 24 h with Caco-2 and HT29-MTX cell lines, and during 4 h for MKN-28. After each time of incubation, the samples were replaced with 100 μL of MTT solution (5 mg mL^{-1}), and incubated for more 2 h. Then, the MTT solution was withdrawn, and the purple crystals were solubilized in 100 μL of dimethyl sulfoxide. The optical density of the solution was measured at a wavelength of 570 nm in a Synergy™ HT Multi-mode microplate reader (BioTek Instruments Inc., Winooski, VT, USA). Untreated cells were taken as control with 100% viability and cells exposed to 4% (v/v) DMSO used as control for free DAP. The MTT test was performed in triplicate and results were expressed as mean values ±SD. The cell viability (%) in relation to control cells (untreated cells) was calculated by Eq. (3):

$$Cell\ viability\ (\%) = \frac{[A]cells\ incubated\ with\ formulation}{[A]cells\ incubated\ with\ culture\ medium} \times 100$$

2.5.2 DAP permeation across Caco-2 monolayers

For the permeability studies, Caco-2 cells were seeded on 12-well Transwell inserts (Corning Transwell Clear, pore size 3 μm, area 0.33 cm^2) at a cell density of 10^5 cells cm^{-1}. The cells were grown in supplemented DMEM, and the culture medium was added to both apical and basolateral compartments, with changes every other day, during 21-23 days, until the monolayer achieve suitable initial transepithelial electrical resistance (TEER) values. The tightness of the Caco-2 monolayer was measured as TEER across the Caco-2 cell monolayer using a Millicell1-ER system (Millipore Corporation, Bedford, MA), equipped with a pair of chopstick electrodes that inserted into the apical medium. The TEER at the beginning of these studies was higher than 400 Ω cm^2, indicating an intact monolayer; TEER values were also obtained after completion of flux experiments at 6 h. The resistance measurement of the medium without cells was considered as blank. The permeability was carried out by adding 0.5 mL of culture medium containing the equivalent of 100 μg.mL^{-1} of DAP (as NPs-EL100-DAP or unloaded DAP) in the apical side of the cell monolayer. The samples were

incubated for 6 h, and at predetermined time intervals (1, 2, 3, 4 and 6 h), 0.5 mL were sampled from the basolateral compartment and replaced with fresh culture medium. The amount of DAP in the samples was analyzed by HPLC according the section 3.5. The experiments were carried out in triplicate. The cumulative amounts of DAP transported across the monolayers were calculated from the concentrations measured in the basolateral compartment. The apparent permeability (Papp) was calculated as described elsewhere [17].

2.6 Dapsone determination by high-performance liquid chromatography

The quantification of DAP in cell culture media was performed by high-performance liquid chromatography (HPLC) with UV detection. The HPLC system (Jasco) comprised a high-pressure pump (PU-2089), an autosampler (AS-2057) and a diode array detector (MD-2015) programmed for peak detection at 280 nm, controlled by ChromNAV software. A reversed phase Kinetex® core-shell C18 column (250 x 4.1 mm, 5 µm particle size, 100 Å; Phenomenex, Torrance, CA, USA) was used as stationary phase. Elution was performed in gradient mode using as mobile phase a mixture of aqueous acetate buffer (final concentration 50 mM, pH 4.8) and acetonitrile, at a flow rate of 1 mL min^{-1}. The selected gradient started with 30% (v/v) of acetonitrile, which was maintained up to 3 min. From 3 to 5.5 min, the contribution of acetonitrile was rapidly changed to 80% (v/v). This composition was maintained up to 7.5 min, after which the initial conditions were re-established and held during 5.5 min more to assure column equilibration. Hence, the total run time was 13 min. The injection volume was 20 µL. Standard dapsone solutions were prepared at 0.5, 1, 2.5, 5, 7.5, 10, 15 and 20 µg mL^{-1} in culture medium containing 40% (v/v) of acetonitrile and 50 mM acetate buffer, pH 4.8. To prepare the samples for HPLC analyses, 200 µL of each sample was added to 160 µL of acetonitrile and 40 µL of acetate buffer 500 mM, pH 4.8, to final concentrations of 40% (v/v) and 50 mM, respectively. The mixtures were vortexed and centrifuged at 18,000 × *g* for 10 min at room temperature. After centrifugation, supernatants were collected and analyzed by HPLC.

2.7 Data analysis

The statistical analysis of the experimental design was performed using STATISTICA10 (StatSoft®) software. GraphPad Prism software (version 6, GraphPad Software, La Jolla, CA, USA) was used for statistical comparisons of the results to control for the

cytotoxicity studies. Statistical analysis of the results was performed using student (unpaired) t-test and one-way ANOVA test. All the other results were presented as mean and standard deviation (SD). The differences were assumed statistical significant when $p < 0.05$ (95% confidence level).

3 Results and discussion

3.1 Experimental design

3.1.1 Preformulation screening: Plackett-Burman

During the development of nanoparticles formulations, it is crucial to define at first the suitable method of preparation, and then set and control production conditions, especially for polymeric nanoparticles in which several steps of the method of preparations may affect the characteristics of the obtained nanoparticles [18].

Plackett-Burman designs are screening models that involve a large number of factors and relatively few runs [19]. Because PBD are fractional factorial designs, the number of runs needed to investigate main effects is equal to $2n$ or multiples of 4 and therefore can be used to identify critical factors with a reasonable number of experimental runs and good degree of accuracy. Therefore, they are very useful to set or eliminate variables in further investigations [20]. Based on these facts, it is essential to perform preliminary studies in order to screen several critical parameters during the development of polymeric nanoparticles as: (i) drug solubility in the organic phase, which may influence the drug loading; (ii) the miscibility of the organic solvents with the aqueous phase considering the choice of the nanoprecipitation method; (iii) inclusion of a suitable stabilizer to prevent the aggregation of the nanosuspensions; (iv) the ratio polymer/drug as well as their concentration in the nanosuspension, which are important to both drug loading and stability of nanosuspensions [19]. Other important parameters were fixed as the type of polymer (EL100) due to its specific pH sensitivity; and the organic solvent used (ethanol:acetone - 1: 1 v/v) due to its miscibility with water and ability to solubilize of both drug and polymer. The obtained responses for the prepared formulations are expressed in Table 1.

Table 1. Layout and observed responses of Plackett–Burman screening design batches

Independent variables								Dependent variable		
batch	X_1	X_2	X_3	X_4	X_5	X_6	X_7	**Size (nm)**	**PDI**	**AE (%)**
1	10 mL	PVA	0.1%	1:5	0.5%	2 mL	N	198.3	0.146	81.9
2	20 mL	PVA	0.1%	1:1	1.0%	2mL	E	133.3	0.085	82.2
3	10 mL	Pluronic	0.1%	1:1	0.5%	4 mL	E	341.0	0.300	93.6
4	20 mL	Pluronic	0.1%	1:5	0.5%	2 mL	N	173.6	0.151	75.1
5	10 mL	PVA	1%	1:5	0.5%	2 mL	E	168.5	0.150	68.9
6	20 mL	PVA	1%	1:1	0.5%	4 mL	N	273.8	0.166	81.8
7	10 mL	Pluronic	1%	1:5	1.0%	2 mL	N	137.6	0.143	94.2
8	20 mL	Pluronic	1%	1:5	1.0%	4 mL	N	156.4	0.167	82.4

*X_1: volume of aqueous phase; X_2: type of surfactant; X_3: surfactant concentration (w/v); X_4: ratio polymer/drug; X_5: polymer concentration (w/v); X_6: volume of organic phase; X_7: method E= emulsion N = nanoprecipitation.

The results of the PBD are shown as a standardized Pareto chart (Figure 1), which consists of bars with a length proportional to the absolute value of the estimated effects, divided by the standard error [21]. The graphs evidence the *p*-values of the independent variables, which were considered to have significant effect when the values were < 0.05, with 95% of confidence [21]. As the design was constructed with continuous and categorical variables, the analysis was performed separately to obtain standardized estimated effects.

The categorical variables did not statistically influence the responses, on the contrary of the continuous variables (Figure 1). The response that suffered major alterations was the size (Figure 1A). Concerning the size, the concentration of the polymer in the organic phase (X_5), the volume of the organic phase (X_6) and the ratio polymer/drug (X_7) seemed to have a significant effect, in this order. The positive sign for the concentration of polymer in the organic phase reveals that the size tends to increase with the increase of the amount of polymer in the solution; on the contrary the opposite effect was observed for the other two significant variables (volume of organic phase and ratio polymer/drug), that presented negative sign. All the other variables as volume of aqueous phase (X_1), type of surfactant X_2), concentration of surfactant (X_3) and method of nanoparticle preparation (X_7) were considered insignificant, with 95% of confidence, and were fixed at level -1 for the subsequent studies.

The PBD allowed to reduce the number of variables from seven to three, namely: concentration of polymer in the organic phase (X_5); volume of organic phase (X_6) and ratio polymer/drug (X_7), which were selected for further optimization studies.

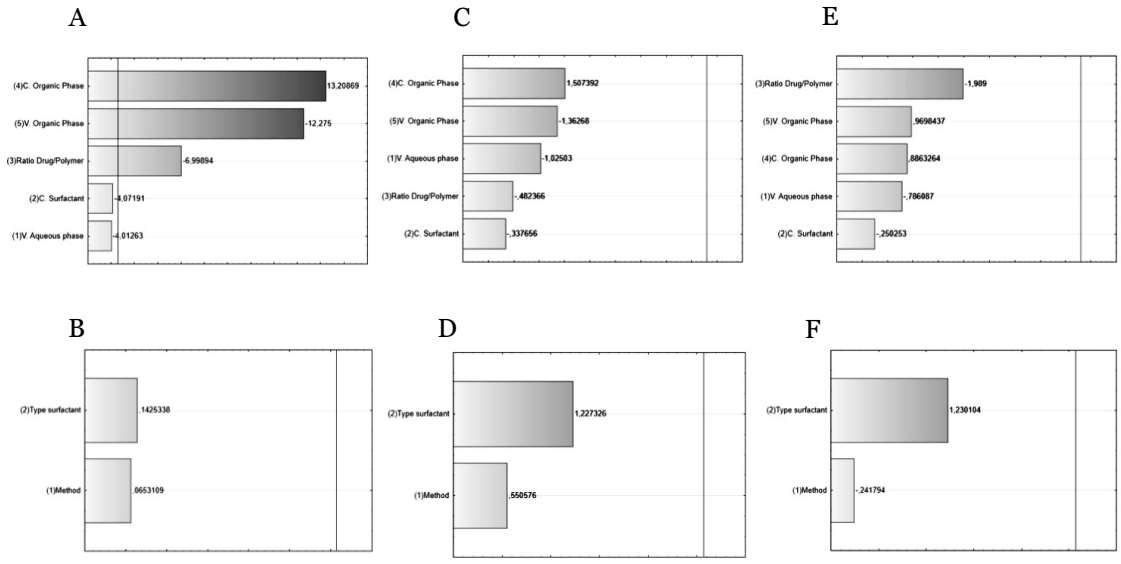

Figure 1. Pareto charts showing the significance of continuous (over) and categorical (down) variables for (A-B) particle size, (C-D) polydispersity index, and (E-F) association efficiency. (*p* values = 0.05)

3.1.2 Optimization: Box-Behnken design

After the preliminary investigation through the PBD model, a deeper investigation was performed with the most significant factors, to optimize the nanoparticles production conditions, using a three-level, three-factor BBD, which requires a minimum number of experiments when three factors are considered, as compared to others designs [1].
According to the previous sections the selected parameters were reassigned as follows: the polymer/drug (X_1); the concentration of the polymer in the organic phase (X_2); and the volume of the organic phase (X_3). The levels of the selected independent variables were chosen based on previous knowledge (Table 2). All the other variables were maintained constant, as described in the section 3.2.1. The responses (dependent variables) studied were the particles size (Y_1), the polydispersity index (PDI, Y_2) and the association efficiency (AE, Y_3). The experimental values of the 15 formulations generated by the BBD were obtained (Table S2).

Table 2. Summary of the coded levels of the Box-Behnken design; including the levels of the optimized formulation, the desirable parameters used for the optimization, and the comparison between predicted and observed values for the considered responses

Independent variables				***Dependent variables***
	Coded Levels			Y_1 = Particle size (nm)
	Low Level (-1)	Medium Level (0)	High Level (+1)	Y_2 = PDI
X_1 = ratio polymer/drug	1:1	2:1	3:1	Y_3 = AE (%)
X_2 = concentration of organic phase (w/v)	0.5 %	1 %	1.5 %	
X_3 = volume organic phase	1 mL	2 mL	3 mL	

The mathematical correlation between the factors coefficients and their *p* values were analyzed via regression analysis, for each response, and are expressed in Table 3.

Table 3. Summary of the regression analysis for the considered responses Y_1–Y_3

	Particle size (Y_1)		***PDI (Y_2)***		***AE (Y_3)***	
	Coeffficient	*p*-Value	Coeffficient	*p*-Value	Coeffficient	*p*-Value
β0	192.067	**0.000**	0.191	**0.000**	37.214	**0.000**
X_1	-4.688	0.373	-0.004	0.639	-7.092	**0.003**
X_1^2	13.996	**0.011**	0.001	0.914	-0.290	0.771
X_2	27.613	**0.002**	0.035	**0.005**	2.691	0.090
X_2^2	-0.054	0.211	0.002	0.662	-3.274	**0.018**
X_3	8.275	0.145	0.011	0.194	4.186	**0.022**
X_3^2	-6.167	**0.006**	-0.011	0.086	-0.142	0.887
$X_1.X_2$	-13.650	0.100	-0.030	**0.035**	-0.112	0.953
$X_1.X_3$	-9.475	0.221	-0.004	0.696	0.883	0.647
$X_2.X_3$	-5.975	0.418	-0.037	**0.016**	-7.264	**0.010**
R^2	**0.945**		**0.913**		**0.937**	

The factors were considered statistically significant, with 95% of confidence level, when *p* values are less than 0.05. The response variables were fitted to different regression models, in which the best fitting was considered. The polynomial equations were statistically validated using ANOVA and were considered statistically significant when *F* was higher than F_{critic} for all responses [1]. The mean values of the obtained response corresponded to the intercept of the model. The magnitude and the sign of the polynomial coefficients, expressed in Table 3, indicate synergistic or antagonistic effect,

when the signs are positive or negative, respectively. Moreover, effects of the change of more than one factor at a time, or quadratic relations of the terms are studied by evaluating the regression coefficients of $X_n.X_m$ *and* X_n^2 respectively.

3.1.2.1 Effect on particle size

The combination of level factors of the BBD result in a range of particle sizes between 135.0 nm (F2) and 253.8 nm (F12). According the regression analysis, the ratio polymer/ drug (X_1) and the concentration of the polymer in the organic phase (X_2) showed to be statistically significant for the particle size. For X_1 only the quadratic coefficient was statistically relevant, which suggest a non-linear response with the change in ratio polymer/drug. The positive sign of the coefficient suggests that the particle size increase with the increasing of the values of the levels of X_1. i.e., when the amount of polymer in the medium is higher than the amount of drug, the particle size seems to increase. Similarly, the linear coefficient of X_2 has a positive sign, suggesting that the particle size increases with the increasing of polymer concentration in the organic phase. Both facts are expectable as, the polymer density in each drop during the particles preparation by the nanoprecipitation is higher when the levels of these variables increase, thus resulting in larger particles [22]. These effects are summarized in the response surface graph **(Figure 2).**
Moreover, the organic solvent volume (X_3) significantly influenced the particle size in a negative way, i.e., the higher is the volume, the smaller seem to be particles.

3.1.2.2 Effect on polydispersity

The PDI values obtained from the 15 formulations ranged from 0.129 (F1) to 0.268 (F10), indicating a narrow distribution. Based on the regression analysis, the simultaneous modification of the ratio polymer/drug (X_1) and the concentration of the polymer in the organic phase (X_2) showed to be statistically significant ($p < 0.05$). The negative sign means that the combination of the variables may influence the decreasing of the PDI value. As observed in Figure 2 the PDI values decrease with the decreasing of the concentration of polymer in the organic phase together with the decreasing of the ratio polymer/drug, as the optimal values are closer to the levels -1 for both variables. Similarly, to the particle size, the density of the polymer in the organic phase may promote the aggregation of the particles due to the supersaturation of the polymer when the solvent drops get in contact with the aqueous phase, leading to the formation of precipitates.

Simultaneous changing of the volume (X_3) and concentration (X_2) of organic phase also promoted significant changing in PDI values. In fact higher concentrations of solute increases the viscosity of the organic phase, making difficult the formation of particles from the solvent dripping, leading to particles with high dispersity index [23].

3.1.2.3 Effect on drug association efficiency

The AE obtained from the formulations varied from 21.6% (F6) to 50.8% (F3). According to the results of the regression analysis the ratio polymer/drug (X_1), the concentration of polymer in organic phase (X_2), the volume of the organic phase (X_3), statistically influenced the AE rate ($p < 0.05$). Besides X_2 seemed to influence the AE in a non-linear way as only quadratic effect was significant. The negative sign before X_1 regression coefficient revels an inverse relation between polymer/drug ratio and AE. Similar results have already been reported [24].

On the other hand, the positive sign of X_3 indicates that the AE increases with the increasing of the volume used during the nanoparticle preparation. This could be explained by the higher degree of DAP solubilization with the increasing of the relation organic to aqueous phase, retarding the solvent diffusion in the media, which may maintain DAP solubilized and viable to be entrapped.

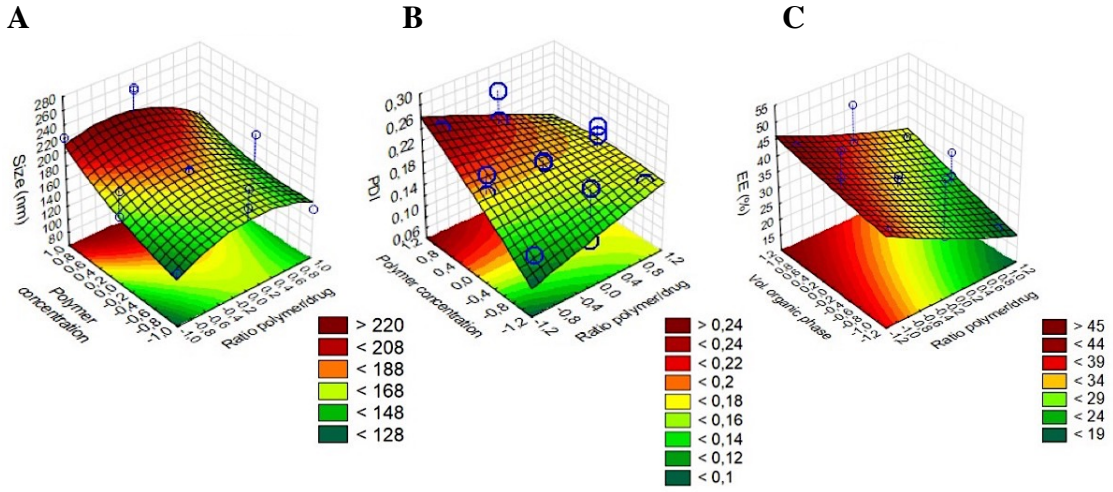

Figure 2. Response surface models showing the influence of the independent variables on the selected responses particles size (Y_1) (A), PDI (Y_2) (B) and AE (Y_3) (C).

3.1.3 Validation of de obtained models

For the optimization, specific values of the responses were selected as particle size (Y_1) was below 200nm; minimum PDI (Y_2); and maximum AE (Y_3). The high R^2 of all the

models (Table 3) indicate good correlation between the experimental and predicted results. Three-dimensional response surface graphs were plotted, for the significant variables in each response, in other to better understand the behavior of the dependent variables.

The optimized nanoparticles were designed using the desirability function of the STATISTCA10 (StatSoft®) software, in which each response is associated with its own partial desirability function. The point possessing the highest value for desirability is termed as optimum. Based on the desirability analysis, the optimized formulation was achieved with the ratio polymer/drug 2:1 (0); with polymer concentration in organic phase of 0.5% w/v (-1) and volume of organic phase of 3 mL (+1).

The optimal nanoparticles were selected and prepared as checkpoint to validate the model. The predicted values for all the responses were closer to the observed, with deviation/bias < 6.5% which characterize the robustness and high extrapolative ability of prediction of the mathematical models.

3.2 Characterization of the optimized nanoparticles

3.2.1 Particle size, polydispersity index and association efficiency

After optimization based on the desirable profile, the check point formulation was formulated in triplicated. Unloaded EL100 nanoparticles were also prepared. The mean of particle size measurements for NPs-EL100-DAP was 198 ± 6 nm and for NPs-EL100 was 185 ± 9 nm, which were in good agreement. PDI values were considered suitable (0.200 and 0.179 for NPs-EL100-DAP and NPs-EL100, respectively). The AE of NPs-EL100-DAP was 47.9% ± 4.8, which was considered a good value, considering loading capacity of the developed system.

3.2.2 Fourier-Transform Infra-Red studies

The FTIR spectra of DAP optimized freeze-dried NPs-EL100 and NPs-EL100-DAP nanoparticles are shown in Figure 3. The FTIR spectrum of NPs-EL100 presents characteristics bands of the polymer Eudragit L100 mainly in the region between 3500-3000 cm^{-1} and in 1740-1695 cm^{-1} which correspond to –OH, and C-O stretching vibrations, respectively. The spectrum of NPs-EL100-DAP is the superposition of the FTIRspectra of NP-EL, with the presence of characteristic peaks of DAP (1590-1550 cm^{-1}), (Figure 3), indicating the presence of DAP [25].

In the DAP spectrum, it can be observed: band at 3300-3400 cm^{-1} corresponding to the stretch of the amine group (N-H); and, characteristic band of the bending vibration of NH_2 group between 1590-1550 cm^{-1}. Bands regarding the symmetric and asymmetric vibrations of the sulfone group ($-SO_2$) in 1143 and 1180 cm^{-1} respectively were also found [9].

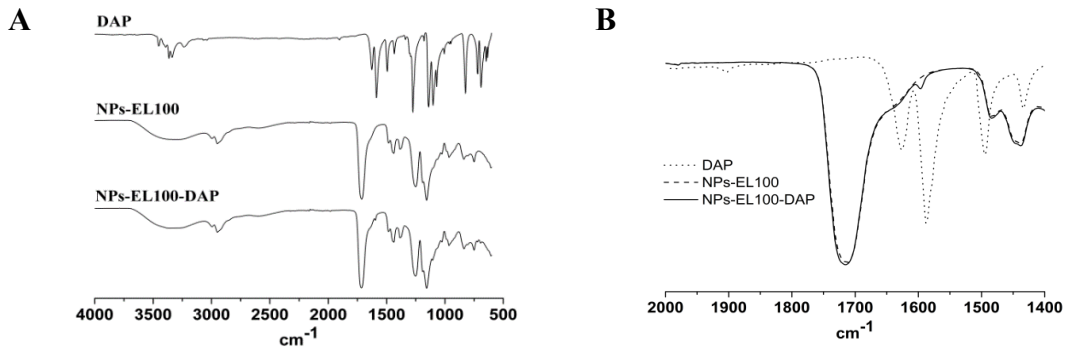

Figure 3. FTIR spectra of (A) DAP, NPs-EL100 and NP-EL100-DAP, and (B) detail of the spectra in the region between 2000-1400 cm^{-1}.

3.2.3 Differential scanning calorimetry studies

DSC thermograms of DAP, EL100, NPs-EL100 and NPs-EL100-DAP are shown in Figure 4. The thermograms of NPs-EL100-DAP did not sow the endothermic event corresponding to the melting of DAP, indicating that the drug is present in the system in the amorphous phase, and may be homogeneously dispersed in the polymer matrix. In addition, the simple superposition of the NPs-EL100 and NPs-EL100-DAP, suggest that no interaction between the drug and the nanoparticles constituents occurred. The thermogram of DAP shows two endothermic events, the first at 83°C corresponding to a polymorphic transition of DAP, and the second at 179°C corresponding to the melting of DAP [1, 26]. The thermogram of EL100 shows an endothermic event at 210°C which could be attributed to the film formation of EL100.

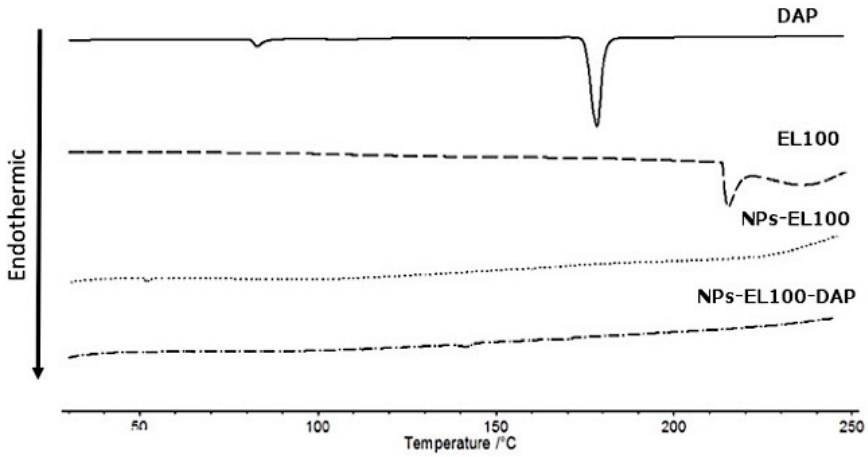

Figure 4. DSC thermograms of DAP, EL100, NPs-EL100 and NPs-EL100-DAP.

3.2.4 Morphology assessment

The morphology of NPs-EL100 and NPs-EL100-DAP are shown in the Figure 5. The TEM micrographs show that the particles were spherical in shape, with homogeneous distributions, and no morphological differences between unloaded and drug loaded nanoparticles was found. The size of the particles seemed to be in accordance to the values obtained by the DLS measurements.

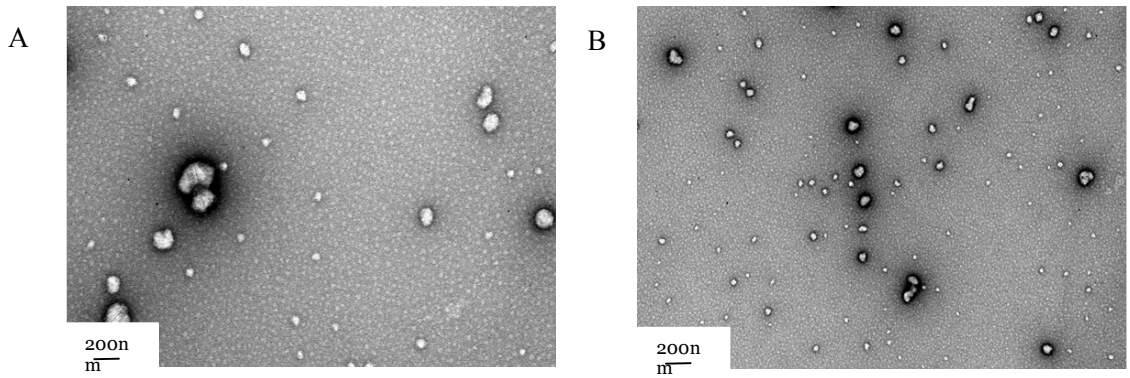

Figure 5. TEM images of NPs-EL100 and NPs-EL100-DAP. Scale bar 200 nm

3.2.5 In vitro drug release assays

The *in vitro* drug release from the optimized NPs-EL100-DAP was evaluated using the dialysis bag diffusion technique. Two different pH conditions (1.2 and 6.8) were

assessed to mimic stomach (2 h, pH 1.2) and intestinal (6h, pH 6.8) physiological conditions, respectively.

The cumulative percentage of drug released from the NPs-EL100-DAP for each pH are represented in the Figure 6. According to the release profile, it could be seen that during the 2 h in acidic conditions, only 30.7% ± 3.2% crossed the diffusion membrane, which may help to reduce DAP side-effects on the gastric mucosa. Considering the AE of the optimized NPs (about 50%) it is possible to infer that most of the released DAP on gastric fluid corresponds to the non-entrapped DAP, proving that, in fact, the highest amount of drug remains entrapped within the NPs.

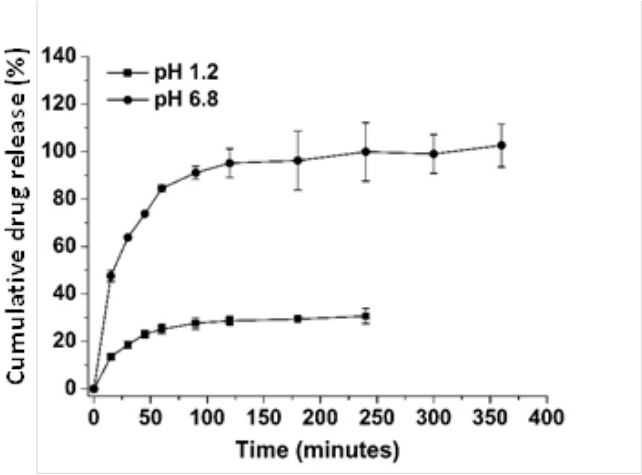

Figure 6: *In vitro* release profile of DAP from NPs-EL100-DAP in different pH conditions.

In intestinal mimetic environment, pH 6.8, the NPs-EL100-DAP revealed a different release profile. A biphasic profile was observed with approximately 80% of DAP was released within the first hour, followed by a sustained release reaching up to 100%. The fast DAP release of the drug at pH 6.8 may be explained by the high loading capacity of the nanoparticles and the fast dissolution of the polymer in more alkaline pH conditions (6.8) (Figure 6). In fact, the swelling behavior of EL100 and the erosion phenomenon have been already reported [2, 5, 6, 25].

According to the results, the developed drug delivery system was able to retain the DAP in acidic environment (pH 1.2), during the initial 2 h, and release the drug immediately when the pH changes close to neutral values (pH 6.8) suggesting that the optimized nanoparticles could overpass the stomach environment (acidic) considering the transit time, and reach the intestine (pH 6.8) where the drug may be delivered and then be available to be absorbed, avoiding possible acid hydrolysis in the stomach. Usually, drug release profile depends on the specific properties of the polymer, on the drug loading and polymer/drug ratio. Cetin and co-workers have described for a fast drug release from Eudragit nanoparticles releated to more water uptake, swelling ratio,

and/or polymer degradation [6]. Moreover, an increasing in the drug release has been observed as a function of polymer/drug ratio [6, 27].

3.3 Cell studies

3.3.1 Cell viability assessment

Following the promising pH-triggered release of DAP under gastro-intestinal conditions, *in vitro* biocompatibility of the NPs-EL100 systems were analyzed in MKN-28, Caco-2 and HT29-MTX cells. The rationale for selecting different cell lines was related to their importance as suitable models mimicking the different cell-types of the GI tract (e.g., stomach, enterocytes and mucus secreting cells) and, therefore, relevant in the oral route of administration [28, 29]. In addition, the aim of this study was to evaluate if the nanoparticles were able to protect the GIT membranes from any adverse effect of DAP alone.

The effects of NP-EL100, NPs-EL100-DAP and free DAP on the cell lines MKN-28, Caco-2 and HT29-MTX are shown in Figure 7. According to data, during the period of 24 h, NPs-EL100-DAP showed cell viabilities higher than 80%, thus it did not present significant reduction on cell viability in the up to 400 μg mL^{-1} in DAP, for the cell lines Caco-2 and HT29-MTX. Similar results were observed with unloaded nanoparticles (Figure 7A and 7B). For the gastric cell line MKN-28, cell viability values for the tested samples were higher than 75% after 4 h, at all the tested concentrations (Figure 7C). Same results were found for free DAP. The absence of cytotoxicity of the NPs-EL100-DAP in both intestinal cells and in most of the tested concentrations in MKN-28 cells could be attributed to EL-100 biocompatibility [30]. Moreover, the polymeric-based system probably avoided instant delivery of DAP to the cellular media which might attribute to the sustained release and consistent diffusion of drug from the nanoparticle (Figure 6).

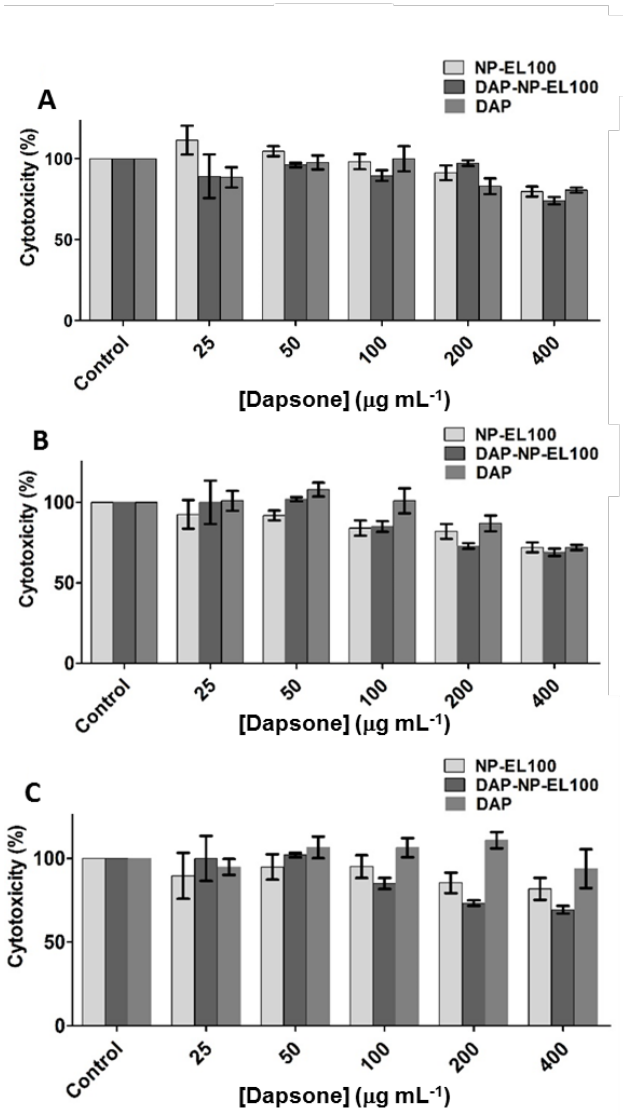

Figure 7. Cell viability of the intestinal and gastric cells exposed to the NP-EL100, NPs-EL100-DAP and free DAP, assessed by the MTT assay. The viability of Caco-2 (A), HT29-MTX (B) and MKN-28 (C) cells after 24 (A and B) and 4 h (C) incubation with different dapsone concentrations (free or loaded in NPs) at 37 °C and equivalent polymeric concentration. Data expressed as the average ± standard deviation (n=5, of three different assays).

3.3.2 DAP permeation across Caco-2 monolayer

The *in vitro* bioassay with Caco-2 cells monolayer has been widely used as model to predict drug permeability and have been well correlated with *in vivo* absorptions in humans [29]. Thus Caco-2 monolayer assay was conducted to analyze the permeability of DAP as loaded in NPs-EL100 formulation and as free drug. The tested concentration was selected according to the cytotoxicity assays, which was 100 µg mL^{-1} of DAP

equivalent to 200 μg mL^{-1} in polymer concentration in the NPs-EL100-DAP formulations.

The cells monolayer integrity was evaluated by TEER analysis throughout the experiment, and no cellular lesion which changes TEER values was detected (data not shown). In the beginning of the experiment the initial TEER values were higher than 400 Ωcm^2, as recommended for absorption studies [31]. The addition of the studied samples did not affect these values until the end of the experiment (6 h).

As can be observed in Figure 8, the permeation profile of NPs-EL100-DAP in comparison to free DAP presented different trends. The polymeric-based nanoparticles were able to significantly enhance the DAP permeation across the intestinal cells (ca. 55% of the initial amount), as compared to free DAP, suggesting that the presence of pharmaceutical adjuvants helped in the permeation process. Given the physicochemical characteristics of the NPs-EL100-DAP, cellular interaction might occur by endocytic and transcytosis processes. Additionally, the DAP release from NPs-EL100 observed in the *in vitro* studies (Figure 6) is in accordance with these results, where a steady permeability profile and improved permeability resulted in significant differences in the apparent permeability values (Fig 8B). The small droplet size of the polymeric nanoparticles enables better adherence to the membrane during transport of the drug and optimizes intestinal absorption and permeation [32]. The low water solubility of free DAP may be related with the reduced amounts of DAP obtained in the basolateral chamber, reaching about 30 % of the initial amount within 6 h. The DAP rapidly precipitates in the medium which hampers its permeation across the monolayer from the apical to the basolateral side. The cumulative permeated amount of DAP across the Caco-2 cells monolayer up to 6 h is shown in Figure 8A. A significant permeability enhancement of DAP was observed for the NPs-EL100-DAP formulation after 6 h of contact with Caco-2 cell monolayers ($^{**}p<0.05$), when compared to free DAP. Therefore, dapsone, a class II drug, when incorporated in a polymeric-based nanoparticle, behaves as a class I drug according to the Biopharmaceutics Classification System, due to its higher solubility and higher permeability, with a Papp of 23.5×10^{-6} cm/sec [33]. Accordingly, both the dose required and the subsequent adverse effects can be reduced, with improved absorption and permeability. In this work, a polymeric-based nanoparticle of EudragitL100 was used and its properties allowed a higher permeability coefficient of DAP that the obtained with other nanoemulsion systems previously described [32, 34, 35].

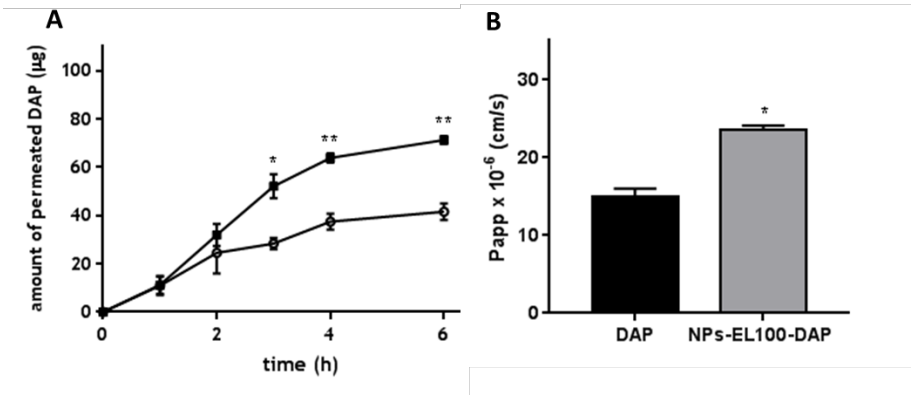

Figure 8. *In vitro* cumulative permeability profile and Papp coefficient of DAP (open circles) and NPs-EL100-DAP (clack squares) across the Caco-2 cells monolayer. The experiments were conducted from the apical-to-basolateral direction in culture medium at 37 °C. Data sets were compared to free DAP (*$p < 0.05$, **$p < 0.01$). Error bars represent mean ± s.d. (n ≥ 3).

4 Conclusions

In this study, pH-sensitive NPs-EL00-DAP was successfully developed and characterized after the identification of most critical variables, through PBD and the optimization employing a three-level, three-factor BBD. The ratio polymer/drug, the concentration of polymer in the organic phase and the volume of the organic phase were found to be the most significant variables that affected the formulations properties. The experimental design strategies allowed to understand the main formulation and process parameters that affected the selected responses namely particle diameter, PDI and AE. The optimized formulation was achieved based on the desirability profile and presented low bias compared to the predicted values for these responses.

FTIR and DSC analysis confirmed the association of DAP and the absence of interactions; TEM micrographs revealed the spherical morphology of the nanoparticles and supported the results obtained from the DLS analysis. The *in vitro* drug release at different pH conditions confirmed the pH sensitivity of NPs-EL00-DAP, being able to provide enhanced drug delivery at intestinal environment. No toxicity was observed in Caco-2, HT29-MTX and MKN-28 cell lines up to 400 µg.mL^{-1} of DAP. Thus, the protection property of the EL100 from acidic environment showed to be promising to delivery strategy at the site of absorption, as 2-fold enhanced permeability was observed when DAP was incorporated within NPs-EL100 in comparison to free DAP. In

fact, the application of NPs-EL100 to deliver DAP, a class II drug, increased its solubility and permeability, resulting in a class I drug behavior.

The present study demonstrated the potential of NPs-EL00-DAP as a therapeutic platform, although further studies using clinical relevant models should be pursued to assess its efficacy for treatment of diseases as leprosy.

Financial & competing interest disclosure

This work received financial support from the European Union (FEDER funds) and National Funds (FCT/MEC, Fundação para a Ciência e Tecnologia and Ministério da Educação e Ciência) under the Partnership Agreement PT2020 UID/MULTI/04378/2013 - POCI/01/0145/FEDER/007728. SCL thanks Operação NORTE-01-0145-FEDER-000011 for her Investigator contract. The authors also thank the CNPq Foundation and CAPES, Ministry of Education of Brazil for the Doctoral fellowship 246514/2012-4 and and 0831-12-3 respectively; and FCT for the Post-Doctoral fellowship SFRH/BPD/99124/2013 and and L. Barreiros thank FCT/MEC and POPH (Programa Operacional Potencial Humano) for her Post-Doc grant (SFRH/BPD/89668/2012). The authors have no other relevant affiliations or financial involvement with any organization or entity with a financial interest in or financial conflict with the subject matter or materials discussed in the manuscript apart from those disclosed.

No writing assistance was utilized in the production of this manuscript.

5 References

1. Vieira, A.C., et al., *Design and statistical modeling of mannose-decorated dapsone-containing nanoparticles as a strategy of targeting intestinal M-cells*. Int J Nanomedicine, 2016. **11**: p. 2601-17.
2. Jog, R., K. Unachukwu, and D.J. Burgess, *Formulation design space for stable, pH sensitive crystalline nifedipine nanoparticles*. Int J Pharm, 2016. **514**(1): p. 81-92.
3. Younis, N., M.A. Shaheen, and M.H. Abdallah, *Silymarin-loaded Eudragit((R)) RS100 nanoparticles improved the ability of silymarin to resolve hepatic fibrosis in bile duct ligated rats*. Biomed Pharmacother, 2016. **81**: p. 93-103.
4. Sahle, F.F., et al., *Formulation and in vitro evaluation of polymeric enteric nanoparticles as dermal carriers with pH-dependent targeting potential*. Eur J Pharm Sci, 2016. **92**: p. 98-109.
5. Hao, S., et al., *Preparation of Eudragit L 100-55 enteric nanoparticles by a novel emulsion diffusion method*. Colloids Surf B Biointerfaces, 2013. **108**: p. 127-33.

6. Cetin, M., A. Atila, and Y. Kadioglu, *Formulation and in vitro characterization of Eudragit(R) L100 and Eudragit(R) L100-PLGA nanoparticles containing diclofenac sodium*. AAPS PharmSciTech, 2010. **11**(3): p. 1250-6.

7. Animesh, K., et al., *Applicability and approaches of (Meth) acrylate copolymers (Eudragits) in novel drug delivery systems*. Curr Drug ther, 2012. **7**(4): p. 219-234.

8. Nollenberger, K. and J. Albers, *Poly(meth)acrylate-based coatings*. Int J Pharm, 2013. **457**(2): p. 461-9.

9. Chaves, L.L., et al., *Rational and precise development of amorphous polymeric systems with dapsone by response surface methodology*. Int J Biol Macromol, 2015. **81**: p. 662-71.

10. Borges, V.R., et al., *Nanoemulsion containing dapsone for topical administration: a study of in vitro release and epidermal permeation*. Int J Nanomedicine, 2013. **8**: p. 535-44.

11. Dhat, S., et al., *Risk management and statistical multivariate analysis approach for design and optimization of satranidazole nanoparticles*. Eur J Pharm Sci, 2017. **96**: p. 273-283.

12. Singh, G. and R.S. Pai, *In-vitro/in-vivo characterization of trans-resveratrol-loaded nanoparticulate drug delivery system for oral administration*. J Pharm Pharmacol, 2014. **66**(8): p. 1062-76.

13. Gandhi, A., S. Jana, and K.K. Sen, *In-vitro release of acyclovir loaded Eudragit RLPO((R)) nanoparticles for sustained drug delivery*. Int J Biol Macromol, 2014. **67**: p. 478-82.

14. Kim, S.R., et al., *Cationic PLGA/Eudragit RL nanoparticles for increasing retention time in synovial cavity after intra-articular injection in knee joint*. Int J Nanomedicine, 2015. **10**: p. 5263-71.

15. Zhang, Y., et al., *Thiolated eudragit-based nanoparticles for oral insulin delivery: preparation, characterization, and evaluation using intestinal epithelial cells in vitro*. Macromol Biosci, 2014. **14**(6): p. 842-52.

16. Zhang, Y., et al., *Thiolated Eudragit nanoparticles for oral insulin delivery: preparation, characterization and in vivo evaluation*. Int J Pharm, 2012. **436**(1-2): p. 341-50.

17. Woitiski, C.B., et al., *Facilitated nanoscale delivery of insulin across intestinal membrane models*. Int J Pharm, 2011. **412**(1-2): p. 123-31.

18. Zazo, H., C.I. Colino, and J.M. Lanao, *Current applications of nanoparticles in infectious diseases*. J Control Release, 2016. **224**: p. 86-102.

19. Shah, S.R., et al., *Application of Plackett–Burman screening design for preparing glibenclamide nanoparticles for dissolution enhancement*. Powder Technol, 2013. **235**: p. 405-411.

20. Awotwe-Otoo, D., et al., *Evaluation of anticancer drug-loaded nanoparticle characteristics by nondestructive methodologies*. AAPS PharmSciTech, 2012. **13**(2): p. 611-22.

21. Cao, W., et al., *Optimization of peptic hydrolysis parameters for the production of angiotensin I-converting enzyme inhibitory hydrolysate from Acetes chinensis through Plackett-Burman and response surface methodological approaches*. J Sci Food Agric, 2012. **92**(1): p. 42-8.

22. Sukhbir, S., S. Yashpal, and A. Sandeep, *Development and statistical optimization of nefopam hydrochloride loaded nanospheres for neuropathic pain using Box-Behnken design*. Saudi Pharm J, 2016. **24**(5): p. 588-599.

23. Park, S.J., et al., *Quality by design: screening of critical variables and formulation optimization of Eudragit E nanoparticles containing dutasteride*. Arch Pharm Res, 2013. **36**(5): p. 593-601.

24. Kilicarslan, M. and T. Baykara, *The effect of the drug/polymer ratio on the properties of the verapamil HCl loaded microspheres*. Int J Pharm, 2003. **252**(1-2): p. 99-109.

25. Nadal, J.M., et al., *Spray-dried Eudragit(R) L100 microparticles containing ferulic acid: Formulation, in vitro cytoprotection and in vivo anti-platelet effect*. Mater Sci Eng C Mater Biol Appl, 2016. **64**: p. 318-28.

26. Grebogi, I.H., et al., *Binary and ternary inclusion complexes of dapsone in cyclodextrins and polymers: preparation, characterization and evaluation*. J Incl Phenom Macrocycl Chem 2011. **73**(1-4): p. 467-474.

27. Das, S., P.K. Suresh, and R. Desmukh, *Design of Eudragit RL 100 nanoparticles by nanoprecipitation method for ocular drug delivery*. Nanomedicine, 2010. **6**(2): p. 318-23.

28. Fernandes, I., et al., *A new approach on the gastric absorption of anthocyanins*. Food Funct, 2012. **3**(5): p. 508-16.

29. Araujo, F. and B. Sarmento, *Towards the characterization of an in vitro triple co-culture intestine cell model for permeability studies*. Int J Pharm, 2013. **458**(1): p. 128-34.

30. Singh, S., S. Neelam, and Y. Singla, *An overview of multifaceted significance of eudragit polymers in drug delivery systems*. Asian J Pharm Clin Res, 2015. **8**(5): p. 1-6.

31. Freichels, H., et al., *Targeting nanoparticles to M cells with non-peptidic ligands for oral vaccination*. Eur J Pharm Biopharm, 2009. **73**(1): p. 16-24.

32. Talegaonkar, S., et al., *Microemulsions: a novel approach to enhanced drug delivery*. Recent Pat Drug Deliv Formul, 2008. **2**(3): p. 238-57.

33. Lam, K.W., et al., *Pharmaceutical Salt Formation Guided by Phase Diagrams*. Ind Eng Chem Res, 2010. **49**(24): p. 12503-12512.

34. Kogan, A. and N. Garti, *Microemulsions as transdermal drug delivery vehicles*. Adv Colloid Interface Sci, 2006. **123-126**: p. 369-85.

35. Monteiro, L.M., et al., *Development and characterization of a new oral dapsone nanoemulsion system: permeability and in silico bioavailability studies*. Int J Nanomedicine, 2012. **7**: p. 5175-82.

5 Supplementary material

Selected independent variables performed during Plackett-Burman design and their respectives low (-1) and high (+1) coded and real levels.

Table S1: Independent variables with the respective levels.

Factor	Factor significance	Level (-1)	Level (+1)
X_1	Vol. of aqueous phase (AP)	10 mL	20 mL
X_2	Type of surfactant	PVA	Pluronic® F68
X_3	Surfactant concentration (w/v)	1%	0.1%
X_4	Ratio polymer/drug*	1 : 1	1 : 5
X_5	Polymer concentration (w/v)	0.5%	1%
X_6	Vol. organic phase (OP)	2 mL	4 mL
X_7	Method	Nanoprecipitation (N)	Emulsion (E)

*the amount of drug was always adjusted to the ratio polymer/drug based on the concentration of polymer in the organic phase.

Experimental values of the 15 formulations generated by the Box-Behnken design with the selected independent variables namely (X_1) the ratio polymer/drug; (X_2) concentration of the polymer in the organic phase and (X_3) volume of organic phase. The levels of the selected independent variables were chosen based on previous knowledge. All the other variables were maintained constant, as described in the section 3.2.1. The dependent variables studied were the particles size (Y_1), the polydispersity index (PDI, Y_2) and the association efficiency (AE, Y_3).

Table S2: Formulation composition and the effects of different formulation variables on the dependent variables.

Formulation	**Independent variables**			**Dependent variables**		
	X_1	X_2	X_3	Y_1 *(nm)*	Y_2	Y_3 *(%)*
F1	-1	-1	0	138.4	0.129	42.9
F2	1	-1	0	135.0	0.165	28.2
F3	-1	1	0	221.4	0.241	50.8
F4	1	1	0	163.4	0.159	35.7
F5	-1	0	-1	162.3	0.181	36.3
F6	1	0	-1	193.2	0.198	21.1
F7	-1	0	1	199.3	0.213	43.4
F8	1	0	1	192.3	0.213	31.7
F9	0	-1	-1	184.0	0.107	26.4
F10	0	1	-1	250.7	0.268	44.0
F11	0	-1	1	211.0	0.200	48.8
F12	0	1	1	253.8	0.215	37.3
F13	0	0	0	182.5	0.191	34.7
F14	0	0	0	183.8	0.194	26.3
F15	0	0	0	181.0	0.154	35.8

*X_1 = ratio polymer/drug (-1 = 1:1; 0 = 2:1; +1 = 3:1); X_2 = concentration of organic phase (-1 = 0.5%; 0 = 1.0%; +1 = 1.5%); X_3 = volume of organic phase (-1 = 1 mL; 0 = 2 mL; +1 = 3 mL); Y_1 = particle size; Y_2 = PDI; Y_3 = AE.

C. Optimization of solid lipid nanoparticles for clofazimine delivery: risk management, statistical design and physicochemical characterization.[5]

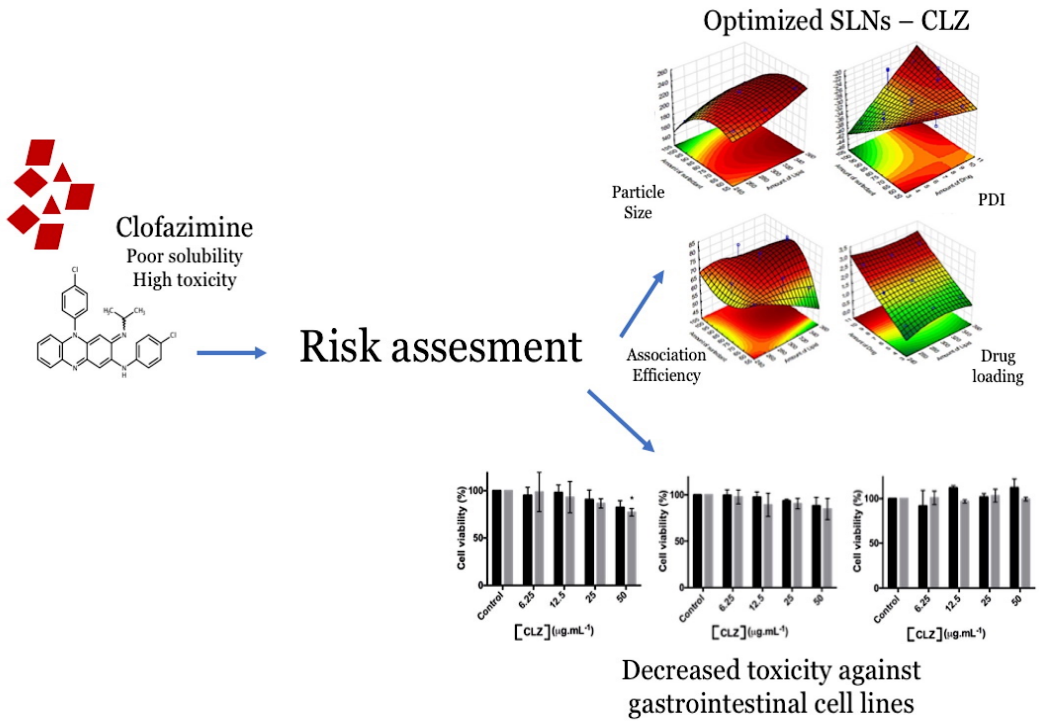

[5] Submitted

Optimization of solid lipid nanoparticles for clofazimine delivery: risk management, statistical design and physicochemical characterization

Luíse L. Chaves[a], Sofia Lima[a,b], Alexandre C.C.Vieira[a], Domingos Ferreira[c], Bruno Sarmento[b,d,e], Salette Reis[*a]

[a]UCIBIO, REQUIMTE, Departamento de Ciências Químicas, Faculdade de Farmácia, Universidade do Porto, Porto, Portugal
[b]CESPU, Instituto de Investigacão e Formação Avançada em Ciências e Tecnologias da Saúde and Instituto Universitário de Ciências da Saúde, Gandra, Portugal
[c]UCIBIO, REQUIMTE, Laboratório de Tecnologia Farmacêutica, Faculdade de Farmácia, Universidade do Porto, Portugal
[d]I3S, Instituto de Investigacão e Inovação em Saúde, Universidade do Porto, Portugal
[e]INEB – Instituto de Engenharia Biomédica, Universidade do Porto, Portugal

ABSTRACT

The aim of this work was to develop solid lipid nanoparticles (SLNs) loaded with clofazimine (CLZ) (SLNs-CLZ), towards drug bioavailability improvement and reduction of its intrinsic high toxicity. Initially, risk assessment of the process and product variables was conducted, helping to select the starting conditions of the pre-formulation. The identification of drug crystals allowed the implementation of control actions during nanoparticles characterization. A spectrophotometric method for the quantification of CLZ in SLNs was developed, validated and showed to be accurate, precise, efficient, specific and sensitive with low limits of detection and quantification. A Box-Behnken design was constructed and the relations between the independent variables in the selected responses could be understood. The optimized SLNs-CLZ with suitable particle size (PS), zeta potential (ZP), association efficiency (AE) and drug loading (DL) parameters for oral delivery. The optimized SLNs-CLZ were also characterized by Fourier transformed infra-red spectroscopy (FTIR) and differential scanning calorimetry (DSC). The optimized SLNs-CLZ presented values of 230 nm, -34.28 mV, 72% and 2.39 % of PS, ZP, AE and DL respectively. FTIR confirmed the presence of the drug and the absence of chemical interactions, while DSC thermograms indicated the amorphous state of CLZ. The storage stability studies ensured the stability of the systems over a period of 12 weeks at 4°C. *In vitro* cytotoxicity studies evidenced no significant effect of both drug-load and unloaded SLNs on MKN-28 gastric cells and on intestinal cells, namely Caco-2 and HT29-MTX cells up to 25 μg mL^{-1} in CLZ. Free CLZ solutions exhibited IC_{50} values of 16.3 and 20.3 μg mL^{-1} for Caco-2 and HT29-MTX cells, respectively. It can be concluded that the optimized system was developed considering important variables for the formulation of poorly soluble drugs. The optimized SLNs-CLZ represent a promising platform to orally deliver CLZ.

Key-words: leprosy, Box-Behnken design, cytotoxicity, UV-Vis quantification

1. Introduction

Clofazimine (CLZ) is an antibiotic and anti-inflammatory drug, classified as a riminophenazine agent [1, 2]. It has been recommended for decades by the World Health Organization for the therapy of multibacillary leprosy. In addition, recent studies have revived its application in the treatment of multidrug-resistant tuberculosis [1, 2].

Despite its clinical approval, it is a highly hydrophobic drug (logP > 7) [1], virtually insoluble in water [2]. This particular feature of CLZ result in a limited absorption (about 40%) due to its extremely high hydrophobicity, associated with a very large volume of distribution and elimination half-life of more than 70 days, as the cells act as drug reservoirs [3]. After long-term administration, the consequent bioaccumulation of CLZ results in yellowish and reddish skin pigmentation, abdominal pain and cardiotoxicity [1].

CLZ has three amine groups, which may be protonated and charged at acidic pH, increasing its solubility. Therefore, in the gastrointestinal tract, CLZ may form supersaturated solutions, as it passes from the stomach (pH 1 - 3) [4] to more alkaline environment of the intestine leading to *in vivo* drug precipitation [2]. In fact, it is already reported that CLZ can form complexes with intracellular membranes, and precipitate as crystal aggregates, being phagocytized by the mononuclear phagocyte system [2]. This phenomenon may be correlated with the undesired and toxicological effects, often resulting in patients' treatment noncompliance [5].

Several strategies are commonly applied to improve poorly soluble drugs solubility namely prodrug formation, salt formation [6], complexation with cyclodextrins [3] or other macromolecules [7, 8], formulation of amorphous dispersions [9], use of co-solvents or surfactants [10], formulation of liposomes [11] and nanosuspensions [12]. Although many types of nanoparticles are available for oral delivery, lipid nanoparticles and especially solid lipid nanoparticles (SLNs), have shown to be one of the most promising delivery systems to improve the oral bioavailability of hydrophobic drugs, due to its high lipid content [13].

SLNs consist of a physiological compatible solid lipid core and of an amphiphilic surfactant shell. The main characteristic of the lipid phase is that they remain in solid state at room temperature [14, 15]. The mechanism by which SLNs can improve the solubility of poorly soluble drugs is based on the formation of a fine lipid dispersion, at the same time that entraps the drug, providing a large surface area of absorption in the gastrointestinal tract [16]. Besides the traditional advantages of the colloidal systems such as improved physical stability, protection of drug from *in vivo* degradation,

controlled drug release, possibility to specific targeting, SLNs are feasible to scale-up with an associated low cost [13, 14].

Despite the great number of works applying different technologies to improve CLZ solubility, the encapsulation into lipid nanoparticles have not been described, yet. The aim of this work was to develop SLNs loaded with CLZ (SLNs-CLZ) to improve CLZ bioavailability and to decrease its associated toxicity, using a rational development. The design of the SLNs-CLZ was carried out by first assessing the risks associated with product and process parameters during SLNs production, with further application of a Box-Behnken design aiming to better underwent the influence of different factors on selected responses. The optimized formulations were physicochemically characterized by dynamic light scattering, Fourier transformed infra-red spectroscopy, differential scattering calorimetry, and, also the storage stability and the *in vitro* cytotoxicity were assessed.

2. Materials and methods

2.1 Materials

Clofazimine (CLZ) was purchased from Hangzhou Heta Pharm & Chem Co. The solid lipids Precirol ATO 5 Cetyl Palmitate, Compritol 888 ATO, Precirol ATO 5, Gelucire 43/01, were kindly provided by Gattefossé (Saint-Priest, France). Softisan 142 was purchased from Cremer Care (Hamburg, Germany); Witepsol E85 from Sasol (Johannesburg, South Africa), and stearic acid was from Merck & Co., Inc. (Whitehouse Station, NJ, USA). Tween® 80 was purchased from Sigma-Aldrich Co. (St Louis, MO, USA). All other chemicals used in the study were of analytical grade. Caco-2 and MKN28 cell lines were acquired from the American Type Culture Collection (ATCC, Wesel, Germany) (passage number 35 - 55); while, HT29-MTX cell line was kindly provided by Dr. T. Lesuffleur (INSERM U178, Villejuif, France). Dulbecco's Modified Eagle Medium (DMEM), Roswell Park Memorial Institute (RPMI), fetal bovine serum (FBS), Pen-Strep (penicillin, streptomycin) and Trypsin-EDTA were all obtained from Gibco (Paisley, UK). Thiazolyl blue tetrazolium bromide (MTT) was obtained from Sigma–Aldrich (St Louis, MO, USA).

2.2 Methods

2.2.1 Preparation of SLNs

All the formulations of the experimental design were prepared by the hot homogenization followed by ultrasonication method, as previously described [15]. Briefly, the selected amounts of Precirol ATO 5 and CLZ (Table 1) were both heated to 75°C to solubilize the drug in the lipid matrix. Further, the aqueous phase containing the established amount of surfactant (Tween® 80) (Table 1) was pre-heated in water bath at the same temperature. The 6 mL of aqueous phase were added into the lipid phase and homogenized using a probe sonicator (VCX130; Sonics & Materials, Inc., Newtown, CT, USA), at 70% of amplitude for 5 min. The colloidal dispersion obtained was rapidly cooled down in an ice bath. Placebo SLNs were prepared similarly, without the addition of CLZ. When appropriate, the formulation was freeze-dried for 48h, under vacuum (0.5 mBar), and -55°C using a LyoQuest 85 plus v.407 Telstar freeze dryer (Telstar® Life Science Solutions, Terrassa, Spain).

2.2.2 Risk assessment of critical variables

To identify the potential risks and determine the cause-effect relationship between potential formulation and process parameters, an Ishikawa fishbone diagram was constructed. This approach was conducted based on prior knowledge, experiment trials and literature review [17-19]. The key parameters identified as Critical Quality Attribute (CQA), which may affect nanoparticles performance *in vivo*, were particle size, polydispersity index (PDI), zeta potential (ZP), association efficiency (AE) and drug loading (DL) [20, 21].

2.2.3 Development and validation of a spectrophotometric method for CLZ quantification

An UV-Vis spectrophometric method was developed and validated regarding linearity, detection limit, quantification limit, precision, accuracy, specificity and robustness [22] using an ultraviolet-visible spectrophotometer (Jasco V-660, Easton, USA). The stock solution was prepared by accurately weighing 5 mg of CLZ with further dissolution in 50 mL of DMSO. The solution was sonicated in water bath for 10 min up to complete solubilization. The linearity was investigated using CLZ stock solutions in HCl 1 M at different concentrations ranging from 0.125 to 1.5 μg mL^{-1} of CLZ, in triplicated. The

limit of detection (LoD) and limit of quantification (LoQ) were determined from angular coefficient (*b*) obtained from the linear equation of the standard curve, and from the standard deviation of five blank samples (S) (LoD = 3.3(*b* /S); LoQ = 10(*b* /S) [22]. Precision was evaluated regarding intermediate precision (assays on different days) and repeatability (different assays on the same day) which were determined with six scans of the CLZ standard solution. Precision levels were calculated by the relative standard deviation percentage (RSD %) from the analytical curves. Accuracy (recovery) was determined by preparing CLZ solutions with unloaded SLNs supernatants. Briefly, known volume of fresh SLNs was diluted with ultrapure water (20 times) and centrifuged at 4,000 x*g* for 10 min, using Amicon® filters devices. The supernatant was diluted (1:1) with HCl 2 M, to reach final HCl concentration of 1 M, and this solution was used to prepare the samples by adding the CLZ stock solutions to obtain 0.25, 0.50 and 0.75 μg mL^{-1} (the equivalent of 50, 100 and 150% of the test sample - 0.5 μg mL^{-1}). The samples were analyzed and concentrations were recalculated from the calibration curve. Assays were performed in triplicated. Specificity was evaluated by obtaining UV-Vis spectra of CLZ samples and supernatant of centrifuged SLNs using Amicon® filter device, with different dilutions, between 350-700 nm. Robustness of the method was evaluated by reading the test samples (0.5 μg mL^{-1}) after 4 h, and by preparation the samples from a HCl 1 M acidified from other pH (1.2 and 6.8) solutions.

2.2.4 Screening of starting conditions

2.2.4.1 Selection of the lipid

The selection of the lipid was based on the solubility of CLZ in different biocompatible lipids commonly used to formulate SLNs, namely Cetyl Palmitate, Compritol 888 ATO, Precirol ATO 5, Gelucire 43/01, Softisan 142 and Witepsol E85 and stearic acid. Briefly, a known amount of physical mixtures (PM) of each type of lipid and CLZ (10:1, w/w) were heated at 100°C and then left at room temperature (25°C) until solidification. The presence of drug crystals in the molten mixtures was observed and chosen as parameter for the choice of the lipid.

2.2.4.2 Preformulation studies

Before the construction of an experimental design, screening studies were conducted to assess the critical parameters (e.g. amount of lipid, amount of surfactant, time and amplitude of sonication) which should be controlled and studied during the

formulation design. For these purpose, preliminary SLNs formulations with CLZ using the selected lipid (Precirol ATO 5) were obtained according to section 2.2.1.

2.2.5 Experimental design

2.2.5.1 Box-Behnken design

In order to assess the correlation between the responses and the factors during the development of SLNs-CLZ, maximizing the experimental efficiency with the minimum number of experiments, a three-level, three-factor Box-Behnken design (BBD) was applied.

The selected independent variables were (X_1) the amount of lipid, (X_2) the amount of surfactant and, (X_3) the amount of drug. These parameters and their lower (-1), medium (0) and higher (+1) values were selected based on previous screening studies for each variable. Other parameters were set as fixed levels. The studied responses were: Y_1 = mean particle diameter, Y_2 = PDI, Y_3 = zeta potential (ZP), Y_4 = association efficiency (AE), and Y_5 = drug loading (DL). The results were studied using analysis of variance (ANOVA), and regression analysis (supplementary material).

The best-fitting experimental model (linear, two-factor interaction, quadratic, and cubic models) was statistically evaluated according to multiple correlation coefficient (R^2) provided by STATISTICA 10 software (StatSoft®, Dell Software, Round Rock, TX, USA). The effects of the obtained models were assessed by analyzing the statistical significance of the coefficients using ANOVA (p-value 0.05).

2.2.5.2 Optimization and validation assays

The optimization of the formulation was performed assuming the values obtained after studying the desirability profile tool of STATISTICA10 software. The constraints parameters were to: reach particles with 250 nm of diameter, minimize PDI, reach charge around -30 mV, and maximize AE and DL, all simultaneously. Three-dimensional response surface plots were obtained for each response in order to better understanding the correlation between the factors.

To evaluate the reliability of the models, the optimized nanoparticle was used as check point for the validation, in which the predicted values of each response were compared to the experimental by calculating the % bias. The linear correlation and residual plots between observed and predicted responses were obtained. The optimized nanoparticles were used for the subsequent characterization.

2.2.6 Characterization of the optimized SLNs-CLZ

2.2.6.1 Mean particle size, PDI and zeta potential

The mean particle size as well as the PDI were analyzed by dynamic light scattering (DLS) using a ZetaPALS, Zeta Potential Analyzer (Brookhaven Instrument Corps, Holtsville, NY, USA), at 25°C with a light incidence angle of 90°.
Before measurement, the formulation was filtered with a nitrocellulose 3 μm pore size filter (Merck Millipore, Billerica, MA, USA),) aiming to exclude the unentrapped precipitated drug. Further, the filtrated nanoparticles were properly diluted with ultrapure water until reaching a suitable concentration for the measurement, that is, Kcps around 500. The obtained values of particle size and PDI were representative to the mean of 6 runs. The zeta potential of the samples was analyzed by electrophoretic light scattering (ELS) using the Smoluchowski mathematical model. The filtered nanoparticles were measured in a folded capillary electrophoresis cell, at 25°. The obtained value represents the mean of multiple runs (n=10).

2.2.6.2 Association efficiency and drug loading

The quantification of entrapped drug within the SLNs was carried out based on methodologies already reported [23]. Briefly, fresh optimized formulation was filtered through 3 μm nitrocellulose membrane filter (Merck Millipore, Billerica, MA, USA) to retain unentrapped drug crystals which were undissolved. The drug retained in the filter was recovered with HCl 1 M, and the amount of free CLZ was measured by UV-Vis spectrophotometer (Jasco V-660, Easton, MD, USA) at 528 nm. The amount of soluble drug in the aqueous phase was determined by the ultrafiltration method. Briefly, SLNs-CLZ was properly diluted in ultrapure water, then transferred into Amicon® Ultra-4 Centrifugal Filter Devices (Millipore, Billerica, MA, USA), and centrifuged using an Allegra X-15Rcentrifuge (Beckman Coulter, Brea, CA, USA) at 4,000 x*g* for 10 min. After centrifugation, the samples were acidified with HCl until reaching the concentration of 1 M, and the free CLZ was detected by spectrophotometer at 528 nm. Standard curves were obtained in HCL 1 M and the supernatant of the aqueous phase solution obtained after Amicon filter centrifugation, used to determine the CLZ concentration. The results are expressed as mean ± standard deviation (n=3). Drug loading (DL) expresses the percent of drug to total lipids and excipients. Association efficiency (AE) was calculated following the equation:

$$AE = \frac{initial\ amount\ of\ drug\ -(drug\ retained\ in\ filter\ 3\ \mu m +\ drug\ soluble\ in\ aqueous\ phase)}{initial\ amount\ of\ drug} \times 100$$

$$DL = \frac{initial\ amount\ of\ drug - recovered\ drug}{total\ weight\ of\ nanoparticles} \times 100$$

2.2.6.3 Fourier transform infrared spectroscopy (FTIR)

FTIR spectra of CLZ, Precirol ATO5 and CLZ physical mixture (PM), and freeze-dried SLNs and SLNs-CLZ were using a PerkinElmer® Spectrum 400 (Waltham, MA, USA) equipped with an attenuated total reflectance (ATR) device and zinc selenite crystals. The samples were transferred directly to the ATR compartment, and the result was obtained by combining the 16 scans. The spectra were recorded between 4000 and 600 cm^{-1} with a resolution of 4 cm^{-1}.

2.2.6.4 Differential scanning calorimetry (DSC)

DSC thermal analysis of CLZ, Precirol ATO 5, PM and freeze-dried SLNs and SLNs-CLZ and were performed using a DSC 200 F3 Maia (Netzsch, Selb, Germany). Briefly, accurately weighted samples (1 - 2 mg) were poured into aluminum pans and hermetically sealed. An empty pan was used as reference. The samples were scanned from 30 to 300 ºC, at 10 ºC/min of flow rate. Nitrogen gas was used as purge gas, at 40 mL/min. The melting point (peak maximum), was calculated using the (NETZSCH Proteus® Software – Thermal Analysis – Version 6.1) software provided for the DSC equipment.

2.2.6.5 Storage stability studies

The storage stability of the SLNs-CLZ nanoparticles was assessed by conducting a study for a period of 12 weeks, at 4ºC. At each time point, the formulation was characterized regarding particle size, PDI, zeta potential, AE and DL. The results were compared to the first day of production.

2.2.7 Cell- SLNs interaction studies

Caco-2 and HT29-MTX cells were cultured in Dulbecco's modified Eagle's medium (DMEM) supplemented with 10% (v/v) of fetal bovine serum (FBS) and 1% (v/v) of penicillin-streptomycin. Gastric MKN-28 cells were cultured in RPMI 1640 culture

medium, with 10% (v/v) FBS and 1% (v/v) of penicillin-streptomycin. Cells were grown in a humidified incubator at 37 ºC and 5% CO_2 atmosphere and 95% relative humidity. To detached the cells, a 0.25% (/w/v) trypsin-EDTA solution was used when cells' confluence reached 80%

The potential cell cytotoxicity of SLNs, SLNs-CLZ and CLZ pure drug was evaluated against Caco-2, HT29-MTX and MKN-28 cells lines using the 3-(4, 5-dimethylthiazol-2-yl)-2,5-diphenyltetrazolium bromide (MTT) colorimetric assay. Separately, each cell line was transferred into 96-well plates, at a density of 5 x 10^4 cells per well for Caco-2 and HT29-MTX and 10^5 cells per well for MKN-28 cells. The plates were incubated for 18- 24 h for cell attachment. Further, the culture media was removed and the wells were incubated with 100 µL of culture media containing different concentrations of SLNs, SLNs-CLZ and CLZ (6.25 – 50 µg mL^{-1} equivalent of CLZ). For CLZ pure drug, the samples were prepared from a stock solution in DMSO, and appropriate dilutions were done to reach maximum of 4% (v/v) of DMSO in the well, immediately before the beginning of the assay. Each sample was incubated during 24 h for Caco-2 and HT29-MTX cell lines; and during 4 h for MKN-28. After the incubation period, the samples were removed and replaced by 100 µL of MTT solution (5 mg mL^{-1}), and incubated for additional 2 h. Further, the MTT solution was removed and 100 µL of DMSO was added into each well to solubilize the formazan crystals. The optical density of the solution was measured at 570 and 650 nm wavelengths using Synergy™ HT Multi-mode microplate reader (BioTek Instruments Inc., Winooski, VT, USA). Untreated cells were taken as positive control with 100% viability and cells incubated with 4% (v/v) DMSO used as control for free CLZ. The MTT test was performed in triplicate and results were expressed as mean values ±SD. The cell viability (%) in relation to control cells (untreated cells) as follows:

$$Cell\ viability\ (\%) = \frac{OD\ 570 - 630\ treated\ cells}{OD570 - 630\ untreated\ cells} \times 100$$

2.2.8 Statistical analyses

All results were expressed as mean ± SD (n=3). The method validation was carried out using ANOVA, regression analysis, and T student test. Data obtained from the experimental design were analyzed by ANOVA and multiple correlation coefficient using STATISTICA10 (StatSoft®) software. GraphPad Prism software (version 6, GraphPad Software, USA) was used for statistical comparisons of the results to control for the cytotoxicity, through student (unpaired) t-test and one-way ANOVA test. The differences were assumed statistical significant when $p < 0.05$ (95% confidence level).

3. Results and discussion

3.1 Risk management: cause-effect relationship

In the Quality by Design (QbD) approach, the formulation by design involves the identification of potential risks that may affect the product quality [24]. In this framework, the Ishikawa diagram is a qualitative tool to explore systematically the causes and sub-causes that may produce an effect [20].

To design an Ishikawa diagram the parameters involved in the production of nanoparticles, such as the materials, the process and the characterization should be considered according to their possible influence along the following lines. In the nanotechnology framework, higher values of AE and DL are essential to reach suitable drug concentration in the site of absorption with improved yield and low amount of excipients. Particle diameter influences the uptake mechanism by the cells. On the other hand, the surface charge is an important indicator of long-term stability and biocompatibility of the colloidal suspensions [20].

Lipid-based nanocarriers seem to be an appropriate system to load poorly soluble drugs as they can solubilize such compounds. There is a variety of biocompatible materials available that have been used to improve oral bioavailability of drugs. On the other hand, lipid nanocarriers are not universal platforms to delivery poorly soluble drugs since lipophilic drugs do not necessarily display a high solubility in lipid phase. Besides, the partition of the drug between aqueous and oil phase should be taken into consideration to maximize AE and DL [25, 26]. Regarding the methods of production, several methods have been reported to produce SLNs such as high-shear homogenization, high-pressure homogenization and ultrasonication. The correct selection of the method is a critical step for obtaining of particles with suitable diameter and narrow size distribution [27].

Furthermore, properly characterization of SLNs is a critical step to control product quality, stability and safety. The particle size and PDI are important parameters to be controlled, and the DLS technique is the most used for this purpose which can provide excellent qualitative and quantitative information [23, 28]. In the case of nanoformulations with poorly soluble drugs, proper dilution sometimes is not enough to solubilize unentrapped drug, leading to a super estimation of the particle size due the drug precipitation [28-30]. In addition, AE and DL should also be well determined without having super estimation or false results, which are common for insoluble drugs [31]. Direct or indirect drug quantification methods have been reported to determine

the entrapped drug. For lipophilic drugs, the drug theoretically soluble is present as a precipitate, leading to an overestimation of the drug loading capacity [32].

In this context, the relationship between potential factors affecting the development of SLNs and the targeted quality attributes namely particle size, polydispersity index, zeta potential, association efficiency and drug loading were established by constructing a cause-and-effect Ishikawa diagram (Figure 1). Figure 1 shows the Ishikawa diagram illustrating the effect of product and process parameters on the targeted product quality profile. Based on prior knowledge and preliminary experiments formulation, the process variables were expressed as risk factors [33, 34].

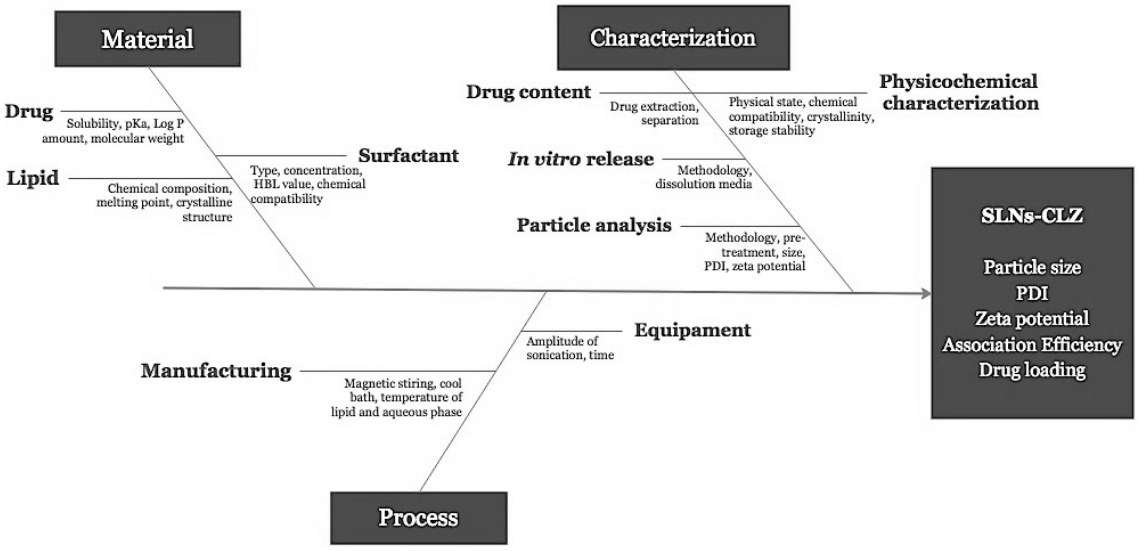

Figure 1. Ishikawa cause-and-effect diagram in the development of SLNs-CLZ.

The first step considered crucial for the development of SLNs-CLZ was the development of a suitable and reliable analytical method for CLZ quantification. Further, process and product variables were assessed by an initial risk management using the aforesaid tool. The study has suggested that factors, as amount lipid, amount of surfactant, and amount of drug were found to strongly influence the risk associated with the selected effects that where attributed as critical. On the other hand, process parameters such as amplitude and time of sonication showed overall medium risk associated. Based on this preliminary evaluation, formulation factors were selected to perform an optimization experimental design.

3.2 Development and validation method for CLZ quantification

The very low water solubility of CLZ is not only an issue during the design of new formulations, but also a challenge to have a proper quantification method, which

requires a minimum amount of organic solvent, and enough sensibility to quantify low drug concentrations [35].

Few methods for the determination of CLZ in biological fluids [36-38] and pharmaceutical preparations [39] are reported in the literature. Even though, the reported techniques, are time consuming and costly, and in the case of UV-Vis methods, are present lack of sensitivity and requires high levels of toxic organic solvents. Thus, the development and validation of a simple and, sensitive and accurate UV-Vis spectrophotometric method would be highly useful for the analysis of CLZ in bulk nanoformulations.

CLZ is present as reddish crystals, and in an aqueous media almost all the drug precipitates. Despite CLZ poor water solubility, it has three sites of protonation [2], which make it soluble in acidic pH, becoming a purple solution (data not shown).

Spectra for CLZ with different concentrations of HCl were obtained in the range between 350 and 700 nm. Figure 2A shows CLZ pH dependence, as the pH of the medium decreases, the maximum wavelength of the spectra shifts to higher values. However, as the pH of the medium increases, the spectra exhibit a different behavior, as the CLZ structure is at molecular conformation resulting in lower intensities of absorbance (Figure 2A). This behavior allows to reach very low detection limits. The minimum concentration of solvent to obtain spectra of protonated CLZ in the visible region was studied. HCl 1 M was selected for the method validation, which provided a maximum wave length of 528 nm. Linearity of the method was obtained in a range concentration of 0.125–1.5 μg mL^{-1} (Figure 2B). Least square regression (R^2) showed a good correlation coefficient (r=0.9995) and the equation obtained was: absorbance = 0.0735 [CLZ] + 0.00006. The LoD and LoQ were 0.0141 μg mL^{-1} and 0.0471 μg mL^{-1} respectively.

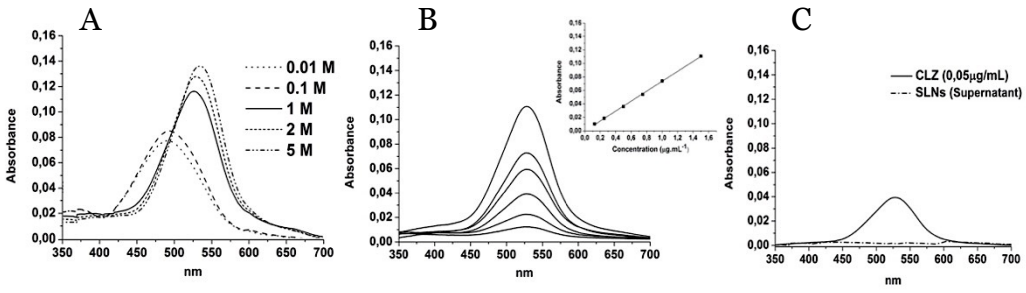

Figure 2. UV-Vis absorption spectra of (A) CLZ samples in different HCl concentrations; (B) calibration curve in the concentration range of 0.125 – 1.500 μg $mL^{-1.}$ in 1 M HCl; and (C) superposition of CLZ sample and SLNs drug-free supernatant, evidencing the selectivity of the method for CLZ.

The relative standard deviation (RSD%) for repeatability, inter-day precision and second analyst analysis were less than 5% (3.8%, 3.2% and 1.3% respectively) indicating reasonable result. The mean percentage of recoveries for the three tested concentrations reached RSD values below 5% (1.82, 1.84 and 0.39% for 0.250, 0.500 and 0.750 μg mL^{-1}, respectively) demonstrating good agreement between added and quantified amounts of CLZ, and that small changes in CLZ concentrations could be accurately determined. The selectivity of the method was assessed by analyzing the interference of nanoparticles constituents in CLZ quantification. Figure 2C shows that the SLNs supernatant did not interfere with the absorption spectra of CLZ at 528 nm.
The robustness of the method was assessed by evaluating the stability of the sample after 4 h, and samples preparation in HCl 1 M from already buffered solution. The results show that there were no significant differences between samples read immediately after preparation, and 4 h after performance of unpaired T test ($p > 0.05$, with 95% of confidence level). ANOVA statistical analysis were performed to compare samples obtained from different pH (1.2, 4.5 and 6.8), and once more no significance was found, with 95% of confidence level.

3.3 Screening of starting conditions

3.3.1 Selection of the lipid

The correct selection of the lipid during the development of SLNs influences their ability to carry the drug and may warrant high values of association efficiency. Moreover, proper melting point of the lipid is essential to maintain the solid state of the particles at room temperature [40, 41].
Among the tested lipids, a more homogenous dispersion of CLZ was observed with Precirol ATO 5, suggesting that this lipid might be able to maximize the association of CLZ in SLNs. The melting temperature was also considered for the selection of the lipid, as it is preferable for storage and process reasons to have lipids with melting point above 50°C. Most of the tested lipids were unable to completely dissolve CLZ and, presented a low phase transition temperature (below 50°C), thus were not considered suitable for SLNs-CLZ production. Compritol 888, cetyl palmitate, stearic acid and Precirol ATO 5 were the lipid with higher melting point. As Precirol ATO 5 was able to visually better disperse CLZ, it was selected for the pre-formulation studies.

3.3.2 Pre-formulation studies

Preliminary studies were considered essential to develop SLNs-CLZ since many factors may strong influence the final performance of the nanoformulation. As discussed before, parameters regarding process and formulation, in addition to methods for the characterization must be well defined and controlled.

In this context, a step-by-step study was performed, in which three formulations at a time were obtained (Table 1), and the subsequent formulations were prepared after evaluation of the results of the previous step. Visual aspect, particle size and PDI were the parameters that were evaluated.

Based on prior knowledge and literature review, 10 mg of CLZ, 250 mg Precirol ATO 5, and 90 mg of Tween® 80 were selected as the constituent of the SLNs. These values were selected considering the ratio lipid:surfactant as well as the ratio lipid:drug. Regarding the process variables, amplitude and time of sonication was assessed at two different levels (90 and 70%; 5 and 10 min, respectively).

Table 1. Formulation and process parameters of preliminary SLNs-CLZ and their characterization (particle size and PDI)

		Amount of Lipid (mg)	Amount of Surfactant (mg)	Time (min)	Amplitude (%)	Mean particle size	PDI
Step 1	F1	250	90	5	70	528	0.148
	F2	250	90	5	90	486	0.116
	F3	250	90	10	90	576	0.148
Step 2	F4	200	60	10	90	537	0.163
	F5	200	60	5	90	615	0.202
	F6	200	40	10	90	553	0.313

The initial three formulations (F1, F2 and F3) presented very high values of size (Table 1) (higher than 400 nm) and values of PDI below 0.2. Besides, the higher percentage of sonication amplitude provided particles with lower sizes (F2) but increasing sonication time to 10 min (F3) did not produced smaller SLNs. Thus, 90% was set as fixed variable for the subsequent step. Less amount of lipid (200 mg) with different amount of Tween® 80 (40 and 60 mg), were studied in the second step (F4, F5 and F6 on Table 1) intending to observe the influence on the particle size and PDI values. Sonication time was also tested (5 and 10 min). It could be inferred that the amount of surfactant had a

negative impact on the PDI (higher values, F5) while the time of sonication had a positive impact on particle size (Table 1, F4). Even though, once more the particles presented sizes above 400 nm.

It is already reported that the reduction in particle size result in increasing surface area of the particles, which seems to prolong the residence time of SLNs in the GI tract and enhance their contact with epithelial membranes, possibly leading to enhanced oral absorption [42]. Thus, particles with diameter much higher than 250 nm are not suitable for our aims.

Therefore, further investigation of nanoparticles dispersion was performed by analyzing the range of the size populations. The histograms of the DLS analysis (Figure 3) revealed that all the tested formulations presented two very distinct populations, one in the nanometer scale, and another much bigger, in the micrometer range. It could be inferred that due to the very poor solubility of CLZ, precipitated crystals of non-entrapped drug were interfering in the DLS analysis. This phenomenon was increasing the mean particle size of the formulation, providing an unrealistic result. To solve this issue, we decided to filter the subsequent formulation with a 3 μm pore size filter, to retain drug crystals, aiming to have more realist results regarding particle size (data not shown).

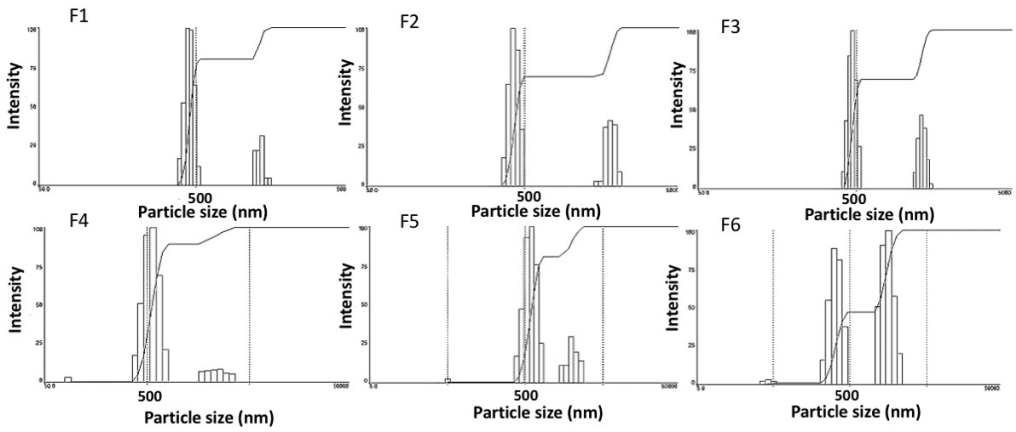

Figure 3. Histograms of size distribution of the preliminary formulations in terms of intensity (F1-F6).

3.4 Experimental design

After a preliminary assessment of the significance of the screened factors, an experimental design was constructed with the identified variables that may influence the critical attributes of the SLNs. In this context, (X_1) amount of lipid, (X_2) amount of

surfactant and (X_3) amount of drug were used to explore individual and synergic effects on the particle size, PDI, zeta potential, AE and DL.

The lower (-1), medium (0), and higher values (+1) for the factors were set out according to preliminary studies and literature research. A three-level, three-factor BBD was applied to optimize SLNs, allowing maximizing the experimental efficiency, with a minimum number of experiments. 15 formulations were prepared and analyzed regarding the adopted responses. The experimental design included three replicates of the central point aiming to estimate the experimental error and accurately test the fit of the model. The data obtained are expressed in Table 2.

The effects of the factors coefficients were evaluated via regression analysis for each independent variable, which were considered statistically significant when p values were less than 0.05, with 95% of confidence level. Because all the PDI values were below 0.2, which is considered to be a homogeneous dispersion, this response was not statistically evaluated.

Table 2. Formulation composition and obtained responses of 15 different formulation obtained from Box-Behnken design

Formulation	***Independent variables***			***Dependent variables***				
	X_1 *(mg)*	X_2 *(mg)*	X_3 *(mg)*	Y_1 *(nm)*	Y_2	Y_3*(mV)*	Y_4 *(%)*	Y_5 (%)
F1	250	60	7	208	0.127	-28.04	67.8	1.88
F2	350	60	7	236.5	0.158	-32.31	61.9	1.26
F3	250	100	7	169	0.174	-23.17	67.0	1.85
F4	350	100	7	195	0.158	-23.62	62.4	1.57
F5	250	80	4	198.1	0.164	-30.88	70.8	1.10
F6	350	80	4	227.1	0.169	-29.08	83.0	0.94
F7	250	80	10	204.3	0.165	-25.73	62.4	2.26
F8	350	80	10	221.2	0.156	-21.78	81.7	2.02
F9	300	60	4	203.3	0.193	-27.18	62.7	0.81
F10	300	100	4	187	0.168	-38.28	77.4	0.97
F11	300	60	10	220.7	0.154	-29.61	75.0	2.39
F12	300	100	10	177.5	0.154	-24.65	69.5	2.24
F13	300	80	7	227.2	0.155	-32.09	71.2	1.63
F14	300	80	7	219.7	0.194	-29.93	80.6	1.87
F15	300	80	7	219.7	0.147	-28.52	74.7	1.61

X_1= amount of lipid, X_2 = amount of surfactant, X_3 = amount of drug, Y_1= particle size, Y_2= PDI, Y_3= zeta potential, Y_4 = AE and Y_5=DL

The polynomial equation generated after fitting in second-order quadratic models showed good correlations (R^2) after multiple linear regression analysis for all the responses (Table 3), with insignificant lack of fit. Moreover, the significance of the obtained models was tested by ANOVA, and tested by evaluating *p* values. All the mathematical models were considered precise in the prediction of the respective response as all the *p* values where 0.05.

Table 3. Summary of the regression analysis of the independent variables Y_1–Y_4

	Particle size (Y_1)		***Zeta potential (Y_2)***		***AE (Y_3)***		***DL (Y_4)***	
	Coefficient	*p*-Value	Coefficient	*p*-Value	Coefficient	*p*-Value	Coefficient	*p*-Value
βo	203.975	**0.000**	-27.861	**0.000**	70.121	**0.000**	1.681	**0.000**
X_1	12.908	**0.015**	-0.308	0.691	0.868	0.671	-0.190	**0.044**
X_1^2	1.131	0.421	-1.614	0.075	1.860	0.269	0.015	0.653
X_2	-18.375	**0.008**	1.748	0.121	0.723	0.721	0.053	0.327
X_2^2	8.906	**0.016**	-0.083	0.875	3.513	0.104	0.043	0.270
X_3	0.708	0.704	3.008	**0.046**	-1.238	0.555	0.704	**0.003**
X_3^2	3.631	0.084	-0.042	0.937	-1.341	0.389	0.002	0.953
$X_1.X_2$	-0.625	0.800	0.955	0.399	0.337	0.900	0.089	0.248
$X_1.X_3$	-1.075	0.555	1.309	0.176	5.236	0.088	0.077	0.187
$X_2.X_3$	2.625	0.229	-2.463	0.061	1.187	0.551	-0.037	0.441
	R^2 = 0.993		R^2 = 0.975		R^2 = 0.940		R^2 = 0.995	

3.4.1 Effect on mean particle size

The size of the nanoparticles is an important parameter to control during the nanoparticles formulation as it seems to influence on *in vivo* distribution, biological fate, toxicity and drug loading capacity [20].

The obtained values of particle size from the formulations generated by the BBD ranged from 169.0 nm (F3) to 236.5 nm (F2), with a mean size (β_0) of 204.0 nm. According to the regression analysis, the amount of lipid (X_1) and the amount of surfactant (X_2) seemed to statistically influence on SLNs particles size, as they presented *p* values <0.05, with 95% of confidence level. The positive sign of X_1 coefficient reveals that the size increases with the increasing of the amount of lipid. On the contrary, the negative sign before the coefficients shows that the higher is the amount of surfactant (X_2) the

smaller are the particles. Also, significance of the X_2 quadratic coefficient evidences a nonlinear relation of the response (particle size) with the changing of the values levels.

3.4.2 Effect on zeta potential

The zeta potential is the measurement of electric charge present on the surface of the particles. This parameter is associated with the colloidal dispersion stability so that generally, the greater the zeta potential the more likely the suspension is to be stable due to the charged particles repel one another, overcoming the tendency to aggregate. It is currently admitted that zeta potentials of |30| mV are required for full electrostatic stabilization [18].

Zeta potential measured from the 15 formulations ranged from -21.78 mV (F8) to -38.28 mV (F10). Only the amount of drug (X_3) seemed to affect the surface charge of the nanoparticles (p value 0.046), with 95% of confidence level. The positive sign of the coefficient means that the zeta potential increases with the augment of the amount of CLZ. Zeta potential expressed as negative values, so that the higher is the value, the closer it is to the neutral.

In this case, it seems that the excess of CLZ may neutralize the surface charge of the nanoparticles, as it may be localized in the outer portion of the nanoparticle, thus influencing the surface charge.

3.4.3 Effect on drug association efficiency

The eassociation efficiency (AE) is one of the most critical attribute when designing nanoformulations as high values of AE improves formulation yield. This fact is even more important when the drug present severe adverse side effect, as is the case of CLZ. The drug entrapment inside nanoparticles depends on the solubility of drug into the solid lipid and on the O/W partition of the drug.

The AE values of all the 15 formulations are shown in Table 2. In general, all the formulations presented satisfactory AE values, ranging from 61.9% (F2) to 83.0% (F6), with mean value (β_0) of 70.121%. The regression analyses evidenced that none of the variables influenced statistically the percentages of drug association. Considering the high values and narrow range of AE percentages, this result may not be considered as negative since the used selected levels for all the variables originated suitable formulations in terms of AE.

3.4.4 Effect on drug loading

During the development of any nanoformulations, high values for DL are preferred as it means less carrier materials and excipients will enter the patient's body, leading to lower risks of toxicity [13].

The DL obtained from the 15 formulations ranged from 0.81% (F9) to 2.39% (F11). The regression analysis of the model showed that the DL statistically alters with the changing of (X_1) the amount of lipid, and (X_3) the amount of drug, with 95% of confidence level. The negative sign of X_1 coefficient demonstrate the inverse relation between amount of lipid and DL, i.e., the DL decreased with the increasing of the amount of lipid. The opposite is observed with the increasing of the amount of drug, as the sign is positive. The result is in accordance with the mathematical equation for the calculation of DL (section 2.2.6).

Although this result seems to be obvious, it is not a rule, mainly in the case of very poorly water soluble drugs as CLZ. The DL is a parameter related to the distribution of the drug between lipid and aqueous phase, which is determined by the drug's solid-state nanocarrier matrix [13]. If the amount of lipid is not enough to solubilize the selected amount of drug, thus this relation would be not so predictable. In this case, this critical step was overcomed by evaluating previously the solubility of CLZ in Precirol ATO 5 during the pre-formulation studies.

3.4.5 Optimization of SLNs-CLZ

After the evaluation of the relationships between factors and responses by the polynomial equations, the optimization of the formulation was carried out. Three-dimensional response surface analyses were plot to provide a graphical representation of the behavior of each response with the simultaneous changing of two factors at a time, maintaining non-used variables fixed at their middle level (Figure 4). Furthermore, the optimization of SLNs-CLZ was carried out using the desirability function of the STATISTICA10 software [43]. This approach is a useful tool to overcome the difficulties of multiples or opposite optimal values for the different responses, as each response is associated with its own partial desirability function. The optimal nanoparticles had to satisfy the selected requirements for each dependent variable, namely nanoparticles with size closer to 250 nm, zeta potential closer to -30 mV, maximum AE and DL. The optimal calculated levels are expressed in Table 4.

The qualities of the models were assessed by plotting predicted versus of the experimental data (supplementary material), confirmed by the low mean percentage of bias (Table 4).

The validation of the models was performed by formulating the optimized formulation with (X_1) 300 mg of lipid, (X_2) 60 mg of surfactant and (X_3) 10 mg of CLZ. The check point responses were then estimated by the mathematical models and the experimental data were compared with the predicted. The lower magnitude of the bias reveals good correlation of the models, and is an indicative of the robustness and high explorative predictive ability of the mathematical models.

Table 4. Summary of the coded levels of the Box-Behnken design; the levels of the optimized formulation, the desirable parameters used for the optimization, and the comparison between predicted and observed values for the considered responses

Factors	**Coded Levels**			**Optimized**
Independent variables	Low Level (-1)	Medium Level (0)	High Level (+1)	
X_1 = Amount of Lipid (mg)	250	300	350	**300 mg**
X_2 = Amount Surfactant (mg)	60	80	100	**60 mg**
X_3 = Amount of Drug (mg)	4	7	70	**10 mg**

Dependent variables	**Constrains**	**Predicted**	**Observed**	**Bias***
Y_1 = Particle size	Optimum (250 nm)	233 nm	230 nm	1.45
Y_2 = Zeta potential	< -30 mV	-32.59 mV	-34.28 mV	4.93
Y_3 = Association efficiency	Maximum	69%	72%	3.93
Y_4= Drug Loading	Maximum	2.44%	2.32	5.23

*Bias (%) = |predicted-observed|/observed x 100

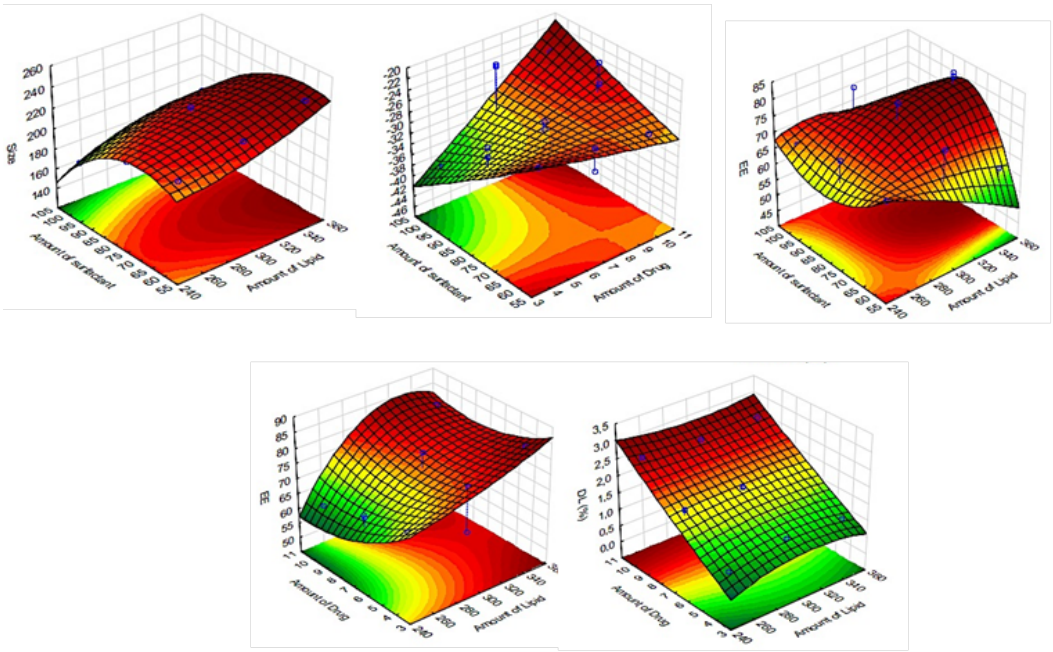

Figure 4. Response surface plots evidencing the influence of the independent variables on the selected responses particles size (Y_1) (A), zeta potential (Y_2) (B), AE (Y_3) (C-D) and DL (E) (Y_4).

3.4.6 Characterization of the optimized SLNs-CLZ

3.4.6.1 Measurement of mean particle size, PDI and zeta potential

The particle size, PDI and zeta potential of the optimized SLNs-CLZ were measured in triplicated. The obtained nanoparticles presented particles size of 230.0 ±8.3 nm which was very closer to the desired value of 250.0 nm; suitable PDI (0.149 ± 0.010) below 0.200 and zeta potential closer to -30 mV (-34.28 ±2.80). Unloaded SLNs were also prepared and values of 216.8± 16.5, 0.166 ± 0.020 and -32.23 mV for particle size, PDI and zeta potential respectively, evidencing that particles were quite similar.

3.4.6.2 Association efficiency and drug loading

The determination of AE and DL of SLNs-CLZ was performed in triplicated and the obtained values were 71 ± 1.8% and 2.39 ± 0.1% respectively. The obtained results were considered satisfactory taking in account the issues during the pre-formulation studies namely the very poor solubility of CLZ in aqueous phase and either in the molten lipid.

3.4.6.3 SLNs-CLZ characterization by Fourier transform infrared spectroscopy

The FTIR spectra of CLZ, PM, SLNs and SLNs-CLZ are shown in Figure 5. Both SLNs and SLNs-CLZ displayed typical bands at 2820 cm^{-1} and 1705 cm^{-1} relative to C- H and C = O (carbonyl) stretching of glyceryl units, respectively. The spectrum of CLZ present characteristic bands of N–H bending frequency at 1550–1620 cm^{-1}, and another regarding C=N stretching at 1625 cm^{-1} [6]. Unknown peaks were not found in the spectra, confirming that there is no chemical interaction between CLZ and SLNs constituents. Due to the amorphous state of entrapped CLZ, the intensity of characteristic peaks may be decreased and/or overlapped by others belonging to the major constituents of SLNs-CLZ.

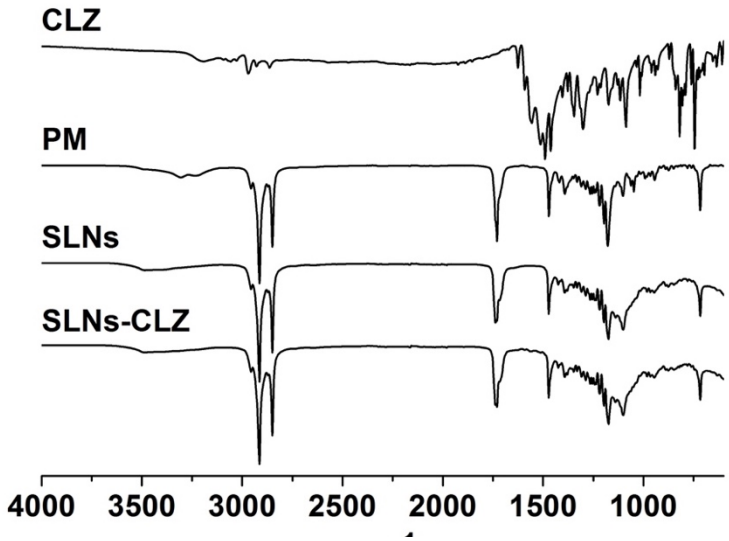

Figure 5: FTIR spectra of CLZ, SLNs and SLNs-CLZ.

3.4.6.4 Assessment of CLZ physical state in the SLNs by differential scanning calorimetry

Differential scanning calorimetry (DSC) studies were conducted to study the physical state of CLZ in the nanoparticles and identify potential Precirol ATO5-CLZ interactions during the production process of obtaining, in addition to evaluate the behavior of the lipid phase.

The thermograms of CLZ, Precirol ATO 5, PM, SLNs and SLNs-CLZ can be observed in Figure 6. The endothermic event of CLZ at 224 ºC was not observed in SLNs-CLZ, which suggests that CLZ is encapsulated in amorphous form in nanoparticle

formulation. Similar results were observed with Precirol ATO 5 and poorly soluble compounds [44, 45]. Furthermore, no additional unknown peaks were found, indicating no incompatibility between Precirol ATO 5 and CLZ.

Precirol ATO 5 thermograms shows an endothermic event at 58°C with a shoulder at 62 °C, characteristic of the diffuse melting in complex glycerides due to the presence of different polymorphs (Figure 6) [46]. This phenomenon was not observed in both load and unloaded nanoparticles, which may suggest that the lipids undergo some polymorphic changes to less ordered structures during particle preparation allowing better incorporation of the drug in the lipid matrix [47].

In PM, the onset temperature of this event shifted to lower temperature, indicating that the presence of CLZ in crystalline form interfered in the lipid melting. This shifting in Precirol ATO onset melting temperature was not observed for both SLNs and SLNs-CLZ. On the other hand, onset temperatures values of lipid transition for both SLNs and SLNs-CLZ were quite similar suggesting that the presence of the drug did not alter the lipid conformation, probably because it is well dispersed. These findings were already reported to Precirol ATO and other compounds [46].

Moreover, in the PM thermogram no endothermic event was found around 224°C, suggesting that CLZ was solubilized in the molten lipid which may be considered a positive interaction between lipid and drug due to the suitable solubility of CLZ in the selected lipid.

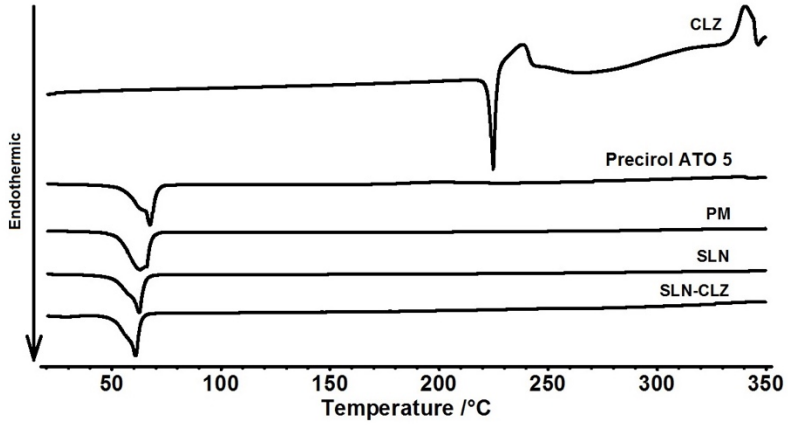

Figure 6. DSC thermograms of CLZ, physical mixture (PM), Precirol ATO 5, SLNs and SLNs-CLZ.

3.4.6.5 Storage stability studies

The physical stability of the optimized SLNs-CLZ was evaluated regarding particle size, PDI, zeta potential, AE and DL, upon storage of the colloidal suspensions at 4°C, during 12 weeks. Changes in particle size and PDI are indicators of formulation instability and the surface charge is commonly related to the aggregation of the particles [18].

Figure 7 show the results obtained after each time point measurement for the tested parameters. At the end of the study, no aggregation or color change were found after visual observations. Moreover, the initial characteristics were maintained, with no significant changes ($p > 0.5$). Particles size varied about 30 nm from the initial values and PDI was always bellow 0.2. The colloidal suspensions remained with negative values closer to -30 mV, which indicate stable dispersion due to the electric repulsion between the particles It was observed that the SLNs did not release CLZ over time, as the AE and DL values were practically constant (Figure 7). This can be considered a positive result since is common to observe drug expulsion after lipid crystallization upon storage [18]. Overall, the developed SLNs-CLZ were stable when stored at 4°C for 12 weeks.

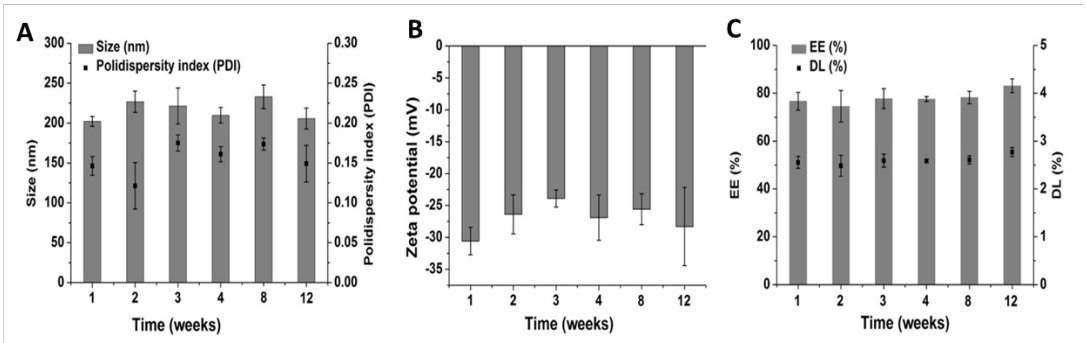

Figure 7. Storage stability at 4°C assessed as (A) particle size and PDI, (B) Zeta potential, (C) drug content of SLNs-CLZ expressed as AE and DL (mean ± SD, n=3).

3.4.7 *In vitro* cell viability studies

SLNs-CLZ development aims oral drug delivery in leprosy therapy. Thus, different cell lines were selected as suitable models mimicking the different cell-types of the GI tract (e.g., stomach, enterocytes and mucus secreting cells) [48, 49]. Caco-2, HT29-MTX (intestinal model cells) and MKN-28 (gastric model cell) cell viability studies were conducted with SLNs and SLNs-CLZ optimized formulations, in addition to CLZ free drug solutions.

The studies were performed with different concentrations of nanoparticles corresponding to 6.26 to 50 μg mL^{-1} in CLZ, equivalent to 0.25 - 2 mg mL^{-1}, in relation to the amount of lipid phase, during 24 h for Caco-2 and HT29-MTX, and 4 h for MKN-28. Cytotoxicity studies were also carried out with CLZ solutions at concentration range of 1.56 – 50 μg mL^{-1}. The obtained results show that for Caco-2 cells, only the highest tested concentration of SLNs-CLZ (50 μg mL^{-1} in CLZ, 2 mg mL^{-1} in lipid) presented cell viability statistically different from the control (Figure 8). Unloaded nanoparticles were considered safe as at all tested concentrations the viability of the cells was superior to 80%. For HT29-MTX and MKN28 cell lines, neither SLNs nor SLNs-CLZ presented statistical significance when compared to the control. These results show that the nanoparticles were not toxic for the studied cell lines when compared to free CLZ solutions. In fact, for all the intestinal cell lines exposure to free CLZ lead to significant reduction on the cell viability, and the IC_{50} values determined were 16.3 and 20.3 μg.mL^{-1} for Caco-2 and HT29-MTX, respectively. No significant effect on the MKN-28 cell viability was observed (Figure 8). Moreover, the high toxicity of CLZ has been already reported [50]. Upon prolonged oral administration CLZ seems to forms intracellular insoluble drug precipitates, leading to high concentration bioaccumulation, being easily associated with unwanted side effects as reddish skin pigmentation, abdominal pain and cardiotoxicity [1].

Based on the exposed results, the successful incorporation of CLZ in SLNs, with the drug in its amorphous state, may prevent drug crystallization and the formation of precipitates *in vitro and in vivo*. In this context, the nanoformulations seems to have an elevated potential to delivery CLZ, decreasing the undesired effect, by protecting the surrounding cells from the toxic effects of the drug.

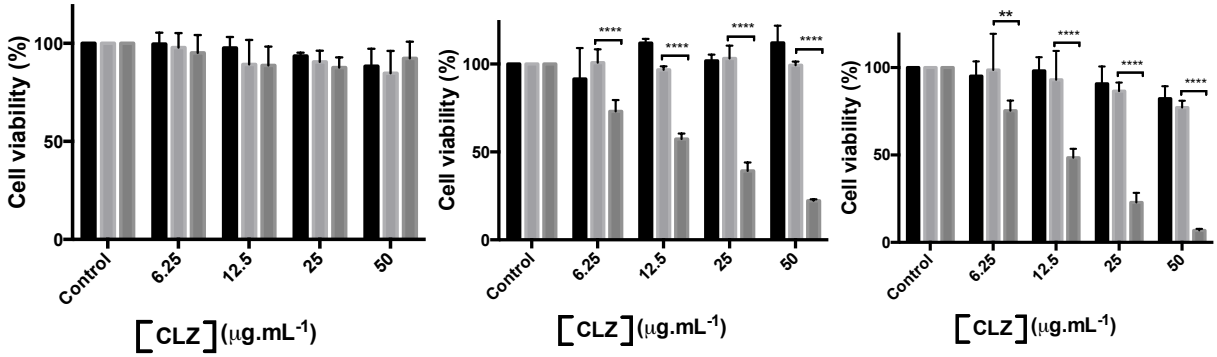

Figure 5. Cell viability of (A) MKN-28, (B) HT29-MTX and (C) Caco-2 cell lines upon exposure to SLNs (dark grey), SLNs-CLZ (light grey), and CLZ (dark grey). Data

expressed as the average ± standard deviation (n=5, for each three independent assays) (*p value <0.05 in relation untreated cells).

4. Conclusion

In the present study, the risk management during the development of SLNs-CLZ helped to identify the main critical variables, through the Ishikawa cause-and-effect diagram, which allowed the construction of an experimental design for further optimization. The studding of the starting conditions namely the selection of the best lipid and other formulation and process variables allowed to identify the presence of drug precipitates, and to implement control actions during nanoparticles characterization. Moreover, the intended analytical method was found to be accurate, precise, efficient, specific and highly sensitive due to the lowest LoD and LoQ, being suitable for the quantification of CLZ in SLNs.

A BBD was successfully obtained and the relations between the independent variables in the selected responses could be understood. The optimized SLNs-CLZ was achieved based on the desirability profile, which presented suitable parameters after characterization, namely particle size, zeta potential, AE and DL. FTIR confirmed the presence of the drug and the absence of chemical interactions, while DSC measurements indicated the amorphous state of CLZ. The stability studies ensured that the developed SLNs are stable over a period of 12 weeks at 4ºC. *In vitro* cytotoxicity studies evidenced that the optimized SLNs-CLZ are not toxic at the teste concentration range, on the contrary of the CLZ solutions that presented low IC_{50} for Caco-2 and HT29-MTX cell lines.

Based on the obtained results, it can be concluded that the optimized system was carefully developed, considering important variables when formulation poorly soluble drugs and SLNs-CLZ is a promising platform to deliver CLZ with reduced associated effects.

Acknowledgments

This work received financial support from the European Union (FEDER funds) and National Funds (FCT/MEC, Fundação para a Ciência e Tecnologia and Ministério da Educação e Ciência) under the Partnership Agreement PT2020 UID/MULTI/04378/2013 - POCI/01/0145/FEDER/007728 and funds through the COMPETE 2020 - Operational Programme for Competitiveness and Internationalisation (POCI), Portugal 2020, and by Portuguese funds through FCT - Fundação para a Ciência e a Tecnologia/ Ministério da Ciência, Tecnologia e Inovação

in the framework of the projects "Institute for Research and Innovation in Health Sciences" (POCI-01-0145-FEDER-007274). SCL thanks Operação NORTE-01-0145-FEDER-000011 for her Investigator contract. The authors also thank the CNPq Foundation, Ministry of Education of Brazil for the Doctoral fellowship 246514/2012-4 (AAV) and LLC thanks the CAPES Foundation, Ministry of Education of Brazil for the Doctoral fellowship 0831-12-3.

5. References

1. Li, S., et al., *Complexation of clofazimine by macrocyclic cucurbit[7]uril reduced its cardiotoxicity without affecting the antimycobacterial efficacy*. Org Biomol Chem, 2016. **14**(31): p. 7563-9.
2. Baik, J. and G.R. Rosania, *Macrophages sequester clofazimine in an intracellular liquid crystal-like supramolecular organization*. PLoS One, 2012. **7**(10): p. e47494.
3. Salem, I., G. Steffan, and N. Düzgünes, *Efficacy of clofazimine–modified cyclodextrin against Mycobacterium avium complex in human macrophages*. Int J pharm, 2003. **260**(1): p. 105-114.
4. Nunes, R., C. Silva, and L. Chaves, *Tissue-based in vitro and ex vivo models for intestinal permeability studies*, in *Concepts and Models for Drug Permeability Studies: Cell and Tissue based In Vitro Culture Models*. 2015. p. 203.
5. Yoon, G.S., et al., *Phagocytosed Clofazimine Biocrystals Can Modulate Innate Immune Signaling by Inhibiting TNFalpha and Boosting IL-1RA Secretion*. Mol Pharm, 2015. **12**(7): p. 2517-27.
6. Bolla, G. and A. Nangia, *Clofazimine Mesylate: A High Solubility Stable Salt*. Cryst Growth Des, 2012. **12**(12): p. 6250-6259.
7. Li, S., et al., *Complexation of clofazimine by macrocyclic cucurbit [7] uril reduced its cardiotoxicity without affecting the antimycobacterial efficacy*. Org Biomol Chem, 2016. **14**(31): p. 7563-7569.
8. Hernandez-Valdepeña, I., et al., *Nanoaggregates of a random amphiphilic polyanion to carry water-insoluble clofazimine in neutral aqueous media*. Eur J Pharm Sci, 2009. **36**(2–3): p. 345-351.
9. Nie, H., et al., *Solid-State Spectroscopic Investigation of Molecular Interactions between Clofazimine and Hypromellose Phthalate in Amorphous Solid Dispersions*. Mol Pharm, 2016. **13**(11): p. 3964-3975.
10. O'Reilly, J., O. Corrigan, and C. O'Driscoll, *The effect of mixed micellar systems, bile salt/fatty acids, on the solubility and intestinal absorption of clofazimine (B663) in the anaesthetised rat*. Int JPharm, 1994. **109**(2): p. 147-154.
11. Patel, V. and A. Misra, *Encapsulation and stability of clofazimine liposomes*. J Microencapsul, 1999. **16**(3): p. 357-367.
12. Peters, K., et al., *Preparation of a clofazimine nanosuspension for intravenous use and evaluation of its therapeutic efficacy in murine Mycobacterium avium infection*. J Antimicrob Chemother, 2000. **45**(1): p. 77-83.

13. Narvekar, M., et al., *Nanocarrier for poorly water-soluble anticancer drugs--barriers of translation and solutions*. AAPS PharmSciTech, 2014. **15**(4): p. 822-33.

14. Righeschi, C., et al., *Enhanced curcumin permeability by SLN formulation: The PAMPA approach*. Food sci technol, 2016. **66**: p. 475-483.

15. Vieira, A.C., et al., *Design and statistical modeling of mannose-decorated dapsone-containing nanoparticles as a strategy of targeting intestinal M-cells*. Int J Nanomedicine, 2016. **11**: p. 2601-17.

16. Attama, A. and C. Umeyor, *The use of solid lipid nanoparticles for sustained drug release*. Ther Deliv, 2015. **6**(6): p. 669-684.

17. Vardhan, H., et al., *Long-circulating polyhydroxybutyrate-co-hydroxyvalerate nanoparticles for tumor targeted docetaxel delivery: Formulation, optimization and in vitro characterization*. Eur J Pharm Sci, 2017. **99**: p. 85-94.

18. Heurtault, B., et al., *Physico-chemical stability of colloidal lipid particles*. Biomaterials, 2003. **24**(23): p. 4283-4300.

19. Shah, B., et al., *Application of quality by design approach for intranasal delivery of rivastigmine loaded solid lipid nanoparticles: Effect on formulation and characterization parameters*. Eur J Pharm Sci, 2015. **78**: p. 54-66.

20. Dhat, S., et al., *Risk management and statistical multivariate analysis approach for design and optimization of satranidazole nanoparticles*. Eur J Pharm Sci, 2017. **96**: p. 273-283.

21. Kola Srinivas, N.S., et al., *A quality by design approach on polymeric nanocarrier delivery of gefitinib: formulation, in vitro, and in vivo characterization*. Int J Nanomedicine, 2017. **12**: p. 15-28.

22. Guideline, I.H.T., *Validation of analytical procedures: text and methodology*. Q2 (R1), 2005. **1**.

23. Das, S., et al., *Formulation design, preparation and physicochemical characterizations of solid lipid nanoparticles containing a hydrophobic drug: effects of process variables*. Colloids Surf B Biointerfaces, 2011. **88**(1): p. 483-9.

24. Chaves, L., et al., *Quality by design: discussing and assessing the solid dispersions risk*. Curr Drug Deliv, 2014. **11**(2): p. 253-269.

25. Fricker, G., et al., *Phospholipids and lipid-based formulations in oral drug delivery*. Pharm Res, 2010. **27**(8): p. 1469-86.

26. H Muller, R., R. Shegokar, and C. M Keck, *20 years of lipid nanoparticles (SLN & NLC): present state of development & industrial applications*. Curr Drug Discov Technol 2011. **8**(3): p. 207-227.

27. Harde, H., M. Das, and S. Jain, *Solid lipid nanoparticles: an oral bioavailability enhancer vehicle*. Expert Opin Drug Deliv, 2011. **8**(11): p. 1407-24.

28. Kathe, N., B. Henriksen, and H. Chauhan, *Physicochemical characterization techniques for solid lipid nanoparticles: principles and limitations*. Drug Dev Ind Pharm, 2014. **40**(12): p. 1565-75.

29. Lin, P.C., et al., *Techniques for physicochemical characterization of nanomaterials*. Biotechnol Adv, 2014. **32**(4): p. 711-26.

30. Wu, L., J. Zhang, and W. Watanabe, *Physical and chemical stability of drug nanoparticles*. Adv Drug Deliv Rev, 2011. **63**(6): p. 456-469.

31. Panyam, J., et al., *Solid-state solubility influences encapsulation and release of hydrophobic drugs from PLGA/PLA nanoparticles*. J Pharm Sci 2004. **93**(7): p. 1804-1814.

32. Bunjes, H., *Lipid nanoparticles for the delivery of poorly water-soluble drugs*. J Pharm Pharmacol, 2010. **62**(11): p. 1637-45.

33. Yerlikaya, F., et al., *Development and evaluation of paclitaxel nanoparticles using a quality-by-design approach*. J Pharm Sci, 2013. **102**(10): p. 3748-61.

34. Beg, S., et al., *QbD-based systematic development of novel optimized solid self-nanoemulsifying drug delivery systems (SNEDDS) of lovastatin with enhanced biopharmaceutical performance*. Drug Deliv, 2015. **22**(6): p. 765-84.

35. Silva-Buzanello, R., et al., *Validation of an Ultraviolet–visible (UV–Vis) technique for the quantitative determination of curcumin in poly(l-lactic acid) nanoparticles*. Food Chem, 2015. **172**: p. 99-104.

36. Borner, K., et al., *HPLC determination of clofazimine in tissues and serum of mice after intravenous administration of nanocrystalline or liposomal formulations*. Int J Antimicrob Agents, 1999. **11**(1): p. 75-9.

37. Queiroz, R.H., et al., *Determination of clofazimine in leprosy patients by high-performance liquid chromatography*. J Anal Toxicol, 2003. **27**(6): p. 377-80.

38. Kapoor, V. and Shishu., *A novel validation of HPTLC method for the quantitative determination of clofazimine*. Int J Pharm Bio Sci, 2013. **4**(2): p. 819 - 828.

39. Saxena, S., et al., *Estimation of Clofazimine in capsule dosage form by using UV-Vis spectroscopy*. . Int J Pharm Pharm Sci, 2013. **5**(3): p. 635-638.

40. Negi, L., M. Jaggi, and S. Talegaonkar, *Development of protocol for screening the formulation components and the assessment of common quality problems of nano-structured lipid carriers*. Int J Pharm, 2014. **461**(1–2): p. 403-410.

41. Patil, H., et al., *Continuous Production of Fenofibrate Solid Lipid Nanoparticles by Hot-Melt Extrusion Technology: a Systematic Study Based on a Quality by Design Approach*. The AAPS Journal, 2015. **17**(1): p. 194-205.

42. Qi, J., Y. Lu, and W. Wu, *Absorption, disposition and pharmacokinetics of solid lipid nanoparticles*. Curr Drug Metab 2012. **13**(4): p. 418-428.

43. Gupta, B., et al., *Effects of Formulation Variables on the Particle Size and Drug Encapsulation of Imatinib-Loaded Solid Lipid Nanoparticles*. AAPS PharmSciTech, 2016. **17**(3): p. 652-62.

44. Makled, S., N. Nafee, and N. Boraie, *Nebulized solid lipid nanoparticles for the potential treatment of pulmonary hypertension via targeted delivery of phosphodiesterase-5-inhibitor*. International Journal of Pharmaceutics, 2017. **517**(1–2): p. 312-321.

45. Fang, J.-Y., et al., *Lipid nanoparticles as vehicles for topical psoralen delivery: Solid lipid nanoparticles (SLN) versus nanostructured lipid carriers (NLC)*. European Journal of Pharmaceutics and Biopharmaceutics, 2008. **70**(2): p. 633-640.

46. Nafee, N., et al., *Antibiotic-free nanotherapeutics: Ultra-small, mucus-penetrating solid lipid nanoparticles enhance the pulmonary delivery and anti-virulence efficacy of novel quorum sensing inhibitors*. Journal of Controlled Release, 2014. **192**: p. 131-140.

47. Araujo, F. and B. Sarmento, *Towards the characterization of an in vitro triple co-culture intestine cell model for permeability studies*. Int J Pharm, 2013. **458**(1): p. 128-34.

48. Fernandes, I., et al., *A new approach on the gastric absorption of anthocyanins*. Food Funct, 2012. **3**(5): p. 508-16.

49. Arbiser, J.L. and S.L. Moschella, *Clofazimine: a review of its medical uses and mechanisms of action*. J Am Acad Dermatol, 1995. **32**(2 Pt 1): p. 241-7.

D. Development of PLGA nanoparticles loaded with clofazimine for oral delivery: assessment of formulation variables and intestinal permeability.[6]

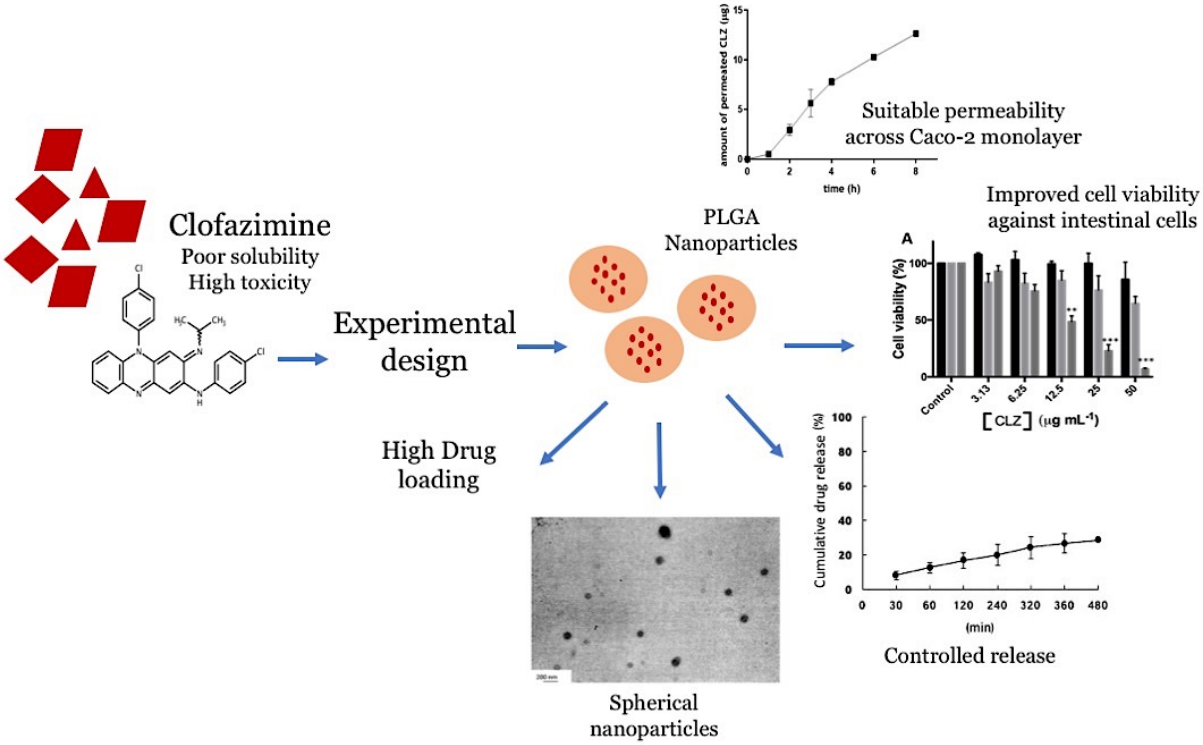

[6] Submitted

Development of PLGA nanoparticles loaded with clofazimine for oral delivery: assessment of formulation variables and intestinal permeability

Luíse L. Chaves[a], Sofia A. Costa Lima[a,b], Alexandre C.C.Vieira[a], Luísa Barreiros[a], Marcela A. Segundo[a], Domingos Ferreira[c], Bruno Sarmento[b,d,e], Salette Reis[*a]

[a]UCIBIO, REQUIMTE, Departamento de Ciências Químicas, Faculdade de Farmácia, Universidade do Porto, Porto, Portugal
[b]CESPU, Instituto de Investigacão e Formação Avançada em Ciências e Tecnologias da Saúde and Instituto Universitário de Ciências da Saúde
[c]Laboratório de Tecnologia Farmacêutica, Departamento de Ciências do Medicamento, Faculdade de Farmácia, Universidade do Porto, Portugal
[d]I3S, Instituto de Investigacão e Inovacão em Saúde, Universidade do Porto, Portugal
[e]INEB – Instituto de Engenharia Biomédica, Universidade do Porto, Portugal

ABSTRACT

The use of polymeric nanoparticles as delivery systems is a promising tool to overcome drawbacks related to low aqueous solubility of drugs, which limit their *in vivo* bioavailability. The aim of this study was to assess critical factors during formulation design of clofazimine (CLZ) loaded in PLGA nanoparticles (NPs-CLZ) through a Plackett–Burman design (PBD). A screening PBD was constructed with twelve formulations involving six variables among process and formulation parameters and the selected responses were particle size, polydispersity index (PDI), association efficiency (AE) and drug loading (DL). The formulation was achieved based on the desirability tool, and the obtained NPs-CLZ formulation was characterized regarding morphology, physicochemical properties and *in vitro* cellular studies. Particle size, PDI, AE and DL were found to be 211 ± 3 nm, 0.211 ± 0.009, 70 ± 5% and 12 ± 1 %, respectively. Fourier transformed infra-red spectroscopy confirmed the absence of chemical interactions between CLZ and other nanoparticles constituents, while differential scanning calorimetry thermograms indicated the amorphous state of CLZ and transmission electron microscopy revealed the spherical shape of the particles. *In vitro* release profile of CLZ from NPs-PLGA showed a slow pattern of drug release. Cytotoxicity studies towards intestinal cells revealed that NPs-CLZ did not show CLZ toxicity on Caco-2 and HT29-MTX cells compared to free CLZ solutions. It can be concluded that experimental design can streamline the formulation of poorly soluble drugs, deploying suitable vehicles with enhanced properties. The optimized NPs-CLZ is a promising platform for oral delivery of CLZ.

Key words: Caco-2 cell monolayer permeation assay; Plackett–Burman design, PLGA nanoparticles; poorly soluble drug

1. Introduction

Leprosy is a chronic infectious disease caused by *Mycobacterium leprae* (*M. leprae*), which is a slowly growing intracellular bacillus that affects mainly peripheral nerves, especially Schwann cells, and skin [1]. Its clinical manifestations are related to the host immune response and bacillary cell loading, being classified as lepromatous (high bacillary load) or tuberculoid (low bacillary load). The actual proposed treatment is classified according to the number of skin lesions namely multibacillary (more than 6 lesion) or paucibacillary (2-5 lesions) [2]. Current therapy consists in a multidrug combination of dapsone, rifampicin, and clofazimine, depending on disease manifestation [1].

Clofazimine (CLZ), is an antibiotic and anti-inflammatory drug and, as other riminophenazines is effective against both slowly and rapidly growing mycobacteria, as well as most other Gram-positive bacteria [3]. The very high hydrophobicity (logP > 7) of CLZ result in a very limited absorption (about 40%) after oral administration [4-6], which lead to an increasing in the administered doses to reach appropriate pharmacokinetic levels and to guarantee the therapeutic effects [4]. Besides, its low solubility CLZ is associated with bioaccumulation in the body's fatty tissue, resulting in a 70 days half-life in humans, causing skin pigmentation, abdominal pain and cardiotoxicity [4-6]. In fact, it is already reported that CLZ may originate *in vivo* drug precipitation, forming complexes with intracellular membranes, and precipitate as crystal aggregates, which is further phagocytized by the mononuclear phagocyte system [7, 8].

Several approaches have been reported to improve CLZ solubility namely salt formation [9], complexation with cyclodextrins [4] or other macromolecules [6, 10], formulation of amorphous dispersions [11], use of co-solvents or surfactants [12], formulation of liposomes [13] and nanosuspensions [14].

In recent years, the encapsulation of poorly soluble drugs into nanoparticles have been gaining attention to improve drug bioavailability due to nanoparticles permeation through the interstitial spaces in tissue which may enhance drug cellular uptake [15]. Furthermore, nanoparticles may offer protection against gastrointestinal degradation, provide improved circulation half-life and possibility to active and passive targeting to specific intestinal cells, reducing systemic undesired effects [16]. The application of polymer based nanodelivery systems are being promising platforms for this purpose due to their ability to prolong drug release, increase drug bioavailability, decrease drug degradation and reduce drug toxicity [17, 18]. The copolymer poly(lactic-co-glycolic acid) (PLGA) is one the polymers widely used in this context as it is biocompatible,

biodegradable and safely administrable [19]. Moreover, it has a particular advantageous to promote controlled and sustained drug delivery [19].
Despite different works have tried to improve CLZ solubility and bioavailability, the encapsulation PLGA nanoparticles has not been already described. The aim of this work was to develop polymeric PLGA nanoparticles loaded with CLZ (NPs-CLZ) aiming to improve CLZ intestinal absorption and decrease its associated toxicity. For these purpose, NPs-CLZ were produced after assessment of Placket-Burman screening designs formulation responses. The obtained NPs-CLZ were physical-chemically characterized regarding particle size distribution, polydispersity index (PDI), association efficiency (AE), in addition morphological studies, and *in vitro* drug release assays. Cell viability of the obtained formulations was also assessed with two different cell lines (Caco-2 and HT29-MTX), aiming to evaluate the toxicity of the particles when in contact with intestinal cells. Finally, the *in vitro* permeability of NPs-CLZ through Caco-2 monolayers was performed to assess the performance of the developed system in an intestinal model.

2. Materials anda methods

2.1. Materials

CLZ was purchased from Hangzhou Heta Pharm & Chem Co. Poly (lactic-co-glycolic acid) (PLGA) (50:50 Purasorb® PDLG 5002A) was a kind gift from Purac Biomaterials (Gorinchem, The Netherlands). Polyvinyl alcohol (PVA) was purchased from Sigma–Aldrich (St. Louis, USA) and acetone obtained from JGMS (Odivelas, Portugal).
Caco-2 cell line was purchased from the American Type Culture Collection (ATCC, Wesel, Germany) (passage number 35 - 55) and HT29-MTX cell line was kindly provided by Dr. T. Lesuffleur (INSERM U178, Villejuif, France). Dulbecco's Modified Eagle Medium (DMEM), fetal bovine serum (FBS, South America origin), penicillin-streptomycin mixture (Pen-Strep) and trypsin-EDTA 0.25% (w/v) were all obtained from Gibco (Paisley, UK). Thiazolyl blue tetrazolium bromide (MTT) was obtained from Sigma–Aldrich (St. Louis, USA).

2.2. Preparation of PLGA nanoparticles

The nanoparticles were prepared following the nanoprecipitation method [20]. Briefly, an accurately weighed amount of PLGA (20 or 40 mg) and CLZ (2 or 4 mg) were dissolved in acetone, at specified volumes (2 or 3 mL). The organic phase was slowly

added to PVA 1% (w/v) solution (5 or 10 mL), under probe sonication, during 2 min, with an amplitude (50 or 70%). A PVA solution (1 or 0.1% w/v) was then used as stabilizer to complete the final volume up to 20 mL. The final emulsion was maintained under magnetic stirring (RT 15 Power IKAMAG Multiposition Magnetic Stirrer, Staufen, Germany) at 350 rpm and room temperature. NPs-CLZ were washed three times with double deionized water, by centrifugation at 11,200 *g* for 30 min, using an Allegra X-15R centrifuge (Beckman Coulter, Brea, CA, USA). The amount of each variable was selected according to the experimental design (see section 2.3). Unloaded nanoparticles (NPs) were obtained for the selected formulation, following the same procedure. The resultant particles were freeze-dried when appropriate for 48 h, using a LyoQuest 85 plus v.407 Telstar freeze dryer (Telstar® Life Science Solutions, Terrassa, Spain).

2.3. Experimental Design

Different process and product variables which may influence the main critical parameters of NPs-CLZ were assessed by constructing a Plackett-Burman design (PBD). The design was constructed with six factors and twelve experiments, using the STATISTICA 10 software (StatSoft®, Dell Software, Round Rock, TX, USA). The parameters studied were chosen according to literature and a preliminary investigation, which were (X_1) volume of organic phase; (X_2) stabilizer concentration; (X_3) amount of polymer; (X_4) amount of drug; (X_5) amplitude of sonication; (X_6) volume of aqueous phase. The parameter level selection was based on prior knowledge and literature [21, 22]. Non-studied variables as type of polymer (PLGA); ratio of PLGA co-polymerization (L:G - 50:50); organic solvent used (acetone); method of preparation (single emulsion – solvent evaporation); method of solvent evaporation (magnetic stirring); final volume of nanosuspension (20 mL) were fixed. The selected responses were: particles size (Y_1), polydispersity index (Y_2), association efficiency (Y_3) and drug loading (Y_4).

2.4. Formulation of CLZ-loaded PLGA nanoparticles (NPs-CLZ)

Selected formulation was obtained after graphical and numerical analyses of the variables using STATISTICA 10 software based on the criteria of desirability namely (Y_1) particle size closer to 200nm; (Y_2) PDI < 0.2; (Y_3) maximum association efficiency (AE) and (Y_4) maximum drug loading (DL).
The models were obtained following the equation:

$$Y = \beta_0 + \beta_1 X_1 + \beta_2 X_2 + \beta_3 X_3 + \cdots + \beta_n X_n$$

where Y is the response, β_0 is a constant and β_0 - β_n are the coefficients of the response values, X_1–X_n are the factors under investigation.

2.5. Physicochemical characterization of NPs-CLZ

2.5.1. Particle size and polydispersity index

Both mean particle size and polydispersity index (PDI) were analyzed using a ZetaPALS, Zeta Potential Analyzer (Brookhaven Instrument Corps, Holtsville, NY, USA), with a light incidence angle of 90º at 25ºC. The fresh colloidal dispersions were properly diluted with ultrapure water until reach a suitable concentration (Kcps 300-500), and the obtained value is the representation of multiples runs (n=6).

2.5.2. Determination of association efficiency and drug loading

The quantification of CLZ within PLGA nanoparticles was carried out by determining the unentrapped drug applying the ultracentrifugation method. Briefly, samples were prepared by properly diluting NPs-CLZ with sodium dodecyl sulphate (SDS) 2% (w/v) so that the maximum concentration of CLZ did not exceed 100 μg mL^{-1} to ensure that unentrapped drug remains soluble. Samples were centrifuged at 11,200 x*g* for 30 min. The supernatant was read at 492 nm by UV-VIS spectroscopy (Jasco V-660, Easton, MD, USA). Standard curves were obtained for CLZ in SDS 2% and then the supernatant containing the aqueous phase was measured to determine the CLZ concentration. The results are expressed as mean ± standard deviation (n=3). Association efficiency (AE) and drug loading (DL) were calculated following the equations:

$$AE = \frac{Initial\ amount\ of\ drug - recovered\ drug}{initial\ amount\ of\ drug} \times 100$$

$$DL = \frac{initial\ amount\ of\ drug - recovered\ drug}{initial\ amount\ of\ drug + initial\ amount\ of\ polymer} \times 100$$

2.5.3. Morphological analysis

The morphology of designed NPs-CLZ and unloaded NPs were examined by transmission electron microscopy (TEM, JeolJEM-1400, JEOL Ltd., Tokyo, Japan). Images were obtained after dropping the colloidal dispersions properly diluted (40 times) over a copper-mesh grid followed by negative staining with 0.75% (w/v) uranyl acetate (30 s at room temperature). The grid was exposed at the accelerating voltage of 60 kV.

2.5.4. Fourier transform infrared spectroscopy (FTIR)

The spectra of CLZ, physical mixture (PM), PLGA NPs and NPs-CLZ were obtained to study possible CLZ-polymer chemical interactions. The IR spectra were obtained using the PerkinElmer® Spectrum 400 (Waltham, MA, USA) equipped with an attenuated total reflectance (ATR) device and zinc selenite crystals. The freeze-dried samples were transferred directly to the ATR compartment, and the result was obtained by combining the 16 scans. The spectra were recorded between 4000 and 600 cm^{-1} with a resolution of 4 cm^{-1}.

2.5.5. Differential scanning calorimetry (DSC)

Differential scanning calorimetry thermograms of CLZ, PM, PLGA NPs and NPs-CLZ were obtained to evaluate the physical changes in CLZ crystallinity before and after the nanoparticles production process. The thermal analysis was performed using a DSC 200 F3 Maia (Netzsch, Selb, Germany).
Accurately weighted samples (1-2 mg) were poured into aluminum pans and hermetically sealed. The samples were scanned from 30 to 300 ^{o}C, at 10 $^{o}C.min^{-1}$. Nitrogen gas was used as purge gas, at 40 $mL.min^{-1}$. The melting point (peak maximum), was calculated using the (NETZSCH Proteus® Software – Thermal Analysis – Version 6.1) software provided for the DSC equipment.

2.5.6. *In vitro* drug release

The *in vitro* drug release was performed using the methodology described elsewhere [22, 23]. Briefly, NPs-CLZ were dispersed into 1.5 mL of sodium dodecyl sulfate (SDS)solution (2% -w/v) aiming to provide solubility of CLZ in the aqueous phase, as already described for other poor soluble drugs [24]. The solubility of CLZ in different

surfactants namely Tween® 80 (1 and 2%), sodium salicylate (1 and 2%) and SDS (1 and 2%) was previous study to select the suitable solubilizing agent (data not shown). Samples were incubated at 37ºC using a shaking water bath, at 250 rpm. Samples were taken at pre-defined time intervals (0.5, 1, 2, 4, 6 and 8 h) and replaced with fresh medium at the same temperature. The recovered samples were centrifuged at 11200 *g* for 30 min using an Allegra X-15R centrifuge (Beckman Coulter, Brea, CA, USA) and free CLZ was determined by UV-VIS spectroscopy (Jasco V-660, Easton, MD, USA) at 492nm, as described in 3.3.2.

2.6 Cell culture assays

Caco-2 and HT29-MTX cells were cultured in Dulbecco's modified Eagle's medium (DMEM) supplemented with 10% (v/v) of fetal bovine serum (FBS) and 1% (v/v) of penicillin-streptomycin. Cells were grown in a humidified incubator at 37 ºC and 5% CO_2 atmosphere and 95% relative humidity. When reaching 80% confluence, cells were detached using trypsinization.

2.6.1 *In vitro* cell viability studies

The cell viability of unloaded NPs, NPs-CLZ and free CLZ was evaluated against Caco-2 and HT29-MTX cells lines to compare its toxicity to the free drug. The method used was the 3-(4, 5-dimethylthiazol-2-yl)-2,5-diphenyltetrazolium bromide (MTT) colorimetric assay. Separately, each cell line was transferred into 96-well plates, at a density of 5 x 10^4 cells per well. After cell adhesion, the culture media was removed and the wells were incubated with 100 µL of culture media containing different concentrations of NPs, NPs-CLZ and free CLZ (6.25 – 50 µg mL^{-1} of CLZ). For free CLZ, the samples were prepared from a stock solution in DMSO, and appropriate dilutions were done to reach a maximum of 4% (v/v) of DMSO in the well, immediately before the assay. After a 24 h incubation period, the supernatant was removed and replaced by 100 µL of MTT solution (0.5 mg mL^{-1}). Upon 2 h at 37ºC, the MTT solution was removed and 100 µL of DMSO was added into each well to solubilizing of formazan crystal. The optical density of the solution was measured at a wavelength of 570 nm using Synergy™ HT Multi-mode microplate reader (BioTek Instruments Inc., Winooski, VT, USA). Untreated cells were taken as positive control with 100% viability and cells treated with 4% (v/v) DMSO in culture media used as control for free CLZ. Three independent MTT assays were performed with quadruplicate samples each and

results were expressed as mean values ±SD. The cell viability (%) in relation to control cells (untreated cells) was calculated by the equation:

$$Cell\ viability\ (\%) = \frac{[A]cells\ incubated\ with\ formulation}{[A]cells\ incubated\ with\ culture\ medium} \times 100$$

2.6.2 CLZ permeation across Caco-2 monolayers

For the permeability studies, Caco-2 cells were seeded on 12-well Transwell inserts (Corning Transwell Clear, pore size 3 μm, area 0.33 cm^2) at a cell density of 10^5 cells per cm. The cells were grown in FBS-supplemented DMEM, and the culture medium was added to both apical and basolateral compartments, with changes every other day, during 21-23 days, until the monolayer achieve minimum of 400 Ω cm^2 of transepithelial electrical resistance (TEER) values [24, 25]. The tightness of the Caco-2 monolayer was assessed as the TEER values using a Millicell® ER-1 system voltohmmeter (Millipore Corporation, Bedford, MA), equipped with a pair of chopstick electrodes inserted into the apical medium. The TEER value at the beginning of the studies was higher than 400 Ω cm^2, indicating an intact monolayer; TEER values were also obtained after completion of flux experiments upon 8 h. The resistance measurement of the medium without cells was considered as blank. The permeability was carried out by adding 0.5 mL of culture medium containing the equivalent of 40 μg mL^{-1} of CLZ as NPs-CLZ in the apical side of the cell monolayer. The formulations were incubated for 8 h, and at predetermined time intervals (1, 2, 3, 4, 6 and 8 h), 0.5 mL were sampled from the basolateral compartment and replaced with fresh culture medium. The amount of CLZ in the samples was analyzed by HPLC according the section 2.7. The experiments were carried out in triplicate. The cumulative amount of CLZ transported across the monolayers was calculated from the samples collected at the basolateral compartment. The apparent permeability (Papp) was calculated as described elsewhere [26].

2.7 CLZ determination by high-performance liquid chromatography

CLZ quantification in cell culture media was performed by high-performance liquid chromatography (HPLC) with UV detection. The HPLC system (Jasco) comprised a high-pressure pump (PU-2089), an autosampler (AS-2057) and a diode array detector (MD-2015) programmed for peak detection at 280 nm, controlled by ChromNAV software. A reversed phase Kinetex® core-shell C18 column (250 x 4.1 mm, 5 μm

particle size, 100 Å; Phenomenex, Torrance, CA, USA) was used as stationary phase. Elution was performed in gradient mode using as mobile phase a mixture of aqueous acetate buffer (final concentration 50 mM, pH 4.8) and acetonitrile, at a flow rate of 1 mL min^{-1}. The selected gradient started with 30% (v/v) of acetonitrile, which was maintained up to 3 min. From 3 to 5.5 min, the contribution of acetonitrile was rapidly changed to 80% (v/v). This composition was maintained up to 7.5 min, after which the initial conditions were re-established and held during 5.5 min more to assure column equilibration. Hence, the total run time was 13 min. The injection volume was 20 µL. Standard CLZ solutions were prepared at 0.5, 1, 2.5, 5, 7.5, 10, 15 and 20 µg mL^{-1} in culture medium containing 40% (v/v) of acetonitrile and 50 mM acetate buffer, pH 4.8. To prepare the samples for HPLC analyses, 200 µL of each sample was added to 160 µL of acetonitrile and 40 µL of acetate buffer 500 mM, pH 4.8, to final concentrations of 40% (v/v) and 50 mM, respectively. The mixtures were vortexed and centrifuged at 18,000 × *g* for 10 min at room temperature. After centrifugation, supernatants were collected and analyzed by HPLC.

2.8 Statistical analyses

The statistical analysis of the experimental design was performed used STATISTICA10 (StatSoft®) software. GraphPad Prism software (version 6, GraphPad Software, USA) was used for statistical comparisons of the results to control for the cytotoxicity studies. Statistical analysis of the results was performed using student (unpaired) t-test and one-way ANOVA test. All the other results were presented as mean and standard deviation (SD). The differences were assumed statistical significant when $p < 0.05$ (95% confidence level), for cytotoxicity studies, and $p < 0.01$ (99% confidence level) for experimental design.

3. Results and discussion

3.1 Experimental Design

Plackett–Burman (PB) designs are screening strategies which can be used to identify critical factors with a reasonable number of experimental runs and good degree of accuracy [27, 28]. In parallel, during the design of polymeric nanoparticles, several factors as: (i) method of preparation, (ii) drug solubility in the organic phase; (iii) choice of organic solvent; (iv) inclusion of a suitable stabilizer; (v) the ratio polymer/drug as well as their concentration in the nanosuspension may influence the

desired performance of the nanosuspension regarding association efficiency, drug loading, nanoparticles dispersity and stability [28, 29].

The emulsion-solvent evaporation is the most common method used to prepare polymeric nanoparticles, though the encapsulation of poorly soluble drugs is yet quite challenging due to the difficulty in achieve satisfactory drug loading [16, 30].

In this context, PBD seemed to be a suitable tool to assess nanoparticles design formulations and process critical factors. This study involved the production of twelve formulations based in six factors defined from on preliminary studies. The independent variables were (X_1) volume of organic phase; (X_2) stabilizer concentration; (X_3) amount of polymer; (X_4) amount of drug; (X_5) amplitude of sonication; (X_6) volume of aqueous phase. From preliminary studies some parameters were considered as the best choice and were fixed namely: the type of polymer (PLGA); the type of PLGA *co*-polymerization (PLA: PGA - 50:50); organic solvent used (acetone); method of preparation (single emulsion- solvent evaporation); method of solvent evaporation (magnetic stirring); final volume of nanosuspension (20 mL). The selected responses, namely (Y_1) particle size, (Y_2) PDI; (Y_3) AE and (Y_4) DL, were determined for each formulation. The designed formulations and the obtained responses are shown in Table 1.

Table 1. Layout and observed responses of Plackett–Burman screening design formulations

Formulation	***X_1*** *(mL)*	X_2 *(%)*	X_3 *(mg)*	X_4 *(mg)*	X_5 *(%)*	X_6 *(mL)*	Size (nm)	PDI	AE (%)	DL (%)
F1	3	1.0	40	2	50	5	221.0	0.180	36.59	1.74
F2	3	0.1	20	4	50	5	209.3	0.215	52.58	8.76
F3	2	0.1	40	2	70	5	241.4	0.138	43.69	2.08
F4	3	1.0	40	4	50	10	121.9	0.208	23.87	2.17
F5	3	0.1	20	4	70	5	227.5	0.223	79.45	13.24
F6	3	0.1	40	2	70	10	108.7	0.211	11.44	0.54
F7	2	0.1	40	4	50	10	136.6	0.152	33.81	3.07
F8	2	1.0	40	4	70	5	218.7	0.125	54.71	4.97
F9	2	1.0	20	4	70	10	181.5	0.326	28.13	4.69
F10	3	1.0	20	2	70	10	142.6	0.324	6.57	0.60
F11	2	0.1	20	2	50	10	120.2	0.201	0.69	0.06
F12	2	1.0	20	2	50	5	177.1	0.220	23.81	2.16

Independent variables: X_1 volume of organic solvent; X_2 stabilizer concentration; X_3 amount of polymer; X_4 amount of drug; X_5 amplitude of sonication; X_6 volume of aqueous phase. Dependent variables: Y_1 particle size; Y_2 PDI; Y_3 AE and Y_4 DL.

The quantitative standardized effects of the variables on the responses were assessed by plotting Pareto charts (Figure 1) which consists in bars with a length proportional to the absolute value of the estimated effects, divided by the standard error. The bars are ordered by magnitude of the effects, with the largest effects at the top [31]. The negative and positive sign of the coefficient indicate an indirect and direct relation to the response respectively [32].

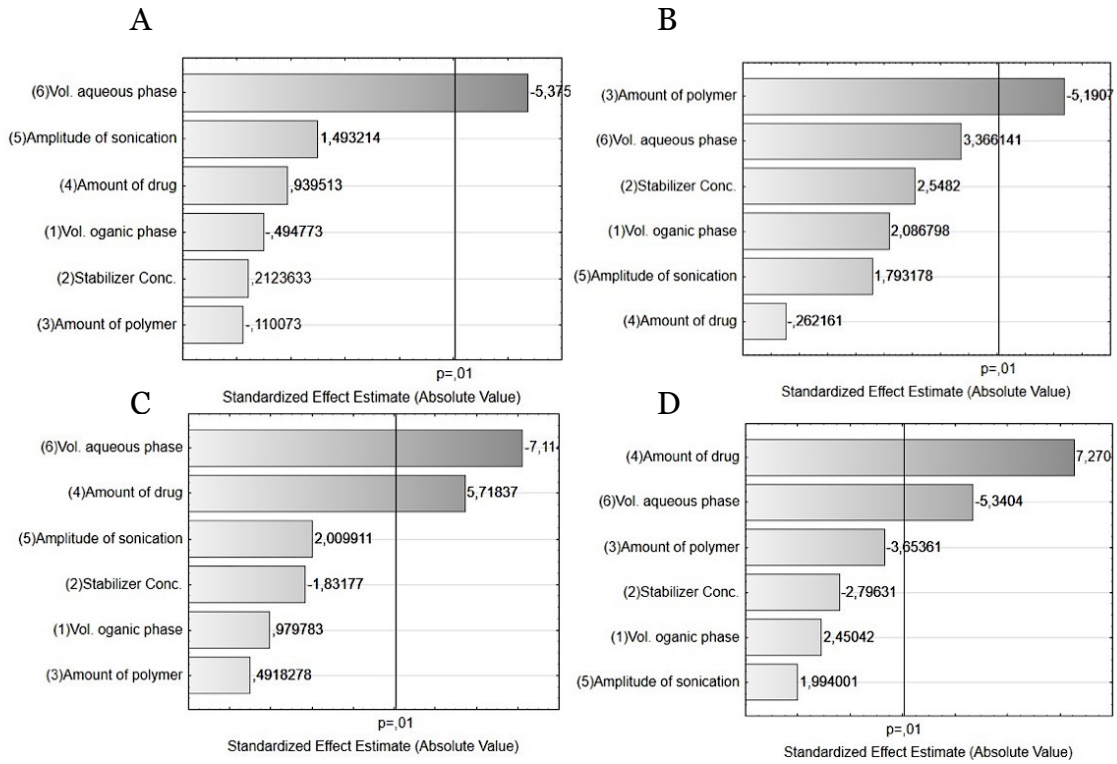

Figure 1. Pareto charts showing the significance of the variables for (A) particle size, (B) polydispersity index, (F) association efficiency and (D) drug loading. The effects were considered statistically significant when $p < 0.01$, with 99% of confidence level.

3.1.1 Effects on particle size

The particles size (Y_1) of the obtained formulations ranged from 108.7 nm (F4) to 241.4 nm (F3). According to the regression analysis of the responses, the volume aqueous phase (X_6) was the only factor that influenced statistically the particle size. The negative sign before the linear coefficient (-40.292) indicates a negative effect of the volume of aqueous phase on particles size, i.e., as the volume increases, the particle size decreases in size. This effect could be explained by the decrease in the levels of entrapped CLZ (see section 4.6.3), with the increasing in the volume of aqueous phase due drug precipitation, leading to formation of particles with lower diameter. In fact, considering only the particles prepared with the lowest volume of aqueous phase (F1, F2, F3, F5, F8

and F12), in general higher values of AE, DL and particle size was observed among the 12 formulations, supporting the suggested explanation.

3.1.2 Effects on PDI

PDI values (Y_2) of the obtained 12 formulations ranges from 0.125 (F8) to 0.326 (F9). The regression analysis showed that the amount of polymer (X_3) statistically influenced the response. The negative sign before the regression coefficient (-0.041) reveals an inverse relationship between the response and changing in the levels of the factor. One possible explanation for this result is drug precipitation of at higher amounts and with lower amounts of the polymer, due to inefficient drug loading capacity. In fact, for formulations (F2, F5, F9, F10, F11 and F12) with low amount of polymer (20 mg), higher values of PDI were obtained. The low water solubility of CLZ lead to the formation of crystals of the non-entrapped drug that may influence the dispersity of the measurement.

3.1.3 Effects on the association efficiency

The AE (Y_3) of the prepared formulations ranged from 0.69% (F11) to 79.45% (F5). The regression analysis evidenced that the volume of aqueous phase (X_6) and drug amount (X_4) significantly interfered in the Ae levels, at this order of significance. The negative sign before the (X_6) coefficient reveals that the AE values decrease with the increasing in volume of aqueous phase. This phenomenon may be explained by the precipitation of CLZ with increased volumes of aqueous phase, due to its very high hydrophobicity as the ratio organic/aqueous phase decreases in a higher degree, even considering the changing in organic solvent volume. With the precipitation of CLZ, less drug is available to interact with the polymer and consequently to be entrapped. On the contrary, the positive sign before (X_6) coefficient indicates a direct relation between the amount of drug and the AE values. The AE is related to the miscibility of the drug into the polymer. In the PLGA nanoparticles, with the same polymer concentration, changings in the initial amount of drug generally results in a maximum drug incorporation. Nevertheless, as the drug content increases, reaches its limiting value, determined by the drug miscibility in the polymer at a given processing conditions, reaching a plateau [33]. Because in PBD only two levels at a time of each variable are studied, the maximum capacity of the process could not be achieved, but a tendency in increasing AE with higher amounts of CLZ was detected.

3.1.4 Effects on the drug loading

The DL (Y_4) of the formulations ranged from 0.06% (F11) to 13.24% (F5). The regression analysis evidenced that the (X_4) amount of drug and the (X_6) volume of aqueous phase significantly interfered in the DL levels, at this order of significance. The amount of drug (p = 0.001) was more relevant than the volume of aqueous phase (p = 0.003) in the values of DL obtained.

The positive sign before the (X_4) coefficient reveals that the DL values increases with the increasing in the initial amount of drug, probably to the same reason as discussed on section 4.4.3. For the calculation of the DL, the initial amount of polymer is considered, even though it seems that it was not relevant for the drug incorporation and the selected levels of the amount of PLGA did not increase significantly the entrapment of CLZ, while considerable differences in changing CLZ amount from 2 to 4 mg promoted several important responses. The negative sign before (X_6) coefficient indicates a negative relation between the volume of aqueous phase and the DL values probably due to drug precipitation when in contact with the aqueous medium, as already discussed.

3.2 Formulation of CLZ-loaded PLGA nanoparticles (NPs-CLZ)

The formulation of NPs-CLZ was based in the effects of the factors after preliminary screening through a PBD. The mathematical correlation between the factors coefficients and their *p* values were analyzed via regression analysis, for each response, and are expressed in Table 2. The mean values of the obtained response (β_0) corresponded to the intercept of the model. The magnitude and the sign of the polynomial coefficients indicate synergistic or antagonistic effect, when the signs are positive or negative, respectively.

As shown in Table 2 the determination coefficients (R^2) were very close to the unit, indicating reasonable agreement between the predicted and the observed values, and variations in the response over 90% could be explained by the obtained models. Moreover, obtained F value were compared with the theoretical value (Fisher test critical value) $F_{\alpha\ (p-1,N-p)}$ (α, chosen risk, p the number of terms of the model, N the number of the experiments) to test the significance of the regression models. The theoretical value $F_{0.05\ (6,5)}$ is 4.95. All the calculated F-ratios were found to be greater than the theoretical value (Table 2) evidencing the significance of the regression models, with a confidence level of 95% [32].

Table 2. Data of the regression analysis for the considered responses Y_1–Y_4.

	Particle size (Y_1)		*PDI (Y_2)*		*AE (Y_3)*		*DL (Y_4)*	
	Coefficient	*p*-Value	Coefficient	*p*-Value	Coefficient	*p*-Value	Coefficient	*p*-Value
β_0	175.542	**0.000**	0.210	0.000	32.946	0.000	3.675	0.000
X_1	-3.708	0.642	0.017	0.091	2.138	0.372	0.835	0.058
X_2	1.592	0.840	0.020	0.051	-3.998	0.126	-0.952	0.038
X_3	-0.825	0.917	-0.041	**0.003**	1.073	0.644	-1.244	0.015
X_4	7.042	0.391	-0.002	0.804	12.480	**0.002**	2.477	**0.001**
X_5	11.192	0.196	0.014	0.133	4.386	0.101	0.679	0.103
X_6	-40.292	**0.003**	0.027	0.020	-15.526	**0.001**	-1.819	**0.003**
	$R^2 = 0.866$		$R^2 = 0.913$		$R^2 = 0.948$		$R^2 = 0.957$	
	$F_{calculated} = 5.39$		$F_{calculated} = 8.73$		$F_{calculated} = 15.32$		$F_{calculated} = 18.76$	

Despite PBD are not commonly used to obtain optimum formulation, the validity of the obtained models allowed to investigate through the desirability software function to design nanoparticles with specific features namely size closer to 200 nm, PDI <0.2, maximum AE and DL. Selected NPs-CLZ were obtained with: (X_1) 3 mL of organic phase; (X_2) 0.1% (w/v) of stabilizer concentration; (X_3) 40 mg of PLGA; (X_4) 4 mg of CLZ; (X_5) 70% of amplitude of sonication and (X_6) 5 mL of aqueous phase. Unload nanoparticles (NPs) were also obtained, and both were characterized.

3.3 Particle size and Polydispersity index

It has been already reported that PLGA particles with diameter close to 200 nm can be taken by the enterocytes via clathrin-coated pit endocytosis [34]. Moreover, kinetic absorption of PLGA nanoparticles was reported to be size- dependent as smaller particles sizes was proved to be uptaken at a higher level compared to particles with diameter closer to 1μm [35].

Thus, our aim was to develop particles closer to the optimal diameter to improve CLZ uptake by intestinal cells, with the lower dispersity as possible. Accordingly, the particle size of the obtained NPs-CLZ was 210.8 ± 2.6 nm. The PDI values (0.211 ± 0.009) were below 0.3, which indicate that distribution is monomodal [24] being suitable for intestinal absorption. Similar results were obtained with PLGA nanoparticles previously [36]. Unloaded nanoparticles (NPs) were obtained as control, and presented values of particle size and PDI of 174.8 ± 13.4 nm and 0.215 ± 0.017, respectively. The presence of drug in the NPs-CLZ leads to ca. 40 nm increase in relation to unloaded NPs.

3.4 Determination of association efficiency and drug loading

The association efficiency and drug loading of NPs-CLZ was 69.6 ± 5.0 % and 11.6 ± 0.8%, respectively. The obtained DL was considered a good result, since this parameter is related to the decrease in the required administrated NPs-CLZ [34].

3.5 Physicochemical characterization of NPs-CLZ

3.5.1 Morphological analysis

Electron micrographs of unloaded-NPs and NPs-CLZ before and after freeze-drying were obtained (Figure 2) to investigate structural and morphological features of the nanoparticles, and the influence of the lyophilization process on the nanoparticles morphology. From the images, it could be seen that the particles were well dispersed, and with spherical morphology. Unloaded-NPs and NPs-CLZ showed similar structures before (Figure 2 A and B) and after freeze-drying (Figure 2 C and D), confirming that the process did not alter the particles morphology. The freeze-drying could then be used to store the formulation.

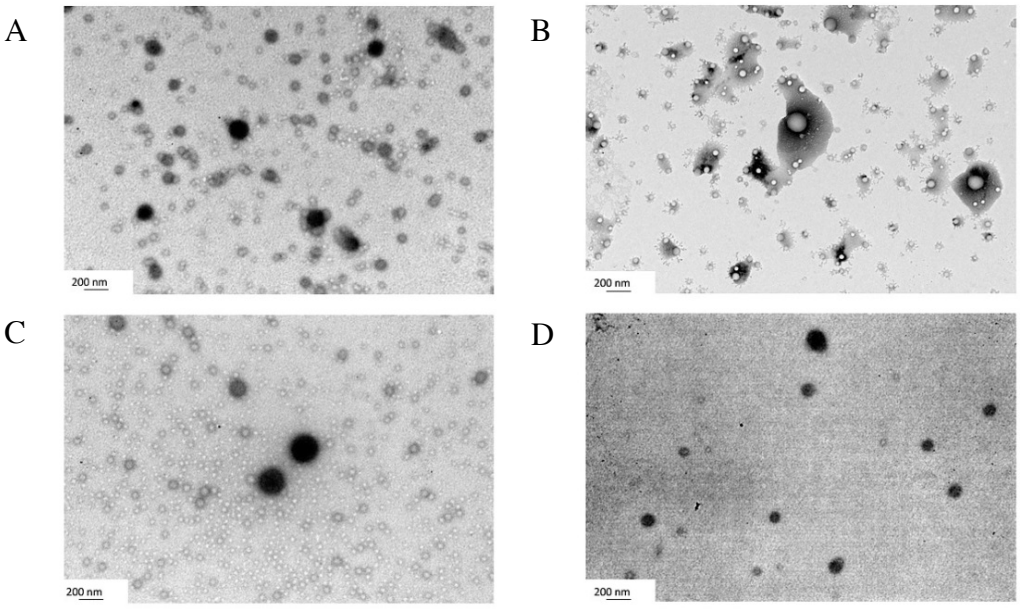

Figure 2. TEM micrographs of (A-C) unloaded NPs and (B-D) NPs-CLZ before (A, B) and after (C, D) freeze-drying process.

3.5.2 Fourier transform infrared spectroscopy studies

The FTIR spectra of CLZ, PM, unloaded-NPs and NPs-CLZ are shown in Figure 3. The spectra of both NPs and NPs-CLZ showed a broader characteristic peak of PLGA at 1750 cm^{-1}, compared to the PM, which are indicative of C = O stretching. This phenomenon could be explained by intermolecular interaction of the nanoparticles constituents in both systems. Moreover, the spectrum of PM evidences characteristics peaks of CLZ namely bands of N–H bending frequency at 1550–1620 cm^{-1}, and C=N stretching at 1625 cm^{-1} [9]. These peaks could not be seen in NPs-CLZ spectrum probably due to the amorphous state of entrapped CLZ as their intensity may be decreased and/or overlapped by others belonging to the major constituents of NPs-CLZ. Overall, no strong chemical interaction was found between CLZ and other nanoparticles' constituents as unknown peaks were not found in the spectra. Thus, all the components of the formulation are compatible.

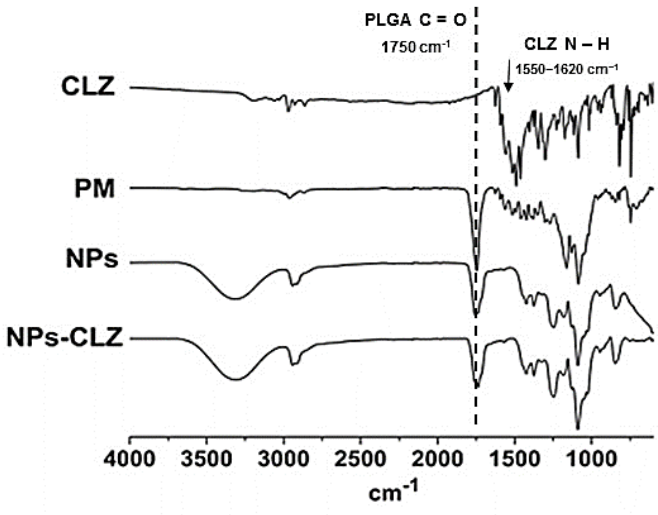

Figure 3. FTIR spectra of CLZ, physical mixture of bulk PLGA and CLZ (PM), unloaded-NPs and NP-CLZ.

3.5.3 Differential scanning calorimetry studies

The DSC thermograms of CLZ, PLGA, PVA, PM, unloaded-NPs and NPs-CLZ are shown in Figure 4. The endothermic event of CLZ melting at 228°C was not observed in NPs-CLZ, suggests that CLZ is entrapped in an amorphous form within the polymeric nanoparticle. Moreover, the thermograms of unloaded-NPs and NPs-CLZ were identical, evidencing that CLZ did not interacted with the formulation constituents.

The PM was performed with the presence of PVA to confirm the origin of any event present in load and unloaded NPs around the phase transition of CLZ (224°C). The thermogram of PM evidences an endothermic peak at 51°C corresponding to the glass transition of PLGA, and a discrete event in 224°C related to the melting of CLZ, suggesting that the formulation process interfered on physical state CLZ, shifting from crystalline to amorphous form, as in NPs-CLZ no endothermic event was found around 224°C. Furthermore, the event related to the phase transition of PVA at 180°C is evident in PM, unloaded-NPs and NPs-CLZ.

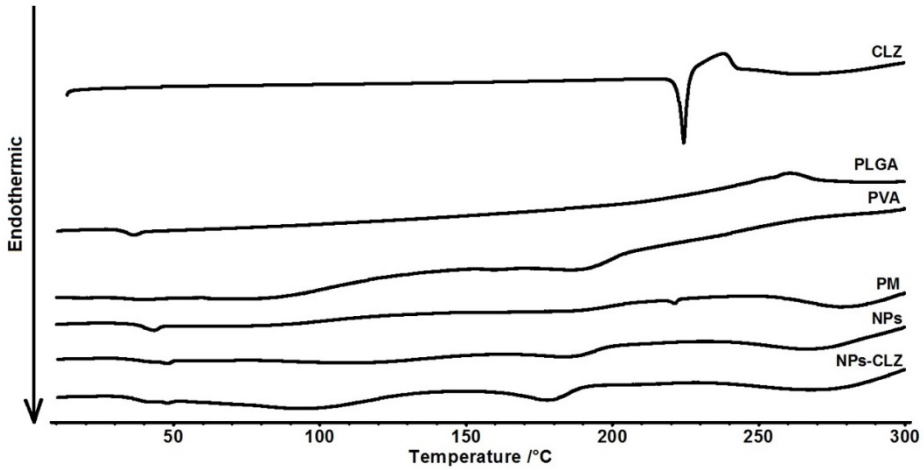

Figure 4. DSC thermograms of CLZ, PLGA, PVA, physical mixtures (PM) and unloaded (NPs) and loaded (NPs-CLZ) nanoparticles.

3.5.4 *In vitro* drug release

The *in vitro* drug release profile of CLZ from NPs-CLZ is show in Figure 5. To simulate the conditions at the small intestine, the experiment was conducted in a buffered solution pH 6.8 for 8 h [37]. The CLZ release profile from the NPs-CLZ is low and controlled reaching about 30 % of released drug at the end of the experiment.

As already reported, drug release from a PLGA matrix depends dramatically on the degradation rate of the PLGA chains, and involves mainly two steps. The first one involves an autocatalytic hydrolysis in the polymer backbone and formation of the relatively high-molecular oligomers, leading to the pores formation in the polymeric matrix. Further on, with the continuing of the scission of the polymeric chain the formation of lower molecular weight products takes place, and the formed oligomers and monomers become water-soluble, and the particle size and weight eventually also decrease [38]. Based on studies performed elsewhere [38, 39], the first step of hydrolytic degradation lasts for at least 24 h. Thus, the release profile of CLZ during 8 h

of incubation is probably determined by drug desorption/from the polymer matrix.
In parallel, the controlled release of CLZ from NPs may prevent drug recrystallization as supersaturated solutions are not formed that tend to change to a thermodynamically more stable system by precipitation of drug microcrystals [40].
Given described intracellular crystallization of CLZ, the release pattern observed may contribute to reduce this unwanted effect by avoiding drug recrystallization. Moreover, at the intestinal lumen, entrapped CLZ into PLGA nanoparticles may allow its absorption by the intestinal cells, avoiding its precipitation, leading to an improved bioavailability [37].

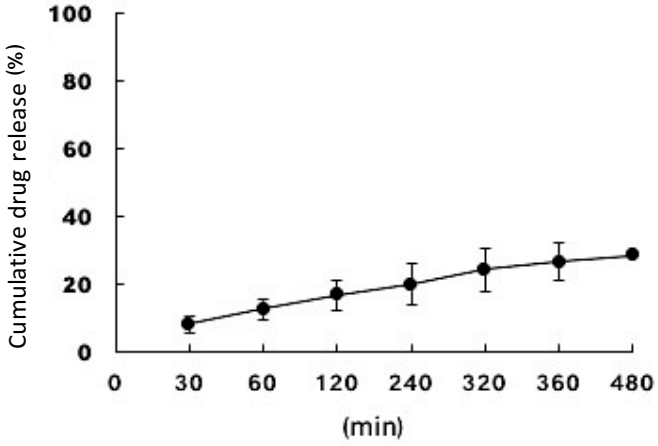

Figure 5 *In vitro* release profile of CLZ from NPs-CLZ in SDS solution (2%) at 37ºC.

3.6 *In vitro* cell viability studies

The developed NPs-CLZ is intended to oral delivery in leprosy therapy. Given the CLZ properties, namely its high hydrophobicity, difficulties may occur in the drug absorption due to drug precipitation at physiological pH, causing toxicity at the intestinal tissue. Thus, two cell lines were selected as models to mimic intestinal cell types, namely Caco-2 ant HT29-MTX [41, 42]. In order to evaluate NPs-CLZ cell viability in these cells, the studies were conducted with unloaded NPs, NPs-CLZ and CLZ as free drug. Different concentration of NPs-CLZ containing 6.26 – 50 μg mL^{-1} in CLZ the equivalent to 15.63 – 250 μg mL^{-1} in relation to the polymer were incubated during 24 h with Caco-2 and HT29-MTX (Figure 6).
Caco-2 cells exposed to unloaded nanoparticles maintained cell viability above 80%, with no statistical differences from the untreated cells. The presence of CLZ in the PLGA nanoparticles leads to a decrease on the cell viability, as the polymer itself did not produce any effect (Figure 6A). Similar results were found for HT29-MTX cell line (Figure 6B). NPs-CLZ led to cell viability around 70 ± 9% and 75 ± 6% for the highest

tested concentration, in Caco-2 and HT-29, respectively. For both the studied intestinal cell lines, the exposure to CLZ solutions lead to a significant reduction of cell viability, resulting in IC_{50} values 16.3 and 20.3 μg mL^{-1} for Caco-2 and HT29-MTX, respectively (Figure 6). In fact, the high toxicity of CLZ has been already reported [43]. Upon prolonged oral administration CLZ seems to form intracellular insoluble drug precipitates, leading to high concentration bioaccumulation, being easily associated with unwanted side effects as reddish skin pigmentation, abdominal pain and cardiotoxicity [6].

In this work, the incorporation of CLZ within the PLGA nanoparticles prevented the drug toxicity effect on the intestinal cells up to 24 h. Taken the results obtained, the encapsulation of CLZ in NPs-CLZ may prevent drug crystallization and the formation of such precipitates *in vivo*, as they are entrapped in its amorphous form. Thus, the formulations have potential to delivery CLZ and decrease the undesired effect, by preventing cells from the drug toxicity.

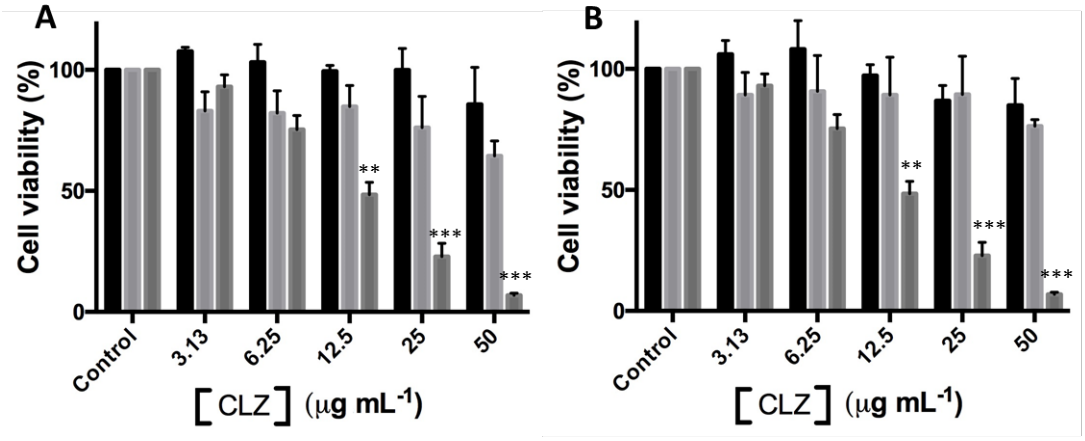

Figure 6. Cell viability of the intestinal cells exposed to the unloaded-NPs (black bar), NPs-CLZ (light grey bar) and free CLZ (dark grey bar) assessed by the MTT assay. The viability of Caco-2 (A), HT29-MTX (B) cells after 24 h incubation with different CLZ concentrations (and equivalent NPs) at 37°C. Data expressed as the average ± standard deviation (n=5, of three different assays). $^{**}p < 0.01$ and $^{***}p < 0.001$ in relation to control cells.

3.7 CLZ permeation across Caco-2 monolayers

The *in vitro* bioassay with Caco-2 cells monolayer has been widely used as model to predict drug permeability and have been well correlated with *in vivo* absorptions in humans [41]. Therefore, Caco-2 monolayer assay was conducted to analyze the permeability of CLZ as loaded in NPs-CLZ. The tested concentrations were selected

according to the cytotoxicity assays, which was 40 μg mL^{-1} of CLZ equivalent to 200 μg mL^{-1} in polymer concentration in the NPs-CLZ formulations. Free CLZ was not included in the intestinal permeability assay due to its toxicity towards Caco-2 cells (Figure 6A).

The cells monolayer integrity was evaluated by TEER measurements throughout the experiments, and no cellular lesion which changes TEER values was detected (data not shown). Initial TEER values were higher than 400 Ωcm^2 in the beginning of the experiment, as recommended for absorption studies [44]. The addition of the studied samples did not affect these values until the end of the experiment (8 h).

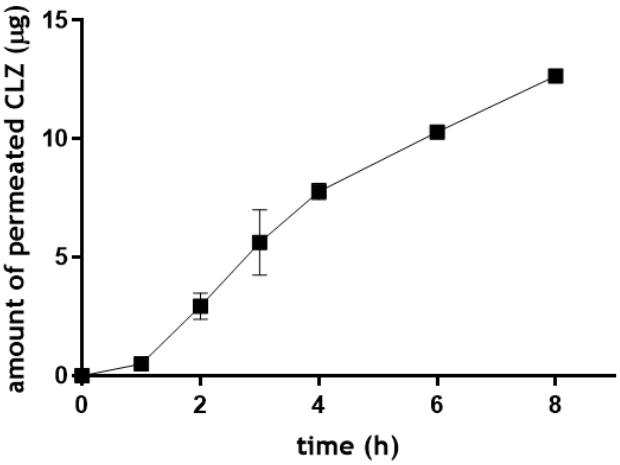

Figure 7. *In vitro* CLZ permeation across Caco-2 monolayers. Amount of permeated CLZ as NPs-CLZ for 8 h. The experiments were conducted from the apical-to-basolateral direction in culture medium at 37 °C. Error bars represent mean ± s.d. (n ≥ 3).

The permeation trend of CLZ as NPs-CLZ across Caco-2 intestinal monolayer is shown in Figure 7. About 12 μg of permeated CLZ was detected at the basolateral chamber, after incubation with NPs-CLZ, representing about 25% of the initial amount. This outcome is similar to the observed in the *in vitro* release studies, as the polymeric matrix slowly diffused CLZ reaching ca. 30 % of drug released within 8 h. Besides the low water solubility of CLZ may also contribute to the low drug amounts quantified at the basolateral chamber of the Caco-2 monolayer. The Papp value for CLZ when incorporated within NPs-CLZ was 3.8± 0.2 x 10^{-6} (cm s^{-1}). The developed NPs-CLZ allowed to assess CLZ intestinal permeability, due to their protector behavior which can be considered an important achievement taking due to the high toxicity of CLZ.

Peak plasma concentrations CLZ were found 8 h after administration. Reports describe concentrations of 0.41 μg mL-1 for CLZ upon 200 mg, thus, NPs-CLZ were able to reach suitable concentration after intestinal permeation, to achieve the intended therapeutic effect [3].

4. Conclusions

In this study, NPs-CLZ were successfully developed and characterized after the identification of critical variables through PBD. The volume of aqueous phase, amount of polymer and the amount of drug were found to be the most significant variables that affected the selected responses namely particle diameter, PDI, AE and DL.

The selected formulation was achieved based on the desirability tool and satisfactory responses regarding particle size (around 200 nm), PDI below 0.3, and feasible AE and DL considering the oral route. FTIR revealed the absence of interactions between CLZ and the other constituents of the formulation; while, DSC evidenced the amorphous characteristic of entrapped CLZ. The polymeric nanoparticles had a spherical morphology. The *in vitro* drug release revealed the sustained pattern of CLZ released from NPs-CLZ upon 8 h under simulated intestinal conditions. The controlled release of CLZ is a promising strategy to overcome its recrystallization at the intestinal lumen and intracellularly avoiding the formation of supersaturated solutions.

In vitro cytotoxicity studies evidenced that the obtained NPs-CLZ prevent the toxic effect of free CLZ, that presented IC_{50} values of 16.3 and 20.3 μg mL^{-1} for Caco-2 and HT29-MTX cells, respectively. In fact, the entrapment of drugs into nanoparticles at their amorphous form may prevent drug precipitation, which is, in the case of CLZ, associated with the formation of intracellular crystal aggregation and correlated with the undesired and toxicological effects. CLZ permeated the Caco-2 cells monolayer as when entrapped in the PLGA nanoparticles, reaching about 25% of the initial added amount. Given the controlled drug release from the NPs-CLZ, a longer time may be required for the CLZ permeate the Caco-2 monolayer at a higher extent.

Based on the obtained results, it can be concluded that the obtained system could be properly designed considering the important variables for poorly soluble drugs. NPs-CLZ represents a promising platform for the oral delivery of CLZ.

Acknowledgments

This work received financial support from the European Union (FEDER funds) and National Funds (FCT/MEC, Fundação para a Ciência e Tecnologia and Ministério da Educação e Ciência) under the Partnership Agreement PT2020

UID/MULTI/04378/2013 - POCI/01/0145/FEDER/007728 and funds through the COMPETE 2020 - Operational Programme for Competitiveness and Internationalisation (POCI), Portugal 2020, and by Portuguese funds through FCT - Fundação para a Ciência e a Tecnologia/ Ministério da Ciência, Tecnologia e Inovação in the framework of the projects "Institute for Research and Innovation in Health Sciences" (POCI-01-0145-FEDER-007274). SCL thanks Operação NORTE-01-0145-FEDER-000011 for her Investigator contract . The authors also thank the CNPq and CAPES Foundation, Ministry of Education of Brazil for the Doctoral fellowships 246514/2012-4 and 0831-12-3 respectively,and FCT for the Post-Doctoral fellowship SFRH/BPD/99124/2013.

5. References

1. Chaves, L., et al., *Rational and precise development of amorphous polymeric systems with dapsone by response surface methodology*. Int J Biol Macromol, 2015. **81**: p. 662-71.
2. Matsuoka, M., *Drug resistance in leprosy*. Jpn J Infect Dis, 2010. **63**(1): p. 1-7.
3. Cholo, M.C., et al., *Clofazimine: current status and future prospects*. J Antimicrob Chemother, 2012. **67**(2): p. 290-8.
4. Salem, II, G. Steffan, and N. Duzgunes, *Efficacy of clofazimine-modified cyclodextrin against Mycobacterium avium complex in human macrophages*. Int J Pharm, 2003. **260**(1): p. 105-14.
5. Bannigan, P., et al., *Investigation into the Solid and Solution Properties of Known and Novel Polymorphs of the Antimicrobial Molecule Clofazimine*. Cryst Growth Des , 2016. **16**(12): p. 7240-7250.
6. Li, S., et al., *Complexation of clofazimine by macrocyclic cucurbit[7]uril reduced its cardiotoxicity without affecting the antimycobacterial efficacy*. Org Biomol Chem, 2016. **14**(31): p. 7563-9.
7. Yoon, G.S., et al., *Phagocytosed Clofazimine Biocrystals Can Modulate Innate Immune Signaling by Inhibiting TNFalpha and Boosting IL-1RA Secretion*. Mol Pharm, 2015. **12**(7): p. 2517-27.
8. Baik, J. and G.R. Rosania, *Macrophages sequester clofazimine in an intracellular liquid crystal-like supramolecular organization*. PLoS One, 2012. **7**(10): p. e47494.
9. Bolla, G. and A. Nangia, *Clofazimine Mesylate: A High Solubility Stable Salt*. Cryst Growth Des , 2012. **12**(12): p. 6250-6259.
10. Hernandez-Valdepena, I., et al., *Nanoaggregates of a random amphiphilic polyanion to carry water-insoluble clofazimine in neutral aqueous media*. Eur J Pharm Sci, 2009. **36**(2-3): p. 345-51.
11. Nie, H., et al., *Solid-State Spectroscopic Investigation of Molecular Interactions between Clofazimine and Hypromellose Phthalate in Amorphous Solid Dispersions*. Mol Pharm, 2016. **13**(11): p. 3964-3975.

12. O'Reilly, J., O. Corrigan, and C. O'Driscoll, *The effect of mixed micellar systems, bile salt/fatty acids, on the solubility and intestinal absorption of clofazimine (B663) in the anaesthetised rat*. Int JPharm, 1994. **109**(2): p. 147-154.

13. Patel, V.B. and A.N. Misra, *Encapsulation and stability of clofazimine liposomes*. J Microencapsul, 1999. **16**(3): p. 357-67.

14. Peters, K., et al., *Preparation of a clofazimine nanosuspension for intravenous use and evaluation of its therapeutic efficacy in murine Mycobacterium avium infection*. J Antimicrob Chemother, 2000. **45**(1): p. 77-83.

15. Sharma, P. and S. Garg, *Pure drug and polymer based nanotechnologies for the improved solubility, stability, bioavailability and targeting of anti-HIV drugs*. Adv Drug Deliv Rev, 2010. **62**(4-5): p. 491-502.

16. Chaves, L., et al., *Nanocarriers as strategy for oral bioavailability improvement of poorly water-soluble drugs*, in *Nanoparticles in the Life Sciences and Biomedicine*, A. Neves and S. Reis, Editors. 2017, Pan Stanford Publishing.

17. Cooper, D.L. and S. Harirforoosh, *Design and optimization of PLGA-based diclofenac loaded nanoparticles*. PLoS One, 2014. **9**(1): p. e87326.

18. Kumari, A., S.K. Yadav, and S.C. Yadav, *Biodegradable polymeric nanoparticles based drug delivery systems*. Colloids Surf B , 2010. **75**(1): p. 1-18.

19. Sharma, S., et al., *PLGA-based nanoparticles: A new paradigm in biomedical applications*. Trends Anal Chem TrAC, 2016. **80**: p. 30-40.

20. Costa Lima, S. and S. Reis, *Temperature-responsive polymeric nanospheres containing methotrexate and gold nanoparticles: A multi-drug system for theranostic in rheumatoid arthritis*. Colloids Surf B , 2015. **133**: p. 378-87.

21. Rahman, Z., et al., *Understanding the quality of protein loaded PLGA nanoparticles variability by Plackett-Burman design*. Int J Pharm, 2010. **389**(1-2): p. 186-94.

22. Akl, M.A., et al., *Factorial design formulation optimization and in vitro characterization of curcumin-loaded PLGA nanoparticles for colon delivery*. J Drug Deliv Sci Technol, 2016. **32**: p. 10-20.

23. Haggag, Y., et al., *Preparation and in vivo evaluation of insulin-loaded biodegradable nanoparticles prepared from diblock copolymers of PLGA and PEG*. Int J Pharm, 2016. **499**(1-2): p. 236-46.

24. Ray, S., S. Ghosh, and S. Mandal, *Development of bicalutamide-loaded PLGA nanoparticles: preparation, characterization and in-vitro evaluation for the treatment of prostate cancer*. Artificial Cells, Nanomedicine, and Biotechnology, 2016: p. 1-11.

25. Spinks, C.B., et al., *Pharmaceutical characterization of novel tenofovir liposomal formulations for enhanced oral drug delivery: in vitro pharmaceutics and Caco-2 permeability investigations*. Clinical Pharmacology : Advances and Applications, 2017. **9**: p. 29-38.

26. Beduneau, A., et al., *A tunable Caco-2/HT29-MTX co-culture model mimicking variable permeabilities of the human intestine obtained by an original seeding procedure*. Eur J Pharm Biopharm, 2014. **87**(2): p. 290-8.

27. Woitiski, C.B., et al., *Facilitated nanoscale delivery of insulin across intestinal membrane models*. Int J Pharm, 2011. **412**(1-2): p. 123-31.

28. Dhat, S., et al., *Risk management and statistical multivariate analysis approach for design and optimization of satranidazole nanoparticles*. Eur J Pharm Sci, 2017. **96**: p. 273-283.

29. Shah, S.R., et al., *Application of Plackett–Burman screening design for preparing glibenclamide nanoparticles for dissolution enhancement*. Powder Technol, 2013. **235**: p. 405-411.

30. Zazo, H., C.I. Colino, and J.M. Lanao, *Current applications of nanoparticles in infectious diseases*. J Control Release, 2016. **224**: p. 86-102.

31. Alshamsan, A., *Nanoprecipitation is more efficient than emulsion solvent evaporation method to encapsulate cucurbitacin I in PLGA nanoparticles*. Saudi Pharmaceutical Journal, 2014. **22**(3): p. 219-222.

32. Cao, W., et al., *Optimization of peptic hydrolysis parameters for the production of angiotensin I-converting enzyme inhibitory hydrolysate from Acetes chinensis through Plackett-Burman and response surface methodological approaches*. J Sci Food Agric, 2012. **92**(1): p. 42-8.

33. Shah, S.R., et al., *Application of Plackett-Burman screening design for preparing glibenclamide nanoparticles for dissolution enhancement*. Powder Technol, 2013. **235**: p. 405-411.

34. Budhian, A., S.J. Siegel, and K.I. Winey, *Haloperidol-loaded PLGA nanoparticles: systematic study of particle size and drug content*. Int J Pharm, 2007. **336**(2): p. 367-75.

35. Reix, N., et al., *In vitro uptake evaluation in Caco-2 cells and in vivo results in diabetic rats of insulin-loaded PLGA nanoparticles*. Int J Pharm, 2012. **437**(1-2): p. 213-20.

36. Desai, M.P., et al., *The Mechanism of Uptake of Biodegradable Microparticles in Caco-2 Cells Is Size Dependent*. Pharmaceutical Research, 1997. **14**(11): p. 1568-1573.

37. Izadifar, M., et al., *Optimization of nanoparticles for cardiovascular tissue engineering*. Nanotechnology, 2015. **26**(23): p. 235301.

38. Chairez-Ramirez, M.H., et al., *Morphological and release characterization of nanoparticles formulated with poly (dl-lactide-co-glycolide) (PLGA) and lupeol: In vitro permeability and modulator effect on NF-kappaB in Caco-2 cell system stimulated with TNF-alpha*. Food Chem Toxicol, 2015. **85**: p. 2-9.

39. Amekyeh, H., et al., *A gastrointestinal transit study on amphotericin B-loaded solid lipid nanoparticles in rats*. AAPS PharmSciTech, 2015. **16**(4): p. 871-7.

40. Malinovskaya, J., et al., *Delivery of doxorubicin-loaded PLGA nanoparticles into U87 human glioblastoma cells*. Int J Pharm, 2017.

41. Mohammad, A.K. and J.J. Reineke, *Quantitative detection of PLGA nanoparticle degradation in tissues following intravenous administration*. Molecular pharmaceutics, 2013. **10**(6): p. 2183-2189.

42. Müller, R.H., et al., *Oral bioavailability of cyclosporine: Solid lipid nanoparticles (SLN®) versus drug nanocrystals*. International Journal of Pharmaceutics, 2006. **317**(1): p. 82-89.

43. Araujo, F. and B. Sarmento, *Towards the characterization of an in vitro triple co-culture intestine cell model for permeability studies*. Int J Pharm, 2013. **458**(1): p. 128-34.

44. Fernandes, I., et al., *A new approach on the gastric absorption of anthocyanins*. Food Funct, 2012. **3**(5): p. 508-16.

45. Arbiser, J.L. and S.L. Moschella, *Clofazimine: a review of its medical uses and mechanisms of action*. J Am Acad Dermatol, 1995. **32**(2 Pt 1): p. 241-7.

46. Freichels, H., et al., *Targeting nanoparticles to M cells with non-peptidic ligands for oral vaccination*. Eur J Pharm Biopharm, 2009. **73**(1): p. 16-24.

E. Polymeric nanosystems combination allows dapsone and clofazimine intestinal permeation[7]

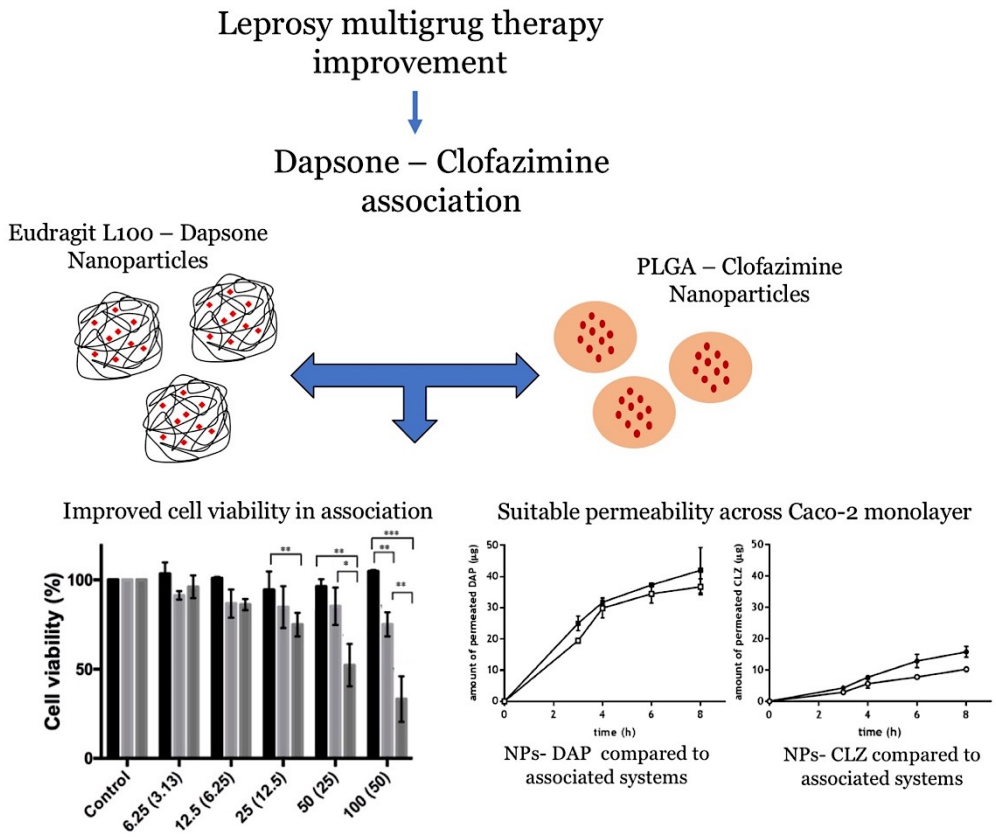

[7] In preparation

Polymeric nanosystems combination allows dapsone and clofazemine intestinal permeation

Luíse L. Chaves[a], Sofia A. Costa Lima[a,b], Alexandre C.C.Vieira[a], Luísa Barreiros[a], Marcela A. Segundo[a], Domingos Ferreira[c], Bruno Sarmento[b,d,e], Salette Reis[*a]

[a]UCIBIO, REQUIMTE, Departamento de Ciências Químicas, Faculdade de Farmácia, Universidade do Porto, Portugal
[b]CESPU, Instituto de Investigacão e Formacão Avançada em Ciências e Tecnologias da Saúde and Instituto Universitário de Ciências da Saúde, Portugal
[c]Laboratório de Tecnologia Farmacêutica, Departamento de Ciências do Medicamento, Faculdade de Farmácia, Universidade do Porto, Portugal
[d]I3S, Instituto de Investigacão e Inovacão em Saúde, Universidade do Porto, Portugal
[d]INEB – Instituto de Engenharia Biomédica, Universidade do Porto, Portugal

ABSTRACT

The aim of this work was to assess the feasibility of drug nanosystems combination for multibacillary leprosy oral therapy. The anti-leprotic drugs dapsone (DAP) and clofazimine (CLZ) were incorporated within polymeric nanosystems and studied *per se* and in combination. DAP was loaded in Eudragit L100 nanoparticles (NPs-DAP) while CLZ was loaded in (poly(lactic-co-glycolic acid) (NPs-CLZ). The nanosystems exhibited around 200 nm in size and a drug loading of 12% for both drugs. *In vitro* cytotoxicity on intestinal Caco-2 cells revealed that after 8 h incubation, DAP alone and within NPs were not toxic up to 100 μg mL^{-1}, while CLZ *per se* was toxic, reducing cell viability to 30% at 50 μg mL^{-1}. Caco-2 exposed to NPs-DAP/ NPs-CLZ combination at 100 and 50 μg mL^{-1}, respectively exhibited 80% viability. Caco-2 monolayer permeability assays revealed that DAP and CLZ in the nanosystems *per se* or in NPs-DAP/ NPs-CLZ combination crossed the intestinal barrier. No significant differences were observed between the single nanosystems or in combination for the apparent permeability values and the amount of permeated drug. Thus, the NPs-DAP/ NPs-CLZ combination seems to be a promising platform to deliver both drugs in association, representing an important step toward the improvement of multibacillary leprosy therapy.

Keywords: Caco-2 cells; Cytotoxicity; Eudragit L-100; Leprosy; PLGA

1. Introduction

Leprosy is a chronic and infectious disease caused by the *Mycobacterium leprae* that continues to be a significant issue of public health globally [1-3], being one of the most common causes of non-traumatic peripheral neuropathy [4]. For treatment purposes, the World Health Organization (WHO) suggests a simple scheme to categorize leprosy patients based on visible symptoms [5], as having paucibacillary (PB) leprosy (1-5 skin patches) or multibacillary (MB) leprosy (with > 5 skin patches) [5]. The actual recommended treatment for leprosy disease is based in a multidrug therapy (MDT), consisting of rifampicin, clofazimine (CLZ), and dapsone (DAP) to treat MB leprosy patients during 12 months, while rifampicin and DAP are used in PB leprosy patients during 6 months [5]. The rifampicin is monthly administered under supervision of healthy regional professionals, while DAP (alone or associated with CLZ) is daily administered without supervision [5].

The standardization of the MDT regarding time of treatment and therapeutic agents appears to be a trend in leprosy eradication program as these strategies may promote patient compliance and efficiency in patient management [6]. Thus, the daily administered drugs (DAP and CLZ) become the most important components of leprosy MDT [7]. On the other hand, the non-supervised administration may highlight the risk of antimicrobial resistance [7]. In this context, research in the leprosy therapy is still needed, and efforts must be done specially to improve delivery of drugs and patient compliance.

Despite their proven effectiveness, the therapeutic potential of DAP and CLZ is limited by their poor water solubility [8], leading to undesired bioavailability, which may compromise the success of MDT. In this context, it is of great relevance the development of new delivery strategies to both drugs in order to overcome these issues, and even improve leprosy therapy through drug association. Few works have reported new approaches to overcome the poor solubility of DAP [9] and CLZ [10]. In the literature, so far there is no report on the drug association through the combination of nanodelivery systems.

The aim of this work was to evaluate the biological properties of the combination of nanosystems containing MB anti-leprosy drugs, namely DAP and CLZ for oral delivery. The previously optimized nanosystems were combined according to MB therapy and assessed for cytotoxicity and permeability using an *in vitro* intestinal barrier model.

2. Materials and methods

2.1. Materials

DAP was purchased from CHEMOS GmbH (Regenstauf, Germany) and clofazimine (CLZ) from Hangzhou Heta Pharm & Chem Co. Pluronic® F-68 and polyvinyl alcohol (PVA) were adquired from Sigma–Aldrich (St. Louis, USA); poly(methacrylic acid-co-methyl methacrylate) 1:1 (Eudragit® L100) was obtained from Evonik Roehm GmbH, (Darmstadt, Germany). Ethanol was purchased from VWR chemicals (Carnaxide, Portugal) and acetone from JGMS (Odivelas, Portugal). Poly (lactic-co-glycolic acid) (PLGA) (50:50 Purasorb® PDLG 5002A) was a kind gift from Purac Biomaterials (Gorinchem, The Netherlands). Caco-2 cell line was obtained from the American Type Culture Collection (ATCC, Wesel, Germany) (passage number 35 - 55) and HT29-MTX cell line was kindly provided by Dr. T. Lesuffleur (INSERM U178, Villejuif, France). Dulbecco's Modified Eagle Medium (DMEM), fetal bovine serum (FBS, South America origin), penicillin-streptomycin mixture (Pen-Strep) and trypsin-EDTA 0.25% (w/v) were all obtained from Gibco (Paisley, UK).

2.2. Methods

2.2.1. Nanoparticles preparation and characterization

Dapsone-loaded nanoparticles (NPs-DAP) were produced with Eudragit L100 (EL100) polymer via the nanoprecipitation method, previously described [11, 12], with slight modifications. Briefly, known amounts of EL100 and DAP were co-dissolved in 3 mL of ethanol-acetone (1:1) mixture. The organic solution was subsequently slowly dripped (0.5 mL min^{-1}) in the 10 mL of PVA 1% (w/v) solution previous acidified to pH 3. The final solution was maintained under magnetic stirring at 350 rpm (RT 15 Power IKAMAG Multiposition Magnetic Stirrer, Staufen, Germany) and room temperature until complete solvent diffusion. Unloaded nanoparticles (EL100 NPs) were obtained for the selected formulation, following the same procedure. Freshly prepared nanosuspensions were used to perform cells assays.

CLZ nanoparticles were prepared using PLGA (NPs-CLZ) also following nanoprecipitation method [11, 12]. Briefly, 20 mg of PLGA and 2 mg of CLZ were dissolved in 3 mL acetone, which was slowly added to 5 mL of PVA 1% (w/v) solution under probe sonication, during 2 min, with an amplitude of 70%. A PVA solution (0.1% w/v) was then used as stabilizer. The final emulsion was maintained under magnetic stirring (RT 15 Power IKAMAG

Multiposition Magnetic Stirrer, Staufen, Germany) at 350 rpm and room temperature. Unloaded nanoparticles (PLGA NPs) were obtained for the selected formulation, following the same procedure.

The nanoparticles were characterized regarding mean particle size using a ZetaPALS, Zeta Potential Analyzer (Brookhaven Instrument Corps, Holtsville, NY, USA), with a light incidence angle of 90º at 25ºC and the obtained value represent multiple runs (n=6). The quantification of DAP and CLZ within the nanoparticles was carried out by determining the unentrapped drug separated by centrifugation (11,200 x*g* for 30 min). For the quantification of CLZ, NPs-CLZ samples were properly diluted with sodium dodecyl sulphate (SDS) 2% (w/v) so that the maximum concentration of CLZ did not exceed 100 μg mL^{-1}. The supernatant was read at 492 nm by UV-VIS spectroscopy (Jasco V-660, Easton, MD, USA). For the quantification of DAP, NPs-DAP were diluted 5 times with acidified ultrapure water (pH 3) and then centrifuged (11,200 x*g* for 30 min). Absorbance of supernatant was measured at 391 nm. Association efficiency (AE) and drug loading (DL) were calculated following the equations:

$$AE = \frac{initial\ amount\ of\ drug - recovered\ drug}{initial\ amount\ of\ drug} \times 100$$

$$DL = \frac{initial\ amount\ of\ drug - recovered\ drug}{initial\ amount\ of\ drug + initial\ amount\ of\ polymer} \times 100$$

2.2.2. Cell culture studies

Caco-2 and HT29-MTX cells were cultured in DMEM supplemented with 10% (v/v) of FBS and 1% (v/v) of penicillin-streptomycin. Cells were grown in a humidified incubator at 37 ºC and 5% CO_2 atmosphere and 95% relative humidity. When reaching 80% confluence, cells were detached using trypsinization.

2.2.2.1. *In vitro* cell viability assessment

The cell viability of unloaded nanoparticles (EL100-NPs and PLGA-NPs), NPs-DAP, NPs-CLZ, and free drugs (DAP and CLZ) was evaluated in Caco-2 cell lines. The method used was the 3-(4, 5-dimethylthiazol-2-yl)-2,5-diphenyltetrazolium bromide (MTT) colorimetric assay. The cells were incubated with 100 μL of culture media containing different concentrations of EL100-NPs, PLGA-NPs, NPs-CLZ, NPs-DAP and free drugs, namely for DAP 12.5 – 100.0 μg mL^{-1} and for CLZ 6.3 – 50.0 μg mL^{-1}, equivalent dosage. For drug association (DAP/ CLZ) the ratio DAP:CLZ (2:1) was selected based on the daily

administered dosage in MB leprosy treatment. After 8 h incubation, the supernatant was removed and replaced by 100 µL of MTT solution (0.5 mg mL^{-1}). The formazan crystals were dissolved with dimethyl sulphoxide and then the optical density of the solution was measured at a wavelength of 570 and 630 nm using Synergy™ HT Multi-mode microplate reader (BioTek Instruments Inc., Winooski, VT, USA). Untreated cells were taken as positive control with 100% viability. Three independent MTT assays were performed with quadruplicate samples each and results were expressed as mean values ± standard deviation. The cell viability (%) in relation to control cells (untreated cells) was calculated by the equation:

$$Cell\ viability\ (\%) = \frac{[A]570-630\ cells\ incubated\ with\ formulation}{[A]570-630\ cells\ incubated\ with\ culture\ medium} \times 100$$

2.2.2.2 Permeation studies using *Caco-2* monolayers

For the permeability studies, Caco-2 cells were seeded on 12-well Transwell inserts (Corning Transwell Clear, pore size 3 µm, area 0.33 cm^2) at a cell density of 10^5 cells per cm. The cells were grown in DMEM supplemented with FBS, during 21-23 days, until the monolayer achieved suitable initial transepithelial electrical resistance (TEER) values. The TEER at the beginning of these studies was higher than 400 Ω cm^2, indicating an intact monolayer; TEER values were also obtained after completion of flux experiments at 8 h. The resistance measurement of the medium without cells was considered as blank. The permeability was carried out by adding 0.5 mL of culture medium containing the equivalent of 80 µg mL^{-1} of DAP (as NPs-DAP), 40 µg mL^{-1} of CLZ (as NPs-CLZ), or the combination NPs-DAP/ NPs-CLZ (80 µg mL^{-1}/ 40 µg mL^{-1}) in the apical side of the cell monolayer. The samples were incubated for 8 h, and at predetermined time intervals (1, 2, 3, 4, 6 and 8 h), 0.5 mL were sampled from the basolateral compartment and replaced with fresh culture medium. The amount of DAP and CLZ in the samples was quantified by HPLC. The experiments were carried out in triplicate. The cumulative amounts of DAP, CLZ and DAP/ CLZ that permeated the monolayers were calculated from the concentrations measured in the basolateral compartment. The apparent permeability (Papp) was calculated following the equation:

$$Apparent\ permeability\ (Papp) = \frac{dQ}{dt} \times \frac{1}{A \times C_0}$$

where, *Papp* is the apparent permeability coefficient (cm s^{-1}), *dQ/dt* is the linear appearance rate of the compound on the receiver end based on its cumulative transport

for 8 h (μg s^{-1}), *A* is the surface area of the cell monolayer (cm) and C_o is the initial concentration of compound in the donor chamber (μg mL^{-1}).

2.2.3. Dapsone and clofazimine determination by high-performance liquid chromatography

The quantification of DAP, CLZ and the DAP/ CLZ association in the permeability studies samples was performed by high-performance liquid chromatography (HPLC) with UV detection. The HPLC system (Jasco) comprised a high-pressure pump (PU-2089), an autosampler (AS-2057) and a diode array detector (MD-2015) programmed for peak detection at 280 nm, controlled by ChromNAV software. A reversed phase Kinetex® core-shell C18 column (250 x 4.1 mm, 5 μm particle size, 100 Å; Phenomenex, Torrance, CA, USA) was used as stationary phase. Elution was performed in gradient mode using as mobile phase a mixture of aqueous acetate buffer (final concentration 50 mM, pH 4.8) and acetonitrile, at a flow rate of 1 mL min^{-1}. The selected gradient started with 30% (v/v) of acetonitrile, which was maintained up to 3 min. From 3 to 5.5 min, the contribution of acetonitrile was rapidly changed to 80% (v/v). This composition was maintained up to 7.5 min, after which the initial conditions were re-established and held during 5.5 min more to assure column equilibration. Hence, the total run time was 13 min. The injection volume was 20 μL. Standard solutions for both drugs were prepared at 0.5, 1, 2.5, 5, 7.5, 10, 15 and 20 μg mL^{-1} in culture medium containing 40% (v/v) of acetonitrile and 50 mM acetate buffer, pH 4.8. To prepare the samples for HPLC analyses, 200 μL of each sample was added to 160 μL of acetonitrile and 40 μL of acetate buffer 500 mM, pH 4.8, to final concentrations of 40% (v/v) and 50 mM, respectively. The mixtures were vortexed and centrifuged at 18,000 × *g* for 10 min at room temperature. After centrifugation, supernatants were collected and analyzed by HPLC.

3.3 Statistical analyses

The statistical analysis was performed using GraphPad Prism software (version 6, GraphPad Software, La Jolla, CA, USA) for statistical comparisons of the results to control for the cell viability studies. Statistical analysis of the results was performed using student (unpaired) t-test and one-way ANOVA test. All the other results were presented as mean and standard deviation (SD). The differences were assumed statistical significant when $p < 0.05$ (95% confidence level).

3. Results and discussion

3.1. Nanoparticles characterization

Nanoparticles with diameter close to 200 nm have an improved uptake by the intestinal tissue when compared to larger particles [13]. The previously optimized nanosystems were characterized regarding particle size, AE and DL. The mean of particle size for NPs-DAP was 198 ± 6 nm and no statistical differences between load and unloaded nanoparticles were found (p<0.05). The AE and DL were 48 ± 4% and 12 ± 1% respectively. As for NPs-CLZ AE and DL were 70 ± 5% and 12 ± 1%, respectively, and the mean particle size was 211 ± 3 nm and unloaded nanoparticles presented values of 175 ± 13 nm.

3.2. *In vitro* cell viability studies

The nanosystems were developed for oral administration in MB leprosy therapy. Given the limited physicochemical properties of DAP and CLZ specifically regarding their high hydrophobicity, difficulties may occur in the drug absorption due to drug precipitation at physiological pH, causing toxicity at the intestinal tissue. To mimic the intestinal absorption barrier Caco-2 cell line was selected as a model [14]. The daily administered doses are in a ratio of 2:1 DAP/ CLZ, thus the drug association assays were conducted in this proportion. The permeability assays studies were performed during 8 h, aiming to unravel the effect of drugs closer to real physiological conditions as the intestinal transit time. The tested concentrations ranged from 6.3 to 100.0 μg mL^{-1} for DAP, and from 3.1 to 50.0 μg mL^{-1} for CLZ as free drug and as loaded within the optimized nanosystems, wherein containing an equivalent polymer concentration between 12.5 to 200.0 μg mL^{-1} of EL100 or PLGA.

The effect of DAP/ CLZ association on the viability of intestinal cells was studied. Figure 1 depicts the cell viability of single DAP, CLZ and of the association DAP/ CLZ. DAP alone was not toxic up to 100 μg mL^{-1}, while single CLZ led to statistically significant differences compared to the untreated samples for the highest tested concentrations (12.5 to 50.0 μg mL^{-1}), in relation to the untreated control. Drug association at 2:1 ratio (DAP/ CLZ) reduced Caco-2 viability for the concentrations 25 to and 100 μg mL^{-1} of DAP, corresponding to 12.5 – 50 μg mL^{-1} of CLZ in relation to the control (untreated cells), resulting in cell viabilities between 75 and 33%. The decrease in Caco-2 viability observed with the drug association treatment was probably due to the presence of CLZ, as the same amount of single CLZ provided similar results. Moreover, statistical differences between DAP and DAP/ CLZ for the highest tested concentrations were found (Figure 1). In fact, it

has been described that upon prolonged oral administration CLZ forms intracellular insoluble drug precipitates, leading to bioaccumulation, which is associated with unwanted side effects as reddish skin pigmentation, abdominal pain and cardiotoxicity [10].

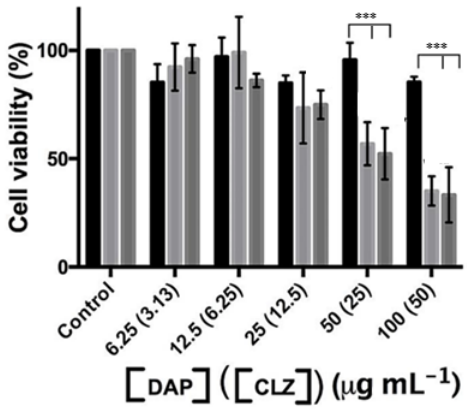

Figure 1. Cell viability of Caco-2 cells, assessed by the MTT assay, when exposed to DAP (black bar), CLZ (light grey bar) and DAP/ CLZ (2:1, dark grey bar) drug association upon 8 h of incubation. Data expressed as the average ± standard deviation (n=5, of three different assays). ***$p < 0.001$

The influence on cell viability of the drug association *per se* and in the developed nanosystems (NPs-DAP and NPs-CLZ) was also evaluated on the Caco-2 cell line. Figure 2 shows that 8 h incubation with NPs-DAP/ NPs-CLZ, at the highest studied concentrations, results in 75 ± 7 % cell viability, while equivalent dose of DAP/ CLZ association reduces significantly cell viability to 35%. The unloaded nanosystems do not exert any significant influence on the Caco-2 cells viability. Moreover, the loading of the drugs into polymeric nanosystems could overcome the reduction in cell viability found for free CLZ. Taken the obtained results, the nanosystems may prevent DAP/ CLZ association toxicity, most probably by preventing CLZ crystallization and the formation of CLZ precipitates. The combination of the nanosystems have the potential to deliver DAP/ CLZ association, and decreases the undesired toxic effect.

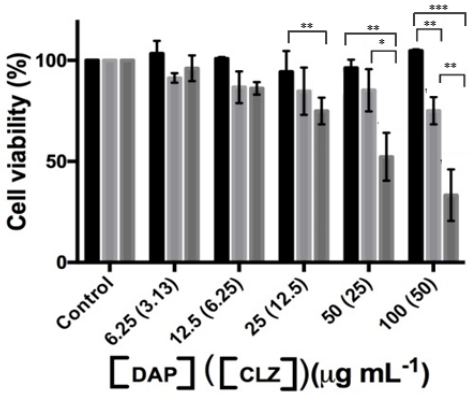

Figure 2. Cell viability of Caco-2 cells, upon 8 h exposure to unloaded NPs (black bar), NPs-DAP/ NPs-CLZ (light grey bar) and DAP/ CLZ (2:1, dark grey bar). Data expressed as the average ± standard deviation (n=5, of three different assays). $^{**}p < 0.01$; $^{***}p < 0.001$

3.3. Nanosystems permeation across Caco-2 monolayers

The *in vitro* bioassay with Caco-2 cells monolayer has been widely used as model to predict drug permeability and have been well correlated with *in vivo* absorptions in humans [14]. Therefore, Caco-2 monolayer assay was conducted to analyze the permeability of DAP and CLZ *per se* and in DAP/ CLZ association, using the developed polymeric nanoparticles. The cells monolayer integrity was evaluated by TEER measurements throughout the experiment (Table 1). It can be inferred that during the 8 h incubation with the developed nanosystems for DAP and CLZ *per se* and the NPs-DAP/ NPs-CLZ combination did not influence statistically the Caco-2 monolayer's integrity. The TEER values were higher than 400 Ωcm^2 in the beginning of the experiment, as recommended for absorption studies [15].

Table 1. TEER values prior, during and after Caco-2 permeation assays

	TEER values (Ohms cm^2)			
	Control	NPs-DAP	NPs-CLZ	NPs-DAP/ NPs-CLZ
0 h	455 ± 30	460 ± 25	460 ± 35	450 ± 25
4 h	480 ± 45	475 ± 30	480 ± 30	465 ± 35
8 h	470 ± 35	480 ± 40	475 ± 40	470 ± 30

Data expressed as mean ± standard deviation (n=3) and 3 independent measurements per well.

The permeation assessment of NPs-DAP and NPs-CLZ *per se* and in combination can be observed in Figure 3.

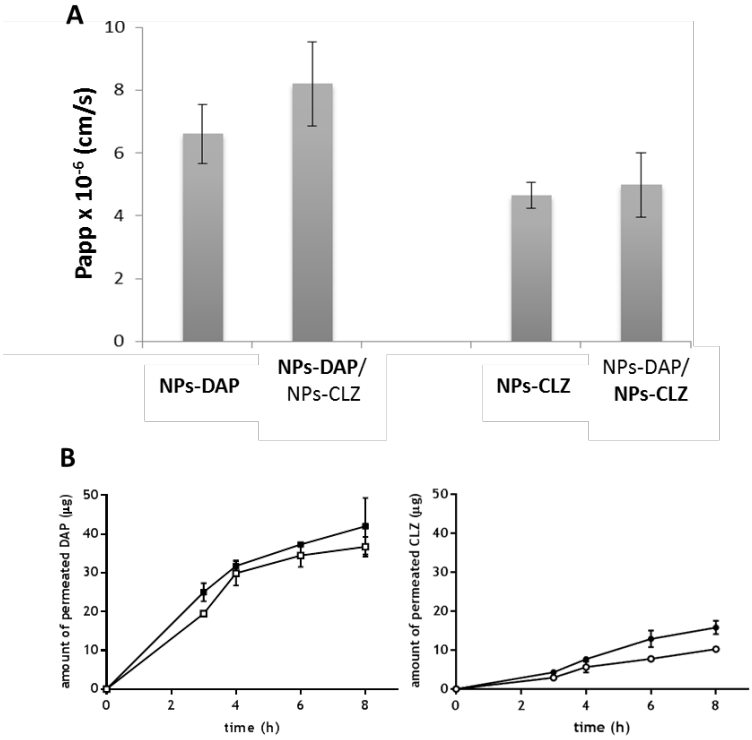

Figure 3. Effect of DAP and CLZ nanosystems on drug (A) apparent permeability (Papp, in relation to the drug in bold) and (B) permeation profile, through Caco-2 monolayer at 37°C. Different formulations were studied: NPs-DAP (open square), NPs-CLZ (open circle) and the association NPs-DAP/ NPs-CLZ (at 2:1, black square/ black circle). Data represents average ± standard deviation (n=3).

The combination of NPs-DAP and NPs-CLZ did not interfere with the Papp values nor the permeation profile of DAP and CLZ in comparison to each individual nanosystem. Due to the toxic effect observed with the free CLZ, the DAP/ CLZ drug association *per se* (Fig 2) was not evaluated in the permeation assay. About 40-50% of the initially added amount of drugs to the apical chamber reached the basolateral chamber after 8 h of exposure, accounting for ca. 40 µg DAP and ca. 15 µg CLZ. Considering the polymeric nature of the nanosystems and the 200-nm size it may be hypothesized that the NPs will interact with the Caco-2 cells through endocytic and transcytosis processes, which allow the drug permeation across the mimetic intestinal barrier [16].

Peak plasma concentrations for DAP and CLZ were found 8 h after administration. Reports describe concentrations of 0.41 µg mL^{-1} for CLZ upon 200 mg administration and 1.35 µg mL^{-1} for DAP after administration of 100 mg. Thus, the developed nanosystems

were able to reach suitable concentration *per se* or in combination after intestinal permeation, to achieve the intended therapeutic effect. Moreover, the ratio DAP/ CLZ adopted in MB leprosy treatment could be achieved as at the end of the assay, the ratio 2:1 was almost maintained.

4. Conclusions

This study demonstrates that DAP/ CLZ drug association delivered as polymeric nanosystems permeates the intestinal barrier. The *in vitro* cytotoxicity studies upon 8 h evidenced that DAP *per se* was not toxic towards Caco-2 cells, while CLZ decreased cell viability to 33%, at 50 μg mL^{-1}. DAP/ CLZ association was similarly toxic most probably due to the CLZ presence. The nanosystems combination did no exert any statistically significant toxic effects. The incorporation of DAP and CLZ into polymeric nanosystem provided good intestinal cell viability, compared to free drug association. Both drugs were able to permeate the intestinal barrier when incorporated in the nanosystems. The NPs-DAP/ NPs-CLZ combination exhibited similar behavior as each of the nanosystem in the Caco-2 permeability. The amount of permeated drugs is above the plasmatic concentration previously reported, which indicates the ability to reach the intended daily therapeutic dosage. Based on the obtained results, it can be concluded that polymeric nanosystems with DAP and CLZ in combination seem to be a promising platform to overcome the toxic effects and low patient compliance related to the actual MB leprosy treatment.

Acknowledgments

This work received financial support from the European Union (FEDER funds) and National Funds (FCT/MEC, Fundação para a Ciência e Tecnologia and Ministério da Educação e Ciência) under the Partnership Agreement PT2020 UID/MULTI/04378/2013 - POCI/01/0145/FEDER/007728. LLC thanks the CAPES Foundation, Ministry of Education of Brazil for the Doctoral fellowship 0831-12-3 and AV thanks the CNPq Foundation, Ministry of Education of Brazil for the Doctoral fellowship 246514/2012-4. SCL thanks Operação NORTE-01-0145-FEDER-000011 for her Investigator contract. LB thanks FCT/MEC and POPH (Programa Operacional Potencial Humano) for her Post-Doc grant (SFRH/BPD/89668/2012).

5. References

1. White, C. and C. Franco-Paredes, *Leprosy in the 21st century*. Clin Microbiol Rev, 2015. **28**(1): p. 80-94.

2. Virmond, M., A. Grzybowski, and L. Virmond, *Leprosy: a glossary*. Clin Dermatol, 2015. **33**(1): p. 8-18.

3. Nath, I., C. Saini, and V.L. Valluri, *Immunology of leprosy and diagnostic challenges*. Clin Dermatol, 2015. **33**(1): p. 90-8.

4. Bhat, R.M. and C. Prakash, *Leprosy: an overview of pathophysiology*. Interdiscip Perspect Infect Dis, 2012. **2012**: p. 181089.

5. World Health Organization. *Global Leprosy Programme*. 2017 March 7]; Available from: http://www.searo.who.int/entity/global_leprosy_programme/disease/en/.

6. Organization, W.H., *Weekly Epidemiological Record, 23 September 2016, vol. 91, 39 (pp. 441–460)*. 2016.

7. Prasad, P.V. and P.K. Kaviarasan, *Leprosy therapy, past and present: can we hope to eliminate it?* Indian J Dermatol, 2010. **55**(4): p. 316-24.

8. Islan, G.A., et al., *Nanopharmaceuticals as a solution to neglected diseases: Is it possible?* Acta Trop, 2017. **170**: p. 16-42.

9. Vieira, A.C., et al., *Design and statistical modeling of mannose-decorated dapsone-containing nanoparticles as a strategy of targeting intestinal M-cells*. Int J Nanomedicine, 2016. **11**: p. 2601-17.

10. Li, S., et al., *Complexation of clofazimine by macrocyclic cucurbit[7]uril reduced its cardiotoxicity without affecting the antimycobacterial efficacy*. Org Biomol Chem, 2016. **14**(31): p. 7563-9.

11. Dhat, S., et al., *Risk management and statistical multivariate analysis approach for design and optimization of satranidazole nanoparticles*. Eur J Pharm Sci, 2017. **96**: p. 273-283.

12. Costa Lima, S. and S. Reis, *Temperature-responsive polymeric nanospheres containing methotrexate and gold nanoparticles: A multi-drug system for theranostic in rheumatoid arthritis*. Colloids Surf B , 2015. **133**: p. 378-87.

13. Reix, N., et al., *In vitro uptake evaluation in Caco-2 cells and in vivo results in diabetic rats of insulin-loaded PLGA nanoparticles*. Int J Pharm, 2012. **437**(1-2): p. 213-20.

14. Araujo, F. and B. Sarmento, *Towards the characterization of an in vitro triple co-culture intestine cell model for permeability studies*. Int J Pharm, 2013. **458**(1): p. 128-34.

15. Fievez, V., et al., *Targeting nanoparticles to M cells with non-peptidic ligands for oral vaccination*. Eur J Pharm Biopharm, 2009. **73**(1): p. 16-24.

16. Talegaonkar, S., et al., *Microemulsions: a novel approach to enhanced drug delivery*. Recent Pat Drug Deliv Formul, 2008. **2**(3): p. 238-57.

F. Integrated Discussion

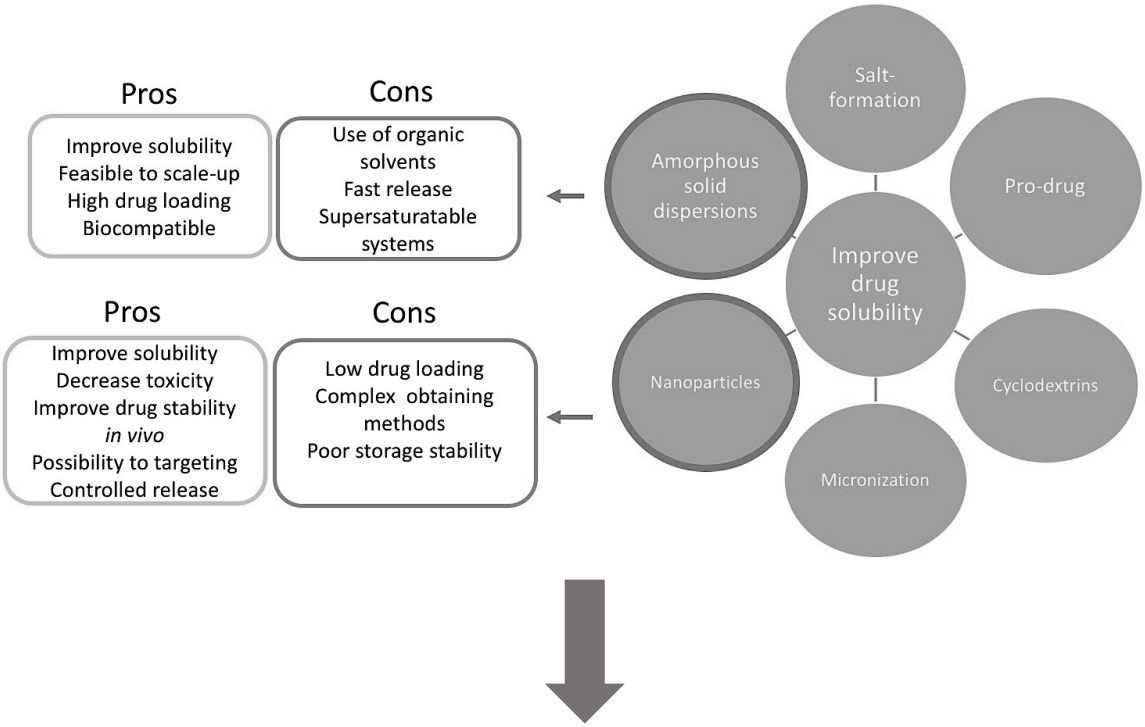

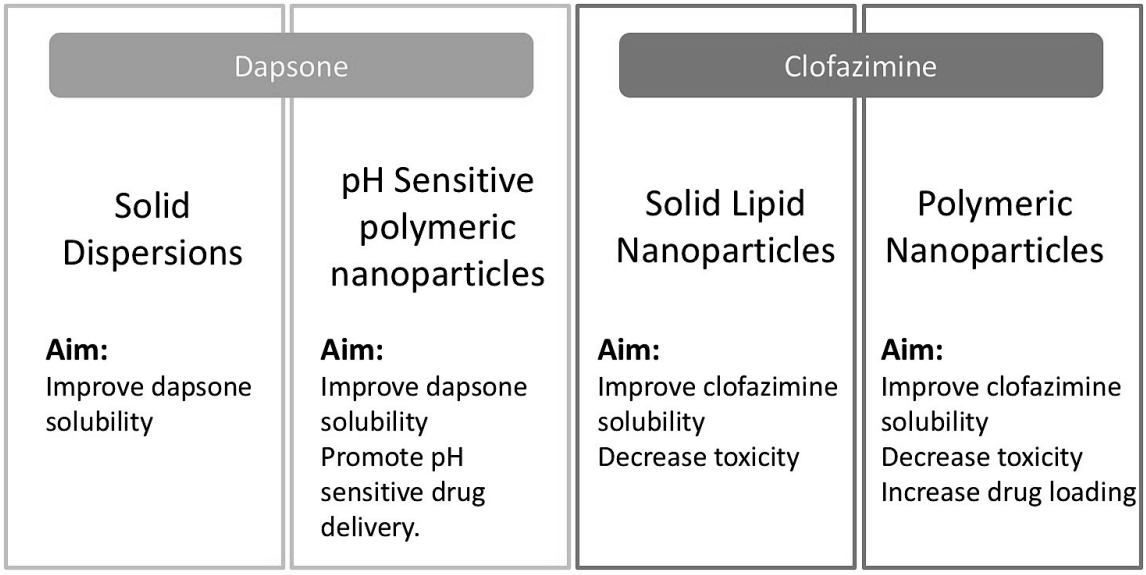

Integrated discussion

The hypothesis of this thesis was based on the current difficulties in the management of leprosy treatment as recommend by the WHO, which results in a lack of patient compliance, most of the times due to duration of treatment, and appearance of undesired side effects. Thus, it was envisaged that the association of the main first-line drugs, DAP and CLZ, could promote leprosy eradication worldwide, particularly in Brazil, endemic country that founded this research. DAP and CLZ are classified according to the BDS as class II drugs, presenting water solubility of 160 and 0.5 μg mL^{-1} respectively, at 25°C [1]. Therefore, the study was always based on the selection of appropriate systems for poorly water-soluble drugs.

The development of drug delivery systems was designed separately for each drug, mainly to avoid chemical interactions between the drugs and other formulations constituents, or degradation acceleration, as already reported before with other studies with drug association [2, 3]. In fact, DAP chemical reactions with other drugs has already been reported, under non-severe conditions [4]. The choice of solid dispersions (SD) as DAP drug delivery system was based on their scale-up feasibility, associated low cost and general physical stability [5]. Indeed, SD could be successfully developed and provided an increasing in DAP solubility three-fold higher compared to free DAP, at physiological pH and 37°C. During the preformuation studies, equilibrium solubility of DAP in different pH conditions (1.2; 4.5 6.8 and 7.4) was performed as recommended by the Food and Drug Administration (FDA)[6]. It was observed that solubility of DAP was much higher at acidic conditions, due to the protonation amino groupings [1]. Despite the positive results obtained from SD with DAP (Chapter IV.A) it was hypothesized that its higher solubility under acidic conditions would be the reason of DAP relevant digestive problems such as nausea, vomiting, and stomatitis. Besides, the DAP hydrolysis under acidic environment have been reported by non-enzymatic manner [7]. Thus, to overcome this drawback, DAP was incorporated within pH-sensitive nanoparticles aiming to achieve site-specific deliver of the drug as an alternative to the solid dispersions and the supersaturated solutions. By this way, DAP would be protected from the acidic gastric environment, and would be delivered only at the intestine for absorption. The selection of nanoparticles as drug delivery systems was based on their supplementary advantages such as: protection of the drug against potential degradation conditions, possibility to attach on nanoparticles surface ligands to further tissue-specific drug delivery, and to provide a controlled release, compared to solid dispersions as drug delivery systems. In fact, the developed nanosystems based on Eudragit L100 (Chapter IV.B) resisted to lower pH (1.2) in

comparison to more alkaline conditions (pH 6.8), with no toxic effects on gastric and intestinal cell lines.

Contrary to DAP, the initial preformulation study with CLZ was not conducted by determining its equilibrium solubility. The solubility assays were hampered due to the lack of a fast and feasible method to quantify the drug using a minimum amount of aqueous phase, and with suitable sensitivity to detect low concentrations. Thus, it was thought that the development of a fast, solvent-free, precise, sensitive and robust method to quantify CLZ would be useful to the work progress (Chapter IV.C). Moreover, after literature review, it could be concluded that the application of solid dispersions to deliver CLZ would not be a suitable strategy. It was already discussed that solid dispersions may improve drugs solubility buy delivering them through a very fine colloidal dispersion, promoting a supersaturated solution in the media [5, 8]. Although it has been demonstrated that amorphous systems can provide faster dissolution rates and higher solution concentrations than their crystalline counter, the drugs tend to crystallize via a solid-to-solid transition [9]. As already mentioned along the thesis, CLZ seems to form insoluble precipitates inside cells, which can be associated to its toxicity as the intracellular crystals act as intracellular drug depots, accounting for the drug's prolonged elimination, bioaccumulation and extended half-life [10, 11]. Thus, the improvement of CLZ absorption *per se* would not be enough to overcome its physicochemical limitations. As alternative, SLNs seemed to be a promising system to deliver CLZ (Chapter IV.C). Besides improve solubility of poorly soluble compounds through the reduction of particle size, SLNs in general could offer additional advantages, such as protection of the drug from gastrointestinal degradation, active and passive targeting to specific intestinal cells and even reduce systemic side effects. Particularly, SLNs were the first chosen nanocarriers due to its theoretical capability to entrap lipophilic compounds considering the lipid nature of the matrix. Moreover, it was considered their feasibility to scale-up, low cost, and production without the use of organic solvents. Despite the lipophilic nature of SLNs, it was found that most of the tested solid lipids during preliminary studies were not able to solubilize CLZ, as crystals were still present after lipid melting, at the ratio 10:1 (w/w) lipid:drug. Precirol ATO was found to be suitable for the development of SLNs loaded with CLZ (SLNs-CLZ), with proper particle size, potential zeta and polydispersity index. Regarding AE (71%) and DL (2.4%), even if the obtained values can be considered positive results for nano-delivery systems, it would be difficult to reach the oral administered dosage adopted in leprosy treatment (50 mg) with this drug payload. Moreover, the hypothesis that SLNs could improve poorly soluble drugs permeability did not apply for SLNs-CLZ. After 8 h of permeation across Caco-2 monolayers, no CLZ was found at the receptor compartment, or the permeated amount of CLZ was below the detection limit of

the quantification method (Chapter III, 6.2). One explanation for this result is that the permeability assay across Caco-2 monolayer using Transwell® systems may not be the most appropriated assay to evaluate SLNs since the lipid density is lower than the medium used for the assay, resulting in false negative or inconclusive results. Likewise, it has been reported that negatively charged SLNs may aggregate in the buffer medium due to the presence of high concentration of salts in the buffer, which may bypass the negative charges on the surface of SLNs, leading to the aggregation, avoiding uptake by Caco-2 cells [12]. On the other hand, high amounts of SLNs-CLZ could be internalized by the Caco-2 cells, and follow some degradation pathway, or simply remain inside cells unable to permeate the monolayer, resulting in not detectable quantification. However, these hypotheses were not confirmed, and need further investigation. To overcome the described issues concerning SLNs, the development of polymeric nanoparticles with CLZ appeared to be an alternative. Compared to lipid-based nanocarriers, polymeric nanoparticles have advantages such as higher stability in acidic environment, and possibility to achieve a more controlled drug release by modulating physicochemical characteristics [13]. In addition, less amount of dispersive matrix is required, compared to SLNs, which would increase the DL of the nanosystem. The choice of poly(lactic-co-glycolic acid) (PLGA) as matrix was due to its ability to encapsulate poor soluble compounds as already reported in the literature [14-17]. In fact, the obtained polymeric nanoparticles loaded with CLZ (NPs-CLZ) (Chapter IV.D) showed higher DL (11.6%) compared to SLNs (2.4%). AE efficiencies were found ca 70% for both nanosystems. Regarding toxicity, both nanoparticles did not affect intestinal cells viability, in relation to pure CLZ that induce toxicity (Chapter IV C and D). The most important outcomes when comparing SLNs and NPs loaded with CLZ were regarding permeability assays across Caco-2 cell monolayer. Differently from SLNs-CLZ, the CLZ within polymeric nanoparticles were able to cross the intestinal cell monolayer. Even though, longer time may be required for the CLZ permeate the Caco-2 monolayer at a higher extent (Chapter IV.D). The data obtained from the permeability assays could emphasizes that further studies should be conduct to compare the uptake mechanism of lipid-based and polymer-based nanoparticles with CLZ by Caco-2 cells.

The final ultimate of this thesis was to perform DAP/CLZ association through the optimized and most promising nanosystems. Intestinal permeability assays with DAP solid dispersions and EL100 nanoparticles were performed, even though no statistical differences were found concerning the amount of permeated DAP. Due the advantages of the NPs-EL100-DAP nanoparticles, this system was chosen to be combined with the NPs-CLZ (Chapter IV.E). Permeability assays across Caco-2 monolayer revealed that DAP and CLZ in the nanosystems *per se* or in combination crossed the intestinal barrier, and no

significant differences were observed between the nanosystems *per se* or in combination. Nevertheless, complementary assays regarding physicochemical characterization of nanosystems combination, and pharmacokinetics profiles must be performed.

Overall, different drug delivery systems with DAP and CLZ could be well designed and have their individual importance, as each of them present negative and positive aspects. In the framework of pharmaceutical technology, it should always be considered several aspects regarding the via of administration, drug physicochemical features, pharmacokinetics profile, elimination and degradation mechanism, duration of treatment, administered dosage, and an infinity of other parameters [5]. On the other hand, the advances in the search for new drug platforms to delivery active compounds is increasing day by day, and different alternatives are being available to overcome the drugs clinical limitations. Fortunately, there are very efficient tools to assess their performance, either *in vitro* or *in vivo,* leading to exhaustive work searching for the "perfect" formulation. Even though, the research will never end, as all pharmaceutical product will have their associated risk, leading the work to the beginning! (Personal note).

1. References

1. Chaves, L.L., *et al.*, *Rational and precise development of amorphous polymeric systems with dapsone by response surface methodology*. Int J Biol Macromol, 2015. **81**: p. 662-71.
2. Kauss, T., *et al.*, *Fixed artesunate–amodiaquine combined pre-formulation study for the treatment of malaria.* International journal of pharmaceutics, 2010. **395**(1): p. 198-204.
3. Gaubert, A., et al., *Preliminary pharmaceutical development of antimalarial–antibiotic cotherapy as a pre-referral paediatric treatment of fever in malaria endemic areas.* International journal of pharmaceutics, 2014. **468**(1): p. 55-63.
4. Yamasaki, P.R., et al., *Synthesis and evaluation of novel dapsone–thalidomide hybrids for the treatment of type 2 leprosy reactions.* Bioorganic & medicinal chemistry letters, 2014. **24**(14): p. 3084-3087.
5. Chaves, L.L., et al., *Quality by Design: Discussing and Assessing the Solid Dispersions Risk.* Current Drug Delivery, 2014. **11**(2): p. 253-269.
6. Food, U. and D. Administration, *Guidance for industry: Dissolution testing of immediate release solid oral dosage forms.* Center for Drug Evaluation and Research, Rockville, 1997.
7. Ellard, G., *Absorption, metabolism, and excretion of di(p-aminophenyl) sulphone (dapsone) and di(p-aminopheny) sulphoxide in man.* British Journal of Pharmacology, 1966. **26**(1): p. 212-217.
8. Chaves, L., et al., *Rational and precise development of amorphous polymeric systems with dapsone by response surface methodology*. Int J Biol Macromol, 2015. **81**: p. 662-71.

9. Alonzo, D.E., et al., *Understanding the behavior of amorphous pharmaceutical systems during dissolution*. Pharmaceutical research, 2010. **27**(4): p. 608-618.

10. Yoon, G.S., et al., *Clofazimine Biocrystal Accumulation in Macrophages Upregulates Interleukin 1 Receptor Antagonist Production To Induce a Systemic Anti-Inflammatory State*. Antimicrobial agents and chemotherapy, 2016. **60**(6): p. 3470-3479.

11. Yoon, G.S., et al., *Phagocytosed Clofazimine Biocrystals Can Modulate Innate Immune Signaling by Inhibiting TNFalpha and Boosting IL-1RA Secretion*. Mol Pharm, 2015. **12**(7): p. 2517-27.

12. Luo, Y., et al., *Solid lipid nanoparticles for oral drug delivery: Chitosan coating improves stability, controlled delivery, mucoadhesion and cellular uptake*. Carbohydrate Polymers, 2015. **122**: p. 221-229.

13. Pathak, K. and S. Raghuvanshi, *Oral bioavailability: issues and solutions via nanoformulations*. Clinical pharmacokinetics, 2015. **54**(4): p. 325-357.

14. Akl, M.A., et al., *Factorial design formulation optimization and in vitro characterization of curcumin-loaded PLGA nanoparticles for colon delivery*. Journal of Drug Delivery Science and Technology, 2016. **32**: p. 10-20.

15. Shaikh, M.V., M. Kala, and M. Nivsarkar, *Formulation and optimization of doxorubicin loaded polymeric nanoparticles using Box-Behnken design: ex-vivo stability and in-vitro activity*. European Journal of Pharmaceutical Sciences, 2017. **100**: p. 262-272.

16. Dhat, S., et al., *Risk management and statistical multivariate analysis approach for design and optimization of satranidazole nanoparticles*. European Journal of Pharmaceutical Sciences, 2017. **96**: p. 273-283.

17. Yerlikaya, F., et al., *Development and Evaluation of Paclitaxel Nanoparticles Using a Quality-by-Design Approach*. Journal of Pharmaceutical Sciences, 2013. **102**(10): p. 3748-3761.

Chapter V

Concluding remarks and future perspectives

1. Concluding remarks

The actual MDT for leprosy disease with CLZ and DAP as daily first-line drugs to treat patients with MB leprosy seems to be a trend in leprosy treatment management. Even though, despite the already stablished efficiency of the anti-leprotic agents, the biopharmaceutical properties of these drugs may be limiting their performance during the treatment. Besides, the reported resistance of DAP, associated with the toxicity effects of CLZ probably due to its tissue accumulation and *in vivo* precipitation may be jeopardizing the patient compliance, and the ultimate success of leprosy treatment. Therefore, the investigation of new strategies to deliver DAP and CLZ in order to overcome their physicochemical limitations was found to be useful for the improvement of leprosy therapy.

The implementation of the Quality by Design (QbD) concept recommended by the International Conference on Harmonization was successfully applied along this thesis by the application of combined analytical approaches such as design of experiments (DoE), response surface methodology (RSM) and optimization aiming to systematically construct suitable drug delivery systems with DAP and CLZ.

Solid dispersions (SD) systems were considered a promising technique to improve the aqueous solubility of DAP. The preparation of amorphous SD with DAP and PVP-K30 was developed based on preliminary investigation of DAP solubility enhancement after phase diagram solubility assay. Moreover, the addition of Pluronic® F68 as a third component in the SD did not interfere in the improvement of DAP solubility. Higher solubility and dissolution rate was found for freeze-dried SD, compared to kneaded and physical mixtures, which could be attribute to the improved wettability and particle size reduction, by the conversion from crystalline to the amorphous form and by the molecular interactions between drug and polymer in resultant dispersions.

pH-sensitive nanoparticles produced with DAP and Eudragit L100 polymer (NPs-EL100-DAP) were successfully developed after the identification of the most critical variables, through Placket-Burman screening design, with subsequent optimization by the application of BBD regarding the selected responses (particle diameter, PDI and AE). The *in vitro* drug release at different pH conditions confirmed the pH sensitivity of NPs-EL100-DAP, being able to provide enhanced drug delivery at the intestinal environment. No toxicity was observed in different gastro-intestinal cell lines up to 400 $\mu g.mL^{-1}$ of DAP. Moreover, 2-fold enhanced intestinal permeability was observed when DAP was incorporated within NPs-EL100 in comparison to free DAP.

Regarding CLZ drug delivery systems, risk management tools helped to identify potential factors that could affect SLNs-CLZ performance, and allowed the

implementation of control actions to obtain suitable nanosystems. A BBD was used to optimize SLNs-CLZ with the desired parameters (particle size, zeta potential, AE and DL). Physicochemical characterization confirmed the amorphous state of CLZ within SLNs. The developed SLNs-CLZ showed to be stable under the established storage conditions (4ºC) for 12 weeks, and no toxicity was found up to 50μg mL^{-1} in CLZ for SLNs-CLZ towards gastrointestinal cells, on the contrary of the free CLZ solutions. SLNs-CLZmay be an useful platform to decrease CLZ associated side effects.

A second nanosystem was developed with CLZ and PLGA, after the identification of critical variables by PBD. Physicochemical characterization confirmed the amorphous state of CLZ into the polymeric nanoparticles, and their spherical morphology The *in vitro* drug release revealed the sustained pattern of CLZ released from NPs-CLZ upon 8 h. *In vitro* cytotoxicity studies evidenced that the obtained NPs-CLZ prevented the toxic effect of free CLZ. CLZ permeated the Caco-2 cells monolayer when entrapped in the PLGA nanoparticles, exhibiting Papp values of 3.8± 0.2 x 10^{-6} (cm s^{-1}). Despite the long-term controlled CLZ release from the NPs-CLZ, the developed nanoparticles were able to reach intended concentration to promote therapeutic effect after 8h or permeability assay, according described reports.DAP/ CLZ association was as toxic as CLZ alone, evidencing that the toxicity of the drug association was probably due to the CLZ presence. The nanosystems combination did no exert any significant toxic effects. On the contrary, the incorporation of DAP and CLZ into polymeric nanosystem provided a good intestinal cell viability.

To summarize, the results of this thesis provided different platforms to deliver DAP and CLZ separately, aiming to overcome the limitations associated with both drugs, representing promising systems to the future leprosy therapy as single systems or in association. Nevertheless, complementary assays regarding physicochemical characterization of nanosystems association, and determination of pharmacokinetics profiles must be conducted to better elucidate the performance of DAP – CLZ association into nanodelivery systems.

2. Future Perspectives

Following the obtained outcomes from presented work, it would be ofgreat value to assess physicochemical stability and characterization of the nanosystems (NPs-DAP and NPs-CLZ) in combination, and compare with the nanosystems alone. Performing *in vitro* drug release studies with the associated nanosystems, using more complex biorelevant media aiming to correlate more precisely with *in vivo* results seem to be an important aspect to be studied. In addition, the uptake mechanisms by intestinal cells

of the nanosystems to better understand the behavior of tissue permeability would be of great relevance. The performance of *in vivo* assays for the assessment of the efficacy of nanosystems combination and determination of pharmacokinetic profile after oral administration to adjust dosages for leprosy treatment purposes would be interesting points to be approached.